KU Leuven

Biomedical Sciences Group

Faculty of Medicine

Neuroelectronics Research Flanders (NERF)

VIB Center for the Biology of Disease

Studying neuronal circuit mechanisms underlying fragile X syndrome in *Drosophila melanogaster*

Luis Manuel FRANCO MÉNDEZ

Jury:

Promoter:	Prof. Emre Yaksi
Co-promoter:	Prof. Bassem Hassan
Chair:	Prof. Peter Janssen
Secretary:	Katleen Vercammen
Jury members:	Prof. Patrick Callaerts
	Prof. Sebastian Haesler
	Prof. Frank Kooy
	Prof. Carlos Ribeiro

Dissertation presented in partial fulfilment of the requirements for the degree of Doctor of Philosophy in Biomedical Sciences

October 2016

To Diana.

Acknowledgements

I would like thank my supervisors, Prof. Emre Yaksi and Prof. Bassem Hassan, firstly, for the opportunity to carry out my PhD in their laboratories, but most importantly, for the excellent scientific guidance they provided to me during the course of my PhD. Thank you very much for your patience, for your advice and for helping me to carry out a successful PhD.

I would like to thank Prof. Patrick Callaerts, Prof. Sebastian Haesler, Prof. Frank Kooy and Prof. Carlos Ribeiro for accepting being part of my jury. In particular, I would like to thank Prof. Patrick Callaerts and Prof. Sebastian Haesler for the constructive feedback provided during the different evaluations of my PhD. In addition, I would like to thank Prof. Peter Marynen and Prof. Peter Janssen for accepting being the chair of my thesis examining committee and the chair of my public defense jury, respectively.

During the course of my PhD I received many brilliant comments that helped to enrich my PhD project from all the members of Prof. Emre Yaksi and Prof. Bassem Hassan laboratories. I feel very lucky and grateful of having had such talented and cooperative colleagues. In particular, I am very thankful to Zeynep Okray, who not only introduced me to the magnificent field of *Drosophila* research, but also contributed considerably to my PhD project by providing very important feedback and by conducting some experiments.

I would like to thank Annelies Claeys, Jiekun Yan and Natalie De Geest for their exceptional technical support. Thank you very much for your patience and your time. In particular, I would like to thank Annelies Claeys, whose essential support contributed to construct the behavioral setup used to carry out some of the experiments for my PhD project. In addition, I would like to thank Ilse Eyckmans and Frédérique Ooms, whose outstanding managerial and technical assistance greatly facilitated carrying out complicated high quality experiments. Thank you very much for your time and never ending energy to help anytime it was required.

I am very grateful to Miep Behets, Katleen Vercammen, Ethel Claes and Anke Van Noten, whose impeccable secretarial assistance enormously helped me to efficiently manage the different procedures required during the course of my PhD. Thank you very much for your time and your outstanding attitude to help every time it was necessary.

I would like to thank KU Leuven for allowing me to be part of this extraordinary university to conduct my PhD. The academic environment provided by KU Leuven not only promoted my personal scientific development but, importantly, permitted me to meet many very talented scientists and to learn about the interesting research they carry out. I feel very proud of having been part of such great university.

I would like to thank the Vlaams Instituut voor Biotechnologie (VIB) for believing and trusting me to award me with one of their prestigious scholarships of the VIB International PhD Program in Life Sciences. I will always be grateful to VIB for allowing me to carry out my PhD in this great scientific institution.

Finally, I would like to thank my family and friends, whose support encouraged me to continue pursuing my PhD even in the most difficult moments. I feel very happy of having such amazing people in my life. In particular, I would like to thank my mother Lourdes, my sister Viridiana and my wife Diana, who were always there to listening to and to supporting me when I needed them most.

Index

Abbreviations

AMPA	α-amino-3-hydroxy-5-methyl-4-isoxazolepropionic acid
BK_{Ca}	calcium-activated potassium channel
$CaCl_2$	calcium chloride
ChR2	channelrhodopsin-2
DNA	deoxyribonucleic acid
dfmr1	*Drosophila melanogaster* homolog of the human FMR1
dFMRP	*Drosophila melanogaster* homolog of the human FMRP
EGTA	ethylene glycol-bis(β-aminoethyl ether)-N,N,N',N'-tetraacetic acid
ELAV	embryonic lethal abnormal visual protein
EMMCD	electron multiplying charged-coupled device
END1-2	ELAV *n*-synaptobrevin-DsRed 1-2
FMR1	fragile X mental retardation 1 gene
FMRP	fragile X mental retardation protein
FXPOI	fragile X related primary ovarian insufficiency
FXTAS	fragile X associated tremor/ataxia syndrome
GABA	γ-aminobutyric acid
$GABA_A$	γ-aminobutyric acid receptor, type A
$GABA_B$	γ-aminobutyric acid receptor, type B
GAD	glutamic acid decarboxylase
GAT	GABA transporter
GCaMP	fusion protein of GFP, calmodulin and M13 (peptide sequence of MLCK)
GFP	green fluorescent protein
KCl	potassium chloride
HEPES	4-(2-hydroxyethyl)-1-piperazineethanesulfonic acid
Kv4.2	voltage-gated potassium channel
Kv3.1	voltage-gated potassium channel
LN	local interneuron
LTD	long-term depression

LTP	long-term potentiation
$MgCl_2$	magnesium chloride
mGluR	metabotropic glutamate receptor
MLCK	myosin light-chain kinase
mRNA	messenger ribonucleic acid
NaCl	sodium chloride
$NaHCO_3$	sodium bicarbonate
NaH_2PO_4	monosodium phosphate
NMDA	N-methyl-D-aspartic acid
ORN	olfactory receptor neuron
PBS	phosphate-buffered saline
PBST	PBS with Triton
PN	projection neuron
RNA	ribonucleic acid
RNAi	RNA interference
SOD1	superoxide dismutase 1
SSADH	succinic semialdehyde dehydrogenase
TES	2-[tris(hydroxymethyl)methylamino]-1-ethanesulfonic acid
WT	wild type

Summary

Fragile X syndrome patients present neuronal alterations that lead to severe intellectual disability, but the underlying neuronal circuit mechanisms are poorly understood. An exciting hypothesis postulates that reduced GABAergic inhibition of excitatory neurons is a key component in the pathophysiology of fragile X syndrome. Here, I directly test this idea. First, I show that a *Drosophila melanogaster* model of fragile X syndrome exhibits strongly impaired olfactory behaviors. In line with this, olfactory representations are less odor-specific due to broader response tuning of excitatory projection neurons. I find that impaired inhibitory interactions underlie reduced specificity in olfactory representations. Finally, I show that defective lateral inhibition across projection neurons is caused by weaker inhibition from GABAergic interneurons. I provide direct evidence that deficient inhibition impairs sensory computations and behavior in an *in vivo* model of fragile X syndrome. Together with evidence of impaired inhibition in autism and Rett syndrome, these findings suggest a potentially general mechanism for intellectual disability.

Samenvatting

Patiënten met het fragiele-X-syndroom vertonen neuronale afwijkingen die een ernstige verstandelijke handicap veroorzaken. De onderliggende mechanismen van het neuronale netwerk zijn echter amper bekend. Een opmerkelijke hypothese stipuleert dat GABAergische inhibitie van de exciterende neuronen een essentiële rol spelen in de pathofysiologie van het fragiele-X-syndroom. In deze thesis testen we deze theorie op een directe manier. Een *Drosophila melanogaster* model van het fragiele-X-syndroom vertoont sterke afwijkingen in hun olfactorisch gedrag. Meerbepaald zijn hun olfactorische hersenkaarten minder geurspecifiek door een bredere respons regeling van exciterende projectieneuronen. We leiden af dat verstoorde inhibitorische interacties de onderliggende reden zijn voor verminderde specificiteit in olfactorische hersenkaarten. We tonen ook aan dat foutieve laterale inhibitie van projectieneuronen veroorzaakt wordt door zwakkere inhibitie van GABAergische interneuronen. We leveren rechtstreeks bewijs dat foutieve inhibitie de sensorische verwerking in de hersenen alsook het gedrag aantasten in een *in vivo* model van het fragiele-X-syndroom. Samen met de aanwijzingen voor verzwakte inhibitie bij autisme en het syndroom van Rett, suggereren onze bevindingen het bestaan van een potentiëel algemeen mechanisme voor verstandelijke handicaps.

Introduction

Fragile X syndrome is one of the most common inherited intellectual disability disorder. Patients with fragile X syndrome exhibit neurological symptoms that include learning disabilities, social anxiety, attention deficits, hyperarousal, hypersensitivity, autism and, in some cases, epileptic seizures (reviewed by Penagarikano *et al.*, 2007). Notwithstanding the complexity of neurophysiological and behavioral alterations, fragile X syndrome is caused by the silencing, deletion or loss of function mutation of a single gene, FMR1. As a result, FMRP, its protein product, is not expressed in the vast majority of cases or is non-functional in the rare cases with a point mutation (Verkerk *et al.*, 1991; Sutcliffe *et al.*, 1992; Okray *et al.*, 2015; Suhl & Warren, 2015). FMRP is a mRNA-binding protein (Ashley et al., 1993) that regulates several aspects of mRNA metabolism such as nuclear export, transport to synaptic terminals, activity-dependent ribosome stalling and gene expression (reviewed by Bagni & Greenough, 2005; Bassell & Warren, 2008; Santoro *et al.*, 2012). Although much of FMRP molecular activity is thought to be specifically related to regulation of synaptic function (Zhang *et al.*, 2001; Edbauer *et al.*, 2010; Darnell *et al.*, 2011), very little is known about the potential defects in neuronal circuit function caused by the absence of FMRP. In particular, how these neurophysiological alterations lead to impairment in neuronal computations and, eventually, behavior in patients with fragile X syndrome.

Initial studies revealed that the number of dendritic spines is increased in the cortical tissue of patients with fragile X syndrome (Rudelli *et al.*, 1985; Hinton *et al.*, 1991; Wisniewski *et al.*, 1991; Irwin *et al.*, 2001). In fact, dendritic abnormalities are the most consistent anatomical correlates of intellectual disability (Kaufmann & Moser, 2000). Further studies on mouse and fruit fly models of fragile X syndrome showed that FMRP regulates neuronal branching (Morales *et al.*, 2002; Galvez *et al.*, 2003; Pan *et al.*, 2004; Reeve *et al.*, 2005; Reeve *et al.*, 2008; Patel *et al.*, 2014) as well as dendritic spine morphology and density (Comery *et al.*, 1997; Nimchinsky *et al.*, 2001; Zhang *et al.*, 2001). In addition to defects in synaptic structure and in axonal branching, impairments in animal behavior were observed (Zhang *et al.*, 2001; Morales *et al.*, 2002). However, further studies showed that

anatomical neuronal circuitry defects and behavioral defects can be genetically uncoupled (Reeve *et al.*, 2005), suggesting that unknown defects in neuronal circuit function underlie behavioral deficits.

FMRP regulates translation of target mRNAs at synapses, some of which encode proteins involved in synaptic plasticity (Brown *et al.*, 2001; Zalfa *et al.*, 2003; Muddashetty *et al.*, 2011; Darnell & Klann, 2013). Importantly, absence of FMRP leads to abnormally and constitutively enhanced group 1 mGluR signaling, which results in exaggerated long-term depression (Huber *et al.*, 2002), with a net loss of AMPA and NMDA receptors (Huber *et al.*, 2000; Snyder *et al.*, 2001; Ireland & Abraham, 2009). Exaggerated group 1 mGluR signaling has additional consequences. Anatomically, enhanced group 1 mGluR signaling contributes to elongation of dendritic spines in rodent models of fragile X syndrome (Comery *et al.*, 1997; Nimchinsky *et al.*, 2001; Vanderklish & Edelman, 2002). Physiologically, enhanced group 1 mGluR signaling leads to increased intrinsic neuronal excitability through downregulation of potassium channels that are important for determination of the resting membrane potential and for action potential afterhyperpolarization (Sourdet *et al.*, 2003; Brager & Johnston, 2007). Moreover, FMRP directly influences neuronal excitability by regulating expression of potassium channels (Strumbos *et al.*, 2010; Gross *et al.*, 2011; Lee *et al.*, 2011), and also, in a translation-independent manner, by interacting with potassium channels. (Brown *et al.*, 2010; Deng *et al.*, 2013). Nevertheless, the recent failure of clinical trials targeting group 1 mGluR signaling (Mullard, 2015), has lead the field to re-examine the assumption that enhanced group 1 mGluR signaling is sufficient to explain the symptomatology associated with fragile X syndrome.

Loss of FMRP was recently shown to result in abnormal network-level hyperexcitability in the mouse somatosensory cortex (Goncalves *et al.*, 2013; Zhang *et al.*, 2014), which has been associated with many of the symptoms observed in patients with fragile X syndrome, such as hypersensitivity, hyperarousal, hyperactivity, anxiety and epilepsy (reviewed by Bear *et al.*, 2004; D'Hulst & Kooy, 2007; Braat & Kooy, 2015a; Contractor *et al.*, 2015). Interestingly, absence of FMRP leads to downregulation of $GABA_A$ receptor subunits in both mice and fruit flies (El Idrissi *et al.*, 2005; D'Hulst *et al.*, 2006;

Gantois *et al.*, 2006; Curia *et al.*, 2009; Adusei *et al.*, 2010; Hong *et al.*, 2012). Furthermore, other components of the GABAergic transmission machinery, such as the enzymes for GABA synthesis and degradation, GABA membrane transporters, a GABA receptor scaffolding protein and a protein that regulates $GABA_B$ receptor signaling were shown to be downregulated in the absence of FMRP (D'Hulst *et al.*, 2009; Adusei *et al.*, 2010; Olmos-Serrano *et al.*, 2010; Pacey *et al.*, 2011; Gatto *et al.*, 2014). These observations suggest a tantalizing, yet poorly understood, link between GABAergic signaling, network hyperexcitability and behavioral deficits in models and patients with fragile X syndrome.

In contrast to the extensively studied group 1 mGluR component of fragile X syndrome, the potential effects of altered synaptic inhibition on neuronal circuits excitability and how these synaptic changes might impact sensory computations and animal behavior remain unexplored. In this study, I explore the changes in neuronal circuit function and connectivity underlying fragile X syndrome by using a combination of quantitative behavioral assays, *in vivo* functional brain imaging, optogenetics and electrophysiology in a fruit fly model of Fragile X Syndrome. Specifically, I focused on the olfactory system of *Drosophila melanogaster*, which is a well-understood and genetically tractable neuronal circuit with a high level of stereotypy. I find that absence of dFMRP, the fly homolog of the human FMRP, results in reduced performance in innate olfactory behaviors such as attraction and aversion. Calcium imaging data show that antennal lobe projection neurons have broader odor response tuning in *dfmr1*$^-$ flies, which leads to reduced specificity in odor coding and alterations in olfactory representations. In line with these results, I observe that lateral inhibition across olfactory glomeruli, as well as the inhibitory connections between local interneurons and projection neurons are impaired in *dfmr1*$^-$ flies. I propose that absence of dFMRP leads to defective lateral inhibition across olfactory glomeruli, which, in turn, results in impaired olfactory coding and odor induced behaviors.

Fragile X Syndrome

Fragile X syndrome was firstly identified after the observation of unusual gaps on the X chromosome long arm in a particular group of patients previously diagnosed with intellectual disability (Lubs, 1969; see Figure I). Such gaps were named fragile sites due to their propensity to break under certain conditions (Sutherland, 1977; Hecht & Sutherland, 1985). The term *Fragile X Syndrome* was thus coined to designate this distinct form of X chromosome related intellectual disability (Santoro *et al.*, 2012). Fragile X syndrome is also known as Martin-Bell syndrome (Webb *et al.*, 1981) or Escalante syndrome (Vianna-Morgante *et al.*, 1982).

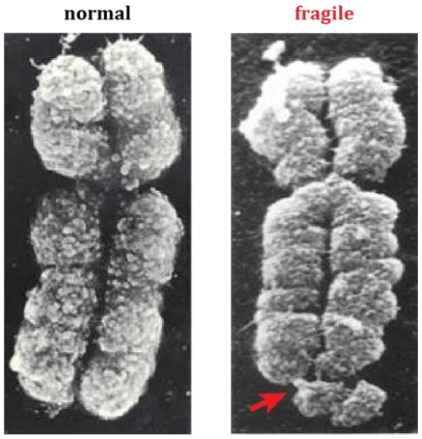

Figure I. Human normal **(left)** and fragile **(right)** X chromosomes observed in metaphase by scanning electron microscopy. The gap denoted by a red arrow indicates the fragile site. (Adapted from Harrison *et al.*, 1983).

Fragile X Syndrome is a developmental disorder that results in a spectrum of physical alterations as well as intellectual disabilities. Fragile X syndrome patients commonly present connective tissue disorders such as prominent ears, long face, high palate, flat feet, hyperextensible joints and hypotonia (Hagerman *et al.*, 1984; Chudley & Hagerman, 1987; Hagerman, 2002; Murphy-Ryan *et al.*, 2010). The looseness of the connective tissue also predisposes them to hernias, joint dislocations, esophageal reflux, eye and vision problems, sinusitis and middle ear infections (Hagerman, 2002). In addition, male subjects present postpubescent macroorchidism (Turner *et al.*, 1980; Chudley & Hagerman, 1987; Hagerman, 2002). Behaviorally, fragile X syndrome patients exhibit perseverative movements such as hand-flapping and hand-biting as well as atypical social interactions such as poor eye

contact, shyness, tactile defensiveness, panic attacks and aggression. Psychiatric conditions such as attention deficit hyperactivity, hypersensitivity, hyperarousal and anxiety are frequently diagnosed in individuals with fragile X syndrome (Chudley & Hagerman, 1987; Hagerman, 2002; Hagerman *et al.*, 2009; Tranfaglia, 2011). These characteristic behaviors significantly overlap with those observed in autistic disorders (Tranfaglia, 2011).

It has been estimated that in approximately 5 % of the cases, fragile X syndrome patients also meet all of the criteria for autism spectrum disorder (Muhle *et al.*, 2004; Schaefer & Mendelsohn, 2008; Budimirovic & Kaufmann, 2011). Nonetheless, most patients display autistic features, with reported rates ranging from 15 to 60 % (Bailey *et al.*, 2001; Rogers *et al.*, 2001; Kaufmann *et al.*, 2004; Lewis *et al.*, 2006; Clifford *et al.*, 2007; Bailey *et al.*, 2008; Harris *et al.*, 2008; Budimirovic & Kaufmann, 2011). This behavioral overlap between autism and fragile X syndrome has been proposed to arise from some overlapping neural mechanisms (Belmonte & Bourgeron, 2006; Braat & Kooy, 2015a).

The observation of increased behavioral responsiveness might reflect neural hyperexcitability (Gibson *et al.*, 2008; Braat & Kooy, 2015b). In consonance with this, fragile X syndrome patients have been reported to present seizures in 10 to 20 % of the cases, whose EEG patterns are characteristic of benign Rolandic epilepsy, suggesting a shared neural mechanism (Berry-Kravis, 2002; Incorpora *et al.*, 2002; Hagerman & Stafstrom, 2009).

A subgroup of individuals diagnosed with fragile X syndrome have been reported to exhibit hyperphagia and obesity, with a physical phenotype similar to that of Prader-Willi syndrome (Fryns *et al.*, 1987; de Vries *et al.*, 1993; Schrander-Stumpel *et al.*, 1994; Nowicki *et al.*, 2007). Importantly, this subgroup presents elevated rates of autism (Hagerman *et al.*, 2009).

Most of the neurological diseases that share behavioral phenotypes with fragile X syndrome do not currently have populational biomarkers. By contrast, fragile X syndrome has been found to be caused by a mutation in one single gene (Verkerk *et al.*, 1991). This

discovery considerably facilitated its diagnosis as well as its study through animal experimentation. Therefore, the study of fragile X syndrome is not only important by itself but also to help elucidating neurological mechanisms related to other disorders.

Mutation in the *FMR1* gene

The variety of symptoms identified as fragile X syndrome have one common origin: an abnormal large expansion of CGG trinucleotide repeats (over 200) in the 5' untranslated region of the *FMR1* gene located in the X chromosome (Verkerk *et al.*, 1991). This abnormal DNA expansion results in hypermethylation of the CGG repeats and of the *FMR1* promoter (Oberle *et al.*, 1991; Sutcliffe *et al.*, 1992). Elevated levels of methylated DNA drive, in turn, deacetylation of the associated histones (Coffee *et al.*, 1999; Coffee *et al.*, 2002). This uncovers positive charges in the histones that interact with negative changers in the DNA, restricting nucleosome mobility and, therefore, rendering the promoter inaccessible to the transcription machinery (Razin, 1998). As a consequence, *FMR1* is silenced and no FMRP is expressed (Pieretti *et al.*, 1991), leading to manifestation of fragile X syndrome symptoms (see Figure II). In addition, nonsense and missense mutations in the *FMR1* gene that result in a premature stop codon or in non-functional FMRP, respectively, have been reported to cause fragile X syndrome (De Boulle *et al.*, 1993; Gronskov *et al.*, 2011; Myrick *et al.*, 2014). However, in the majority of cases, fragile X syndrome is caused by the expansion of CGG repeats (Santoro *et al.*, 2012).

Premutation of the FMR1 gene

Premutation of the *FMR1* gene occurs when the CGG triplet island undergoes a milder expansion between 50 and 200 repeats (Fu *et al.*, 1991; see Figure II). This results in a substantial increase of *FMR1* mRNA levels (Tassone *et al.*, 2000), which excessively bind to a number of nuclear proteins, leading to the formation of intranuclear aggregates (Greco *et al.*, 2002; Hagerman & Hagerman, 2007). By contrast, FMRP levels are only slightly reduced (Kenneson *et al.*, 2001), and are not thought to contribute to *FMR1* premutation disorders (Hagerman & Hagerman, 2007). Importantly, the CGG repeat number has been observed to proportionally correlate with the increase and decrease of *FMR1* mRNA and FMRP levels, respectively (Kenneson *et al.*, 2001).

Although premutation of *FMR1* does not produces fragile X syndrome, it can lead to other distinct diseases. For instance, fragile X related primary ovarian insufficiency (FXPOI) is a disorder that affects about 20 % of female premutation carriers (Sherman, 2000). FXPOI is characterized by a premature onset of menopause, which in some cases occurs as early as in adolescence. The number of CGG repeats has been reported to correlate with the penetrance and age of onset of FXPOI (Sullivan *et al.*, 2005). Fragile X associated tremor/ataxia syndrome (FXTAS), on the other hand, is a neurodegenerative disease with a late onset affecting approximately 40 % of male premutation carriers, with an age-related penetrance of 17 %, 38 %, 47 % and 75 % for male carriers aged 50 to 59, 60 to 69, 70 to 79 and ≥80 years, respectively. Clinical features include intention tremor and cerebellar gait ataxia, accompanied by characteristic white matter abnormalities. Some patients also show progressive cognitive decline (Berry-Kravis *et al.*, 2007; Jacquemont *et al.*, 2007). The pathological hallmark of FXTAS is the presence of intranuclear inclusions both in neurons and in astrocytes (Greco *et al.*, 2002; Hagerman & Hagerman, 2007). Similarly, the number of CGG repeats has been found to correlate with the onset of FXTAS, the age of death and the number of intranuclear inclusions (Greco *et al.*, 2006; Tassone *et al.*, 2007).

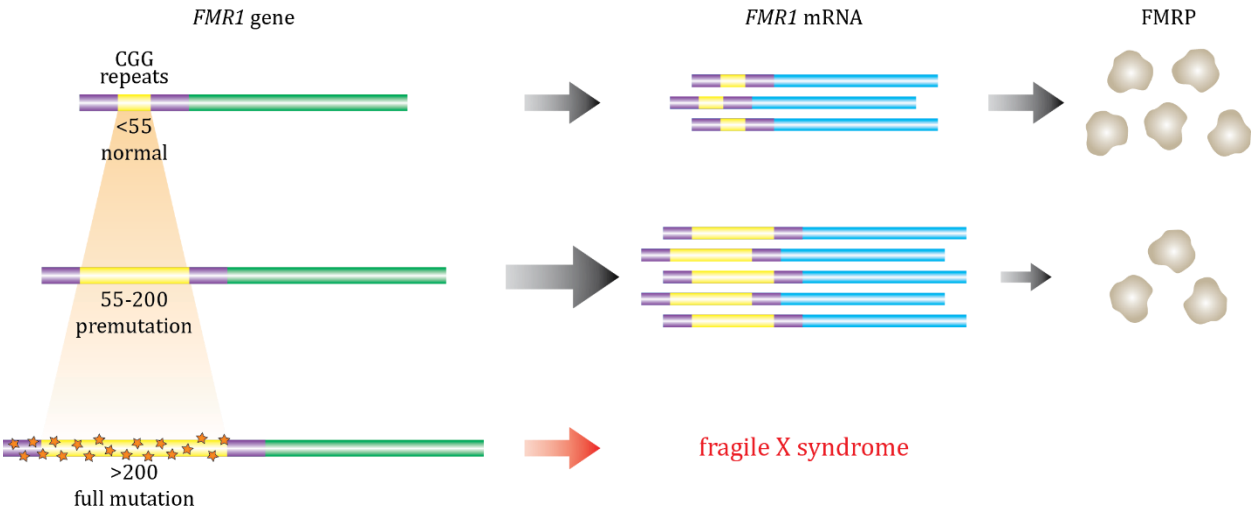

Figure II. (Up) The *FMR1* gene contains less than 55 CGG repeats (yellow) in its 5' untranslated region (purple). This allows for physiologically appropriate transcription of *FMR1* into its mRNA and, subsequently, translation into FMRP. **(Middle)** Premutation of *FMR1* results in substantially higher levels of its mRNA and, conversely, in slightly lower levels of FMRP. This premutation causes fragile X associated tremor/ataxia syndrome (FXTAS) and fragile X related primary ovarian insufficiency (FXPOI). **(Bottom)** Full mutation of *FMR1* leads to methylation (orange spots) in the CGG triplets as well as in the promoter of *FMR1*. As a consequence, FMRP is not expressed and symptoms of fragile X syndrome are manifested. (Adapted from Santoro *et al.*, 2012).

Cellular functions of FMRP

In order to understand how the absence of a single protein such as FMRP results in a disorder with the phenotypic variety and variability of fragile X syndrome it is necessary to know what functions FMRP carries out in the cell. FMRP is a RNA-binding protein (Ashley *et al.*, 1993) that participates in many aspects of mRNA metabolism. It is thought that FMRP binds to other proteins in the nucleus to form a ribonucleoprotein complex that exports mRNA to the cytoplasm. In the cytoplasm, FMRP, in association with some other cytosolic proteins and some of its nuclear partners, forms a different complex that is involved in mRNA transport along dendrites to synapses and in regulation of mRNA translation into proteins. Additionally, FMRP interacts with non-coding RNA in the nucleus to regulate gene expression by performing epigenetic DNA modifications (Bagni & Greenough, 2005; Pasciuto & Bagni, 2014a; see Figure III). Hence, FMRP regulates gene expression at the RNA level.

The implications of silencing the *FMR1* gene are, therefore, naturally related to the particular mRNA targets regulated by FMRP. It has been estimated that FMRP binds to as much as 4 % of the mRNA in the mammalian brain (Ashley *et al.*, 1993; Brown *et al.*, 2001), although only few have been validated by showing direct biochemical interaction (Santoro *et al.*, 2012; Pasciuto & Bagni, 2014b). Interestingly, several FMRP mRNA targets have been related with autism (Darnell *et al.*, 2011; Santoro *et al.*, 2012; Pasciuto & Bagni, 2014b), a recurrent phenotype of fragile X syndrome patients (Budimirovic & Kaufmann, 2011).

FMRP inhibits mRNA translation by stalling ribosomal translocation during elongation (Darnell *et al.*, 2011). This permits mRNA transport to distal sites of the neuron for protein synthesis while protecting mRNA from degradation and also allows rapid protein synthesis in response to synaptic activation (Aakalu *et al.*, 2001; Krichevsky & Kosik, 2001; Martin & Ephrussi, 2009; Darnell *et al.*, 2011). In fact, it has been shown that phosphorylated FMRP is associated with stalled ribosomes, whereas unphosphorylated FMRP allows translation to proceed (Ceman *et al.*, 2003; Muddashetty *et al.*, 2011). Thus, FMRP can dynamically modulate protein synthesis at the synapse in response to neuronal activity changes (Zalfa *et al.*, 2003; Muddashetty *et al.*, 2011). Dysregulation of these processes in the

absence of FMRP is likely to contribute to the symptoms observed in fragile X syndrome (Bear *et al.*, 2004; Kelleher & Bear, 2008).

FMRP has also been reported to enhance the expression of SOD1, an enzyme involved in mitigating oxidative stress (Bechara *et al.*, 2009). In the absence of FMRP, SOD1 levels decrease, which in turn leads to increased oxidative stress in the brain (el Bekay *et al.*, 2007; Juarez *et al.*, 2008; Bechara *et al.*, 2009). Oxidative stress in the brain has been linked to anxiety, sleeping difficulties and autism, all of which typically affect individuals with fragile X syndrome (Gingrich, 2005; Ming *et al.*, 2005; Cirelli, 2006). Nevertheless, it is considered that the main function of FMRP is to constitutively repress mRNA translation and to allow it upon activation of specific cell signaling pathways (Santoro *et al.*, 2012).

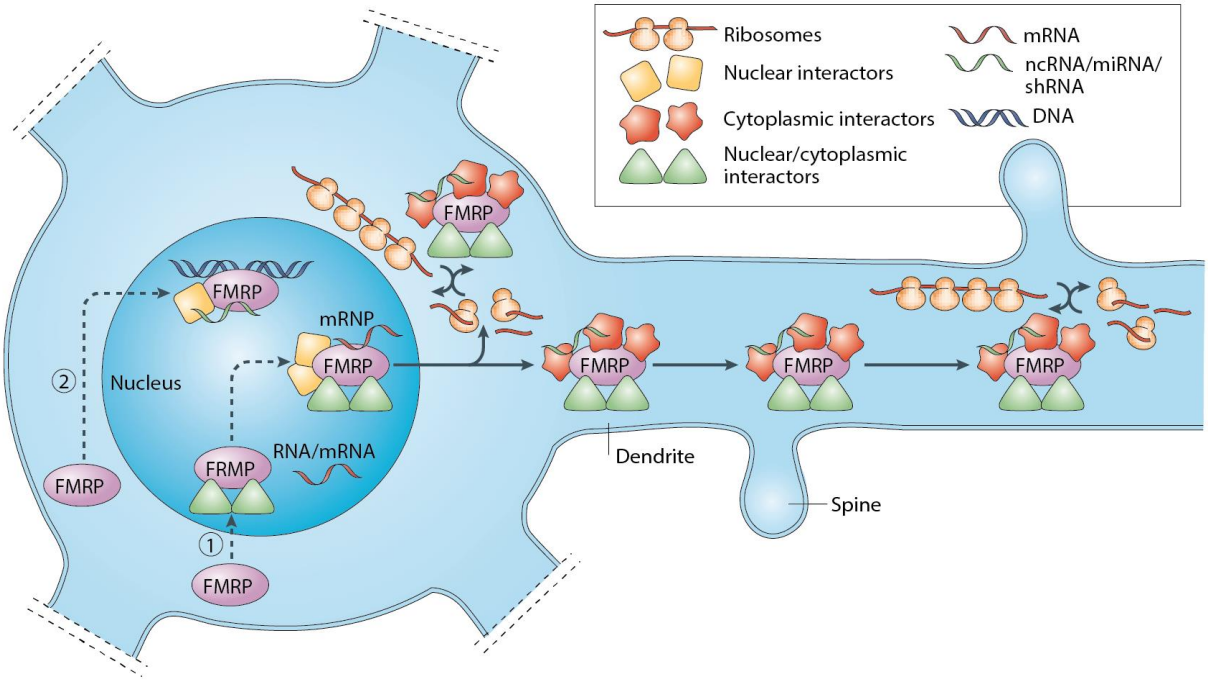

Figure III. (1) FMRP enters the nucleus and interacts with other proteins and with mRNA to form a ribonucleocomplex that is involved in mRNA export from the nucleus to the cytoplasm. Once in the cytoplasm, a 'core' complex, containing FMRP and some of its nuclear partners, would interact with cytoplasm-specific proteins and move along dendrites to the synapses, transporting mRNA and, later, regulating synaptic protein synthesis. **(2)** FMRP is involved in the nuclear RNA interference pathway that is associated with small, non-coding RNAs and specific nuclear partners. ncRNA, non-coding RNA; miRNA, microRNA; shRNA, short hairpin RNA. (Adapted from Bagni & Greenough, 2005).

The mGluR theory

Synaptic activity can trigger long-lasting changes in synaptic strength called long-term potentiation (LTP) and long-term depression (LTD). During development, LTP plays a role in retaining nascent synapses, whereas LTD is important for synapse pruning. In postnatal life, these same mechanisms, working in concert, contribute to learning and memory storage. Although different mechanisms resulting in long-term plasticity have been described, mGluR-LTD is of particular relevance to fragile X syndrome (Bear *et al.*, 2004).

In mGluR-LTD, activation of postsynaptic group 1 mGluRs results in internalization of AMPA receptors (Snyder *et al.*, 2001) as well as lateral movement of synaptic NMDA receptors (Ireland & Abraham, 2009), which reduces synaptic efficacy. This process requires rapid translation of preexisting mRNA in the postsynaptic dendrites. If protein synthesis does not occur, these changes are reverted within 30 minutes (Huber *et al.*, 2000; Snyder *et al.*, 2001). Importantly, mGluR-LTD was found to be enhanced in the absence of FMRP (Huber *et al.*, 2002), suggesting that upon mGLuR activation, FMRP repression on translation is released and proteins involved in stabilization of LTD are synthetized. By contrast, in the absence of FMRP, proteins involved in stabilizing LTD are expressed in abnormal higher levels, resulting in exaggerated LTD, even in the absence of mGluR activation (Bear *et al.*, 2004; see Figure IV).

It has been reported that activation of group 1 mGluRs leads to a net loss of AMPA and NMDA receptors (Snyder *et al.*, 2001) as well as to elongation of dendritic spines (Vanderklish & Edelman, 2002), which probably represents a mechanism to eliminate synapses during development (Bear *et al.*, 2004). In the absence of FMRP, however, synaptic maturation might be delayed as a result of exaggerated group 1 mGluR signaling (Bear *et al.*, 2004). Additionally, FMRP might regulate translation of proteins involved in stabilization of mature synapses during development. In this scenario, absence of FMRP would result in constitutive expression of this machinery, leading to stabilization of synapses that would otherwise be removed, giving rise to an increased number of immature synapses (Bagni & Greenough, 2005).

Besides exaggerated LTD, overactive or inappropriate group 1 mGluR signaling might lead to epilepsy (Merlin *et al.*, 1998; Stoop *et al.*, 2003; Chuang *et al.*, 2005), hyperarousal to sensory stimuli (Chen & Toth, 2001; Walker *et al.*, 2001; Nielsen *et al.*, 2002), anxiety (Paradee *et al.*, 1999; Rodrigues *et al.*, 2002), developmental delay and cognitive impairment (Huber *et al.*, 2000; Raymond *et al.*, 2000; Snyder *et al.*, 2001; Zho *et al.*, 2002), increased density of elongated dendritic spines (Vanderklish & Edelman, 2002) and loss of motor coordination (Karachot *et al.*, 2001), all of which are phenotypes present in fragile X syndrome. It was therefore reasonable to hypothesize that the psychiatric and neurological aspects of fragile X syndrome are a consequence of exaggerated responses to group 1 mGluR activation (Bear *et al.*, 2004).

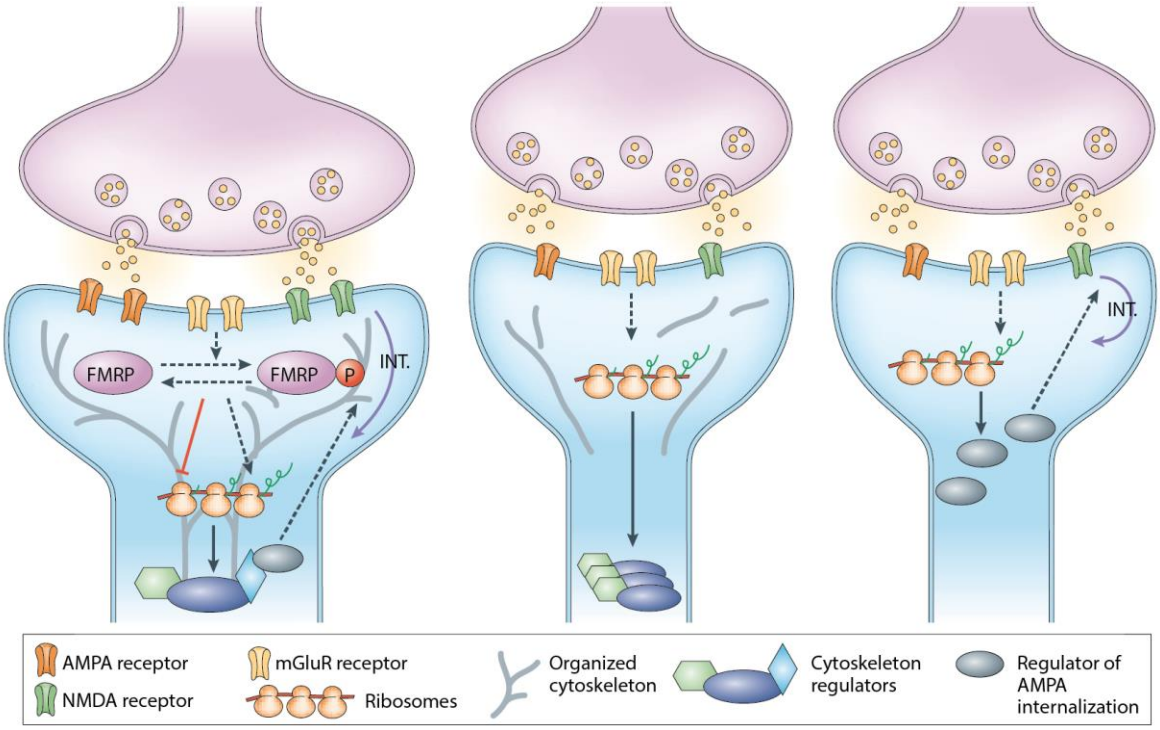

Figure IV. (Left) In a wild type spine, stimulation of mGluRs enhances the synthesis of FMRP, which could act to negatively regulate the translation of proteins that are involved in ionotropic receptor internalization during LTD and of proteins that regulate the cytoskeleton. This signaling pathway might also be responsible for FMRP phosphorylation and the consequent release of mRNAs from translational inhibition and/or the activation of translation of other specific dendritic mRNAs. The correct balance between synthesis and degradation of these proteins would promote and maintain the mature shape of the synapse. **(Middle)** In a spine of a patient with fragile X syndrome, the absence of FMRP would lead to an increase and/or decrease in the translation of protein regulators of the cytoskeleton, both of which might have an effect on the lengthening of dendritic spines. **(Right)** The absence of FMRP could also lead to an increase in the translation of proteins that are involved in AMPA receptor internalization as well as and NMDA receptor lateral movement during LTD, which could lead to fewer receptors being present on the postsynaptic membrane and to thinner spines. (Adapted from Bagni & Greenough, 2005).

GABAergic deficits.

GABA is the main inhibitory neurotransmitter in the brain. It exerts its effect through binding to ionotropic $GABA_A$ receptors and to metabotropic $GABA_B$ receptors, which results in hyperpolarization of the membrane potential of the neuron, reducing the probability of generation of an action potential. Upon activation, $GABA_A$ receptors open their pore, which are mostly permeable to Cl^-, allowing influx of negative current into the neuron (reviewed by Farrant & Nusser, 2005; Jacob *et al.*, 2008). $GABA_B$ receptors, by contrast, are coupled to G-proteins, which in turn activate postsynaptic K^+ channels or inhibit presynaptic Ca^{2+} channels, allowing efflux of positive current from the neuron or blocking influx of positive current into the neuron, respectively (reviewed by Bettler *et al.*, 2004; Gassmann & Bettler, 2012).

The $GABA_A$ receptor is a heteropentamer assembled from a range of homologous subunits (α_{1-6}, β_{1-3}, γ_{1-3}, δ, ε_{1-3}, θ y π), although most of them are composed of two α, two β and one γ (or δ) subunits (reviewed by Jacob *et al.*, 2008). The $GABA_B$ receptor, on the other hand, is a heterodimer composed of one B1 and one B2 subunits (reviewed by Benarroch, 2012). Importantly, absence of FMRP leads to a reduction in expression of some of the $GABA_A$ receptor subunits (D'Hulst *et al.*, 2006; Curia *et al.*, 2009; Adusei *et al.*, 2010; Hong *et al.*, 2012; Gatto *et al.*, 2014) as well as the $GABA_B$ receptor B1 subunit (Pacey *et al.*, 2011). Moreover, expression of other proteins that are important for GABAergic transmission is also reduced in the absence of FMRP (D'Hulst *et al.*, 2009; Adusei *et al.*, 2010). These include the GABA synthesizing enzyme (GAD), the GABA membrane transporter (GAT), an enzyme important in degradation of GABA (SSADH) and a protein involved in the clustering and targeting of $GABA_A$ receptors to the postsynaptic membrane (gephyrin).

Downregulation of RGS4, a protein that negatively regulates $GABA_B$ receptor signaling, was reported to rescue some of the phenotypes observed in fragile X syndrome, such as altered synaptic protein expression, abnormal social behaviors, susceptibility to audiogenic seizures and increased body weight (Pacey *et al.*, 2009; Pacey *et al.*, 2011). Conversely, combined pharmacological upregulation of group 1 mGluR signaling and downregulation of $GABA_B$ receptor signaling was found to mimic the effect of the absence of

FMRP on audiogenic seizures (Pacey *et al.*, 2009). Hence, enhancement of $GABA_B$ receptor signaling represents a potential therapeutic strategy for the treatment of fragile X syndrome.

During development, GABA has a depolarizing action and activates $GABA_A$ receptors to increase Ca^{2+} influx through NMDA receptors which promotes maturation of glutamatergic synapses (Akerman & Cline, 2006; Wang & Kriegstein, 2008). In fact, in the absence of this early GABA depolarizing action, neuronal circuits exhibit imbalances in excitatory and inhibitory transmission and disrupted dendrite maturation (Akerman & Cline, 2006; Wang & Kriegstein, 2008), which is consistent with the physiological and anatomical alterations observed in cortical neurons of mouse models of fragile X syndrome (Nimchinsky *et al.*, 2001; Gibson *et al.*, 2008). Moreover, GABA also participates in maturation of inhibitory synapses during development (Chattopadhyaya *et al.*, 2007). Interestingly, mouse models of fragile X syndrome exhibit reduced expression of GAD, the enzyme that synthesizes GABA (D'Hulst *et al.*, 2009; Adusei *et al.*, 2010), as well as reduced number of inhibitory synapses (Centonze *et al.*, 2008; Olmos-Serrano *et al.*, 2010). Therefore, it is likely that both pathways, increased group 1 mGluR signaling and reduced GABAergic transmission, affect the development of neuronal circuits in fragile X syndrome.

Hyperexcitability

One remarkable feature of fragile X syndrome is the occurrence of behaviors that reflect neuronal hyperexcitability, such as hypersensitivity, hyperarousal, hyperactivity, anxiety or epilepsy (Hagerman *et al.*, 2009; Tranfaglia, 2011). In consonance with this, it has been reported that cortical excitatory neurons harbor an intrinsic increased excitability (Gibson *et al.*, 2008; Hays *et al.*, 2011; Goncalves *et al.*, 2013). Moreover, excitatory drive onto inhibitory interneurons was found to be reduced in cortical circuits (Gibson *et al.*, 2008). Together, this evidence suggests that neuronal circuits are hyperexcitabile, which could explain the exaggerated responses to sensory stimuli observed in animal models of fragile X syndrome (Goncalves *et al.*, 2013; Zhang *et al.*, 2014).

The finding that principal neurons are intrinsically hyperexcitable indicates that, in addition to GABA and glutamate receptors, other channels might be affected by the absence

of FMRP. In fact, the conductances mediated by the voltage-gated potassium channels HCN and BK_{Ca} have been found to be reduced in the absence of FMRP (Brager & Johnston, 2007; Deng *et al.*, 2013; Zhang *et al.*, 2014). These channels are important for regulating neuronal excitability. HCN channels, for instance, are involved in generation of neuronal resonance, determination of the resting membrane potential and dendritic integration (Kole *et al.*, 2006; Wahl-Schott & Biel, 2009). BK_{Ca} channels participate in establishing the threshold for distal action potential initiation, regulation of action potential repolarization and determination of action potential duration (Faber & Sah, 2003; Benhassine & Berger, 2009). In physiological conditions, the net effect of these channels is the reduction of neuronal excitability. However, in the absence of FMRP, their conductances are decreased, giving rise to hyperexcitable neurons (Zhang *et al.*, 2014).

Absence of FMRP results in downregulation of other potassium channels such as Kv4.2 and Kv3.1 (Strumbos *et al.*, 2010; Gross *et al.*, 2011; Lee *et al.*, 2011). Kv4.2 channels decrease back-propagating action potentials in dendrites and are, thus, important for dampening neuronal firing (Birnbaum *et al.*, 2004; Chen *et al.*, 2006). Interestingly, a truncation mutation of Kv4.2 leads to epilepsy in humans (Singh *et al.*, 2006), and mice lacking Kv4.2 exhibit increase sensitivity to convulsant stimuli (Barnwell *et al.*, 2009). Kv4.2 channels are, hence, important for regulating neuronal excitability. Kv3.1 channels produce fast delayed rectifier currents that permit neurons to fire prolonged trains of action potentials at very high frequencies with little adaptation (Gan & Kaczmarek, 1998; Rudy & McBain, 2001). Kv3.1 channels are particularly enriched in cortical GABAergic fast-spiking interneurons (Weiser *et al.*, 1995). Downregulation of Kv3.1 channels in cortical inhibitory interneurons is likely to contribute to neuronal circuits with increased excitability.

Activation of the group 1 mGluR signaling pathway leads to neuronal epileptiform burst firing (Merlin *et al.*, 1998; Stoop *et al.*, 2003), which is, at least in part, caused by reduction of potassium conductances (Sourdet *et al.*, 2003). Therefore, the abnormal and constitutive enhanced group 1 mGluR signaling observed in fragile X syndrome (Bear *et al.*, 2004), additionally participates in increasing neuronal excitability. Furthermore, downregulation of $GABA_A$ receptor subunits (Curia *et al.*, 2009) as well as reduced $GABA_B$

signaling (Pacey *et al.*, 2011) possibly result in decreased neuronal inhibitory dynamics in fragile X syndrome. Taken together, this evidence supports a model in which an imbalance of neuronal excitation and inhibition leads to circuit hyperexcitability (Gibson *et al.*, 2008), giving rise to neurons with a lower dynamic range to process sensory stimuli, which could be responsible for the alterations in neuronal computations related to fragile X syndrome. In fact, autism, a disorder whose behavioral phenotypes highly overlap with those of fragile X syndrome, as well as epilepsy, present in a subpopulation of patients with fragile X syndrome, have been associated with excitation/inhibition imbalance in key neuronal circuits (Rubenstein & Merzenich, 2003; Belmonte & Bourgeron, 2006).

Hyperconnectivity

Initial neuroanatomical studies of patients with intellectual disability revealed alterations in dendritic spine structure (Marin-Padilla, 1972; Purpura, 1974). In fact, dendritic abnormalities are the most consistent anatomical correlates of intellectual disability (Kaufmann & Moser, 2000). In the case of fragile X syndrome, the first evidence of altered synaptic structure came from postmortem studies, which revealed an increased number of dendritic spines in cortical tissue (Rudelli *et al.*, 1985; Hinton *et al.*, 1991; Wisniewski *et al.*, 1991; Irwin *et al.*, 2001). Moreover, a large proportion of spines appeared abnormally long, thin and tortuous, a phenotype reminiscent of the immature spine precursors, filopodia, and indicative of alterations in synapse development (Fiala *et al.*, 1998). Nevertheless, the mechanism by which these changes occur is not fully understood.

For instance, it is known that at early stages in development an overproduction of synapses takes place. However, at later stages, some synapses are eliminated, a physiological process called pruning (reviewed by Bagni & Greenough, 2005; Pfeiffer & Huber, 2009). Importantly, further research has provided evidence that FMRP promotes synapse pruning (Pfeiffer & Huber, 2007; Patel *et al.*, 2014), suggesting that absence of FMRP leads to defective spine removal (see Figure V).

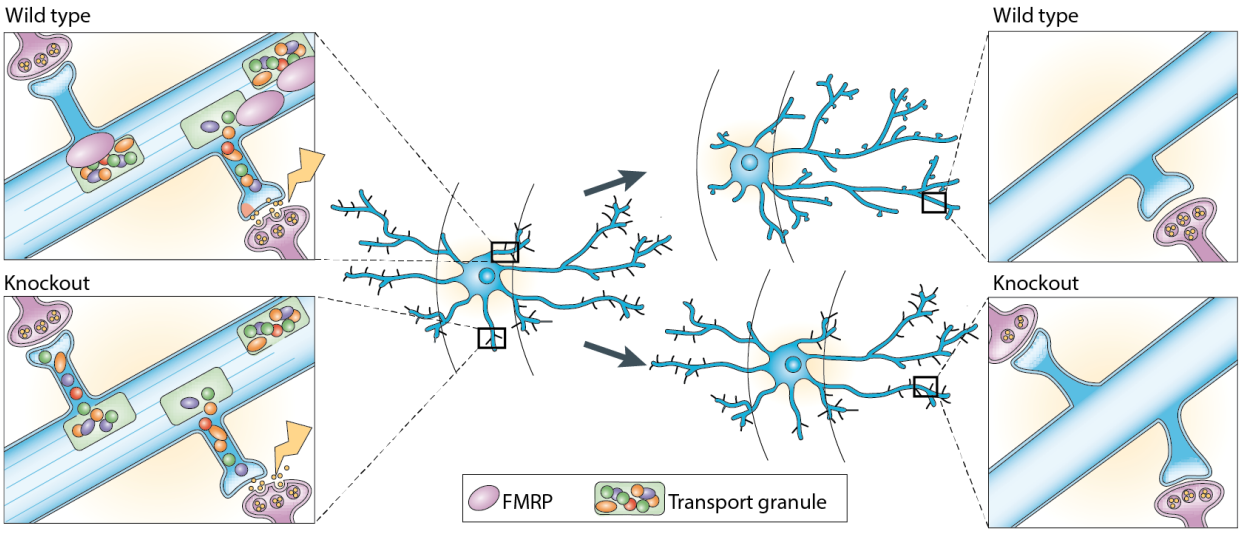

Figure V. Under this hypothetical paradigm, absence of FMRP leads to failure of synapse pruning and, as a consequence, dendrite pruning. This model assumes that FRMP regulates the synthesis of structural proteins, such as PSD-95, or signaling proteins that form part of a complex that is important for stabilizing and maturing developing synapses. When FMRP is present, this stabilization complex (carried by the transport granule) is selectively targeted to active synapses **(upper left)**, which results in selective maturation and stabilization of spines **(upper right)** and pruning of non-stabilized synapses. In the absence of FMRP **(lower left)**, the stabilization complex is equally targeted to active and inactive synapses, which results in a weaker form of maturation and stabilization, giving rise to greater numbers of synapses as well as an immature morphology **(lower right)**. (Adapted from Bagni & Greenough, 2005).

Animal models of fragile X syndrome

The discovery of the *FMR1* gene has greatly facilitated the study of the pathogenesis of fragile X syndrome. Its protein product, FMRP, possesses a high extent of functional homology to the mouse FMRP (Ashley *et al.*, 1993) and to the *Drosophila melanogaster* dFMRP (Wan *et al.*, 2000; Ishizuka *et al.*, 2002). Hence, knockout animal models have been generated for both, the mouse (Bakker *et al.*, 1994) and the fruit fly (Zhang *et al.*, 2001). These models present several behavioral, anatomical and cognitive phenotypes that are comparable to those of human fragile X syndrome, therefore representing valuable tools to study this disease and to identify potential routes for therapeutic intervention (reviewed by Bhogal & Jongens, 2010). In addition, a zebrafish model has been generated, which also displays similarities to the human disease (Tucker *et al.*, 2006; den Broeder *et al.*, 2009). The fact that *FMR1* is so well conserved across phylogeny reflects the importance this gene has for animal biology.

Due to the consistency between human phenotypes and those displayed by animal models, animal research has provided mechanistic explanations of how the absence of FMRP gives rise to the cognitive problems associated with fragile X syndrome. These models have also been useful for exploring pharmacological approaches that eventually have led to clinical trials on human patients (Bhogal & Jongens, 2010). As a consequence, alterations in mGluR signaling (Bear *et al.*, 2004) as well as GABA transmission deficiencies (Braat & Kooy, 2015b) have been proposed to account for the cognitive impairment observed in fragile X syndrome patients. Nevertheless, further investigation is needed in order to understand how the affected cellular pathways impact neuronal circuit computations.

The *Drosophila melanogaster* model of fragile X syndrome

Several strong hypomorphic and null alleles of the *dfmr1* gene have been generated and characterized in *Drosophila melanogaster* (Wan *et al.*, 2000; Zhang *et al.*, 2001; Dockendorff *et al.*, 2002; Inoue *et al.*, 2002; Ishizuka *et al.*, 2002; Morales *et al.*, 2002; Lee *et al.*, 2003; Michel *et al.*, 2004; Pan *et al.*, 2004; Zhang *et al.*, 2004; McBride *et al.*, 2005; Reeve *et al.*, 2005; Pan & Broadie, 2007; Bolduc *et al.*, 2008; Gatto & Broadie, 2008; Pan *et al.*, 2008; Reeve *et al.*, 2008; Gatto *et al.*, 2014). These flies present abnormalities in axonal and dendritic branching as well as in synaptic architecture and transmission. Physically, male flies are reported to have enlarged testes. Behaviorally, it has been found that mutant *dfmr1* flies lack the ability to maintain a normal circadian rhythm and to exhibit erratic patterns of locomotor activity. Alterations in courtship activity as well as in short-term and long-term memory have also been described. Thus, the fly model of fragile X syndrome displays significant social and cognitive deficits that can be used to examine the underlying mechanisms that cause fragile X syndrome symptoms (reviewed by Pfeiffer & Huber, 2009; Bhogal & Jongens, 2010). Furthermore, some neuronal alterations can be comparable to those of human subjects, and therefore useful in elucidating the associated emerging neuronal circuit deficits.

Although different *Drosophila melanogaster* neuronal strains have been characterized in the context of fragile X syndrome, no apparent common phenotype has been found to arise from the absence of dFMRP. Thus, it is possible that particular neurons are affected differently when dFMRP is not expressed. For instance, neuromuscular junction

terminals display pronounced synaptic overgrowth and overelaboration (Zhang *et al.*, 2001), whereas dorsal cluster neurons, which form part of the fly visual system, exhibit strong loss of neurite extension and irregular branching (Morales *et al.*, 2002). Ventrolateral neurons, another component of the fly visual system, present aberrant collateral branching and defasiculation (Reeve *et al.*, 2005; Reeve *et al.*, 2008). Therefore, in order to understand how neuronal circuit function is affected by the absence of dFMRP, it is firstly necessary to define a circuit, preferentially one that has been widely studied and whose functions are considerably well-understood. In this regard, it is worth mentioning that the antennal lobe, which forms part of the *Drosophila melanogaster* olfactory system, is one of the most studied and understood neuronal circuits (Wilson, 2013). Moreover, since the antennal lobe presents a high level of anatomical stereotypy (Vosshall *et al.*, 2000; Fishilevich & Vosshall, 2005) and its functional connectivity as well as the computations it carries out are considerably well-understood (Masse *et al.*, 2009; Wilson, 2013), the antennal lobe represents an excellent substrate to study neuronal circuit function in fine detail in the context of fragile X syndrome.

The *Drosophila melanogaster* olfactory system

The olfactory sensory organs of *Drosophila melanogaster* are the antennae and the maxillary palps (see Figure VI). These organs contain a large number of small hairs known as sensilla, which house and protect the olfactory receptor neurons. Other antenna sensilla contain neurons involved in processing thermosensation, mechanosensation and hygrosensation (Stocker, 1994). Nevertheless, only olfactory sensilla contain pores along their shaft, which are thought to allow access to odors. A total of about 410 olfactory sensilla cover the antenna, while the maxillary palp has about 60 olfactory sensilla. Sensilla are divided in three distinct morphological and functional classes: club-shaped basiconic sensilla, sharp-tipped trichoid sensilla and short, peg-shaped coeloconic sensilla (Laissue & Vosshall, 2008; see Figure VI).

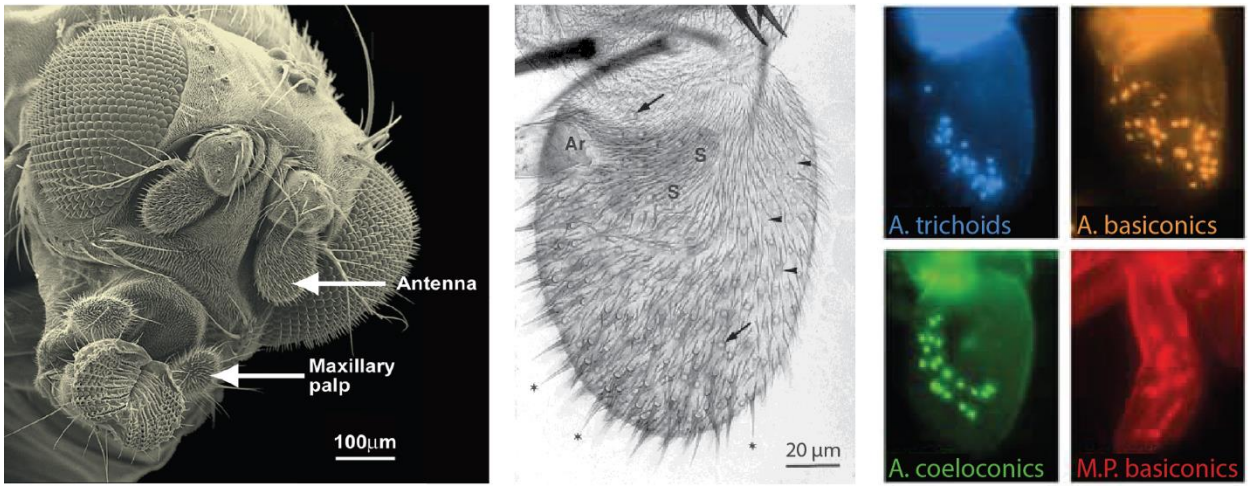

Figure VI. (Left) Scanning electron micrograph of a *Drosophila melanogaster* head indicating the two major olfactory sensory organs, the antenna and the maxillary palp. These organs are covered with a large number of sensory hairs, called sensilla. (Adapted from Laissue & Vosshall, 2008). **(Middle)** Micrograph of the funiculus, also known as third antennal segment, depicting the three principal types of sensilla: the sharp-tipped trichoid (asterisks), the translucent, club-shaped basiconic (arrowheads) and the short, peg-shaped coeloconic with prominent sockets (arrows). The basis of the arista (Ar) and the sacculus (S) are also indicated. (Adapted from Stocker, 2001). **(Right)** Images of the olfactory organs showing the distribution of four representative sensillum types from the different classes of sensilla, respectively. Blue, antennal trichoids (Or88a-GAL4); yellow, antennal basiconics (Or47a-GAL4); green, antennal coeloconics (Ir92a-GAL4); and red, maxillary palp basiconics (Or42a-GAL4). (Adapted from Grabe *et al.*, 2015).

Each antenna and each maxillary palp contain approximately 1 200 and 120 olfactory receptor neurons, respectively (Stocker, 1994), while each sensillum houses the dendrites

of 1 to 4 olfactory receptor neurons (de Bruyne *et al.*, 1999; Shanbhag *et al.*, 1999; de Bruyne *et al.*, 2001). Olfactory receptor neurons generally express only 1 odorant receptor, with a unique molecular receptive range, from a repertoire of 62 different odorant receptors (Gao *et al.*, 2000; Vosshall *et al.*, 2000; Robertson *et al.*, 2003; Couto *et al.*, 2005; Hallem & Carlson, 2006). However, in some cases, 2 or even 3 odorant receptors are expressed by the same olfactory receptor neuron (Couto *et al.*, 2005; Fishilevich *et al.*, 2005; Fishilevich & Vosshall, 2005; Vosshall & Stocker, 2007). Moreover, the co-receptor encoded by the *Or83b* gene is co-expressed in most olfactory receptor neurons and is essential for olfaction (Larsson *et al.*, 2004; Benton *et al.*, 2006).

Odorant receptors, which are proteins comprising seven membrane-spanning domains, but with inverted topology relative to that of G-protein-coupled receptors (Benton *et al.*, 2006), are expressed by the majority of olfactory receptor neurons. Nevertheless, approximately 25 % of olfactory receptor neurons do not express odorant receptors (Couto *et al.*, 2005; Fishilevich & Vosshall, 2005). Instead, these neurons express a second family of olfactory receptors called ionotropic receptors, which bear structural homology to ionotropic glutamate receptors (Benton *et al.*, 2009; Abuin *et al.*, 2011), and display a particular odorant receptive range (Silbering *et al.*, 2011). Interestingly, whereas odorant receptors are, in general, more broadly tuned to esters, aldehydes and alcohols (Hallem & Carlson, 2006), ionotropic receptors are more broadly tuned to amines and acids (Silbering *et al.*, 2011).

Olfactory receptor neurons project their axons to the antennal lobe, where they innervate specific clusters of neuropil called glomeruli (Stocker *et al.*, 1983; Naresh Singh & Nayak, 1985; Stocker *et al.*, 1990). Olfactory receptor neurons expressing the same collection of odorant or ionotropic receptors innervate a particular glomerulus (Figure VII) This innervation pattern is bilaterally symmetric and invariant across different animals (Stocker *et al.*, 1990; Gao *et al.*, 2000; Vosshall *et al.*, 2000; Silbering *et al.*, 2011). Conventionally, it is agreed that there are approximately 54 olfactory receptor neuron types, which map to their cognate 54 glomeruli in the antennal lobe (Laissue *et al.*, 1999; Couto *et al.*, 2005; Laissue & Vosshall, 2008; Grabe *et al.*, 2015).

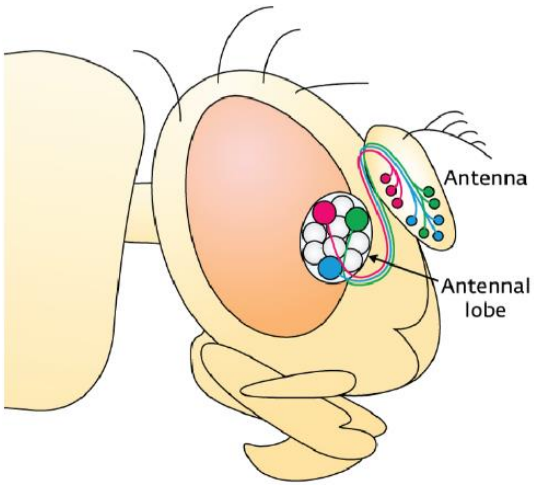

Figure VII. Axons of olfactory receptor neurons expressing the same collection of olfactory receptors (colored equally) converge onto the same glomerulus in the antennal lobe. (Adapted from Adrian Moore, RIKEN Brain Science Institute).

Neuronal populations in the antennal lobe

Olfactory receptor neurons establish cholinergic excitatory synapses in the antennal lobe with excitatory second-order neurons called projection neurons and with inhibitory neurons called local interneurons (Stocker, 1994; Ng *et al.*, 2002; Wilson *et al.*, 2004; Kazama & Wilson, 2008; see Figure VIII). Typically, the dendrites of a single projection neuron innervate only 1 glomerulus (Stocker, 1994; Jefferis *et al.*, 2001; Marin *et al.*, 2002; see Figure VIII), whereas the dendrites of a single local interneuron innervate many or all glomeruli (Stocker, 1994; Chou *et al.*, 2010; Seki *et al.*, 2010; see Figure VIII). There are approximately 150 projection neurons as well as 200 local interneurons per antennal lobe (Ng *et al.*, 2002; Seki *et al.*, 2010). Projection neurons extend their axons to higher brain centers in the *Drosophila* protocerebrum, namely the mushroom body and the lateral horn (Jefferis *et al.*, 2001; Marin *et al.*, 2002; Wong *et al.*, 2002). Local interneurons, by contrast, lack axons and release GABA from their dendrites instead (Ng *et al.*, 2002; Wilson & Laurent, 2005; Das *et al.*, 2008; Seki *et al.*, 2010).

Almost all projection neurons are cholinergic (Yasuyama & Salvaterra, 1999). They release acetylcholine from their axonal arbors in higher brain regions and from their dendrites in the antennal lobe (Ng *et al.*, 2002; Wilson *et al.*, 2004; Kazama & Wilson, 2008; Yaksi & Wilson, 2010). Within the antennal lobe, projection neurons excite other sister

projection neurons innervating the same glomerulus, as well as target lateral interneurons (Wilson, 2013).

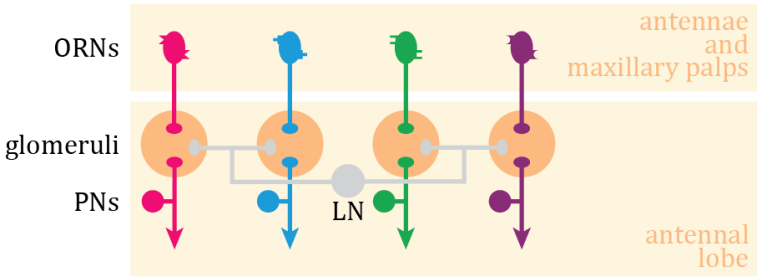

Figure VIII. Connectivity of the *Drosophila* antennal lobe. The cell body and dendrites of olfactory receptor neurons (ORNs) reside in the peripheral olfactory organs, namely antennae and maxillary palps. All of the ORNs that express a given odorant receptor converge onto the same glomerulus in the antennal lobe, schematized here as a single ORN per glomerulus. The dendrites of individual projection neurons (PNs) arborize in specific glomeruli, where they receive monosynaptic input from their cognate ORNs. Although each glomerulus contains dendrites of several sister PNs, only one PN for each glomerulus is shown here. Glomeruli are laterally interconnected by a network of local interneurons (LNs), which interact with PNs, ORNs, and other LNs. Many individual LNs innervate most or all glomeruli, but some are more selective. (Adapted from Wilson, 2013).

Local interneurons mediate lateral inhibition of projection neurons in the antennal lobe. This inhibition is predominantly presynaptic, occurring at axon terminals of olfactory receptor neurons. In fact, when olfactory receptor neurons are silent, most lateral inhibition disappears (Olsen & Wilson, 2008). Moreover, olfactory receptor neuron terminals show immunoreactivity for GABA receptors (Root *et al.*, 2008), and iontophoretic GABA inhibits synaptic transmission between olfactory receptor neurons and projection neurons at a presynaptic locus (Olsen & Wilson, 2008; Root *et al.*, 2008). Similarly, activating local interneurons with odor stimuli also inhibits synaptic currents in projection neurons at a presynaptic locus (Olsen & Wilson, 2008).

Although presynaptic inhibition is perhaps the most functionally important target of inhibition in the antennal lobe, projection neurons also receive synaptic inhibition. Iontophoretic GABA hyperpolarizes projection neurons through $GABA_A$ and $GABA_B$ receptors (Wilson & Laurent, 2005). Moreover, in paired recordings, injecting depolarizing current into local interneurons produces a train of spikes in local interneurons and a weak hyperpolarization of projection neurons (Yaksi & Wilson, 2010). Nevertheless, clear unitary synaptic currents are never observed in these paired recordings. Instead, a train of spikes in

local interneurons is always required to see any measurable inhibitory response in projection neurons, which grows slowly throughout the train. This suggests that these connections might represent volume transmission rather than true synapses (Wilson, 2013). Similarly, local interneurons are themselves targets of inhibition. Local interneurons are hyperpolarized by iontophoretic GABA (Wilson & Laurent, 2005), and paired recordings from connected local interneurons reveal inhibitory connections (Huang *et al.*, 2010; Yaksi & Wilson, 2010). However, as for projection neurons, these connections seem to be weak and slow (Wilson, 2013).

In addition to lateral inhibition, projection neurons receive lateral excitatory inputs (Olsen *et al.*, 2007; Shang *et al.*, 2007; Root *et al.*, 2008). These connections transmit both hyperpolarizing and depolarizing voltage steps (Huang *et al.*, 2010; Yaksi & Wilson, 2010). Moreover, these connections are abolished by a mutation in a gap junction subunit, and the same mutation abolishes odor-evoked lateral excitation (Yaksi & Wilson, 2010), implying that lateral excitation is attributable to electrical connections formed by excitatory local interneurons onto projection neurons (Wilson, 2013). Complementarily, it has been reported that some excitatory local interneurons are cholinergic (Shang *et al.*, 2007) and some are glutamatergic (Chou *et al.*, 2010; Das *et al.*, 2011). Nonetheless, since lateral excitation is essentially unaffected by pharmacological blockade of nicotinic acetylcholine receptors or voltage-dependent calcium channels, and it is blocked by a gap junction mutation (Yaksi & Wilson, 2010), the contribution of acetylcholine and glutamate to lateral excitation in the antennal lobe is small as compared to electrical excitation.

Olfactory computations in the antennal lobe

All of the olfactory receptor neurons that express the same olfactory receptor wire precisely to the same projection neurons (Gao *et al.*, 2000; Vosshall *et al.*, 2000). Computationally, this connectivity arrangement has the advantage of favoring summation of synchronous presynaptic inputs to effectively drive a projection neuron above its spike threshold (Wilson, 2013). This is especially important for the *Drosophila melanogaster* olfactory system, as the antennal lobe receives approximately 20 000 spikes/s from the total population of approximately 2 500 olfactory receptor neurons, even when no odor is present (Stocker,

1994; de Bruyne *et al.*, 1999; de Bruyne *et al.*, 2001). Hence, summation provides an efficient mechanism for projection neurons to integrate even small increases in the firing rates of olfactory receptor neurons. If, for instance, olfactory receptor neurons of the same type would randomly connect with projection neurons innervating different glomeruli, detection of increases in the firing rate of olfactory receptor neurons by projection neurons would be much more difficult, given the elevated background activity of the population of olfactory receptor neurons (Wilson, 2013).

Projection neurons respond most strongly at the onset of olfactory receptor neuron spiking (Wilson *et al.*, 2004; Bhandawat *et al.*, 2007). Two mechanisms are responsible for this: lateral inhibition (Wilson & Laurent, 2005; Olsen & Wilson, 2008) and synaptic depression (Kazama & Wilson, 2008). This response profile is functionally important because it predicts that projection neurons should respond better to fluctuating inputs than to sustained inputs (Wilson, 2013). Since natural odor plumes produce large fluctuations in odor concentration (Murlis *et al.*, 1992), onset-oriented projection neuron responses may be an adaptation to the natural distribution of odors in the environment as well as a selective pressure for speed in olfactory behaviors. In fact, olfactory behaviors in *Drosophila* can be observed within 100 ms of the onset of olfactory receptor neuron activity (Bhandawat *et al.*, 2010; Gaudry *et al.*, 2013). Moreover, as olfactory receptor neurons spike most strongly at the onset of transduction, and projection neurons spike most strongly at the onset of olfactory receptor neurons spiking, the *Drosophila* olfactory system promotes rapid olfactory perception by an iterative process of response speeding (Wilson, 2013).

Another important property of projection neurons is their high sensitivity to small increases in the firing rates of olfactory receptor neurons (Wilson, 2013). When sister olfactory receptor neurons fire at a low rate, they produce relatively large increases in the firing rates of their postsynaptic projection neurons. By contrast, when olfactory receptor neurons fire at high rates, they tend to saturate their postsynaptic projection neurons (Bhandawat *et al.*, 2007; Olsen *et al.*, 2010). Consequently, odor stimuli that elicit low firing rates in olfactory receptor neurons occupy the major part of the dynamic range of a projection neuron. Furthermore, since most odor-evoked firing rates of olfactory receptor

neurons are low, below 50 spikes/s, as compared to their maximum firing rate, approximately 300 spikes/s (Hallem & Carlson, 2006), most of the dynamic range of a projection neuron may be devoted to the most common odor stimuli. Thus, this property of projection neuron should maximize rates of information transmission (Wilson, 2013). In fact, in computational simulations, the compressive nonlinearity in the relationship between the firing rates of olfactory receptor neurons and projection neurons substantially improves odor discrimination (Luo *et al.*, 2010; Olsen *et al.*, 2010).

Lateral inhibition adjusts projection neuron sensitivity to the level of total activity of olfactory receptor neurons (see Figure IX). Local interneurons collectively pool input from all glomeruli and inhibit neurotransmitter release as the activity of olfactory receptor neurons increases. This mechanism renders projection neurons less sensitive to the firing rates of their cognate olfactory receptor neurons (Olsen & Wilson, 2008; Root *et al.*, 2008; Olsen *et al.*, 2010). As a consequence of inhibition, firing rates of projection neurons do not saturate as easily as they would otherwise, and their dynamic range becomes more closely matched to that of their inputs (Wilson, 2013). In simulations, this type of lateral inhibition substantially improves odor discrimination by a linear decoder. In particular, it improves the ability of a decoder to identify an odor over a broader range of concentrations (Luo *et al.*, 2010; Olsen *et al.*, 2010), implying that lateral inhibition may help flies to identify odors in spite of natural variations in odor concentration (Wilson, 2013).

Lateral inhibition is also important for decorrelating the activity of different projection neurons (see Figure IX). Indeed, different types of olfactory receptor neurons provide a highly correlated input to projection neurons, which could easily lead to network saturation at high firing rates in the absence of the gain control provided by local interneurons (Haddad *et al.*, 2010; Luo *et al.*, 2010; Olsen *et al.*, 2010). The computation implemented by this type of lateral inhibition has been called divisive normalization, and it appears to be present in a wide variety of sensory systems (Carandini & Heeger, 2012).

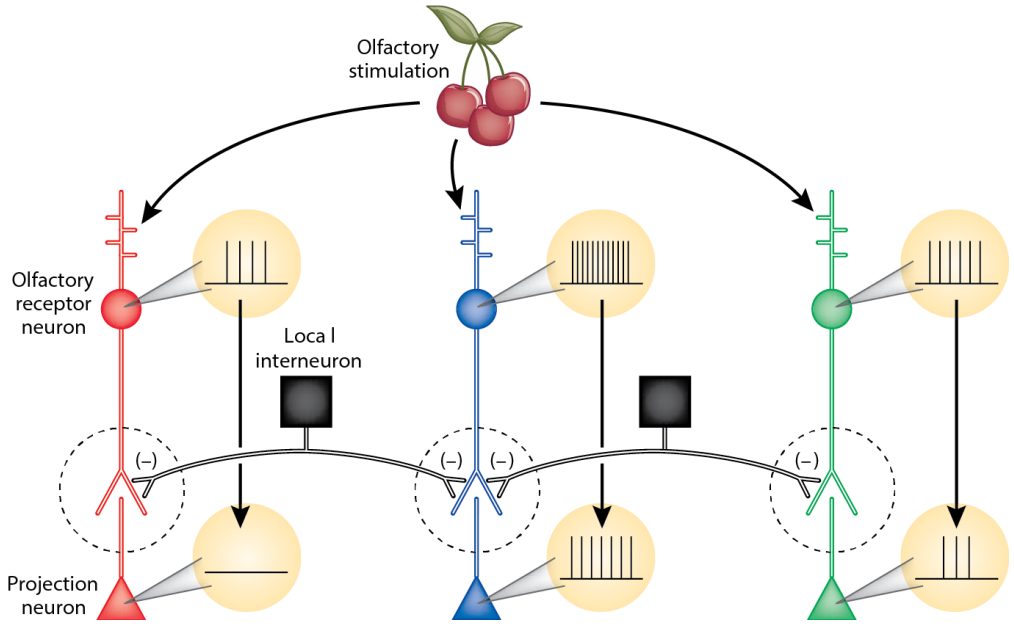

Figure IX. Lateral inhibition mediates gain control in the *Drosophila melanogaster* antennal lobe. Olfactory stimuli activate multiple classes of olfactory receptor neurons (ORNs) that each express a single receptor protein subtype. Since receptor proteins are broadly tuned, even simple olfactory stimuli activate many different classes of receptor cells (red, blue and green). This organization is continued at the next processing step, in which one receptor subtype (for example, red) activates antennal lobe projection neurons (PNs) with dendrites that innervate the red glomerular input station. Presynaptic lateral inhibition attenuates signal transfer from ORN to PN, resulting in less firing in downstream PNs (bottom row of simulated recordings) than in the ORNs (top row) that originate olfactory signals. The magnitude of presynaptic inhibition reflects the overall drive to the antennal lobe, allowing this local circuitry to regulate gain and to prevent input saturation when animals are exposed to strong stimuli. (Adapted from Strowbridge, 2008).

It has been recently reported that lateral inhibition increases with odor concentration, is almost completely untuned to odor identity, and that specific glomeruli exhibit different sensitivities to inhibition (Hong & Wilson, 2015). This organization may represent a way to effectively implement lateral inhibition while minimizing some of the associated problems, such as noise and ambiguity. In fact, projection neuron activity is noisy, and most of this noise is attributable to the high level of background activity of their cognate olfactory receptor neurons (Bhandawat *et al.*, 2007; Kazama & Wilson, 2009). Since noise in different olfactory receptor neurons is independent (Kazama & Wilson, 2009), pooling signals over many glomeruli may provide an avenue for local interneurons to reduce the noise that they re-inject into the circuit (Hong & Wilson, 2015). Moreover, glomeruli that are insensitive to inhibition would be immune to this noise and, therefore, better able to convey information to higher brain areas even when odor signals are weak and near the noise threshold for detection. Glomeruli that are insensitive to inhibition are also potentially useful

encoders of absolute odor concentration. This is particularly relevant for the antennal lobe, as inhibition increases with stimulus intensity and could potentially create ambiguity about odor concentration (Hong & Wilson, 2015).

Olfactory computations in the absence of dFMRP: hypotheses

One of the most known effects of absence of FMRP is that neurons experience constitutively enhanced mGluR signaling, which is probably the cause of the observed neuronal hyperexcitability associated with fragile X syndrome (Bear *et al.*, 2004). In the antennal lobe of *Drosophila melanogaster*, excitatory transmission is cholinergic, although few interneurons are glutamatergic (Wilson, 2013). Hence, it is unlikely that elevated mGluR produced by absence of dFMRP would impact on olfactory computations in the antennal lobe. Nevertheless, neuronal hyperexcitability could potentially be produced by downregulation of potassium channels occurring in the absence of dFMRP (Contractor *et al.*, 2015).

In the antennal lobe of *Drosophila melanogaster*, lateral inhibition mediated by local interneurons is GABAergic (Wilson, 2013). Increasing evidence obtained during the last decade has pointed towards GABAergic deficits as an important component of the neurophysiology related to fragile X syndrome (reviewed by Belmonte & Bourgeron, 2006; Braat & Kooy, 2015b). As described above, lateral inhibition participates in important olfactory computations, such as shaping the response dynamic range of projection neurons, reducing populational background noise of projection neurons due to constant input from olfactory receptor neurons, gain control of olfactory receptor neuron input upon olfactory stimulation, and, along with the differential glomerular sensitivity to inhibition, providing a mechanism for odor concentration encoding (Wilson, 2013). Therefore, downregulation of proteins involved in GABAergic transmission resulting from the absence of dFMRP (D'Hulst *et al.*, 2006; D'Hulst *et al.*, 2009) is likely to produce reduced inhibition in the antennal lobe, which would lead to neuronal computation as well as behavioral alterations in fruit flies.

Odor discrimination, which relies on an appropriate level of network lateral inhibition so that specific projection neurons carrying information about odor identity can

reliably convey this information to higher brain centers (Wilson, 2013), would be most likely affected by downregulation of proteins involved in GABAergic transmission. In this sense, reduced inhibition could lead to less specific projection neuron responses, rendering representations of different odors more similar to each other, thus, reducing the computational power of the antennal lobe to identify particular odors. Furthermore, since activation of specific glomeruli can be sufficient to elicit attraction (Semmelhack & Wang, 2009) or aversion (Suh *et al.*, 2007) behaviors in *Drosophila melanogaster*, it is possible that reduced odor discriminability in the antennal lobe would have an impact on olfactory behaviors.

Another possible consequence of the absence of dFMRP in the fruit fly antennal lobe is that odor concentration encoding would be impaired. According to recent evidence, concentration encoding requires that specific projection neurons are less sensitive to inhibition, whereas the rest of projection neurons are more sensitive to inhibition (Hong & Wilson, 2015). If inhibition is decreased, the whole population of projection neurons would be equally insensitive to inhibition, reducing the capacity of the antennal lobe to encode concentration.

Nonetheless, there is no physiological evidence that inhibitory synapses are affected in the absence of FMRP. Studying how neuronal computations are affected in the antennal lobe of fruit flies not expressing dFMRP could provide mechanistic principles that might help to better understand the neurophysiological implications of fragile X syndrome in humans.

Hypothesis

In the absence of dFMRP, the antennal lobe neuronal circuit will have altered olfactory information processing and exhibit less specificity to odors due to reduced inhibition. These alterations in odor processing will result in aberrant olfactory behaviors.

Objectives

1. Generate *dfmr1*$^{-}$ flies that express GCaMP6, ChR2 or GFP under specific promoter control. These flies will be used in behavioral, electrophysiological and functional imaging experiments.

2. Test whether *dfmr1*$^{-}$ flies exhibit reduced performance in olfactory attraction or aversion assays.

3. Evaluate whether odor representations are altered in the antennal lobe of *dfmr1*$^{-}$ flies by recording calcium responses to a number of odors in flies expressing GCaMP6. Moreover, I will study whether lateral interactions are affected by analyzing the calcium responses to odor mixtures.

4. Investigate whether the morphology of specific projection neurons expressing GFP undergoes modifications in *dfmr1*$^{-}$ flies by examining their neurite branching.

5. Examine whether inhibitory GABAergic transmission is affected in *dfmr1*$^{-}$ flies by recording whole cell patch-clamp responses in projection neurons to light stimulation of lateral neurons expressing ChR2.

Methods

Flies

For behavioral assays, 3-5 days post eclosion flies were used. Their genotypes are w^{1118};; (WT), w^{1118};;$dfmr1^{B55}$ (*dfmr1*$^{-}$), w^{1118};*dfmr1*;$dfmr1^{B55}$ (*dfmr1*-rescue), ;GH146-GAL4/UAS-*dfmr1*-RNAi; (*dfmr1*-RNAi) and ;GH146-GAL4/+; (control-RNAi). This control RNAi fly results from the cross between the same GAL4 line used to produce the *dfmr1*-RNAi fly and a WT fly with the same genetic background as the UAS fly used to produce the *dfmr1*-RNAi. Calcium imaging experiments were conducted on 5-10 days post eclosion female flies. Their genotypes are ;GH146-GAL4/UAS-GCaMP6m;+/+ (WT) and ;GH146-GAL4/UAS-GCaMP6m;$dfmr1^{B55}$/$dfmr1^{\Delta 113}$ (*dfmr1*$^{-}$). Patch-clamp experiments were conducted in 2 days post eclosion female flies. Their genotypes are NP2426-GAL4;UAS-ChR2/+;+/+ (WT) and NP2426-GAL4;UAS-ChR2/+;$dfmr1^{B55}$/$dfmr1^{\Delta 113}$ (*dfmr1*$^{-}$). The NP2426-GAL4 insertion drives expression in a population of GABAergic local interneurons (Das *et al.*, 2008; Okada *et al.*, 2009). Anatomical study of specific glomeruli was assessed in 3-5 days post eclosion female flies. Their genotypes are ;NP5221-GAL4,UAS-mCD8-GFP; (WT), NP3062-GAL4,UAS-mCD8-GFP;; (WT), ;NP5221-GAL4,UAS- mCD8-GFP; $dfmr1^{B55}$/$dfmr1^{\Delta 113}$ (*dfmr1*$^{-}$) and NP3062-GAL4,UAS- mCD8-GFP;; $dfmr1^{B55}$/$dfmr1^{\Delta 113}$ (*dfmr1*$^{-}$).

Olfactory stimulation

All odors were diluted 1:100 v/v in paraffin oil, except p-cresol which was diluted 1:100 w/v in water. Odors were delivered through a custom-built mechanism (for details, see Figures 2 and 6A), which dilutes the headspace of the odor vial a further 10-fold in clean air. The flow rate of odor delivery was 2.2 L/min. For physiological experiments, odor stimuli were applied for 500 ms every 15 s for 3 trials per odor. The stimulation protocol was controlled by a Master-8 stimulator (A.M.P.I.).

Behavioral assays

For each experimental session, ~50 flies were starved for 18-20 h at 25 ^{0}C in scintillation vials containing a piece of humidified filter paper. Flies were then transferred to a custom

made four-quadrant arena and filmed from the top of the arena for trials with a duration of 10 min (2 min, clean air; 3 min, odor exposure; 5 min, clean air). An automated mechanism was used to inject odors to the arena (for details, see Figure 1). The flow rate of odor delivery was 0.5 L/min.

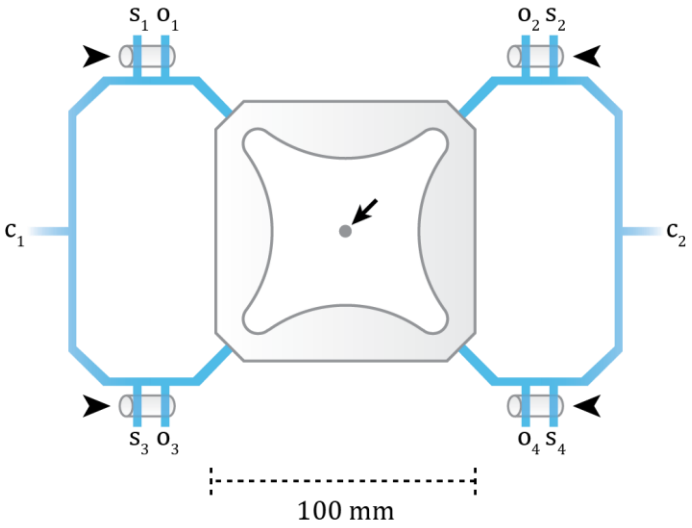

Figure 1. Experimental setup used for behavioral assays. Four quadrant arena used for evaluating innate olfactory behaviors in fruit flies (Semmelhack & Wang, 2009). Odors are injected independently to any of the four corners of the arena. A vacuum in the center (arrow) acts as a sink and constantly extracts air from the arena. This configuration favors separated air profiles in each of the four quadrants of the arena. Carrier air stream (C1+C2) is 0.35 L/min. Secondary air stream (S1+S2+S3+S4) or odor stream (O1+O2+O3+O4) is 0.15 L/min. Electronically controlled valves (arrowheads) precisely control switching between secondary air stream and odor stream for a programmed amount of time. Flies are imaged from the top using a standard webcam.

Calcium imaging

For each experiment, a fly was secured to an aluminum chamber with wax and the cuticle above the antennal lobes was removed (Figure 2). The antennal lobes were imaged *in vivo* from the dorsal side while constantly perfusing the brain with oxygenated saline. The saline contained (in mM): 103 NaCl, 3 KCl, 1 NaH_2PO_4, 1.5 $CaCl_2$, 4 $MgCl_2$, 26 $NaHCO_3$, 5 TES, 10 glucose and 8 trehalose. GCaMP6 fluorescence was imaged using an EMCCD camera (Hamamatsu Photonics) installed on an Olympus BX51 fluorescence microscope (Olympus Corporation).

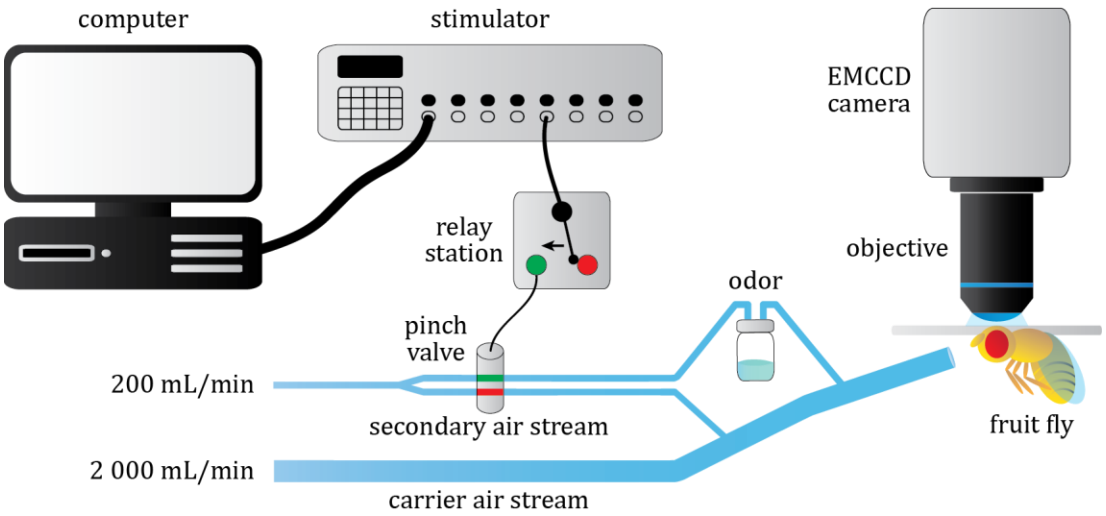

Figure 2. Experimental setup used for *in vivo* imaging of calcium responses to odors in the antennal lobe of *Drosophila melanogaster*. Experimental setup used to record calcium responses to odors in the antennal lobe of *Drosophila melanogaster*. After opening a small window on top of the antennal lobes, the fly is secured to an aluminum foil and placed in front of a clean air stream (2 200 L/min) that is constantly delivered to the antennae of the fly. To apply the odor stimuli, a pulse is sent from a computer to a stimulator (MASTER-8, A.M.P.I.), which in turn switches (black arrow) a relay station to the 'on' position (green). This activates a pinch valve (Bio-Chem Fluidics) that changes the direction of the secondary air flux, which pushes odor contained in a vial to the carrier air stream. An EMMCD camera simultaneously records GCaMP6m fluorescence from the antennal lobes and send them to the computer to be stored for offline analyses.

Immunohistochemistry

Brains were extracted from flies expressing either GCaMP6m or GFP and fixated in 4 % formaldehyde PBS solution. PBS contained (in mM): 137 NaCl, 2.7 KCl, 10 Na_2HPO_4 and 1.8 KH_2PO_4. Brains were incubated in primary antibody cocktails for ~24 h and then incubated in secondary antibody cocktails for ~2 h. Primary antibodies anti-GFP (A-11222, Life Technologies, dilution 1:500), anti-dFMRP (20E4, specifically generated for our lab by EMBL-MACF Hybridoma, dilution 1:50), anti-ELAV (7E8A10, Hybridoma Bank, dilution 1:100) and Alexa Fluor® secondary antibodies (Life Technologies) were dissolved in 5 % bovine serum albumin PBS solution. After each step, brains were washed 3 times in 0.1 % Triton PBS solution. Images of stained brains were visualized by confocal microscopy using a Nikon A1R+ confocal unit mounted on a Nikon Eclipse Ti-E inverted microscope (Nikon Corporation). Confocal stacks were preprocessed and exported using Fiji (ImageJ).

Electrophysiology

Flies were prepared similarly as for calcium imaging experiments. Although, for electrophysiology, the sheath covering the antennal lobes was carefully removed. *In vivo,* whole-cell patch-clamp recordings were performed from the somata of projection neurons and local interneurons. The external saline solution was identical to the one used for calcium imaging experiments. Patch-clamp electrodes were filled with an internal solution containing (in mM): 1 KCl, 140 potassium aspartate, 10 HEPES, 1 EGTA, 4 MgATP and 0.5 Na_3GTP. Recordings were performed in current-clamp mode with an Axopatch 200B amplifier (Molecular Devices). Recorded voltages were low-pass filtered at 1 kHz and digitalized at 10 kHz. Data acquisition was performed with a custom code written in MATLAB (MathWorks). Blue light for optogenetic stimulation of local interneurons was delivered via the fluorescence lamp HXP 120 C.

Data analysis

Fluorescence imaging stacks were processed by independent component analysis. This method allows automated detection of individual glomeruli (Mukamel *et al.*, 2009; Strauch & Galizia, 2012; for details, see Figure 3). Time series of detected glomeruli were then reconstructed from original fluorescence stacks. Behavior movies were binarized and numbers of flies per quadrant were calculated based on pixels occupied by flies (Figure 4). All quantifications and statistical tests of all the data obtained from the different experiments were performed using custom made codes written in MATLAB (MathWorks). Sparseness was calculated using the formula (Rolls & Tovee, 1995; Vinje & Gallant, 2000):

$$S = \frac{1 - \frac{\left(\frac{\sum r_i}{n}\right)^2}{\sum\left(\frac{r_i^2}{n}\right)}}{1 - \frac{1}{n}}$$

For lifetime sparseness, r_i is the response of a particular glomerulus to the i^{th} odor and n is the total number of odors. For population sparseness, r_i is the response of the i^{th} glomerulus to a particular odor and n is the total number of glomeruli per fly. Values near 0 indicate low selectivity whereas values near 1 indicate high selectivity of a particular glomerulus for a

given odor set (lifetime sparseness), or, of a population of glomeruli for a particular odor (population sparseness).

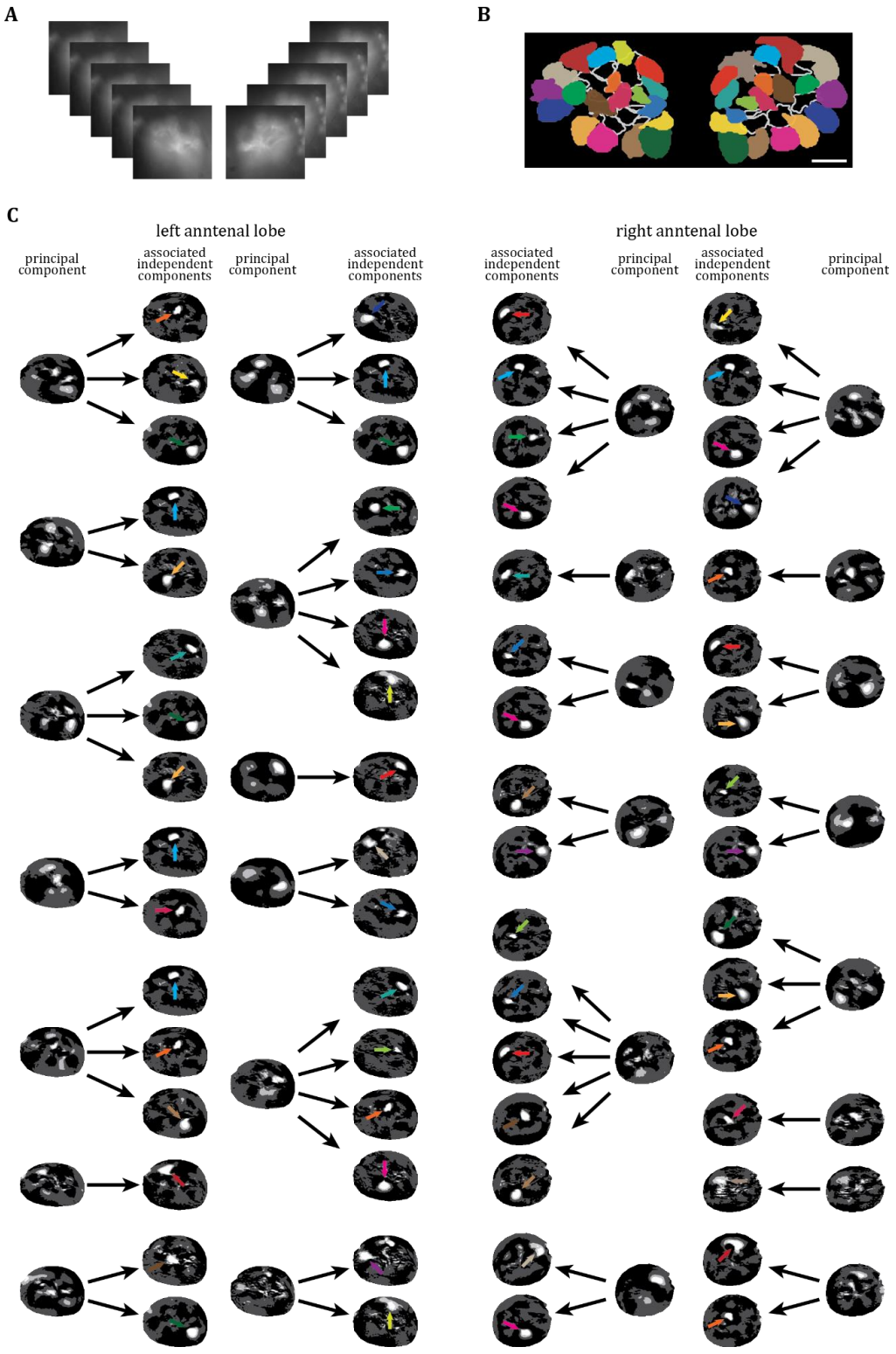

Figure 3. Automated extraction of glomerular activity by independent component analysis. A. To perform automated detection of glomeruli, raw florescence stacks are split into two so that each antennal lobe is processed by separate. This facilitates detection of sister glomeruli, which present very similar activity. **B.** Glomeruli map of detected glomeruli for one fly. Example glomeruli shown in C are highlighted in color. Other detected glomeruli are shown in gray contours. Scale bar = 10 µm. **C.** Individual glomeruli are detected by independent component analysis (Mukamel *et al.*, 2009; Strauch & Galizia, 2012). First, frame-based principal components are calculated from raw fluorescence stacks. Principal components contain different features of often more than one glomerulus. In the next step, independent components are calculated from principal components. Independent components bring together the different features of single glomerulus contained in several principal components. Independent components represent isolated single glomerulus. This information was then used to construct activity time series from raw fluorescence stacks.

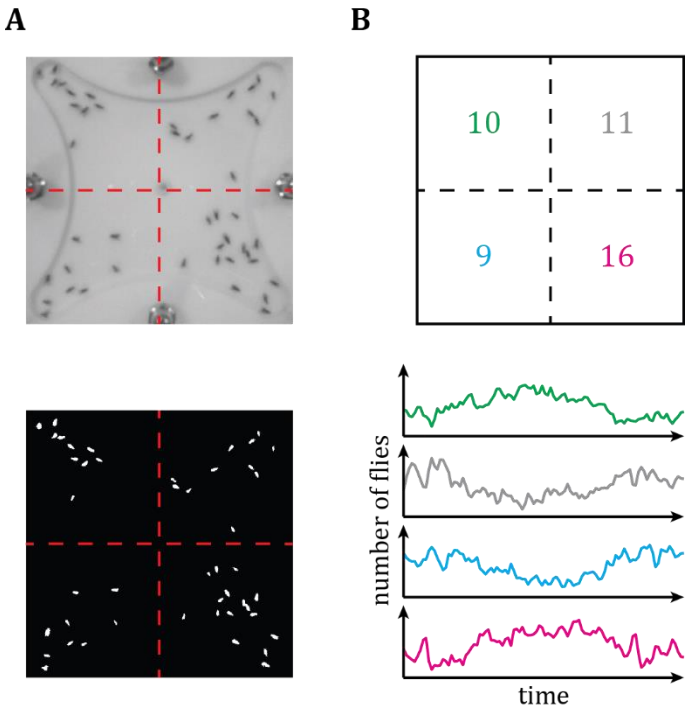

Figure 4. Estimation of number of flies per quadrant. A. Individual raw video frames (top) collected by the webcam are binarized (bottom) by MATLAB functions, so that pixels occupied by flies can be delineated. **B.** Binarized frames allow precise identification of number of flies in each quadrant in every video frame (top). Automated processing of binarized frames yields time series with the number of flies in each quadrant.

Results

dfmr1^{-} flies exhibit deficits in odor induced attraction and aversion

It was previously shown that *dfmr1*$^{-}$ flies present learning deficits in olfactory behavioral assays (Bolduc *et al.*, 2008). However, it was not clear whether this was a consequence of deficits in olfactory processing itself or in associative learning. In order to evaluate whether the olfactory system of *Drosophila melanogaster* is affected by the absence of FMRP, I conducted olfactory attraction and aversion assays (Figure 5; for details, see Figures 1 and 4). Some odors such as ethyl acetate are known to induce attraction in fruit flies, whereas others such as benzaldehyde induce aversion (Steck *et al.*, 2012; Farhan *et al.*, 2013). I presented these odors to freely walking starved fruit flies and quantified attraction and aversion by counting the number of flies in odorized and non-odorized sections of the behavioral arena, before, during and after odor delivery. I found that *dfmr1*$^{-}$ flies exhibit significantly weaker odor induced attraction and aversion as compared to WT flies (Figure 5B-C,H-I,L-M). In particular, I observed that *dfmr1*$^{-}$ flies spend less time exploring the quadrant odorized with the attractive odor ethyl acetate (Figure 5B,H,L). Similarly, *dfmr1*$^{-}$ flies were not repelled as much as WT flies were by the aversive odor benzaldehyde (Figure 5C,I,M). Furthermore, impaired olfactory performance in *dfmr1*$^{-}$ flies can be restored by the genomic rescue of dFMRP, demonstrating specificity (Figure 5D-E,H-I,L-M). To test whether reduced olfactory performance was due to the absence of dFMRP in the antennal lobe circuit, I knocked down dFMRP expression specifically in excitatory antennal lobe projection neurons. Downregulation of dFMRP in the antennal lobe projection neurons also led to a significant impairment of olfactory behaviors (Figure 5F-G,J-K,L-M), confirming the prominent role of dFMRP for antennal lobe circuit function and odor induced behaviors in fruit flies.

Figure 5. Absence of dFMRP results in deficits in olfactory attraction and aversion. A. Scheme of the olfactory behavior arena with 4 input ports. A vacuum in the center generates a 4-quadrant air profile (humidified air pressure = 500 ml/min). In olfactory attraction assays, the attractive odor ethyl acetate was delivered from a single port of the 4 quadrant arena (arrowhead) and clean air (white quadrants) was delivered through the remaining three ports. In olfactory aversion assays, the aversive odor benzaldehyde was delivered from three ports (arrowheads) of the 4 quadrant arena while clean air (white quadrant) was delivered through the remaining single port. For these experiments, the arena is populated with fifty 20h-starved flies. Flies were recorded during 10 min (odorless air = 2 min, odor = 3 min, odorless air = 5 min). *Continued on next page*.

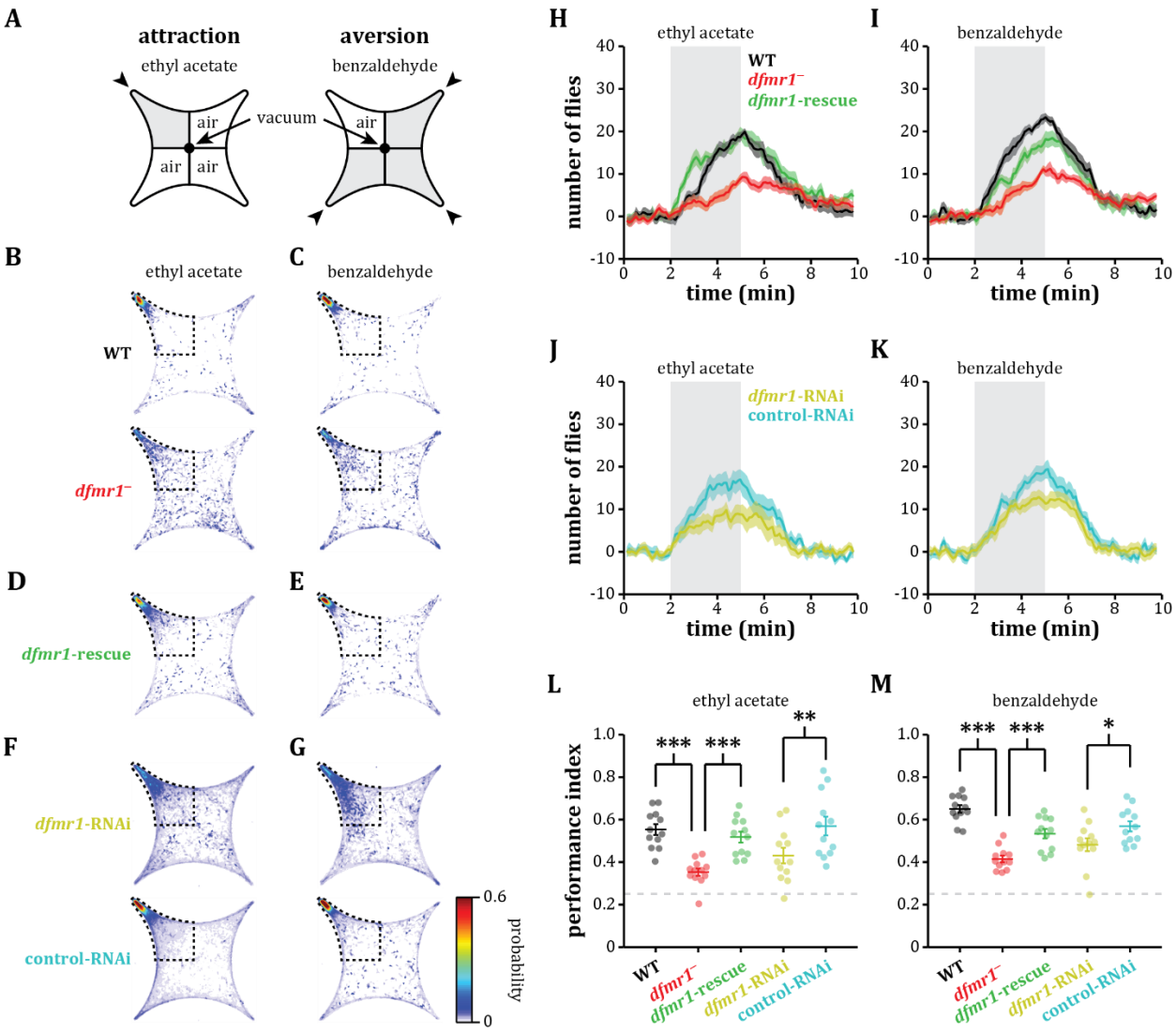

Figure 5 (*continued*). B-G. Heat maps showing the density of flies across all trials from all experimental sessions during the last minute of odor exposure. Note that WT, *dfmr1*-rescue and control-RNAi flies cluster in the ethyl acetate quadrant (dotted quadrant) in olfactory attraction assays and in the clean air quadrant (dotted quadrant) in olfactory aversion assays using benzaldehyde. *dfmr1*$^{-}$ and *dfmr1*-RNAi flies, by contrast, are more distributed across all quadrants and, hence, exhibited a poorer performance in olfactory attraction or olfactory aversion assays. **H-K.** Temporal course showing the change in number of flies in the odorized quadrant for olfactory attraction assays and in the clean air quadrant for olfactory aversion assays depicted by a dotted line in B-D. Note that WT flies (black) and *dfmr1*-rescue flies (green) performed better than *dfmr1*$^{-}$ flies (red). Also note that flies expressing RNAi against the RNA product of *dfmr1* in projection neurons (yellow) performed significantly worse than flies of the same genetic background (cyan), but that do express dFMRP (for details, see Experimental Procedures). Shadowed traces represent s.e.m. for the number of flies (n = ~200 flies per genotype tested across 4 experimental sessions representing 3 repetitions of each odor per session). **L-M.** Preference index defined by the fraction of flies being present in the corresponding odorized (for ethyl acetate) or clean air (for benzaldehyde) quadrant during the last minute of odor exposure (4 to 5 min). Note that both, full mutants *dfmr1*$^{-}$ flies and flies expressing RNAi against *dfmr1* in projection neurons (*dfmr1*-RNAi), exhibited a lower performance in ethyl acetate-guided attraction (n = 12 trials, Wilcoxon rank-sum test; WT vs *dfmr1*$^{-}$, $p = 3.0\text{x}10^{-5}$; *dfmr1*-rescue vs *dfmr1*$^{-}$, $p = 6.2\text{x}10^{-5}$; *dfmr1*-control vs *dfmr1*-RNAi, $p = 1.8\text{x}10^{-2}$) as well as in benzaldehyde-guided aversion (n = 12 trials, Wilcoxon rank-sum test; WT vs *dfmr1*$^{-}$, $p = 1.8\text{x}10^{-5}$; *dfmr1*-rescue vs *dfmr1*$^{-}$, $p = 3.7\text{x}10^{-4}$; *dfmr1*-control vs *dfmr1*-RNAi, $p = 3.4\text{x}10^{-2}$).

Broader odor response tuning in projection neurons leads to less selective olfactory representations in *dfmr1*$^{-}$ flies

Reduced performance of *dfmr1*$^{-}$ flies in odor-induced behaviors suggests that olfactory coding is compromised in these animals. In order to evaluate whether olfactory computations are affected by the absence of dFMRP, I measured glomerular responses of antennal lobe projection neurons to different odors using fluorescence calcium imaging (Figure 6A-B; for details, see Figure 2) in WT and *dfmr1*$^{-}$ flies (Figure 6D). To extract the location of individual glomeruli, I adopted a previously described method called independent component analysis (Mukamel *et al.*, 2009; Strauch & Galizia, 2012). I show that this method performs very well for identifying even the sister glomeruli across antennal lobes with very similar locations and response profiles (Figure 6C; for details, see Figure 3).

Using this approach, I investigated the combinatorial glomerular activation patterns of antennal lobe projection neurons, and compared the neuronal representations of 24 odors in WT and *dfmr1*$^{-}$ flies. I observed that overall responsiveness of olfactory glomeruli is significantly altered, with more excitatory and fewer inhibitory odor responses in *dfmr1*$^{-}$ flies (Figure 7A-C). In order to evaluate olfactory coding in the antennal lobe, I carried out a pairwise comparison of odor evoked glomerular activation patterns using two commonly used and complementary measures of similarity, cosine distance and Euclidean distance. Cosine distance is a measure to compare odor responses irrespective of their amplitude. Euclidean distance, by contrast, takes the strength of odor responses into account. In general, high cosine and Euclidean distances indicate increased difference among odor representations, and vice versa. Hence, high cosine and Euclidean distances describe greater specificity in odor encoding. These results show significantly lower cosine and Euclidean distance values between pairs of odors in *dfmr1*$^{-}$ flies (Figures 8A-D). This indicates that loss of *dfmr1* causes odor evoked glomerular activation patterns to become less distinct from each other and, therefore, harder to discriminate. Reduced odor specificity of glomerular activation patterns could, in principle, explain why *dfmr1*$^{-}$ flies are impaired in both attractive and aversive olfactory behavioral tasks.

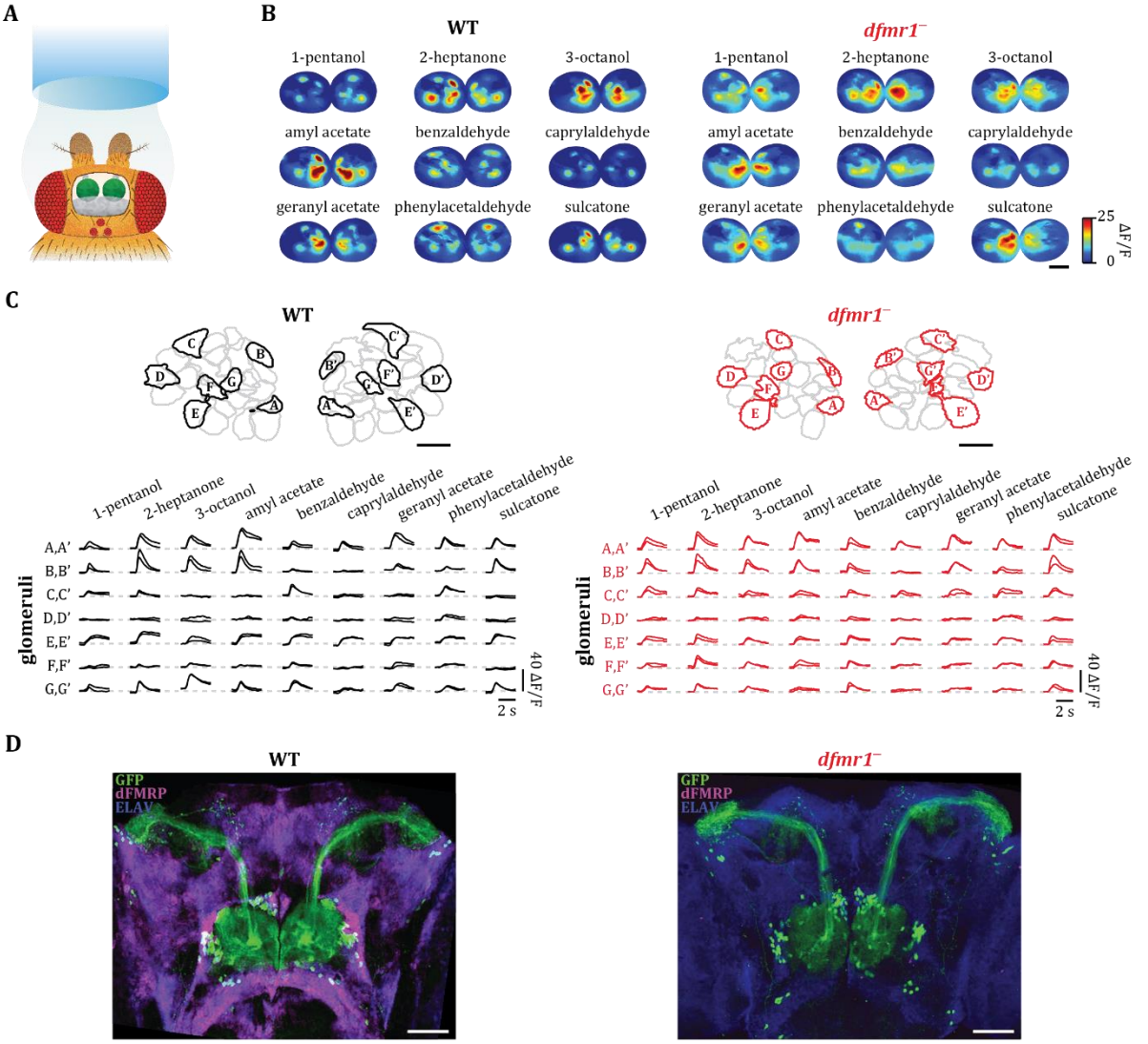

Figure 6. Odor representations in the antennal lobe of WT and *dfmr1*⁻ flies. A. Experimental setup depicting a fly expressing the transgenic calcium indicator GCaMP6 in projection neurons. Briefly, the fly is secured to a chamber and the cuticle above the antennal lobes is removed, which allows imaging of the antennal lobes from the dorsal side. A tube is placed in front of its antennae for odors to be delivered (for details, see Figure 2). **B.** Activity maps elicited by different odors in the antennal lobes of WT and *dfmr1*⁻ flies. These maps are obtained by calculating the percent change of fluorescence intensity (ΔF/F) during 1 s after response onset. Warmer colors signify strong responses. Note that glomerular responses are more dispersed and localized in WT than in *dfmr1*⁻ flies. Scale bar = 20 µm. **C.** Examples for the location and the response time course of antennal lobe glomeruli in WT and in *dfmr1*⁻ flies. Different activity dynamics can be observed in response to different odors in different glomeruli. Please note that potential sister glomeruli identified via our detection algorithm (for details, see Figure 3) exhibit similar response profiles. Scale bar = 10 µm. **D.** Immunostainings on brains obtained from flies used in calcium imaging experiments confirmed expression of dFMRP in WT flies (left) and lack of dFMRP in *dfmr1*⁻ flies (right). Scale bar = 50 µm.

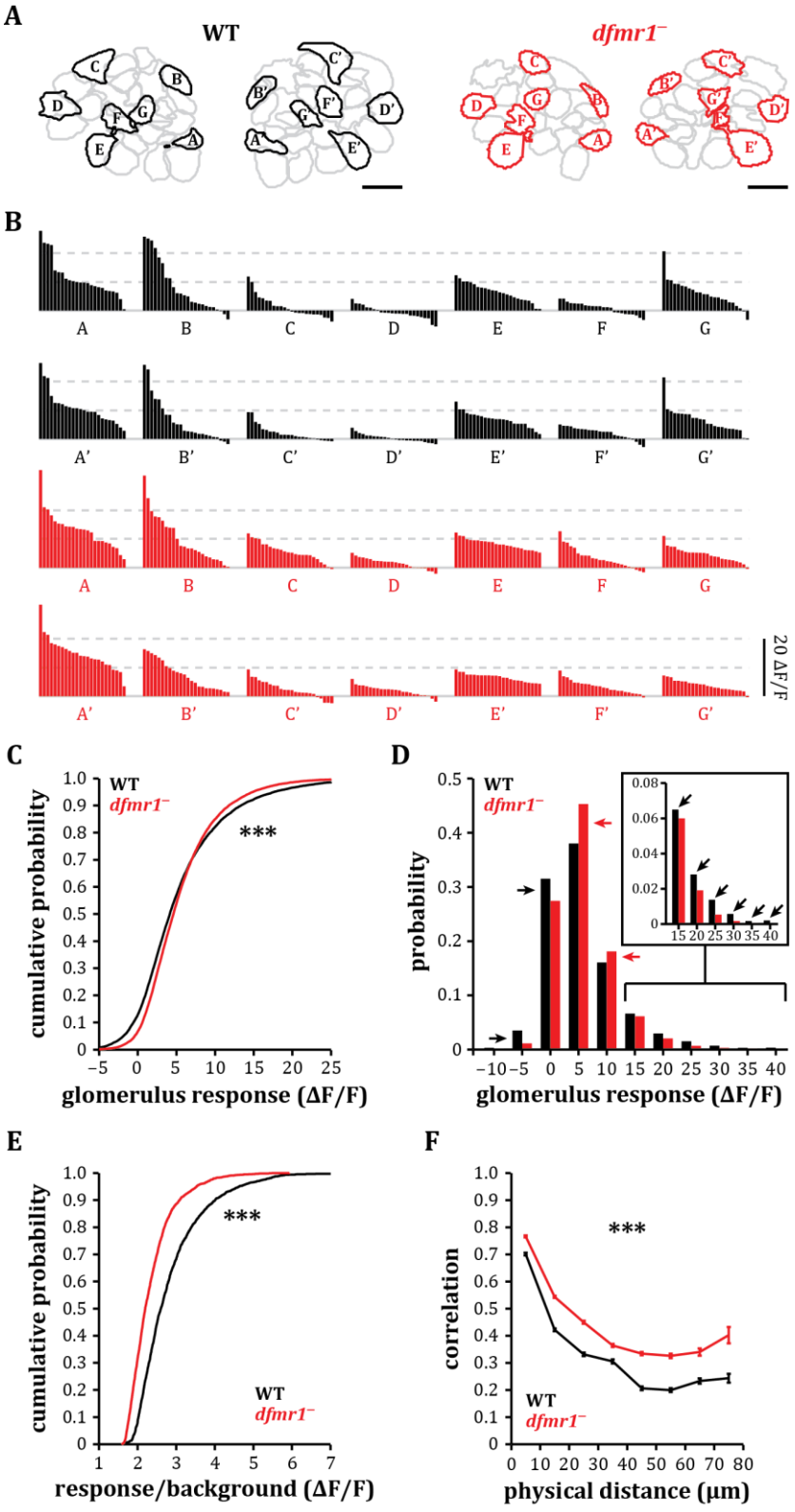
A
WT
dfmr1⁻
B
20 ΔF/F
C
WT
dfmr1⁻
***
cumulative probability
glomerulus response (ΔF/F)
D
WT
dfmr1⁻
probability
glomerulus response (ΔF/F)
E
***
WT
dfmr1⁻
cumulative probability
response/background (ΔF/F)
F
***
WT
dfmr1⁻
correlation
physical distance (μm)

Figure 7. Olfactory glomeruli in *dfmr1*$^{-}$ flies are broadly tuned and have narrower dynamic response range. A. Examples of glomerular response profiles obtained from one WT fly and one *dfmr1*$^{-}$ fly, respectively. Black contour lines mark the location of the displayed glomeruli within the antennal lobes. Calibration bar = 10 µm. **B.** Responses of individual glomeruli to 24 different odors. The responses are sorted so that the most preferred odor of a given glomerulus is always on the left and the least preferred odor is on the right. Note that odor responses in WT flies are sparser than *dfmr1*$^{-}$ flies. Also note that there are little or no inhibitory odor responses in *dfmr1*$^{-}$ flies, whereas most WT glomeruli would display some inhibition in response to its least preferred odor. Responses are sorted equally for sister glomeruli. **C.** Cumulative distribution showing the response amplitudes of all glomeruli to all presented odors. *dfmr1*$^{-}$ glomeruli exhibited increased number of weak odor responses as well as reduced number of high amplitude odor responses and less inhibitory odor responses. This indicates significantly different and narrower dynamic range for odor responses in *dfmr1*$^{-}$ flies (WT, n = 10 flies, 492 glomeruli; *dfmr1*$^{-}$, n = 12 flies, 560 glomeruli; Kolmogorov-Smirnov test, $p = 1.1\text{x}10^{-30}$). **D.** Histogram illustrating the probability of glomerular response amplitudes for the assessed population of flies (WT, n = 10 flies, 492 glomeruli; *dfmr1*$^{-}$, n = 12 flies, 560 glomeruli). WT flies exhibited increased number of inhibitory odor responses, silent glomeruli and strong excitatory responses (black arrows) as compared to *dfmr1*$^{-}$ flies. By contrast, *dfmr1*$^{-}$ glomeruli were more likely to produce weak excitatory responses to odor stimulation (red arrows). **E.** Cumulative distribution of odor response to background activity ratios. Glomerular activity above one standard deviation from the mean antennal lobe activity was considered a response. The mean antennal lobe activity was taken as background. *dfmr1*$^{-}$ flies exhibited reduced response to background activity ratios, indicating nosier odor representations (WT, n = 10 flies, 492 glomeruli; *dfmr1*$^{-}$, n = 12 flies, 560 glomeruli; Kolmogorov-Smirnov test, $p = 6.0\text{x}10^{-65}$). **F.** Correlation of glomerular odor response profiles versus their physical distance within the antennal lobes (mean ± s.e.m.; Wilcoxon rank-sum test; WT, n = 10 flies, 492 glomeruli; *dfmr1*$^{-}$, n = 12 flies, 560 glomeruli; 10 µm, $p = 4.2\text{x}10^{-24}$; 20 µm, $p = 8.4\text{x}10^{-65}$; 30 µm, $p = 4.9\text{x}10^{-38}$; 40 µm, $p = 1.3\text{x}10^{-8}$; 50 µm, $p = 7.6\text{x}10^{-43}$; 60 µm, $p = 6.5\text{x}10^{-30}$; 70 µm, $p = 9.4\text{x}10^{-12}$; 80 µm, $p = 3.8\text{x}10^{-6}$). Increased correlation indicates that *dfmr1*$^{-}$ glomeruli are more similar in their odor responses and exhibit less specific responses for encoding particular odors.

What underlies the increased similarity among odor representations in *dfmr1*$^{-}$ flies? To answer this question, I visualized odor response selectivity by plotting the odor responses of each individual glomerulus normalized to its maximum odor response. I qualitatively observed that *dfmr1*$^{-}$ glomeruli have broader response profiles, and thus reduced odor selectivity, represented by warmer colors (Figure 8E). To quantify this effect, I calculated the lifetime sparseness, a measure of response selectivity (Yaksi *et al.*, 2007), of all recorded glomeruli. A glomerulus with a high sparseness value responds to only one or very few odors. Conversely, a glomerulus with a low sparseness value responds to many odors equally. I found that *dfmr1*$^{-}$ glomeruli have lower lifetime sparseness values (Figure 8F), suggesting they are less selective to odors. Complementary to these analyses, I computed the population sparseness, which is a measure of the number of glomeruli activated by a single odor. A high population sparseness value signifies that few glomeruli were activated by a given odor, whereas a low population sparseness value signifies that many glomeruli were activated. I found that the antennal lobe circuit of *dfmr1*$^{-}$ flies has lower population sparseness values

(Figure 8G), which is consistent with a complementary analysis showing reduced response to background (signal to noise) ratios (Figure 7D-E) and increased correlations across antennal lobe glomeruli in *dfmr1*⁻ flies (Figure 7F).

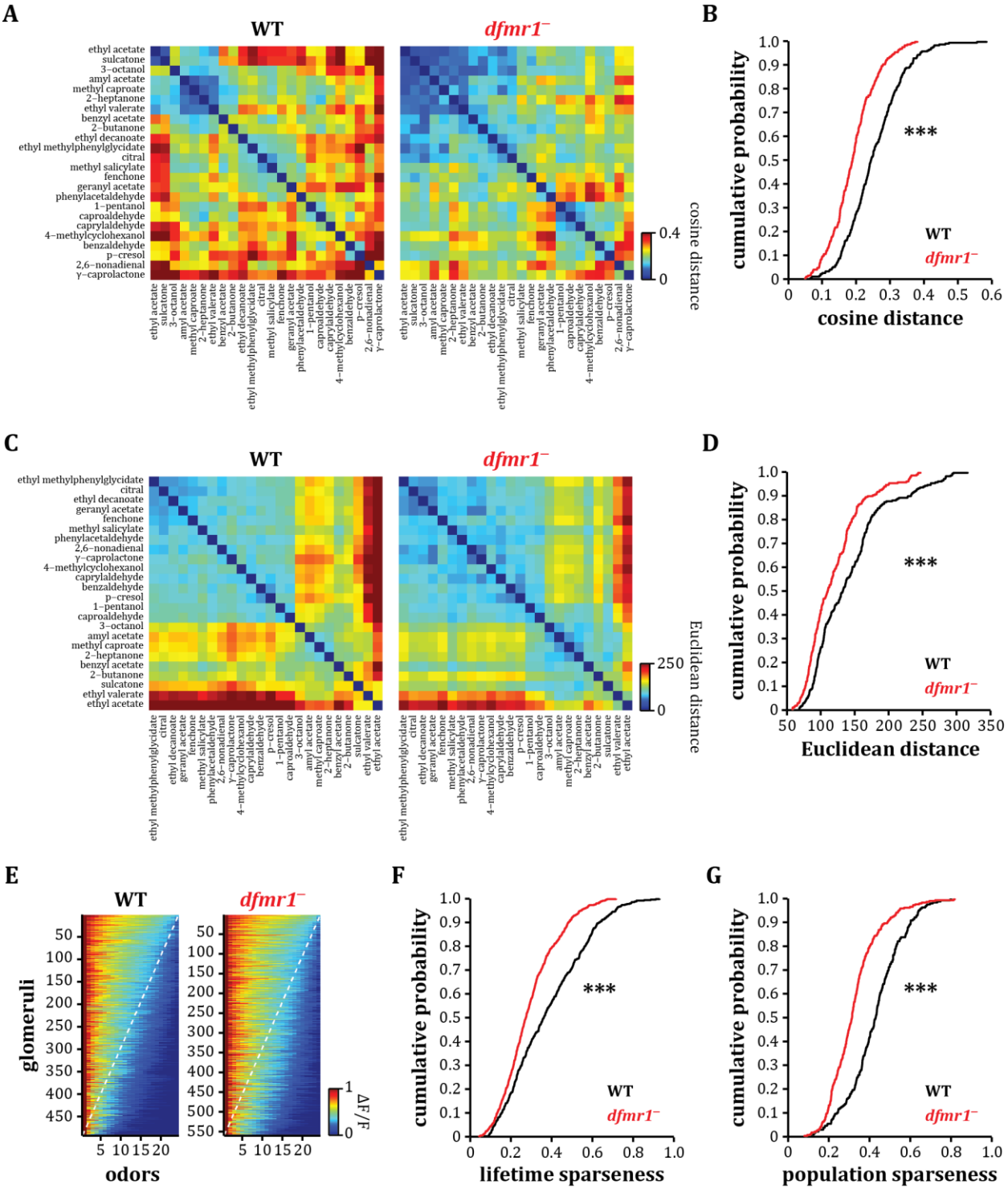

Figure 8. Broader glomerular odor tuning leads to less specific odor representations in *dfmr1*$^{-}$ flies. A. Cosine distance matrices representing pairwise similarities among representations of 24 different odors in glomerular responses of WT and *dfmr1*$^{-}$ flies (WT, n = 10 flies, 492 glomeruli; *dfmr1*$^{-}$, n = 12, 560 glomeruli). Lower cosines distances (cooler colors) indicate that different odors are encoded more similarly in the antennal lobes of *dfmr1*$^{-}$ flies. **B.** Cumulative distribution of cosine distances in WT (black) and in *dfmr1*$^{-}$ flies (red). Significantly lower cosine distance values in *dfmr1*$^{-}$ flies show that odors are represented more similarly in the antennal lobes of *dfmr1*$^{-}$ flies as compared to WT flies (WT, n = 10 flies, 492 glomeruli; *dfmr1*$^{-}$, n = 12 flies, 560 glomeruli; Kolmogorov-Smirnov test, $p = 7.4 \times 10^{-16}$). **C.** Euclidean distance matrices representing pairwise similarities among representations of 24 different odors in glomerular responses of WT and *dfmr1*$^{-}$ flies (WT, n = 10 flies, 492 glomeruli; *dfmr1*$^{-}$, n = 12 flies, 560 glomeruli). Reduced Euclidean distances (cooler colors) indicate that different odors are encoded more similarly in the antennal lobes of *dfmr1*$^{-}$ flies. **D.** Cumulative distribution of Euclidean distances in WT (black) and in *dfmr1*$^{-}$ flies (red). Significantly lower Euclidean distance values in *dfmr1*$^{-}$ flies show that odors are represented more similarly in the antennal lobes of *dfmr1*$^{-}$ flies as compared to WT flies (WT, n = 10 flies, 492 glomeruli; *dfmr1*$^{-}$, n = 12 flies, 560 glomeruli; Kolmogorov-Smirnov test, $p = 4.1 \times 10^{-7}$). **E.** Normalized odor responses of all individual WT and *dfmr1*$^{-}$ glomeruli (WT, n = 10 flies, 492 glomeruli; *dfmr1*$^{-}$, n = 12 flies, 560 glomeruli). Glomeruli on the ordinates are sorted on the basis of their response selectivity. The least selective glomeruli are located at the top, whereas the most selective glomeruli are located at the bottom. Odor responses on the abscissas are sorted on the basis of the response strength, after normalizing to the strongest odor response of individual glomeruli (warmest colors) on the left side. A dashed white line was added to help with the comparison of WT versus *dfmr1*$^{-}$ glomeruli. **F**. Cumulative distribution of glomerulus lifetime sparseness for all recorded glomeruli in WT (black) and *dfmr1*$^{-}$ (red) flies. Reduced lifetime sparseness indicates that *dfmr1*$^{-}$ glomeruli exhibited broader tuning to odors, reflecting reduced specificity (WT, n = 10 flies, 492 glomeruli; *dfmr1*$^{-}$, n = 12 flies, 560 glomeruli; Kolmogorov-Smirnov test, $p = 9.8 \times 10^{-14}$). **G.** Cumulative distribution of population sparseness for all measured odors in WT (black) and *dfmr1*$^{-}$ (red) flies. Lower population sparseness indicates that odors activate more glomeruli equally in *dfmr1*$^{-}$ flies. By contrast, odors activate fewer odor specific glomeruli in WT flies (WT, n = 10 flies, 492 glomeruli; *dfmr1*$^{-}$, n = 12 flies, 560 glomeruli; Kolmogorov-Smirnov test, $p = 8.4 \times 10^{-22}$).

These results thus far reveal impairment in olfactory coding and odor selectivity in *dfmr1*$^{-}$ flies due to broader response tuning and reduced odor selectivity of antennal lobe projection neurons. This reduced odor selectivity can, in principle, arise from less selective glomerular innervation patterns of individual antennal lobe projection neurons in *dfmr1*$^{-}$ flies. However, I did not observe any significant changes in glomerular morphology or size in any of the genetically identified projection neurons that I tested in *dfmr1*$^{-}$ flies (Figure 9).

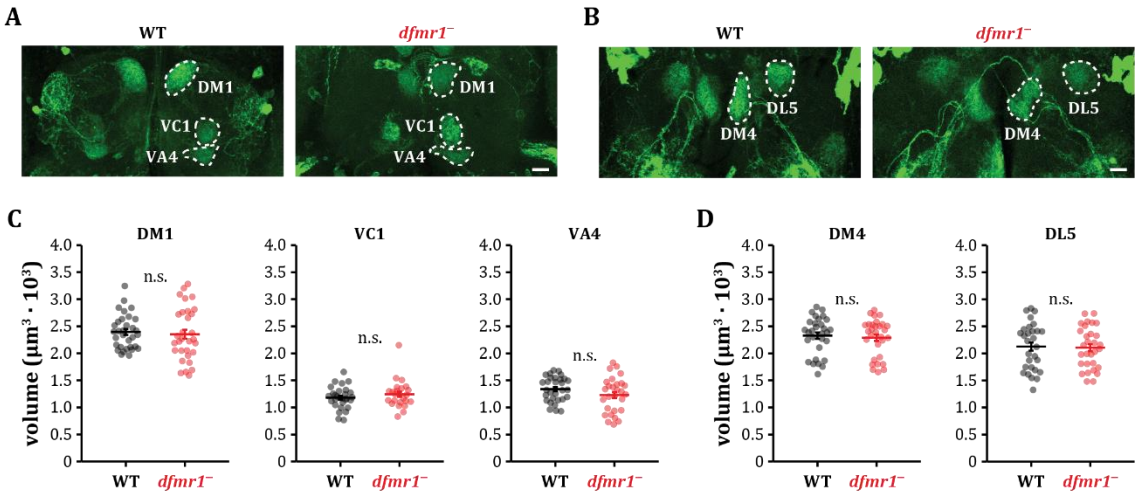

Figure 9. Glomerular innervation patterns of antennal lobe projection neurons are not affected in *dfmr1*⁻ flies. A. Maximum intensity projections of representative WT and *dfmr1*⁻ flies expressing GFP in projection neurons innervating glomeruli DM1, VC1 and VA4. Calibration bar = 20 µm. **B.** Maximum intensity projections of representative WT and *dfmr1*⁻ flies expressing GFP in projection neurons innervating glomeruli DL5 and DM4. Calibration bar = 20 µm. **C.** Scatter plots showing the calculated volumes for glomeruli DM1, VC1 and VA4. No significant differences were found between WT and *dfmr1*⁻ flies (WT, n = 16 flies; *dfmr1*⁻, n = 16 flies; Wilcoxon rank-sum test). **D.** Scatter plots showing the calculated volumes for glomeruli DL5 and DM4. No significant differences were found between WT and *dfmr1*⁻ flies (WT, n = 15 flies; *dfmr1*⁻, n = 15 flies; Wilcoxon rank-sum test).

Impaired lateral interactions alter olfactory information processing in *dfmr1*⁻ flies

The lack of gross morphological alterations in antennal lobe projection neurons, combined with the observations of increased excitatory and reduced inhibitory odor responses, suggests that defective lateral interactions among antennal lobe neurons are responsible for the reduced specificity of olfactory representations in *dfmr1*⁻flies. In the fruit fly antennal lobe, lateral interactions across olfactory glomeruli were shown to mediate the spread of both excitation (Olsen *et al.*, 2007), through gap junctions (Yaksi & Wilson, 2010), and inhibition, through local interneurons (Wilson & Laurent, 2005; Olsen & Wilson, 2008; Root *et al.*, 2008).

It was previously shown that when odors are mixed, lateral interactions across antennal lobe glomeruli can alter odor representations, both through lateral excitation and lateral inhibition (Olsen *et al.*, 2010). In order to compare the level of lateral interactions in WT and *dfmr1*⁻ flies, I applied mixtures of odorants, in which the concentration of one of the components is kept constant while the concentration of the other mixture component is

gradually increased (Figure 10A; see also Figure 11). This experimental design is based on the fact that different odors recruit different subsets of projection neurons and different local interneurons. This, in turn, will change the odor evoked activity patterns, creating new odor representations depending on the degree of lateral interactions among all recruited neurons (Olsen *et al.*, 2007; Hong & Wilson, 2015).

I observed that the odor representation of the component with fixed concentration became progressively different with increasing concentrations of the second mixture component. These mixing related changes in odor representations were more pronounced in WT flies than in *dfmr1*$^{-}$ flies (Figure 10A-C, see also Figure 11). Next, I quantified the changes in response amplitudes in individual glomeruli. These results showed that, on average, WT flies exhibited significantly more mixture related suppression whereas *dfmr1*$^{-}$ flies exhibited significantly more mixture related excitation (Figure 10D,E). This suggests that while lateral inhibition is impaired in *dfmr1*$^{-}$ flies, the later excitatory interactions might be spared (see also Figure 15). These lateral inhibitory and lateral excitatory effects were variable across populations of projection neurons. In line with this, these results suggest that populations of individual glomeruli in WT flies have a significantly larger variety of both inhibitory and excitatory effects at all mixture concentrations, when compared to *dfmr1*$^{-}$ flies (Figure 10F; see also Figure 11). Altogether, these results further support the idea that lateral inhibitory interactions are impaired in the antennal lobe of *dfmr1*$^{-}$ flies, which eventually results in reduced contrast across odor evoked activity patterns and, therefore, poorer performance in olfactory behavioral assays.

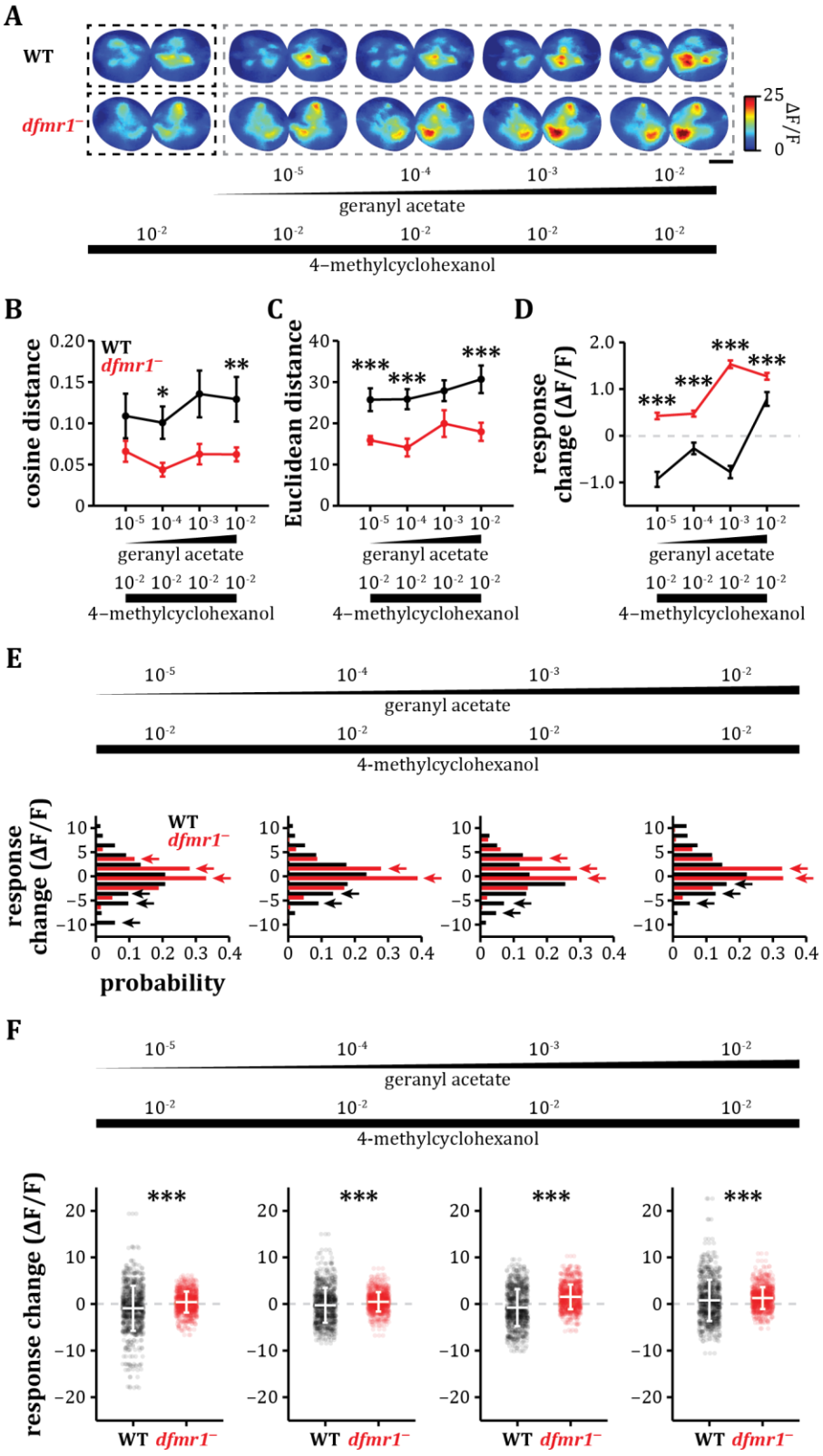
A
WT
dfmr1⁻
25
ΔF/F
0
10-5
10-4
10-3
10-2
geranyl acetate
10-2
4–methylcyclohexanol
B
cosine distance
WT
dfmr1⁻
C
Euclidean distance
D
response change (ΔF/F)
E
4-methylcyclohexanol
probability
F

Figure 10. Lateral interactions across olfactory glomeruli are reduced in *dfmr1*$^{-}$ flies. A. Activity maps elicited by odor mixtures of a constant concentration of 4-methylcyclohexanol and a progressively increasing concentration of geranyl acetate in the antennal lobes of representative WT and *dfmr1*$^{-}$ flies. These activity maps are obtained by calculating the percent change of fluorescence intensity (ΔF/F) during 1 s after response onset. Warmer colors signify strong responses. Single odors are circumscribed by a dashed black box. Mixtures are circumscribed by a dashed gray box. Scale bar = 20 μm. **B.** Cosine distances representing pairwise similarities among representations of the indicated odor mixtures. Note that the representations of 4-methylcyclohexanol become progressively different as the concentration of geranyl acetate increases. These changes are reduced in *dfmr1*$^{-}$ flies (mean ± s.e.m.; WT, n = 6 flies, 298 glomeruli; *dfmr1*$^{-}$, n = 7 flies, 345 glomeruli; Wilcoxon rank-sum test; [10^{-5}], $p = 6.9x10^{-2}$; [10^{-4}], $p = 3.7x10^{-2}$; [10^{-3}], $p = 5.1x10^{-2}$; [10^{-2}], $p = 1.1x10^{-2}$). **C.** Euclidean distances representing pairwise similarities among representations of the indicated odor mixtures. Note that the representations of 4-methylcyclohexanol become progressively different as the concentration of geranyl acetate increases. These changes are reduced in *dfmr1*$^{-}$ flies (mean ± s.e.m.; WT, n = 6 flies, 298 glomeruli; *dfmr1*$^{-}$, n = 7 flies, 345 glomeruli; Wilcoxon rank-sum test; [10^{-5}], $p = 5.8x10^{-4}$; [10^{-4}], $p = 2.3x10^{-3}$; [10^{-3}], $p = 6.9x10^{-2}$; [10^{-2}], $p = 4.1x10^{-3}$). **D.** Average change in 4-methylcyclohexanol responses of all individual glomeruli when mixed with different concentrations of geranyl acetate. On average, WT glomeruli (black) decreased the amplitude of their 4-methylcyclohexanol responses when geranyl acetate was added in the mixture. By contrast, *dfmr1*$^{-}$ glomeruli (red) increase their amplitude when geranyl acetate was added in the mixture(mean ± s.e.m.; WT, n = 6 flies, 298 glomeruli; *dfmr1*$^{-}$, n = 7 flies, 345 glomeruli; Wilcoxon rank-sum test; [10^{-5}], $p = 7.5x10^{-16}$; [10^{-4}], $p = 6.4x10^{-11}$; [10^{-3}], $p = 7.9x10^{-46}$; [10^{-2}], $p = 3.7x10^{-7}$). **E.** Histograms illustrating the distribution of response changes for all recorded glomeruli in WT (black, n = 6 flies, 298 glomeruli) and *dfmr1*$^{-}$flies, (red, n = 7 flies, 345 glomeruli). Note that WT glomeruli exhibited more prominent decrease in their 4-methylcyclohexanol responses after geranyl acetate is added to the mixture (black arrows). By contrast, *dfmr1*$^{-}$ glomeruli showed more increase or no change in their 4-methylcyclohexanol responses (red arrows). **F.** Scatter plots depicting the response changes in every individual glomeruli when 4-methylcyclohexanol is mixed with the indicated concentrations of geranyl acetate in WT (black) and *dfmr1*$^{-}$ (red) flies. Larger variability in response changes is observed for WT glomeruli (mean ± std.; WT, n = 6; *dfmr1*$^{-}$, n = 7; *F*-test; [10^{-5}], $p = 1.6x10^{-7}$; [10^{-4}], $p = 1.4x10^{-8}$; [10^{-3}], $p = 1.5x10^{-10}$; [10^{-2}], $p = 2.6x10^{-15}$).

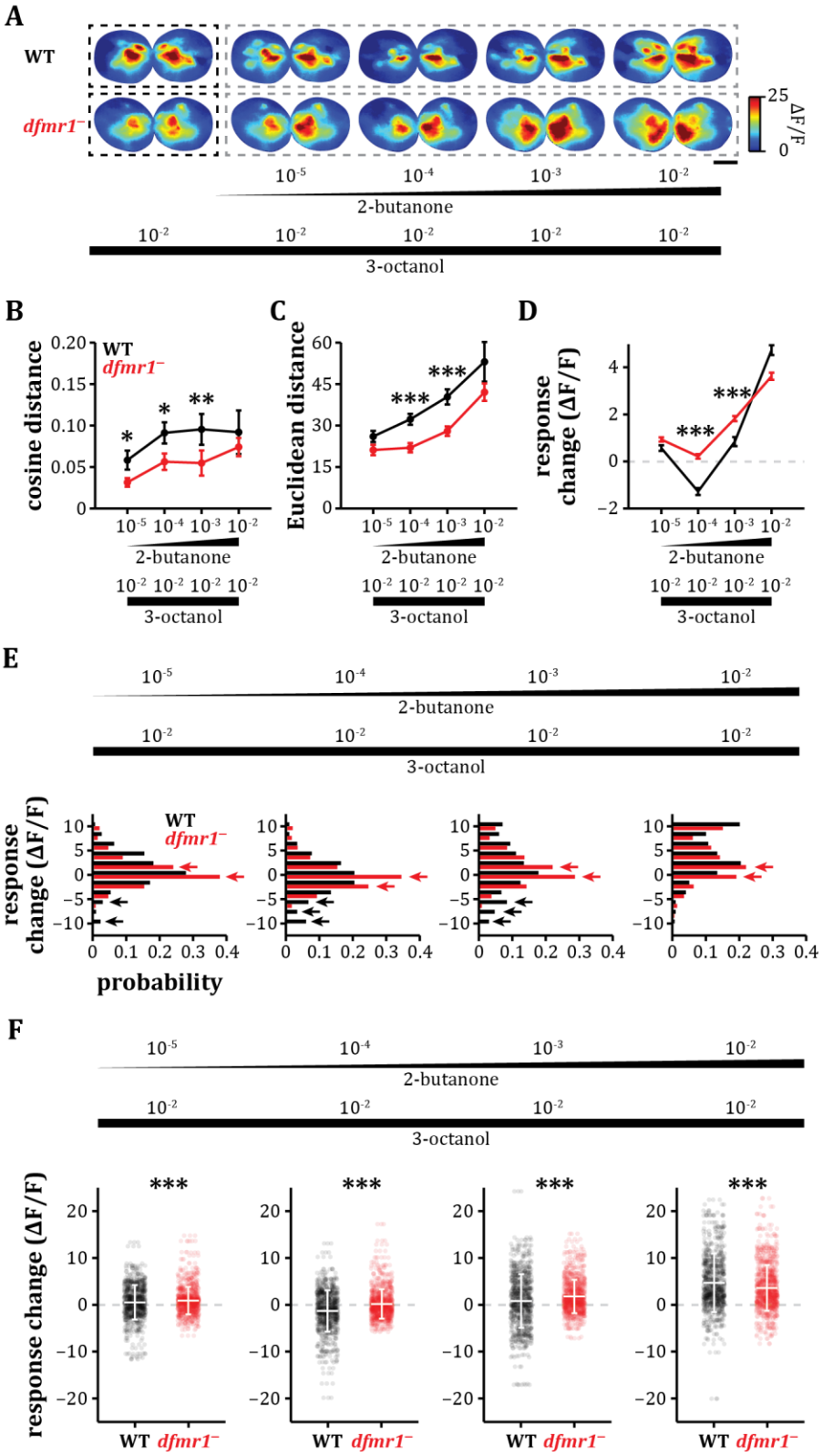
A
WT
dfmr1⁻
25
ΔF/F
0
10-5
10-4
10-3
10-2
2-butanone
10-2
3-octanol
B
cosine distance
WT
dfmr1⁻
C
Euclidean distance
D
response change (ΔF/F)
E
response change (ΔF/F)
probability
F
response change (ΔF/F)
***

Figure 11. Lateral interactions across olfactory glomeruli are reduced in *dfmr1*$^{-}$ flies. A. Activity maps elicited by odor mixtures of a constant concentration of 3-octanol and a progressively increasing concentration of 2-butanone in the antennal lobes of representative WT and *dfmr1*$^{-}$ flies. These activity maps are obtained by calculating the percent change of fluorescence intensity (ΔF/F) during 1 s after response onset. Warmer colors signify strong responses. Single odors are circumscribed by a dashed black box. Mixtures are circumscribed by a dashed gray box. Scale bar = 20 μm. **B.** Cosine distances representing pairwise similarities among representations of the indicated odor mixtures. Note that the representations of 3-octanol become progressively different as the concentration of 2-butanone increases. These changes are reduced in *dfmr1*$^{-}$ flies (mean ± s.e.m.; WT, n = 6 flies, 298 glomeruli; *dfmr1*$^{-}$, n = 7 flies, 345 glomeruli; Wilcoxon rank-sum test; [10^{-5}], $p = 3.7\text{x}10^{-2}$; [10^{-4}], $p = 3.7\text{x}10^{-2}$; [10^{-3}], $p = 2.6\text{x}10^{-2}$; [10^{-2}], $p = 4.7\text{x}10^{-1}$). **C.** Euclidean distances representing pairwise similarities among representations of the indicated odor mixtures. Note that the representations of 3-octanol become progressively different as the concentration of 2-butanone increases. These changes are reduced in *dfmr1*$^{-}$ flies (mean ± s.e.m.; WT, n = 6 flies, 298 glomeruli; *dfmr1*$^{-}$, n = 7 flies, 345 glomeruli; Wilcoxon rank-sum test; [10^{-5}], $p = 6.9\text{x}10^{-2}$; [10^{-4}], $p = 7.0\text{x}10^{-3}$; [10^{-3}], $p = 2.3\text{x}10^{-3}$; [10^{-2}], $p = 1.5\text{x}10^{-1}$). **D.** Average change in 3-octanol responses of all individual glomeruli when mixed with different concentrations of 2-butanone. On average, WT glomeruli (black) decreased the amplitude of their 3-octanol responses when 2-butanone was added in the mixture. By contrast, *dfmr1*$^{-}$ glomeruli (red) increase their amplitude when 2-butanone was added in the mixture(mean ± s.e.m.; WT, n = 6 flies, 298 glomeruli; *dfmr1*$^{-}$, n = 7 flies, 345 glomeruli; Wilcoxon rank-sum test; [10^{-5}], $p = 1.3\text{x}10^{-1}$; [10^{-4}], $p = 3.6\text{x}10^{-11}$; [10^{-3}], $p = 6.3\text{x}10^{-5}$; [10^{-2}], $p = 9.9\text{x}10^{-1}$). **E.** Histograms illustrating the distribution of response changes for all recorded glomeruli in WT (black, n = 6 flies, 298 glomeruli) and *dfmr1*$^{-}$flies, (red, n = 7 flies, 345 glomeruli). Note that WT glomeruli exhibited more prominent decrease in their 3-octanol responses after 2-butanone is added to the mixture (black arrows). By contrast, *dfmr1*$^{-}$ glomeruli showed more increase or no change in their 3-octanol responses (red arrows). **F.** Scatter plots depicting the response changes in every individual glomeruli when 3-octanol is mixed with the indicated concentrations of 2-butanone in WT (black) and *dfmr1*$^{-}$ (red) flies. Larger variability in response changes is observed for WT glomeruli (mean ± std.; WT, n = 6; *dfmr1*$^{-}$, n = 7; *F*-test; [10^{-5}], $p = 2.4\text{x}10^{-13}$; [10^{-4}], $p = 1.5\text{x}10^{-25}$; [10^{-3}], $p = 2.1\text{x}10^{-47}$; [10^{-2}], $p = 5.1\text{x}10^{-15}$).

Lateral inhibition is impaired in the antennal lobe of *dfmr1*$^{-}$ flies

The findings using odor mixtures point to reduced lateral inhibition among olfactory glomeruli in *dfmr1*$^{-}$ flies. In consonance with this idea, it has been reported that several components of the GABAergic transmission machinery are downregulated, both in mouse and in fruit fly models of fragile X syndrome (D'Hulst *et al.*, 2006; Curia *et al.*, 2009; D'Hulst *et al.*, 2009; Adusei *et al.*, 2010; Hong *et al.*, 2012). Moreover, GABAergic signaling appears to be disrupted in the brains of patients with autism (Robertson *et al.*, 2016), a recurrent phenotype in fragile X syndrome. All this evidence led to the hypothesis that reduced inhibition may be a major mechanism underlying neuronal deficits in fragile X syndrome (Braat & Kooy, 2015b). However, direct *in vivo* physiological evidence that inhibitory connections between neurons are impaired in any *in vivo* model of fragile X syndrome is lacking.

In the fruit fly antennal lobe, lateral inhibition across olfactory glomeruli is mediated by a large population of GABAergic local interneurons that can act on both olfactory receptor neuron terminals and on antennal lobe projection neurons (Wilson & Laurent, 2005; Olsen & Wilson, 2008; Chou *et al.*, 2010). In order to directly test the action of local interneurons on the activity of projection neurons, I performed intracellular recordings of projection neurons while optogenetically stimulating a large population of GABAergic local interneurons expressing channelrhodopsin-2 (Figure 12A; Das *et al.*, 2008; Okada *et al.*, 2009; Hong & Wilson, 2015). Optogenetic activation of local interneurons consistently hyperpolarized the membrane potential of WT projection neurons (Figure 12B-D). Instead, *dfmr1*$^{-}$ projection neurons exhibited significantly smaller or no hyperpolarization in their membrane potential (Figure 12B-D). Importantly, I observed a prominent initial excitation upon optogenetic local interneuron stimulation (Figure 12C), which is mediated by the gap junctions established between local interneurons and projection neurons (Yaksi & Wilson, 2010).

During these recordings, I kept the antennae dry and the olfactory nerve intact, which ensures that the olfactory receptor neurons are undamaged and sustain a healthy level of background activity. As previously shown (Kazama & Wilson, 2009), this remaining olfactory

receptor neuron background firing results in prominent subthreshold synaptic activity and spontaneous action potential firing in the recorded projection neurons (Figure 12 B,E,G). I tested whether activating local interneurons can reduce the firing rate of projection neurons, and thus, influence the strength of their output onto the next stage of olfactory processing, the mushroom body and the lateral horn neurons. In fact, optogenetic activation of local interneurons reduced the spontaneous firing of WT projection neurons significantly more than that of *dfmr1*$^{-}$ projection neurons (Figure 12E-H). In line with the remaining gap junction mediated lateral excitation, I observed a slight initial increase in projection neuron firing rates of *dfmr1*$^{-}$ flies (Figure 12E-F).

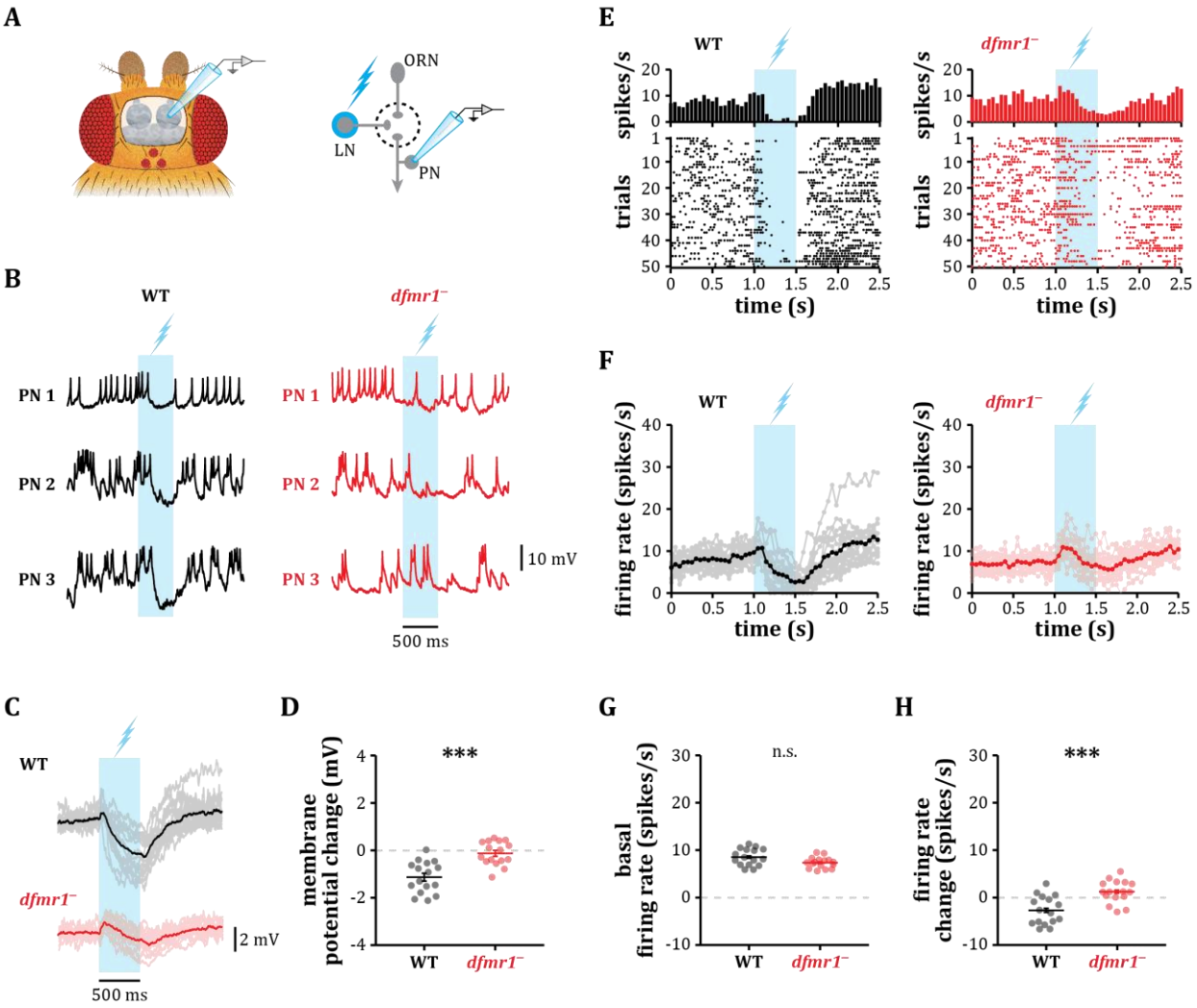

Figure 12. Lateral inhibition of projection neurons is impaired in *dfmr1*$^{-}$ flies. A. Experimental setup depicting a fly expressing the light inducible channel ChR2 in GABAergic (Das *et al.*, 2008; Okada *et al.*, 2009) local interneurons (LN). Patch clamp recordings were conducted in projection neurons (PN), while stimulating a large group of local interneurons with a flash of blue light. **B.** Representative voltage traces of projection neurons (PN). In response to optogenetic activation of local interneurons, WT projection neurons typically show a hyperpolarization of their membrane potential accompanied by inhibition of action potentials. By contrast, *dfmr1*$^{-}$ projection neurons exhibit little hyperpolarization and mild suppression of action potentials. Blue shade depicts the period of 500 ms blue light stimulation. **C.** Membrane potential of every individual projection neuron averaged over 50 trials (transparent traces) in response to optogenetic activation of local interneurons in WT and *dfmr1*$^{-}$ flies (WT, n = 16 cells; *dfmr1*$^{-}$, n = 16 cells). On average (full color traces), optogenetic activation of local interneurons drives a brief initial depolarization followed by a more pronounced hyperpolarization in WT flies. By contrast, in *dfmr1*$^{-}$ flies, activation of local interneurons drives a more pronounced initial depolarization followed by little or no hyperpolarization. **D.** Scatter plot depicting the light evoked changes in the membrane potential of projection neurons calculated during a 1 s window after stimulus onset. Inhibitory responses in WT projection neurons were found to be larger than in *dfmr1*$^{-}$ projection neurons (mean ± s.e.m.; WT, n = 16 cells; *dfmr1*$^{-}$, n = 16 cells; Wilcoxon rank-sum test, $p = 7.6\text{x}10^{-5}$). **E.** Firing rates (above) and raster plots (below) of two representative projection neurons from a WT and a *dfmr1*$^{-}$ fly, respectively. Note that optogenetic activation of local interneurons effectively suppresses action potential firing in the WT projection neuron. This effect is reduced in this *dfmr1*$^{-}$ projection neuron example. **F.** Firing rates (transparent traces) of all recorded WT and *dfmr1*$^{-}$ projection neurons (WT, n = 16 cells; *dfmr1*$^{-}$, n = 16 cells). On average (full color traces), activation of local interneurons consistently decreases the spontaneous firing of WT projection neurons. By contrast, spontaneous firing of *dfmr1*$^{-}$ projection neurons is slightly increased, albeit some delayed suppression. **G.** Scatter plot illustrating the basal spontaneous firing of all recorded WT and d*fmr1*$^{-}$ projection neurons, quantified during a 500 ms window before the onset of the light stimulus. No differences were found between the basal spontaneous firing of WT and that of *dfmr1*$^{-}$ projection neurons (mean ± s.e.m.; WT, n = 16 cells; *dfmr1*$^{-}$, n = 16 cells; Wilcoxon rank-sum test, $p = 8.0\text{x}10^{-2}$). **H.** Scatter plot showing the suppression in the spontaneous firing of all recorded WT and *dfmr1*$^{-}$ projection neurons by optogenetic activation of local interneurons, calculated as the difference between the basal spontaneous firing (G) and the firing during the 500 ms window of blue light stimulation. The firing rates of WT projection neurons was observed to be significantly more suppressed when compared to *dfmr1*$^{-}$ projection neurons (mean ± s.e.m.; WT, n = 16 cells; *dfmr1*$^{-}$, n = 16 cells; Wilcoxon rank-sum test, $p = 4.3\text{x}10^{-4}$).

The observed impaired inhibition in the projection neurons of *dfmr1*$^{-}$ flies could, in principle, be the consequence of a less effective optogenetic activation of local interneurons. In order to rule out this possibility, I recorded the responses to optogenetic activation in local interneurons expressing channelrhodopsin-2, both in WT and *dfmr1*$^{-}$ flies (Figure 13A-B). Optogenetic stimulation elicited significantly larger membrane depolarization and higher firing rates in *dfmr1*$^{-}$ local interneurons, when compared to WT local interneurons (Figure 13C-H). Furthermore, optogenetic stimulation of local interneurons expressing channelrhodopsin-2 consistently hyperpolarized the membrane potential of local interneurons not expressing channelrhodopsin-2 in WT flies (Figure 14). By contrast, little or no hyperpolarization was observed in *dfmr1*$^{-}$ local interneurons not expressing channelrhodopsin-2 (Figure 14). Altogether, these results indicate that the reduced inhibition observed in *dfmr1*$^{-}$ projection neurons (Figure 12) cannot be due to less effective

optogenetic activation of *dfmr1*⁻ local interneurons. One the contrary, these results suggest that optogenetic stimulation is more effective in activating populations of *dfmr1*⁻ local interneurons, especially at the late stage of the stimulation (Figure 13B-C,E-F), presumably, due to less effective GABAergic inhibition across *dfmr1*⁻ local interneurons. In summary, these experiments revealed that deficient inhibition of *dfmr1*⁻ projection neurons (Figure 12) is due to less effective GABAergic inhibition from local interneurons onto the whole antennal lobe circuit, both at the level of projections neurons and local interneurons.

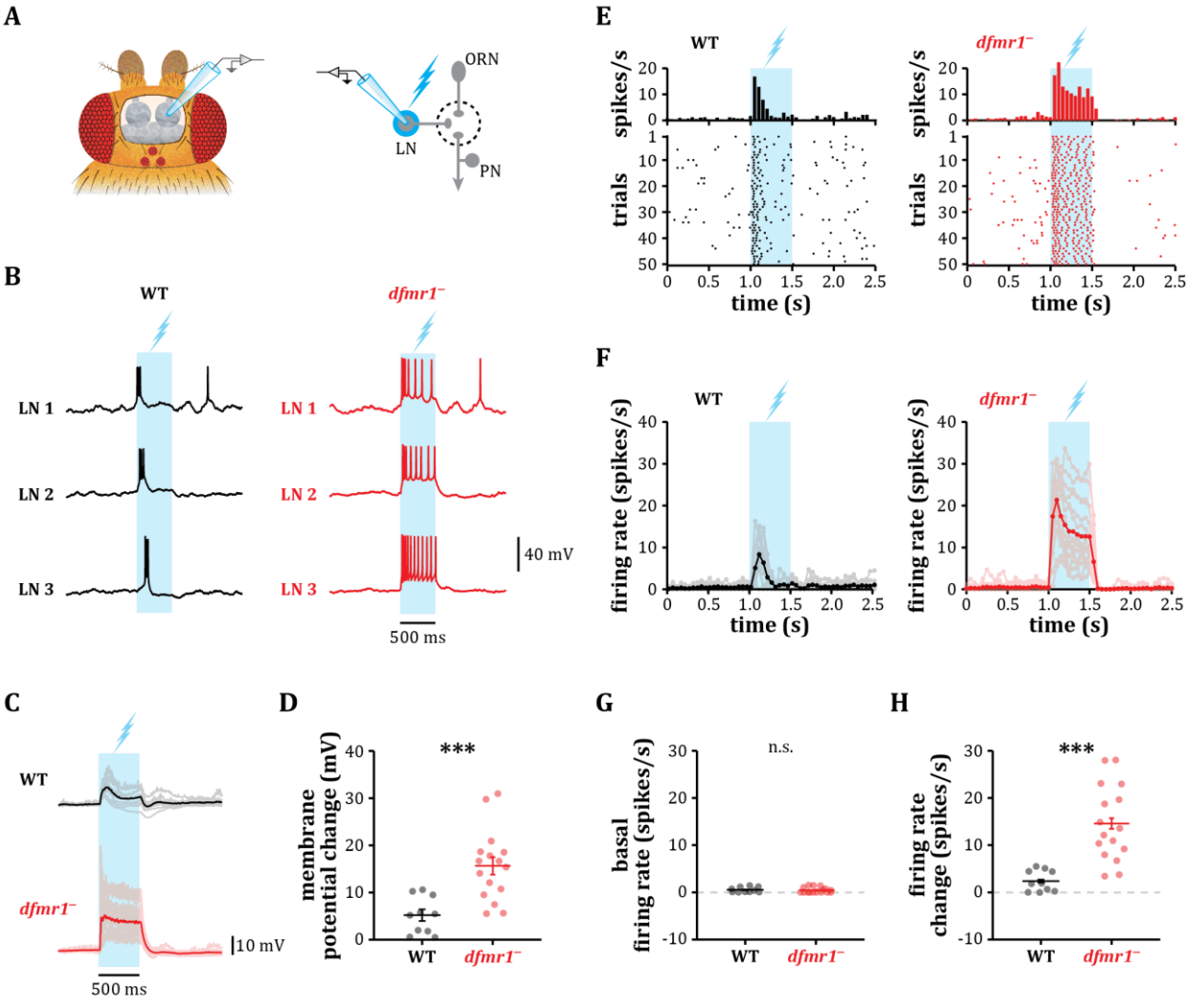

Figure 13. Local interneurons are hyperexcitable in *dfmr1*$^{-}$ flies. A. Experimental setup depicting a fly expressing the light inducible channel ChR2 in GABAergic (Das *et al.*, 2008; Okada *et al.*, 2009) local interneurons (LN). Patch clamp recordings were conducted in local interneurons (LN) expressing Ch2, while stimulating them with a flash of blue light. **B.** Representative voltage traces of local interneurons (LN). In response to optogenetic, WT local interneurons typically show a transient depolarization of their membrane potential accompanied by the firing of action potentials, followed by a period of hyperpolarization and the suppression of action potentials. By contrast, *dfmr1*$^{-}$ projection neurons exhibit a sustained depolarization accompanied by the firing of action potentials. Blue shade depicts the period of 500 ms blue light stimulation. **C.** Membrane potential of every individual local interneuron averaged over 50 trials (transparent traces) in response to optogenetic activation in WT and *dfmr1*$^{-}$ flies (WT, n = 10 cells; *dfmr1*$^{-}$, n = 16 cells). On average (full color traces), optogenetic activation of local interneurons drives an initial depolarization followed by a hyperpolarization of the membrane potential in WT flies. By contrast, in *dfmr1*$^{-}$ flies, activation of local interneurons drives a sustained depolarization with little or no inhibition. **D.** Scatter plot depicting the light evoked changes in the membrane potential of WT and *dfmr1*$^{-}$ local interneurons calculated during a 500 ms window after the onset of the blue light stimulation. *dfmr1*$^{-}$ local interneurons exhibited a larger depolarization as compared to WT local interneurons (mean ± s.e.m.; WT, n = 10 cells; *dfmr1*$^{-}$, n = 16 cells; Wilcoxon rank-sum test, $p = 2.3\text{x}10^{-4}$). **E.** Firing rates (above) and raster plots (below) of two representative local interneurons from a WT and a *dfmr1*$^{-}$ fly, respectively. Note that the initial firing of action potentials is effectively suppressed after 250 ms in the WT local interneuron. This effect is reduced in this *dfmr1*$^{-}$ projection neuron example. **F.** Firing rates (transparent traces) of all recorded WT and *dfmr1*$^{-}$ local interneurons (WT, n = 10 cells; *dfmr1*$^{-}$, n = 16 cells). On average (full color traces), the initial firing evoked by light stimulation is suppressed after 250 ms in WT local interneurons. By contrast, the initial firing of *dfmr1*$^{-}$ local interneurons is only slightly decreased. **G.** Scatter plot illustrating the basal spontaneous firing of all recorded WT and d*fmr1*$^{-}$ local interneurons, quantified during a 500 ms window before the onset of the light stimulus. No differences were found between the basal spontaneous firing of WT and *dfmr1*$^{-}$ local interneurons (mean ± s.e.m.; WT, n = 10 cells; *dfmr1*$^{-}$, n = 16 cells; Wilcoxon rank-sum test, $p = 1.9\text{x}10^{-1}$). **H.** Scatter plot showing the changes in the firing of optogenetically activated WT and d*fmr1*$^{-}$ local interneurons, calculated as the difference between the basal spontaneous firing (G) and the evoked firing during the 500 ms window of the light stimulation. The firing of action potentials evoked by light stimulation was observed to be significantly higher in *dfmr1*$^{-}$ local interneurons as compared to the firing of WT local interneurons (mean ± s.e.m.; WT, n = 10 cells; *dfmr1*$^{-}$, n = 16 cells; Wilcoxon rank-sum test, $p = 8.2\text{x}10^{-5}$).

One interesting observation is that *dfmr1*$^{-}$ flies present less strongly activated glomeruli (Figure 7A-D). This suggests that lateral excitation might be affected in the absence of dFMRP. I, therefore, recorded lateral excitatory responses in projection neurons not exhibiting spontaneous activity to optogenetic stimulation of local interneurons expressing channelrhodopsin-2 (Figure 15A). This experimental arrangement minimizes the effects produced by lateral inhibition, as most of the lateral inhibition in the antennal lobe is presynaptic (Olsen & Wilson, 2008). Optogenetic activation of local inteneurons produced an excitatory response in both, WT and *dfmr1*$^{-}$ projection neurons (Figure 15B-C). However, lateral excitatory responses tended to decay faster in *dfmr1*$^{-}$ projection neurons (Figure 15B-C) and therefore were slightly, but significantly, smaller in amplitude (Figure 15D). This observation could, in principle, explain the lower incidence of strongly activated glomeruli upon odor stimulation in *dfmr1*$^{-}$ flies (Figure 7A-D).

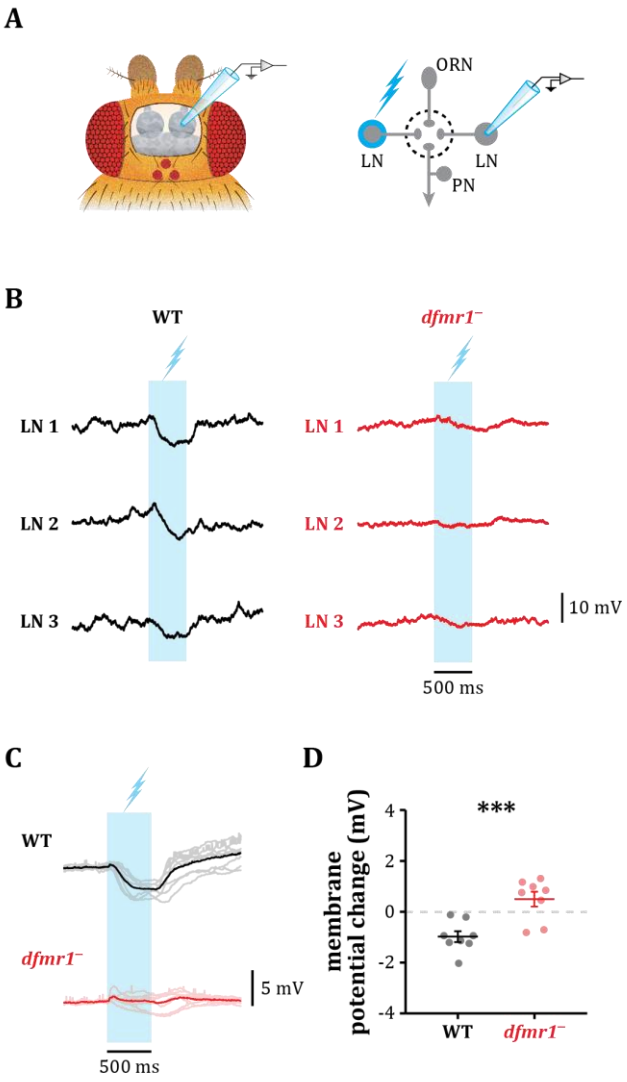

Figure 14. Lateral inhibition of local interneurons is impaired in *dfmr1*⁻ flies
A. Experimental setup depicting a fly expressing the light inducible channel ChR2 in GABAergic (Das et al., 2008; Okada et al., 2009) local interneurons (LN). Patch clamp recordings were conducted in local interneurons (LN) not expressing Ch2, while stimulating the subpopulation of local interneurons expressing ChR2 with a flash of blue light. **B.** Representative voltage traces of local interneurons (LN) not expressing ChR2. In response to optogenetic stimulation, WT local interneurons typically show a hyperpolarization of their membrane potential. By contrast, *dfmr1*⁻ projection neurons exhibit little or no hyperpolarization. Blue shade depicts the period of 500 ms blue light stimulation. **C.** Membrane potential of every individual local interneuron not expressing ChR2 averaged over 50 trials (transparent traces) in response to optogenetic activation of local interneurons expressing ChR2 in WT and *dfmr1*⁻ flies (WT, n = 7 cells; *dfmr1*⁻, n = 8 cells). On average (full color traces), optogenetic activation of local interneurons expressing ChR2 drives a hyperpolarization of the membrane potential in WT local interneurons not expressing ChR2. By contrast, in *dfmr1*⁻ flies, activation of local interneurons expressing ChR2 drives little or no inhibition in local interneurons not expressing ChR2. **D.** Scatter plot depicting the light evoked changes in the membrane potential of WT and *dfmr1*⁻ local interneurons not expressing ChR2 calculated during a 1 s window after the onset of the blue light stimulation. WT local interneurons exhibited a larger hyperpolarization as compared to *dfmr1*⁻ local interneurons (mean ± s.e.m.; WT, n = 8 cells; *dfmr1*⁻, n = 8 cells; Wilcoxon rank-sum test, $p = 9.3 \times 10^{-4}$).

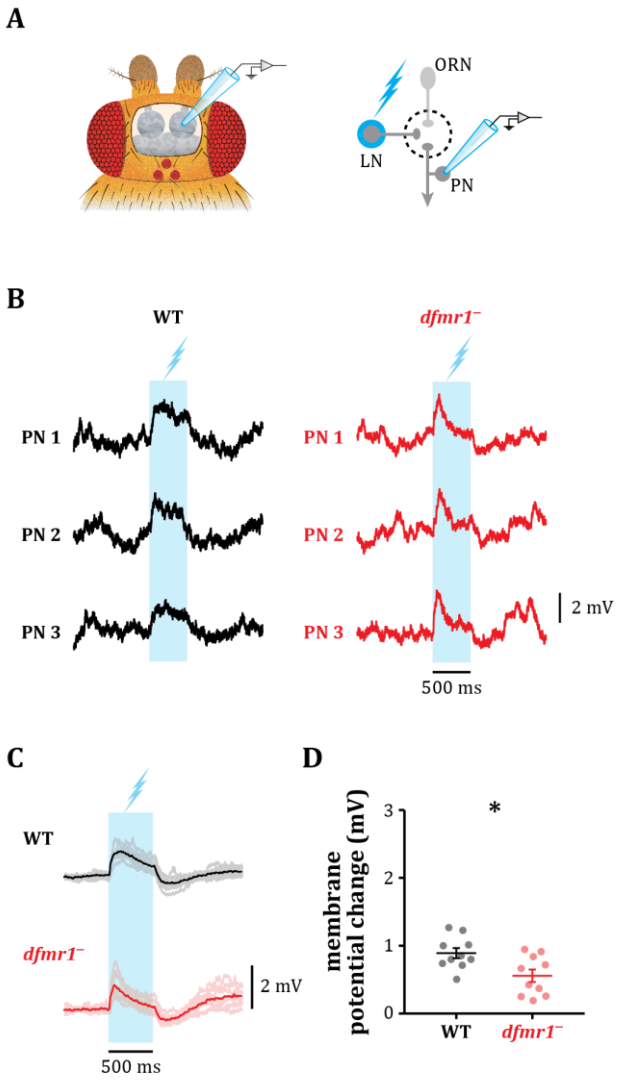

Figure 15. Lateral excitation of projection neurons is slightly reduced in *dfmr1*⁻ flies
A. Experimental setup depicting a fly expressing the light inducible channel ChR2 in GABAergic (Das et al., 2008; Okada et al., 2009) local interneurons (LN). Patch clamp recordings were conducted in projection neurons (PN) not receiving constant synaptic input from olfactory receptor neurons (ORN), while stimulating a large group of local interneurons with a flash of blue light. **B.** Representative voltage traces of projection neurons (PN). In response to optogenetic stimulation, and in the absence of spontaneous activity, WT and *dfmr1*⁻ projection neurons typically show a depolarization of their membrane potential. However, *dfmr1*⁻ projection neuron responses decay faster. Blue shade depicts the period of 500 ms blue light stimulation. **C.** Membrane potential of every individual projection neuron averaged over 50 trials (transparent traces) in response to optogenetic activation of local interneurons in WT and *dfmr1*⁻ flies (WT, n = 10 cells; *dfmr1*⁻, n = 10 cells). On average (full color traces), in the absence of spontaneous activity, optogenetic activation of local interneurons drives a depolarization of the membrane potential in WT and *dfmr1*⁻ projection neurons. However, in *dfmr1*⁻ flies, these responses decay faster. **D.** Scatter plot depicting the light evoked changes in the membrane potential of WT and *dfmr1*⁻ projection neurons calculated during a 500 ms window after the onset of the blue light stimulation. WT projection neurons exhibited a slightly larger depolarization as compared to *dfmr1*⁻ projection neurons (mean ± s.e.m.; WT, n = 10 cells; *dfmr1*⁻, n = 10 cells; Wilcoxon rank-sum test, $p = 2.6 \times 10^{-2}$).

Discussion

Deficient lateral inhibition leads to circuit hyperexcitability

Since the discovery of reduced $GABA_A$ receptor subunit expression in the absence of FMRP (D'Hulst *et al.*, 2006), accumulated evidence over the past decade has pointed towards alterations in GABAergic transmission as a key component in the neurophysiology of fragile X syndrome (reviewed by Braat & Kooy, 2015b; Contractor *et al.*, 2015). In fact, *in vitro* intracellular recordings on acute brain slices suggested that reduced inhibitory input from interneurons onto pyramidal neurons could result in an excitation/inhibition imbalance (Gibson *et al.*, 2008; Curia *et al.*, 2009). Whether this is true *in vivo* and how it might impact neuronal circuit function and behavior remained unclear. The findings reported in this thesis demonstrate that GABAergic connections established by local interneurons, which mediate lateral inhibition across antennal lobe glomeruli (Olsen & Wilson, 2008; Chou *et al.*, 2010; Hong & Wilson, 2015), are impaired in a *Drosophila melanogaster* model of fragile X syndrome. This could be a consequence of decreased GABA release from presynaptic terminals of local interneurons, reduced expression of postsynaptic GABA receptors, or both. Expression analyses support both views, as the GABA synthesizing enzyme (D'Hulst *et al.*, 2009) as well as GABA receptor subunits (D'Hulst *et al.*, 2006) are downregulated in the brain of *Drosophila melanogaster* in the absence of dFMRP. Although, further studies focusing on the particular protein expression profiles for the specific types of antennal lobe neurons are needed to elucidate this.

In addition, I show that excitatory projection neurons are hyperexcitable and exhibit reduced stimulus selectivity, which, in turn, leads to impaired olfactory computations. Importantly, the fact that less inhibitory responses are observed when parallel olfactory channels are activated by odor mixtures, which is known to activate local interneurons, indicates that impaired lateral inhibition is responsible for the hyperexitability of the antennal lobe in *dfmr1*$^{-}$ flies. Moreover, since lateral inhibition is a general information processing tool ubiquitously present in many different neuronal circuits, it is possible that absence of FMRP can produce similar deficits in lateral inhibition that impact on circuit

excitability, and thus, neuronal computations, in other sensory modalities. In consonance with this, it has been reported that circuit hyperexcitability leads to behavioral alterations in tactile, auditory and olfactory tasks in mouse models of fragile X syndrome (Rotschafer & Razak, 2013; Zhang *et al.*, 2014; Schilit Nitenson *et al.*, 2015).

Previous studies have shown that neurons are hyperexcitable in the absence of FMRP (Gibson *et al.*, 2008; Olmos-Serrano *et al.*, 2010; Goncalves *et al.*, 2013; Zhang *et al.*, 2014). However, since activation of the group 1 mGluR signaling pathway results in increased neuronal excitability (Sourdet *et al.*, 2003; Brager & Johnston, 2007), circuit hyperexcitability has been mostly attributed to the constitutively enhanced group 1 mGluR signaling observed in mouse models of fragile X syndrome (reviewed by Bear *et al.*, 2004; Dolen & Bear, 2008). Here, I show that defects in lateral GABAergic inhibition significantly contribute to circuit hyperexcitability in the fruit fly model of fragile X syndrome, which is consistent with downregulation of proteins involved in GABAergic transmission both in fruit flies and in rodents (D'Hulst *et al.*, 2006; D'Hulst *et al.*, 2009). This mechanism might explain phenotypes observed in patients with fragile X syndrome such as hypersensitivity, hyperarousal and hyperactivity, all of which reflect hyperexcitable brain states, although more studies are needed in order to validate this. Additionally, epilepsy, present in about 10-20 % of patients with fragile X syndrome (Berry-Kravis, 2002; Incorpora *et al.*, 2002; Hagerman & Stafstrom, 2009), could also be a consequence of reduced inhibition between neurons.

Absence of dFMRP does not alter the anatomical stereotypy in the antennal lobe

Every projection neuron in the fruit fly antennal lobe specifically innervates one antennal lobe glomeruli, which corresponds to a single olfactory receptor neuron type. This precise targeting of projection neuron dendrites to individual olfactory glomeruli is crucial for their odor response profiles and specificity (Wilson, 2013). Previous studies reported anatomical alterations in the branching of axons and dendrites in *dfmr1*$^{-}$ flies (Zhang *et al.*, 2001; Morales *et al.*, 2002; Galvez *et al.*, 2003; Pan *et al.*, 2004; Reeve *et al.*, 2005; Reeve *et al.*, 2008; Patel *et al.*, 2014). A potential explanation for the reduced odor specificity of projection neurons and the associated impaired olfactory coding in the antennal lobe of *dfmr1*$^{-}$ flies could be that

projection neurons present aberrant dendritic processes, innervating more than one glomerulus or a larger area within the antennal lobe. However, I did not find changes in the morphology, innervation pattern and dendritic size of identified projection neurons in *dfmr1*$^{-}$ flies.

Functional implications of deficient lateral inhibition

It has been proposed that lateral inhibition across olfactory glomeruli is important for increasing contrast among odor representations, which is important for discriminating odors (Wilson & Laurent, 2005; Olsen & Wilson, 2008; Root *et al.*, 2008; Olsen *et al.*, 2010). Interestingly, classic studies have suggested such a mechanism to be relevant for several other sensory modalities (Kuffler, 1953; Barlow *et al.*, 1957; v. Békésy, 1958; Mountcastle & Powell, 1959; Katsuki *et al.*, 1962; Rupert *et al.*, 1963; Furman, 1965). In this winner-takes-it-all model, glomeruli with most prominent odor responses would strongly activate surrounding interneurons, spreading inhibition to nearby weakly activated glomeruli. The spread of lateral inhibition, in turn, would inhibit the odor responses of weakly activated glomeruli, while strongly activated glomeruli remain as the unique encoder of the particular odor. This model also suggests that the lack of many weakly activated glomeruli, in addition to few strongly responding but very odor specific glomeruli enhances the separation of odor response patterns from one another. In line with this model, I observed that lack of lateral inhibition in the antennal lobe of *dfmr1*$^{-}$ flies indeed leads to an increase in the number of weakly activated and less odor specific glomeruli. By contrast, WT flies present more inhibitory and less weak excitatory responses, sparing strongly responding olfactory glomeruli that are more odor specific. Importantly, defects in olfactory processing have been observed in other animal models of fragile X syndrome (Schilit Nitenson *et al.*, 2015), as well as in human patients, which display hypersensitivity to smells (Rogers *et al.*, 2003), and to other sensory modalities involving lateral inhibitory mechanisms such as tactility and audition (Rogers *et al.*, 2003).

Here, I demonstrate that lateral inhibition within the antennal lobe is strongly affected in *dfmr1*$^{-}$ flies due to impaired inhibitory connections from local interneurons onto projection neurons and onto other local interneurons. The lack of this lateral inhibition on

projection neurons is probably the major cause for the increased excitability and reduced specificity in their odor responses. I propose that this compromised olfactory coding consequently leads to impaired olfactory behaviors in *dfmr1*$^{-}$ flies. More generally, I provide the missing *in vivo* evidence that the lack of dFMRP has a direct impact on sensory processing and animal behavior through a weakening of lateral inhibitory connections, which broadens response tuning of principal neurons. This mechanism might be ubiquitously present in the brain of patients with fragile X syndrome. Given the overlap between the phenotypes of fragile X syndrome and those of other neurological diseases, such as autism, Rett syndrome or Dravet syndrome and their corresponding perturbations in GABAergic transmission (Braat & Kooy, 2015a; Abdala *et al.*, 2016; Robertson *et al.*, 2016), it is possible that similar mechanisms involving reduced lateral inhibition are also present in these neurological syndromes, which are yet to be discovered.

Conclusions

Towards a unified theory of fragile X syndrome

Fragile X syndrome is a neurodevelopmental disorder whose behavioral phenotype spectrum has been attributed to a lack of maturation in the anatomy of neurons, particularly in their synapses (Irwin *et al.*, 2000). These neuronal alterations have been found to originate, at least in part, from exacerbated group 1 mGluR signaling (Bear *et al.*, 2004; Bagni & Greenough, 2005). Interestingly, it has been reported that fragile X syndrome phenotypes could be rescued by administration of group 1 mGluR antagonists, both in mice (Yan *et al.*, 2005) and in fruit flies (McBride *et al.*, 2005). Nevertheless, clinical trials on human patients using drugs that target the group 1 mGluR signaling pathway have not shown significant results so far (Braat & Kooy, 2014; Mullard, 2015).

It is possible that the observed alterations in the group 1 mGluR signaling pathway constitute just one of the components of the pathophysiology associated with fragile X syndrome. In this regard, deficits in GABAergic transmission may also play an important part in producing neurophysiological changes that underlie behavioral alterations in patients with fragile X syndrome (Braat & Kooy, 2015b). In fact, several reports indicate that absence of FMRP results in downregulation of proteins involved in GABAergic transmission (Curia *et al.*, 2009; D'Hulst *et al.*, 2009; Adusei *et al.*, 2010; Hong *et al.*, 2012; Gatto *et al.*, 2014), and, consistent with a lower inhibitory tone, that neurons are hyperexcitable in animal models of fragile X syndrome (Gibson *et al.*, 2008; Hays *et al.*, 2011; Goncalves *et al.*, 2013). The results reported in this thesis provide the missing physiological evidence showing that absence of FMRP leads to an impairment in GABAergic transmission, which further supports the idea of an inhibition impairment in fragile X syndrome. Additionally, it is likely that increased group 1 mGluR signaling (Bear *et al.*, 2004) as well as reduced GABAergic transmission (Paluszkiewicz *et al.*, 2011), both of which occur during development in the absence of FMRP, produce neuronal circuits with immature anatomy and physiological properties. Taken together, this evidence invites to consider a more integrative perspective of the pathophysiology associated with fragile X syndrome involving impaired group 1 mGluR

signaling and GABAergic transmission, which could eventually help to design effective therapies to treat this disorder.

Notably, other neurodevelopmental disorders, such as autism, Rett syndrome and Dravet syndrome have been shown to present deficits in GABAergic transmission and to share similarities in behavioral alterations (Braat & Kooy, 2015a), arguing that impaired inhibition might be an ubiquitous mechanism related to autistic disorders and epilepsy.

Neuronal computations in the absence of FMRP

One of the main consequences of the absence of FMRP is the development of neuronal circuits that are hyperexcitable (Gibson *et al.*, 2008; Hays *et al.*, 2011; Goncalves *et al.*, 2013; Zhang *et al.*, 2014). This could be either a consequence of exaggerated group 1 mGluR signaling (Merlin *et al.*, 1998; Sourdet *et al.*, 2003; Stoop *et al.*, 2003; Hays *et al.*, 2011) or reduced GABAergic transmission (this thesis; D'Hulst *et al.*, 2006; D'Hulst *et al.*, 2009), or both.

How hyperexcitability affects neuronal computations in the absence of FMRP is not fully understood. In this thesis, I present calcium imaging and electrophysiological evidence indicating that neuronal circuits exhibit a reduced computational power as a consequence of impaired lateral inhibition. This is reflected in a larger number of neurons recruited to encode a particular piece of information, which, probably, convey aberrant, not fully processed, information to downstream neuronal circuits. Moreover, given the increased overlap in the particular subsets of neurons needed to encode different pieces of information, neuronal representations are more similar to each other, which possibly influences how the brain understands its surrounding environment. In the case of patients with fragile X syndrome, this could explain not only their lower intelligence quotient, but also their particular propensity to exhibit behaviors such as hypersensitivity, hyperarousal, hyperactivity or anxiety (Hagerman *et al.*, 2009; Tranfaglia, 2011).

Another consequence of reduced inhibition is the generation of neuronal circuits that exhibit an excitation/inhibition imbalance (Paluszkiewicz *et al.*, 2011; Cea-Del Rio &

Huntsman, 2014). Importantly, it has been proposed that disruption of the excitation/inhibition balance in the brain reduces neuronal coding efficiency, deteriorating the statistics of spike trains by reducing signal entropy and increasing noise entropy. Furthermore, energy efficiency also deteriorates due to an increase in spike rates. Therefore, intact inhibitory connections are important for making spikes more informative (Sengupta *et al.*, 2013). In this regard, it is important to mention that neuronal excitation/inhibition imbalances have been associated with different types of autistic disorders, including fragile X syndrome (Rubenstein & Merzenich, 2003; Belmonte & Bourgeron, 2006).

Appendix

In vivo 3D map of the antennal lobe

For the *in vivo* calcium imaging experiments reported in this thesis, I employed fruit flies expressing the transgenic calcium indicator GCaMP6m under genetic control of the GH146 promoter. The GH146 promoter drives expression in projection neurons innervating 39 out of the 54 glomeruli of the antennal lobe (Figure A1; Grabe *et al.*, 2015).

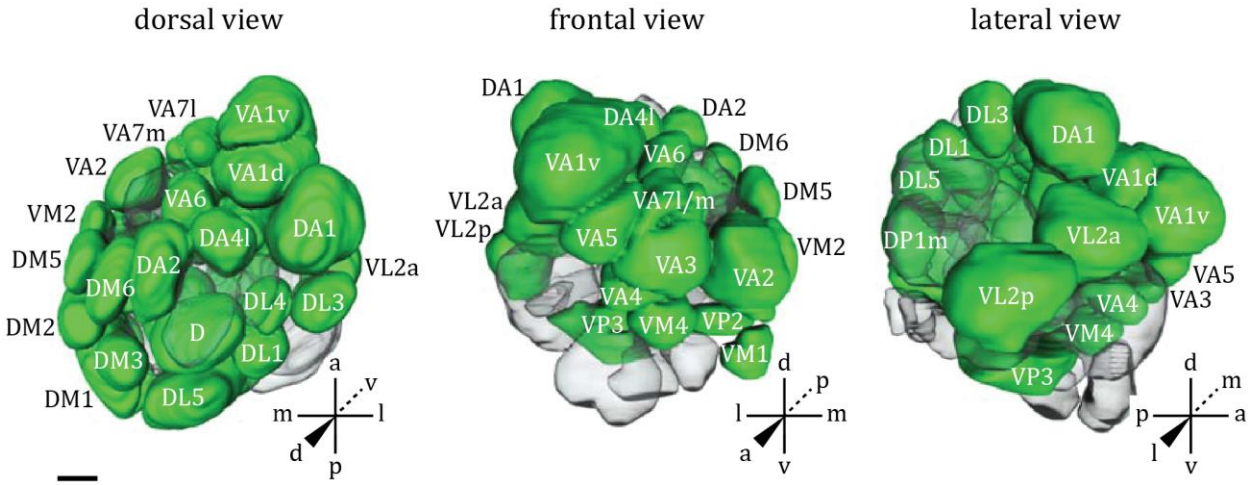

Figure A1. Innervation pattern of GH146 projection neurons. *In vivo* 3D reconstruction of the antennal lobe showing the glomerular innervations of projection neurons in which the GH146 promoter is active. Green, innervated; transparent, not innervated. Scale bar = 20 µm. (Adapted from Grabe *et al.*, 2015).

The antennal lobes were imaged dorsally using a widefield microscope. However, the focal plane was adjusted to cover as many glomeruli as possible, usually at a depth of 35 to 45 µm from the dorsal surface of the antennal lobes (Figure A2). Compare, for instance, the example map obtained by independent component analysis (Figure 3) and the map obtained by confocal microscopy at 45 µm (Figure A2).

Figure A2. *In vivo* 3D atlas of the *Drosophila* antennal lobe. A. Representative confocal stack of an *in vivo* antennal lobe expressing the END1-2 neuropil labeling. Eight planes from dorsal to ventral (top to bottom) through a female antennal lobe are shown at 10 µm intervals displayed in an inverted gray scale. **B.** Identified and reconstructed glomeruli of the confocal stack shown in A. **C.** Dorsal view on the 3D reconstruction of the labels shown in B. The glomeruli are successively removed as the scan moves from dorsal to ventral through the antennal lobe. The color code indicates the classes of sensilla as shown in Figure VI, extended by glomeruli that receive input from the grooved coeloconic sensilla of the sacculus and the aristal shaft (shown in gray). Scale bar = 20 µm. (Adapted from Grabe *et al.*, 2015).

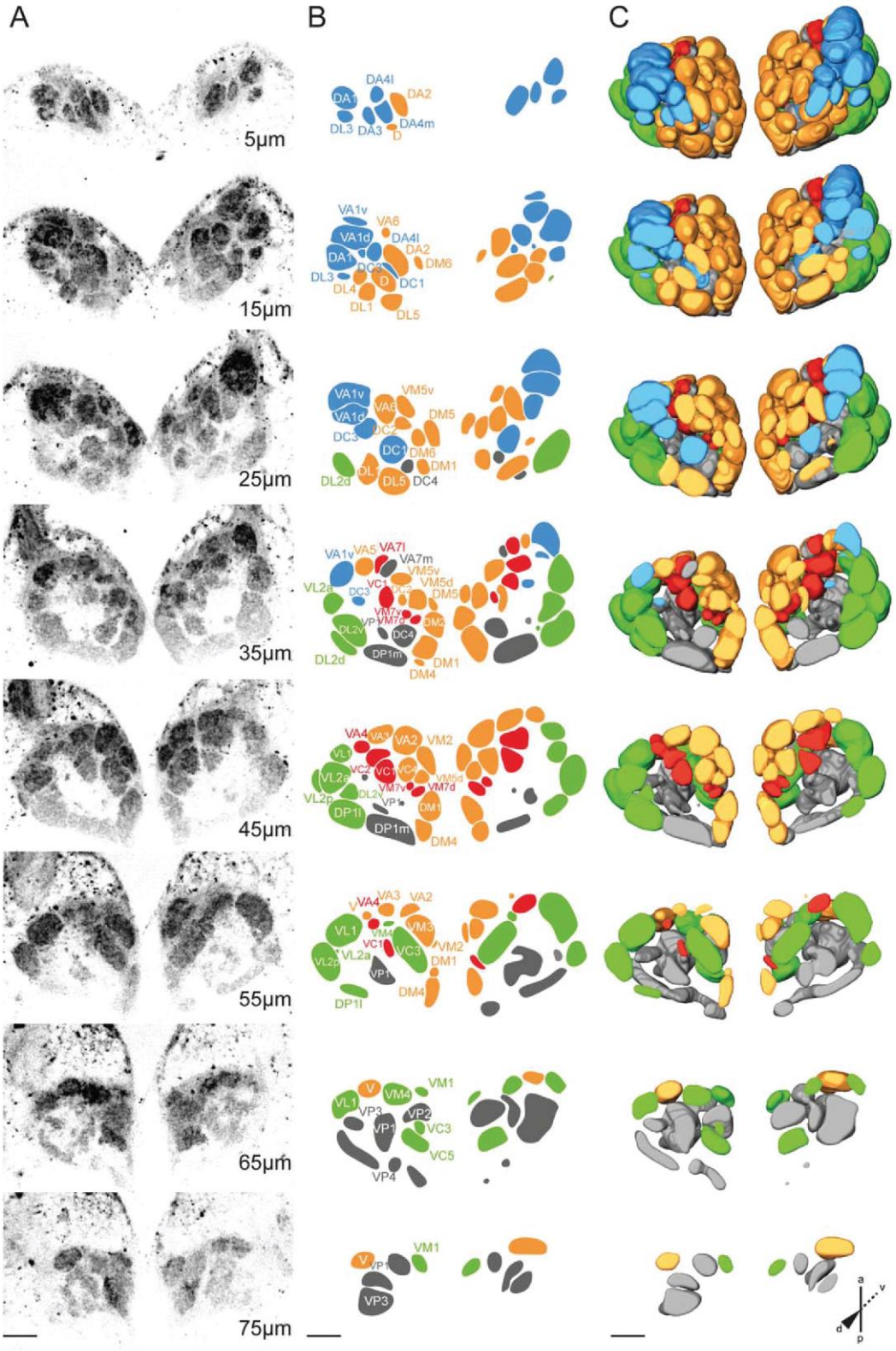
A
B
C
5µm
15µm
25µm
35µm
45µm
55µm
65µm
75µm
DA4l
DA1
DA2
DL3
DA3
DA4m
D
VA1v
VA6
VA1d
DA4l
DA2
DA1
DM6
DC3
DL3
D
DC1
DL4
DL1
DL5
VM5v
VA6
VA1d
DM5
DC2
DC3
DC1
DM6
DM1
DL2d
DL
DL5
DC4
VA1v
VA5
VA7l
VA7m
VM5v
VL2a
DC3
VC1
VM5d
DM5
VM7v
VP1
VM7d
DM2
DL2v
DC4
DL2d
DP1m
DM1
DM4
VA4
VA3
VA2
VM2
VL1
VC2
VC1
VC4
VM5d
VL2a
VM7v
VM7d
VL2p
DL2v
VP1
DP1l
DM1
DP1m
DM4
VA4
VA3
VA2
VL1
VM4
VM3
VC1
VM2
VL2a
VC3
DM1
VL2p
VP1
DM4
DP1l
VM1
VL1
VM4
VP3
VP2
VP1
VC3
VC5
VP4
VM1
VP3
a
v
d
p

Pairwise distances

In this thesis, I compare olfactory neuronal representations by calculating the pairwise distances between them. Different metrics have been developed for this. However, I only focused on two of them, Euclidean and cosine. The main difference between them is that the Euclidean metric takes the amplitude of the responses into account, whereas the cosine metric focuses on the given *direction* of the representation.

The Euclidean distance between two vectors p and q in a n-space is defined as:

$$d(p,q) = \sqrt{\sum_{i=1}^{n}(q_i - p_i)^2}$$

In turn, the cosine distance between two vectors p and q in a n-space is:

$$d(p,q) = 1 - \cos\theta = 1 - \frac{\sum_{i=1}^{n} p_i q_i}{\sqrt{\sum_{i=1}^{n} p_i^2}\sqrt{\sum_{i=1}^{n} q_i^2}}$$

In the particular case of the olfactory computations studied in this thesis, these equations describe how similar odors (vectors) are represented by the n glomeruli (space) of the antennal lobe.

Consider, for instance, that three odors, A, B and C, are encoded by the calcium responses (ΔF/F) of three glomeruli, 1, 2 and 3:

	odor A	odor B	odor C
glomerulus 1	8	0	0
glomerulus 2	0	6	3
glomerulus 3	4	8	4

The Euclidean distances among the vectors representing the neuronal encoding of odors A, B and C are the geometrical distances among them in the space denoted by glomeruli 1, 2 and 3 (see Figure A3A):

	odor A	odor B	odor C
odor A	0	10.8	8.5
odor B	10.8	0	5
odor C	8.5	5	0

Additionally, their corresponding cosine distances are the complement of the cosine of the angles among such vectors (see Figure A3B):

	odor A	odor B	odor C
odor A	0	0.6	0.6
odor B	0.6	0	0
odor C	0.6	0	0

It is important to mention when two vectors of different magnitude project to the same space, in this particular example odors B and C, they might be separated by a given Euclidean distance, but they might not be separated by a cosine distance (Figure A3). In the case of the calcium glomerular representations reported in this thesis, this signifies that the cosine metric is a more robust metric better positioned to compare odor representations based on the particular olfactory channels (glomeruli) being activated or inhibited by the different odors. By contrast, the Euclidean metric is a more sensible metric better position to measure differences in odor representations encoded by similar subsets of glomeruli displaying similar response profiles.

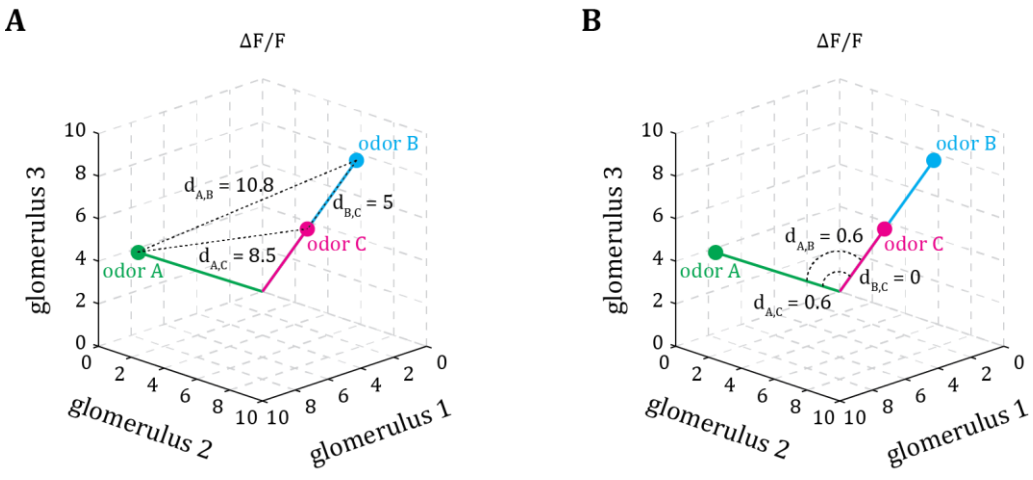

Figure A3. Euclidean and cosine distances. **A.** The Euclidean distance between two vectors is the geometrical distance between them. **B.** The cosine distance between two vectors is the complement of the cosine of the angle between them, or, 1-cos(θ).

Physiological identification of projection neurons and local interneurons

For the electrophysiological experiments reported in this thesis, proper discrimination of projection neurons and local interneurons was required. In this regard, it is worth mentioning that projection neuron somas are relatively smaller than lateral interneuron somas. Moreover, projection neuron action potentials are typically lower than 10 mV in amplitude whereas local interneuron action potentials usually present an amplitude of 40 mV (Figure A4; Wilson *et al.*, 2004).

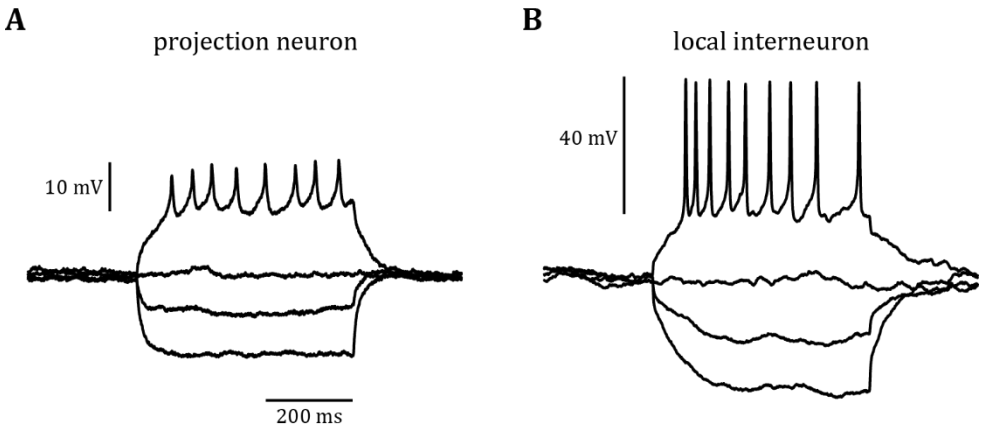

Figure A4. Projection neuron and lateral interneuron. **A.** Voltage steps corresponding to a projection neuron. **B.** Voltage steps corresponding to a lateral interneuron. Note that action potentials fired by projection neurons present a lower amplitude than action potentials fired by local interneurons.

Additionally, and for the particular conditions of the optogenetics experiments carried out in this thesis, identification of projection neurons and local interneurons was possible via their corresponding characteristic responses to the light stimulation of local interneurons expressing channelrhodopsin-2. Projection neurons typically show a hyperpolarization of their membrane potential accompanied by a decrease in their spontaneous firing of action potentials. Local interneurons, by contrast, exhibit an initial depolarization accompanied by the firing of action potentials, which is followed by a hyperpolarization of their membrane potential and the cessation of firing of action potentials (Figure A5). The hyperpolarization of both projection neurons and local interneurons reflects the inhibition driven by GABAergic lateral connections established by local interneurons on sister local interneurons as well as on olfactory receptor neuron presynaptic terminals (Okada *et al.*, 2009; Tanaka *et al.*, 2011).

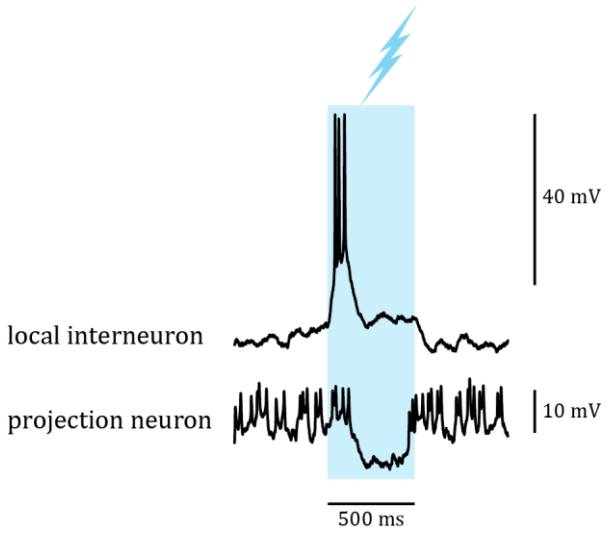

Figure A5. Projection neuron and local interneuron responses to light stimulation. Upon light stimulation of local interneurons expressing channelrhodopsin-2, projection neurons typically show hyperpolarization of their membrane potential as well as a decrease in their spontaneous firing of action potentials. By contrast, light stimulation of those local interneurons expressing channelrhodopsin-2 results in an initial depolarization accompanied by the firing of action potentials, which is followed by a hyperpolarization of their membrane potential. The latter hyperpolarization reflects lateral inhibition from other local interneurons expressing channelrhodopsin-2.

References

Aakalu, G., Smith, W.B., Nguyen, N., Jiang, C. & Schuman, E.M. (2001) Dynamic visualization of local protein synthesis in hippocampal neurons. *Neuron*, 30, 489-502.

Abdala, A.P., Toward, M.A., Dutschmann, M., Bissonnette, J.M. & Paton, J.F. (2016) Deficiency of GABAergic synaptic inhibition in the Kolliker-Fuse area underlies respiratory dysrhythmia in a mouse model of Rett syndrome. *J. Physiol.*, 594, 223-237.

Abuin, L., Bargeton, B., Ulbrich, M.H., Isacoff, E.Y., Kellenberger, S. & Benton, R. (2011) Functional architecture of olfactory ionotropic glutamate receptors. *Neuron*, 69, 44-60.

Adusei, D.C., Pacey, L.K., Chen, D. & Hampson, D.R. (2010) Early developmental alterations in GABAergic protein expression in fragile X knockout mice. *Neuropharmacology*, 59, 167-171.

Akerman, C.J. & Cline, H.T. (2006) Depolarizing GABAergic conductances regulate the balance of excitation to inhibition in the developing retinotectal circuit in vivo. *J. Neurosci.*, 26, 5117-5130.

Ashley, C.T., Jr., Wilkinson, K.D., Reines, D. & Warren, S.T. (1993) FMR1 protein: conserved RNP family domains and selective RNA binding. *Science*, 262, 563-566.

Bagni, C. & Greenough, W.T. (2005) From mRNP trafficking to spine dysmorphogenesis: the roots of fragile X syndrome. *Nat. Rev. Neurosci.*, 6, 376-387.

Bailey, D.B., Jr., Hatton, D.D., Skinner, M. & Mesibov, G. (2001) Autistic behavior, FMR1 protein, and developmental trajectories in young males with fragile X syndrome. *J. Autism Dev. Disord.*, 31, 165-174.

Bailey, D.B., Jr., Raspa, M., Olmsted, M. & Holiday, D.B. (2008) Co-occurring conditions associated with FMR1 gene variations: findings from a national parent survey. *Am. J. Med. Genet.*, 146A, 2060-2069.

Bakker, C.E., Verheij, C., Willemsen, R., van der Helm, R., Oerlemans, F., Vermey, M., Bygrave, A., Hoogeveen, A.T., Oostra, B.A., Reynierse, E., De Boulee, K., D'Hoogeg, R., Crasf, P., van Velzene, D., Nagelsg, G., Martinf, J.J., De Deyng, P.P., Darbye, J.K. & Willems, P.J. (1994) Fmr1 knockout mice: a model to study fragile X mental retardation. The Dutch-Belgian Fragile X Consortium. *Cell*, 78, 23-33.

Barlow, H.B., Fitzhugh, R. & Kuffler, S.W. (1957) Change of organization in the receptive fields of the cat's retina during dark adaptation. *J. Physiol.*, 137, 338-354.

Barnwell, L.F., Lugo, J.N., Lee, W.L., Willis, S.E., Gertz, S.J., Hrachovy, R.A. & Anderson, A.E. (2009) Kv4.2 knockout mice demonstrate increased susceptibility to convulsant stimulation. *Epilepsia*, 50, 1741-1751.

Bassell, G.J. & Warren, S.T. (2008) Fragile X syndrome: loss of local mRNA regulation alters synaptic development and function. *Neuron*, 60, 201-214.

Bear, M.F., Huber, K.M. & Warren, S.T. (2004) The mGluR theory of fragile X mental retardation. *Trends Neurosci.*, 27, 370-377.

Bechara, E.G., Didiot, M.C., Melko, M., Davidovic, L., Bensaid, M., Martin, P., Castets, M., Pognonec, P., Khandjian, E.W., Moine, H. & Bardoni, B. (2009) A novel function for fragile X mental retardation protein in translational activation. *PLoS Biol.*, 7, e16.

Belmonte, M.K. & Bourgeron, T. (2006) Fragile X syndrome and autism at the intersection of genetic and neural networks. *Nat. Neurosci.*, 9, 1221-1225.

Benarroch, E.E. (2012) GABAB receptors: structure, functions, and clinical implications. *Neurology*, 78, 578-584.

Benhassine, N. & Berger, T. (2009) Large-conductance calcium-dependent potassium channels prevent dendritic excitability in neocortical pyramidal neurons. *Pflugers Arch*, 457, 1133-1145.

Benton, R., Sachse, S., Michnick, S.W. & Vosshall, L.B. (2006) Atypical membrane topology and heteromeric function of *Drosophila* odorant receptors in vivo. *PLoS Biol.*, 4, e20.

Benton, R., Vannice, K.S., Gomez-Diaz, C. & Vosshall, L.B. (2009) Variant ionotropic glutamate receptors as chemosensory receptors in *Drosophila*. *Cell*, 136, 149-162.

Berry-Kravis, E. (2002) Epilepsy in fragile X syndrome. *Dev. Med. Child Neurol.*, 44, 724-728.

Berry-Kravis, E., Abrams, L., Coffey, S.M., Hall, D.A., Greco, C., Gane, L.W., Grigsby, J., Bourgeois, J.A., Finucane, B., Jacquemont, S., Brunberg, J.A., Zhang, L., Lin, J., Tassone, F., Hagerman, P.J., Hagerman, R.J. & Leehey, M.A. (2007) Fragile X-associated tremor/ataxia syndrome: clinical features, genetics, and testing guidelines. *Mov. Disord.*, 22, 2018-2030.

Bettler, B., Kaupmann, K., Mosbacher, J. & Gassmann, M. (2004) Molecular structure and physiological functions of GABA(B) receptors. *Physiol. Rev.*, 84, 835-867.

Bhandawat, V., Maimon, G., Dickinson, M.H. & Wilson, R.I. (2010) Olfactory modulation of flight in *Drosophila* is sensitive, selective and rapid. *J. Exp. Biol.*, 213, 3625-3635.

Bhandawat, V., Olsen, S.R., Gouwens, N.W., Schlief, M.L. & Wilson, R.I. (2007) Sensory processing in the *Drosophila* antennal lobe increases reliability and separability of ensemble odor representations. *Nat. Neurosci.*, 10, 1474-1482.

Bhogal, B. & Jongens, T.A. (2010) Fragile X syndrome and model organisms: identifying potential routes of therapeutic intervention. *Dis. Model. Mech.*, 3, 693-700.

Birnbaum, S.G., Varga, A.W., Yuan, L.L., Anderson, A.E., Sweatt, J.D. & Schrader, L.A. (2004) Structure and function of Kv4-family transient potassium channels. *Physiol. Rev.*, 84, 803-833.

Bolduc, F.V., Bell, K., Cox, H., Broadie, K.S. & Tully, T. (2008) Excess protein synthesis in *Drosophila* fragile X mutants impairs long-term memory. *Nat. Neurosci.*, 11, 1143-1145.

Braat, S. & Kooy, R.F. (2014) Fragile X syndrome neurobiology translates into rational therapy. *Drug Discov. Today*, 19, 510-519.

Braat, S. & Kooy, R.F. (2015a) The GABAA Receptor as a Therapeutic Target for Neurodevelopmental Disorders. *Neuron*, 86, 1119-1130.

Braat, S. & Kooy, R.F. (2015b) Insights into GABAAergic system deficits in fragile X syndrome lead to clinical trials. *Neuropharmacology*, 88, 48-54.

Brager, D.H. & Johnston, D. (2007) Plasticity of intrinsic excitability during long-term depression is mediated through mGluR-dependent changes in I(h) in hippocampal CA1 pyramidal neurons. *J. Neurosci.*, 27, 13926-13937.

Brown, M.R., Kronengold, J., Gazula, V.R., Chen, Y., Strumbos, J.G., Sigworth, F.J., Navaratnam, D. & Kaczmarek, L.K. (2010) Fragile X mental retardation protein controls gating of the sodium-activated potassium channel Slack. *Nat. Neurosci.*, 13, 819-821.

Brown, V., Jin, P., Ceman, S., Darnell, J.C., O'Donnell, W.T., Tenenbaum, S.A., Jin, X., Feng, Y., Wilkinson, K.D., Keene, J.D., Darnell, R.B. & Warren, S.T. (2001) Microarray identification of FMRP-associated brain mRNAs and altered mRNA translational profiles in fragile X syndrome. *Cell*, 107, 477-487.

Budimirovic, D.B. & Kaufmann, W.E. (2011) What can we learn about autism from studying fragile X syndrome? *Dev. Neurosci.*, 33, 379-394.

Carandini, M. & Heeger, D.J. (2012) Normalization as a canonical neural computation. *Nat. Rev. Neurosci.*, 13, 51-62.

Cea-Del Rio, C.A. & Huntsman, M.M. (2014) The contribution of inhibitory interneurons to circuit dysfunction in Fragile X Syndrome. *Front. Cell. Neurosci.*, 8, 245.

Ceman, S., O'Donnell, W.T., Reed, M., Patton, S., Pohl, J. & Warren, S.T. (2003) Phosphorylation influences the translation state of FMRP-associated polyribosomes. *Hum. Mol. Genet.*, 12, 3295-3305.

Centonze, D., Rossi, S., Mercaldo, V., Napoli, I., Ciotti, M.T., De Chiara, V., Musella, A., Prosperetti, C., Calabresi, P., Bernardi, G. & Bagni, C. (2008) Abnormal striatal GABA transmission in the mouse model for the fragile X syndrome. *Biol. Psychiatry*, 63, 963-973.

Chattopadhyaya, B., Di Cristo, G., Wu, C.Z., Knott, G., Kuhlman, S., Fu, Y., Palmiter, R.D. & Huang, Z.J. (2007) GAD67-mediated GABA synthesis and signaling regulate inhibitory synaptic innervation in the visual cortex. *Neuron*, 54, 889-903.

Chen, L. & Toth, M. (2001) Fragile X mice develop sensory hyperreactivity to auditory stimuli. *Neuroscience*, 103, 1043-1050.

Chen, X., Yuan, L.L., Zhao, C., Birnbaum, S.G., Frick, A., Jung, W.E., Schwarz, T.L., Sweatt, J.D. & Johnston, D. (2006) Deletion of Kv4.2 gene eliminates dendritic A-type K+ current and enhances induction of long-term potentiation in hippocampal CA1 pyramidal neurons. *J. Neurosci.*, 26, 12143-12151.

Chou, Y.H., Spletter, M.L., Yaksi, E., Leong, J.C., Wilson, R.I. & Luo, L. (2010) Diversity and wiring variability of olfactory local interneurons in the *Drosophila* antennal lobe. *Nat. Neurosci.*, 13, 439-449.

Chuang, S.C., Zhao, W., Bauchwitz, R., Yan, Q., Bianchi, R. & Wong, R.K. (2005) Prolonged epileptiform discharges induced by altered group I metabotropic glutamate receptor-mediated synaptic responses in hippocampal slices of a fragile X mouse model. *J. Neurosci.*, 25, 8048-8055.

Chudley, A.E. & Hagerman, R.J. (1987) Fragile X syndrome. *J. Pediatr.*, 110, 821-831.

Cirelli, C. (2006) Sleep disruption, oxidative stress, and aging: new insights from fruit flies. *Proc. Natl. Acad. Sci. USA*, 103, 13901-13902.

Clifford, S., Dissanayake, C., Bui, Q.M., Huggins, R., Taylor, A.K. & Loesch, D.Z. (2007) Autism spectrum phenotype in males and females with fragile X full mutation and premutation. *J. Autism Dev. Disord.*, 37, 738-747.

Coffee, B., Zhang, F., Ceman, S., Warren, S.T. & Reines, D. (2002) Histone modifications depict an aberrantly heterochromatinized FMR1 gene in fragile X syndrome. *Am. J. Hum. Genet.*, 71, 923-932.

Coffee, B., Zhang, F., Warren, S.T. & Reines, D. (1999) Acetylated histones are associated with FMR1 in normal but not fragile X-syndrome cells. *Nat. Genet.*, 22, 98-101.

Comery, T.A., Harris, J.B., Willems, P.J., Oostra, B.A., Irwin, S.A., Weiler, I.J. & Greenough, W.T. (1997) Abnormal dendritic spines in fragile X knockout mice: maturation and pruning deficits. *Proc. Natl. Acad. Sci. USA*, 94, 5401-5404.

Contractor, A., Klyachko, V.A. & Portera-Cailliau, C. (2015) Altered Neuronal and Circuit Excitability in Fragile X Syndrome. *Neuron*, 87, 699-715.

Couto, A., Alenius, M. & Dickson, B.J. (2005) Molecular, anatomical, and functional organization of the *Drosophila* olfactory system. *Curr. Biol.*, 15, 1535-1547.

Curia, G., Papouin, T., Seguela, P. & Avoli, M. (2009) Downregulation of tonic GABAergic inhibition in a mouse model of fragile X syndrome. *Cereb. Cortex*, 19, 1515-1520.

D'Hulst, C., De Geest, N., Reeve, S.P., Van Dam, D., De Deyn, P.P., Hassan, B.A. & Kooy, R.F. (2006) Decreased expression of the GABAA receptor in fragile X syndrome. *Brain Res.*, 1121, 238-245.

D'Hulst, C., Heulens, I., Brouwer, J.R., Willemsen, R., De Geest, N., Reeve, S.P., De Deyn, P.P., Hassan, B.A. & Kooy, R.F. (2009) Expression of the GABAergic system in animal models for fragile X syndrome and fragile X associated tremor/ataxia syndrome (FXTAS). *Brain Res.*, 1253, 176-183.

D'Hulst, C. & Kooy, R.F. (2007) The GABAA receptor: a novel target for treatment of fragile X? *Trends Neurosci.*, 30, 425-431.

Darnell, J.C. & Klann, E. (2013) The translation of translational control by FMRP: therapeutic targets for FXS. *Nat. Neurosci.*, 16, 1530-1536.

Darnell, J.C., Van Driesche, S.J., Zhang, C., Hung, K.Y., Mele, A., Fraser, C.E., Stone, E.F., Chen, C., Fak, J.J., Chi, S.W., Licatalosi, D.D., Richter, J.D. & Darnell, R.B. (2011) FMRP stalls ribosomal translocation on mRNAs linked to synaptic function and autism. *Cell*, 146, 247-261.

Das, A., Chiang, A., Davla, S., Priya, R., Reichert, H., Vijayraghavan, K. & Rodrigues, V. (2011) Identification and analysis of a glutamatergic local interneuron lineage in the adult *Drosophila* olfactory system. *Neural Syst. Circuits*, 1, 4.

Das, A., Sen, S., Lichtneckert, R., Okada, R., Ito, K., Rodrigues, V. & Reichert, H. (2008) *Drosophila* olfactory local interneurons and projection neurons derive from a common neuroblast lineage specified by the empty spiracles gene. *Neural Dev.*, 3, 33.

De Boulle, K., Verkerk, A.J., Reyniers, E., Vits, L., Hendrickx, J., Van Roy, B., Van den Bos, F., de Graaff, E., Oostra, B.A. & Willems, P.J. (1993) A point mutation in the FMR-1 gene associated with fragile X mental retardation. *Nat. Genet.*, 3, 31-35.

de Bruyne, M., Clyne, P.J. & Carlson, J.R. (1999) Odor coding in a model olfactory organ: the *Drosophila* maxillary palp. *J. Neurosci.*, 19, 4520-4532.

de Bruyne, M., Foster, K. & Carlson, J.R. (2001) Odor coding in the *Drosophila* antenna. *Neuron*, 30, 537-552.

de Vries, B.B., Fryns, J.P., Butler, M.G., Canziani, F., Wesby-van Swaay, E., van Hemel, J.O., Oostra, B.A., Halley, D.J. & Niermeijer, M.F. (1993) Clinical and molecular studies in fragile X patients with a Prader-Willi-like phenotype. *J. Med. Genet.*, 30, 761-766.

den Broeder, M.J., van der Linde, H., Brouwer, J.R., Oostra, B.A., Willemsen, R. & Ketting, R.F. (2009) Generation and characterization of FMR1 knockout zebrafish. *PLoS One*, 4, e7910.

Deng, P.Y., Rotman, Z., Blundon, J.A., Cho, Y., Cui, J., Cavalli, V., Zakharenko, S.S. & Klyachko, V.A. (2013) FMRP regulates neurotransmitter release and synaptic information transmission by modulating action potential duration via BK channels. *Neuron*, 77, 696-711.

Dockendorff, T.C., Su, H.S., McBride, S.M., Yang, Z., Choi, C.H., Siwicki, K.K., Sehgal, A. & Jongens, T.A. (2002) *Drosophila* lacking dfmr1 activity show defects in circadian output and fail to maintain courtship interest. *Neuron*, 34, 973-984.

Dolen, G. & Bear, M.F. (2008) Role for metabotropic glutamate receptor 5 (mGluR5) in the pathogenesis of fragile X syndrome. *J. Physiol.*, 586, 1503-1508.

Edbauer, D., Neilson, J.R., Foster, K.A., Wang, C.F., Seeburg, D.P., Batterton, M.N., Tada, T., Dolan, B.M., Sharp, P.A. & Sheng, M. (2010) Regulation of synaptic structure and function by FMRP-associated microRNAs miR-125b and miR-132. *Neuron*, 65, 373-384.

el Bekay, R., Romero-Zerbo, Y., Decara, J., Sanchez-Salido, L., Del Arco-Herrera, I., Rodriguez-de Fonseca, F. & de Diego-Otero, Y. (2007) Enhanced markers of oxidative stress, altered antioxidants and NADPH-oxidase activation in brains from Fragile X mental retardation 1-deficient mice, a pathological model for Fragile X syndrome. *Eur. J. Neurosci.*, 26, 3169-3180.

El Idrissi, A., Ding, X.H., Scalia, J., Trenkner, E., Brown, W.T. & Dobkin, C. (2005) Decreased GABA(A) receptor expression in the seizure-prone fragile X mouse. *Neurosci. Lett.*, 377, 141-146.

Faber, E.S. & Sah, P. (2003) Ca2+-activated K+ (BK) channel inactivation contributes to spike broadening during repetitive firing in the rat lateral amygdala. *J. Physiol.*, 552, 483-497.

Farhan, A., Gulati, J., Grobetae-Wilde, E., Vogel, H., Hansson, B.S. & Knaden, M. (2013) The CCHamide 1 receptor modulates sensory perception and olfactory behavior in starved *Drosophila*. *Sci. Rep.*, 3, 2765.

Farrant, M. & Nusser, Z. (2005) Variations on an inhibitory theme: phasic and tonic activation of GABA(A) receptors. *Nat. Rev. Neurosci.*, 6, 215-229.

Fiala, J.C., Feinberg, M., Popov, V. & Harris, K.M. (1998) Synaptogenesis via dendritic filopodia in developing hippocampal area CA1. *J. Neurosci.*, 18, 8900-8911.

Fishilevich, E., Domingos, A.I., Asahina, K., Naef, F., Vosshall, L.B. & Louis, M. (2005) Chemotaxis behavior mediated by single larval olfactory neurons in *Drosophila*. *Curr. Biol.*, 15, 2086-2096.

Fishilevich, E. & Vosshall, L.B. (2005) Genetic and functional subdivision of the *Drosophila* antennal lobe. *Curr. Biol.*, 15, 1548-1553.

Fryns, J.P., Haspeslagh, M., Dereymaeker, A.M., Volcke, P. & Van den Berghe, H. (1987) A peculiar subphenotype in the fra(X) syndrome: extreme obesity-short stature-stubby hands and feet-diffuse hyperpigmentation. Further evidence of disturbed hypothalamic function in the fra(X) syndrome? *Clin. Genet.*, 32, 388-392.

Fu, Y.H., Kuhl, D.P., Pizzuti, A., Pieretti, M., Sutcliffe, J.S., Richards, S., Verkerk, A.J., Holden, J.J., Fenwick, R.G., Jr., Warren, S.T. & et al. (1991) Variation of the CGG repeat at the fragile X site results in genetic instability: resolution of the Sherman paradox. *Cell*, 67, 1047-1058.

Furman, G.G. (1965) Comparison of models for subtractive and shunting lateral-inhibition in receptor-neuron fields. *Kybernetik*, 2, 257-274.

Galvez, R., Gopal, A.R. & Greenough, W.T. (2003) Somatosensory cortical barrel dendritic abnormalities in a mouse model of the fragile X mental retardation syndrome. *Brain Res.*, 971, 83-89.

Gan, L. & Kaczmarek, L.K. (1998) When, where, and how much? Expression of the Kv3.1 potassium channel in high-frequency firing neurons. *J. Neurobiol.*, 37, 69-79.

Gantois, I., Vandesompele, J., Speleman, F., Reyniers, E., D'Hooge, R., Severijnen, L.A., Willemsen, R., Tassone, F. & Kooy, R.F. (2006) Expression profiling suggests underexpression of the GABA(A) receptor subunit delta in the fragile X knockout mouse model. *Neurobiol. Dis.*, 21, 346-357.

Gao, Q., Yuan, B. & Chess, A. (2000) Convergent projections of *Drosophila* olfactory neurons to specific glomeruli in the antennal lobe. *Nat. Neurosci.*, 3, 780-785.

Gassmann, M. & Bettler, B. (2012) Regulation of neuronal GABA(B) receptor functions by subunit composition. *Nat. Rev. Neurosci.*, 13, 380-394.

Gatto, C.L. & Broadie, K. (2008) Temporal requirements of the fragile X mental retardation protein in the regulation of synaptic structure. *Development*, 135, 2637-2648.

Gatto, C.L., Pereira, D. & Broadie, K. (2014) GABAergic circuit dysfunction in the *Drosophila* Fragile X syndrome model. *Neurobiol. Dis.*, 65, 142-159.

Gaudry, Q., Hong, E.J., Kain, J., de Bivort, B.L. & Wilson, R.I. (2013) Asymmetric neurotransmitter release enables rapid odour lateralization in *Drosophila*. *Nature*, 493, 424-428.

Gibson, J.R., Bartley, A.F., Hays, S.A. & Huber, K.M. (2008) Imbalance of neocortical excitation and inhibition and altered UP states reflect network hyperexcitability in the mouse model of fragile X syndrome. *J. Neurophysiol.*, 100, 2615-2626.

Gingrich, J.A. (2005) Oxidative stress is the new stress. *Nat. Med.*, 11, 1281-1282.

Goncalves, J.T., Anstey, J.E., Golshani, P. & Portera-Cailliau, C. (2013) Circuit level defects in the developing neocortex of Fragile X mice. *Nat. Neurosci.*, 16, 903-909.

Grabe, V., Strutz, A., Baschwitz, A., Hansson, B.S. & Sachse, S. (2015) Digital in vivo 3D atlas of the antennal lobe of *Drosophila melanogaster*. *J. Comp. Neurol.*, 523, 530-544.

Greco, C.M., Berman, R.F., Martin, R.M., Tassone, F., Schwartz, P.H., Chang, A., Trapp, B.D., Iwahashi, C., Brunberg, J., Grigsby, J., Hessl, D., Becker, E.J., Papazian, J., Leehey, M.A., Hagerman, R.J. & Hagerman, P.J. (2006) Neuropathology of fragile X-associated tremor/ataxia syndrome (FXTAS). *Brain*, 129, 243-255.

Greco, C.M., Hagerman, R.J., Tassone, F., Chudley, A.E., Del Bigio, M.R., Jacquemont, S., Leehey, M. & Hagerman, P.J. (2002) Neuronal intranuclear inclusions in a new cerebellar tremor/ataxia syndrome among fragile X carriers. *Brain*, 125, 1760-1771.

Gronskov, K., Brondum-Nielsen, K., Dedic, A. & Hjalgrim, H. (2011) A nonsense mutation in FMR1 causing fragile X syndrome. *Eur. J. Hum. Genet.*, 19, 489-491.

Gross, C., Yao, X., Pong, D.L., Jeromin, A. & Bassell, G.J. (2011) Fragile X mental retardation protein regulates protein expression and mRNA translation of the potassium channel Kv4.2. *J. Neurosci.*, 31, 5693-5698.

Haddad, R., Weiss, T., Khan, R., Nadler, B., Mandairon, N., Bensafi, M., Schneidman, E. & Sobel, N. (2010) Global features of neural activity in the olfactory system form a parallel code that predicts olfactory behavior and perception. *J. Neurosci.*, 30, 9017-9026.

Hagerman, P.J. & Hagerman, R.J. (2007) Fragile X-associated tremor/ataxia syndrome--an older face of the fragile X gene. *Nat. Clin. Pract. Neurol.*, 3, 107-112.

Hagerman, P.J. & Stafstrom, C.E. (2009) Origins of epilepsy in fragile X syndrome. *Epilepsy Curr.*, 9, 108-112.

Hagerman, R.J. (2002) The Physical and Behavioural Phenotype. In Hagerman, R.J., Hagerman, P.J. (eds) *Fragile X Syndrome: Diagnosis, Treatment and Research*. Johns Hopkins University Press, Baltimore, Maryland, pp. 3-109.

Hagerman, R.J., Berry-Kravis, E., Kaufmann, W.E., Ono, M.Y., Tartaglia, N., Lachiewicz, A., Kronk, R., Delahunty, C., Hessl, D., Visootsak, J., Picker, J., Gane, L. & Tranfaglia, M. (2009) Advances in the treatment of fragile X syndrome. *Pediatrics*, 123, 378-390.

Hagerman, R.J., Van Housen, K., Smith, A.C. & McGavran, L. (1984) Consideration of connective tissue dysfunction in the fragile X syndrome. *Am. J. Med. Genet.*, 17, 111-121.

Hallem, E.A. & Carlson, J.R. (2006) Coding of odors by a receptor repertoire. *Cell*, 125, 143-160.

Harris, S.W., Hessl, D., Goodlin-Jones, B., Ferranti, J., Bacalman, S., Barbato, I., Tassone, F., Hagerman, P.J., Herman, H. & Hagerman, R.J. (2008) Autism profiles of males with fragile X syndrome. *Am. J. Ment. Retard.*, 113, 427-438.

Harrison, C.J., Jack, E.M., Allen, T.D. & Harris, R. (1983) The fragile X: a scanning electron microscope study. *J. Med. Genet.*, 20, 280-285.

Hays, S.A., Huber, K.M. & Gibson, J.R. (2011) Altered neocortical rhythmic activity states in Fmr1 KO mice are due to enhanced mGluR5 signaling and involve changes in excitatory circuitry. *J. Neurosci.*, 31, 14223-14234.

Hecht, F. & Sutherland, G.R. (1985) Detection of fragile sites on human chromosomes. *Clin. Genet.*, 28, 95-96.

Hinton, V.J., Brown, W.T., Wisniewski, K. & Rudelli, R.D. (1991) Analysis of neocortex in three males with the fragile X syndrome. *Am. J. Med. Genet.*, 41, 289-294.

Hong, A., Zhang, A., Ke, Y., El Idrissi, A. & Shen, C.H. (2012) Downregulation of GABA(A) beta subunits is transcriptionally controlled by Fmr1p. *J. Mol. Neurosci.*, 46, 272-275.

Hong, E.J. & Wilson, R.I. (2015) Simultaneous encoding of odors by channels with diverse sensitivity to inhibition. *Neuron*, 85, 573-589.

Huang, J., Zhang, W., Qiao, W., Hu, A. & Wang, Z. (2010) Functional connectivity and selective odor responses of excitatory local interneurons in *Drosophila* antennal lobe. *Neuron*, 67, 1021-1033.

Huber, K.M., Gallagher, S.M., Warren, S.T. & Bear, M.F. (2002) Altered synaptic plasticity in a mouse model of fragile X mental retardation. *Proc. Natl. Acad. Sci. USA*, 99, 7746-7750.

Huber, K.M., Kayser, M.S. & Bear, M.F. (2000) Role for rapid dendritic protein synthesis in hippocampal mGluR-dependent long-term depression. *Science*, 288, 1254-1257.

Incorpora, G., Sorge, G., Sorge, A. & Pavone, L. (2002) Epilepsy in fragile X syndrome. *Brain Dev.*, 24, 766-769.

Inoue, S., Shimoda, M., Nishinokubi, I., Siomi, M.C., Okamura, M., Nakamura, A., Kobayashi, S., Ishida, N. & Siomi, H. (2002) A role for the *Drosophila* fragile X-related gene in circadian output. *Curr. Biol.*, 12, 1331-1335.

Ireland, D.R. & Abraham, W.C. (2009) Mechanisms of group I mGluR-dependent long-term depression of NMDA receptor-mediated transmission at Schaffer collateral-CA1 synapses. *J. Neurophysiol.*, 101, 1375-1385.

Irwin, S.A., Galvez, R. & Greenough, W.T. (2000) Dendritic spine structural anomalies in fragile-X mental retardation syndrome. *Cereb. Cortex*, 10, 1038-1044.

Irwin, S.A., Patel, B., Idupulapati, M., Harris, J.B., Crisostomo, R.A., Larsen, B.P., Kooy, F., Willems, P.J., Cras, P., Kozlowski, P.B., Swain, R.A., Weiler, I.J. & Greenough, W.T. (2001) Abnormal dendritic spine characteristics in the temporal and visual cortices of patients with fragile-X syndrome: a quantitative examination. *Am. J. Med. Genet.*, 98, 161-167.

Ishizuka, A., Siomi, M.C. & Siomi, H. (2002) A *Drosophila* fragile X protein interacts with components of RNAi and ribosomal proteins. *Genes Dev.*, 16, 2497-2508.

Jacob, T.C., Moss, S.J. & Jurd, R. (2008) GABA(A) receptor trafficking and its role in the dynamic modulation of neuronal inhibition. *Nat. Rev. Neurosci.*, 9, 331-343.

Jacquemont, S., Hagerman, R.J., Hagerman, P.J. & Leehey, M.A. (2007) Fragile-X syndrome and fragile X-associated tremor/ataxia syndrome: two faces of FMR1. *Lancet Neurol.*, 6, 45-55.

Jefferis, G.S., Marin, E.C., Stocker, R.F. & Luo, L. (2001) Target neuron prespecification in the olfactory map of *Drosophila*. *Nature*, 414, 204-208.

Juarez, J.C., Manuia, M., Burnett, M.E., Betancourt, O., Boivin, B., Shaw, D.E., Tonks, N.K., Mazar, A.P. & Donate, F. (2008) Superoxide dismutase 1 (SOD1) is essential for H2O2-mediated oxidation and inactivation of phosphatases in growth factor signaling. *Proc. Natl. Acad. Sci. USA*, 105, 7147-7152.

Karachot, L., Shirai, Y., Vigot, R., Yamamori, T. & Ito, M. (2001) Induction of long-term depression in cerebellar Purkinje cells requires a rapidly turned over protein. *J. Neurophysiol.*, 86, 280-289.

Katsuki, Y., Suga, N. & Kanno, Y. (1962) Neural Mechanism of the Peripheral and Central Auditory System in Monkeys. *J. Acoust. Soc. Am.*, 34, 1396-1410.

Kaufmann, W.E., Cortell, R., Kau, A.S., Bukelis, I., Tierney, E., Gray, R.M., Cox, C., Capone, G.T. & Stanard, P. (2004) Autism spectrum disorder in fragile X syndrome: communication, social interaction, and specific behaviors. *Am. J. Med. Genet.*, 129A, 225-234.

Kaufmann, W.E. & Moser, H.W. (2000) Dendritic anomalies in disorders associated with mental retardation. *Cereb. Cortex*, 10, 981-991.

Kazama, H. & Wilson, R.I. (2008) Homeostatic matching and nonlinear amplification at identified central synapses. *Neuron*, 58, 401-413.

Kazama, H. & Wilson, R.I. (2009) Origins of correlated activity in an olfactory circuit. *Nat. Neurosci.*, 12, 1136-1144.

Kelleher, R.J., 3rd & Bear, M.F. (2008) The autistic neuron: troubled translation? *Cell*, 135, 401-406.

Kenneson, A., Zhang, F., Hagedorn, C.H. & Warren, S.T. (2001) Reduced FMRP and increased FMR1 transcription is proportionally associated with CGG repeat number in intermediate-length and premutation carriers. *Hum. Mol. Genet.*, 10, 1449-1454.

Kole, M.H., Hallermann, S. & Stuart, G.J. (2006) Single Ih channels in pyramidal neuron dendrites: properties, distribution, and impact on action potential output. *J. Neurosci.*, 26, 1677-1687.

Krichevsky, A.M. & Kosik, K.S. (2001) Neuronal RNA granules: a link between RNA localization and stimulation-dependent translation. *Neuron*, 32, 683-696.

Kuffler, S.W. (1953) Discharge patterns and functional organization of mammalian retina. *J. Neurophysiol.*, 16, 37-68.

Laissue, P.P., Reiter, C., Hiesinger, P.R., Halter, S., Fischbach, K.F. & Stocker, R.F. (1999) Three-dimensional reconstruction of the antennal lobe in *Drosophila melanogaster*. *J. Comp. Neurol.*, 405, 543-552.

Laissue, P.P. & Vosshall, L.B. (2008) The olfactory sensory map in *Drosophila*. *Adv. Exp. Med. Biol.*, 628, 102-114.

Larsson, M.C., Domingos, A.I., Jones, W.D., Chiappe, M.E., Amrein, H. & Vosshall, L.B. (2004) Or83b encodes a broadly expressed odorant receptor essential for *Drosophila* olfaction. *Neuron*, 43, 703-714.

Lee, A., Li, W., Xu, K., Bogert, B.A., Su, K. & Gao, F.B. (2003) Control of dendritic development by the *Drosophila* fragile X-related gene involves the small GTPase Rac1. *Development*, 130, 5543-5552.

Lee, H.Y., Ge, W.P., Huang, W., He, Y., Wang, G.X., Rowson-Baldwin, A., Smith, S.J., Jan, Y.N. & Jan, L.Y. (2011) Bidirectional regulation of dendritic voltage-gated potassium channels by the fragile X mental retardation protein. *Neuron*, 72, 630-642.

Lewis, P., Abbeduto, L., Murphy, M., Richmond, E., Giles, N., Bruno, L. & Schroeder, S. (2006) Cognitive, language and social-cognitive skills of individuals with fragile X syndrome with and without autism. *J. Intellect. Disabil. Res.*, 50, 532-545.

Lubs, H.A. (1969) A marker X chromosome. *Am. J. Hum. Genet.*, 21, 231-244.

Luo, S.X., Axel, R. & Abbott, L.F. (2010) Generating sparse and selective third-order responses in the olfactory system of the fly. *Proc. Natl. Acad. Sci. USA*, 107, 10713-10718.

Marin-Padilla, M. (1972) Structural abnormalities of the cerebral cortex in human chromosomal aberrations: a Golgi study. *Brain Res.*, 44, 625-629.

Marin, E.C., Jefferis, G.S., Komiyama, T., Zhu, H. & Luo, L. (2002) Representation of the glomerular olfactory map in the *Drosophila* brain. *Cell*, 109, 243-255.

Martin, K.C. & Ephrussi, A. (2009) mRNA localization: gene expression in the spatial dimension. *Cell*, 136, 719-730.

Masse, N.Y., Turner, G.C. & Jefferis, G.S. (2009) Olfactory information processing in *Drosophila*. *Curr. Biol.*, 19, R700-713.

McBride, S.M., Choi, C.H., Wang, Y., Liebelt, D., Braunstein, E., Ferreiro, D., Sehgal, A., Siwicki, K.K., Dockendorff, T.C., Nguyen, H.T., McDonald, T.V. & Jongens, T.A. (2005) Pharmacological rescue of synaptic plasticity, courtship behavior, and mushroom body defects in a *Drosophila* model of fragile X syndrome. *Neuron*, 45, 753-764.

Merlin, L.R., Bergold, P.J. & Wong, R.K. (1998) Requirement of protein synthesis for group I mGluR-mediated induction of epileptiform discharges. *J. Neurophysiol.*, 80, 989-993.

Michel, C.I., Kraft, R. & Restifo, L.L. (2004) Defective neuronal development in the mushroom bodies of *Drosophila* fragile X mental retardation 1 mutants. *J. Neurosci.*, 24, 5798-5809.

Ming, X., Stein, T.P., Brimacombe, M., Johnson, W.G., Lambert, G.H. & Wagner, G.C. (2005) Increased excretion of a lipid peroxidation biomarker in autism. *Prostaglandins Leukot. Essent. Fatty Acids*, 73, 379-384.

Morales, J., Hiesinger, P.R., Schroeder, A.J., Kume, K., Verstreken, P., Jackson, F.R., Nelson, D.L. & Hassan, B.A. (2002) *Drosophila* fragile X protein, DFXR, regulates neuronal morphology and function in the brain. *Neuron*, 34, 961-972.

Mountcastle, V.B. & Powell, T.P. (1959) Neural mechanisms subserving cutaneous sensibility, with special reference to the role of afferent inhibition in sensory perception and discrimination. *Bull. Johns Hopkins Hosp.*, 105, 201-232.

Muddashetty, R.S., Nalavadi, V.C., Gross, C., Yao, X., Xing, L., Laur, O., Warren, S.T. & Bassell, G.J. (2011) Reversible inhibition of PSD-95 mRNA translation by miR-125a, FMRP phosphorylation, and mGluR signaling. *Mol. Cell*, 42, 673-688.

Muhle, R., Trentacoste, S.V. & Rapin, I. (2004) The genetics of autism. *Pediatrics*, 113, e472-486.

Mukamel, E.A., Nimmerjahn, A. & Schnitzer, M.J. (2009) Automated analysis of cellular signals from large-scale calcium imaging data. *Neuron*, 63, 747-760.

Mullard, A. (2015) Fragile X disappointments upset autism ambitions. *Nat. Rev. Drug Discov.*, 14, 151-153.

Murlis, J., Elkinton, J.S. & Carde, R.T. (1992) Odor Plumes and How Insects Use Them. *Annu. Rev. Entomol.*, 37, 505-532.

Murphy-Ryan, M., Psychogios, A. & Lindor, N.M. (2010) Hereditary disorders of connective tissue: a guide to the emerging differential diagnosis. *Genet. Med.*, 12, 344-354.

Myrick, L.K., Nakamoto-Kinoshita, M., Lindor, N.M., Kirmani, S., Cheng, X. & Warren, S.T. (2014) Fragile X syndrome due to a missense mutation. *Eur. J. Hum. Genet.*, 22, 1185-1189.

Naresh Singh, R. & Nayak, S.V. (1985) Fine structure and primary sensory projections of sensilla on the maxillary palp of *Drosophila melanogaster* Meigen (Diptera : Drosophilidae). *Int. J. Insect Morphol. Embryol.*, 14, 291-306.

Ng, M., Roorda, R.D., Lima, S.Q., Zemelman, B.V., Morcillo, P. & Miesenbock, G. (2002) Transmission of olfactory information between three populations of neurons in the antennal lobe of the fly. *Neuron*, 36, 463-474.

Nielsen, D.M., Derber, W.J., McClellan, D.A. & Crnic, L.S. (2002) Alterations in the auditory startle response in Fmr1 targeted mutant mouse models of fragile X syndrome. *Brain Res.*, 927, 8-17.

Nimchinsky, E.A., Oberlander, A.M. & Svoboda, K. (2001) Abnormal development of dendritic spines in FMR1 knock-out mice. *J. Neurosci.*, 21, 5139-5146.

Nowicki, S.T., Tassone, F., Ono, M.Y., Ferranti, J., Croquette, M.F., Goodlin-Jones, B. & Hagerman, R.J. (2007) The Prader-Willi phenotype of fragile X syndrome. *J. Dev. Behav. Pediatr.*, 28, 133-138.

Oberle, I., Rousseau, F., Heitz, D., Kretz, C., Devys, D., Hanauer, A., Boue, J., Bertheas, M.F. & Mandel, J.L. (1991) Instability of a 550-base pair DNA segment and abnormal methylation in fragile X syndrome. *Science*, 252, 1097-1102.

Okada, R., Awasaki, T. & Ito, K. (2009) Gamma-aminobutyric acid (GABA)-mediated neural connections in the *Drosophila* antennal lobe. *J. Comp. Neurol.*, 514, 74-91.

Okray, Z., de Esch, C.E., Van Esch, H., Devriendt, K., Claeys, A., Yan, J., Verbeeck, J., Froyen, G., Willemsen, R., de Vrij, F.M. & Hassan, B.A. (2015) A novel fragile X syndrome mutation reveals a conserved role for the carboxy-terminus in FMRP localization and function. *EMBO Mol. Med.*, 7, 423-437.

Olmos-Serrano, J.L., Paluszkiewicz, S.M., Martin, B.S., Kaufmann, W.E., Corbin, J.G. & Huntsman, M.M. (2010) Defective GABAergic neurotransmission and pharmacological rescue of neuronal hyperexcitability in the amygdala in a mouse model of fragile X syndrome. *J. Neurosci.*, 30, 9929-9938.

Olsen, S.R., Bhandawat, V. & Wilson, R.I. (2007) Excitatory interactions between olfactory processing channels in the *Drosophila* antennal lobe. *Neuron*, 54, 89-103.

Olsen, S.R., Bhandawat, V. & Wilson, R.I. (2010) Divisive normalization in olfactory population codes. *Neuron*, 66, 287-299.

Olsen, S.R. & Wilson, R.I. (2008) Lateral presynaptic inhibition mediates gain control in an olfactory circuit. *Nature*, 452, 956-960.

Pacey, L.K., Doss, L., Cifelli, C., van der Kooy, D., Heximer, S.P. & Hampson, D.R. (2011) Genetic deletion of regulator of G-protein signaling 4 (RGS4) rescues a subset of fragile X related phenotypes in the FMR1 knockout mouse. *Mol. Cell. Neurosci.*, 46, 563-572.

Pacey, L.K., Heximer, S.P. & Hampson, D.R. (2009) Increased GABA(B) receptor-mediated signaling reduces the susceptibility of fragile X knockout mice to audiogenic seizures. *Mol. Pharmacol.*, 76, 18-24.

Paluszkiewicz, S.M., Martin, B.S. & Huntsman, M.M. (2011) Fragile X syndrome: the GABAergic system and circuit dysfunction. *Dev. Neurosci.*, 33, 349-364.

Pan, L. & Broadie, K.S. (2007) *Drosophila* fragile X mental retardation protein and metabotropic glutamate receptor A convergently regulate the synaptic ratio of ionotropic glutamate receptor subclasses. *J. Neurosci.*, 27, 12378-12389.

Pan, L., Woodruff, E., 3rd, Liang, P. & Broadie, K. (2008) Mechanistic relationships between *Drosophila* fragile X mental retardation protein and metabotropic glutamate receptor A signaling. *Mol. Cell. Neurosci.*, 37, 747-760.

Pan, L., Zhang, Y.Q., Woodruff, E. & Broadie, K. (2004) The *Drosophila* fragile X gene negatively regulates neuronal elaboration and synaptic differentiation. *Curr. Biol.*, 14, 1863-1870.

Paradee, W., Melikian, H.E., Rasmussen, D.L., Kenneson, A., Conn, P.J. & Warren, S.T. (1999) Fragile X mouse: strain effects of knockout phenotype and evidence suggesting deficient amygdala function. *Neuroscience*, 94, 185-192.

Pasciuto, E. & Bagni, C. (2014a) SnapShot: FMRP interacting proteins. *Cell*, 159, 218-218 e211.

Pasciuto, E. & Bagni, C. (2014b) SnapShot: FMRP mRNA targets and diseases. *Cell*, 158, 1446-1446 e1441.

Patel, A.B., Loerwald, K.W., Huber, K.M. & Gibson, J.R. (2014) Postsynaptic FMRP promotes the pruning of cell-to-cell connections among pyramidal neurons in the L5A neocortical network. *J. Neurosci.*, 34, 3413-3418.

Penagarikano, O., Mulle, J.G. & Warren, S.T. (2007) The pathophysiology of fragile X syndrome. *Annu. Rev. Genomics Hum. Genet.*, 8, 109-129.

Pfeiffer, B.E. & Huber, K.M. (2007) Fragile X mental retardation protein induces synapse loss through acute postsynaptic translational regulation. *J. Neurosci.*, 27, 3120-3130.

Pfeiffer, B.E. & Huber, K.M. (2009) The state of synapses in fragile X syndrome. *Neuroscientist*, 15, 549-567.

Pieretti, M., Zhang, F.P., Fu, Y.H., Warren, S.T., Oostra, B.A., Caskey, C.T. & Nelson, D.L. (1991) Absence of expression of the FMR-1 gene in fragile X syndrome. *Cell*, 66, 817-822.

Purpura, D.P. (1974) Dendritic spine "dysgenesis" and mental retardation. *Science*, 186, 1126-1128.

Raymond, C.R., Thompson, V.L., Tate, W.P. & Abraham, W.C. (2000) Metabotropic glutamate receptors trigger homosynaptic protein synthesis to prolong long-term potentiation. *J. Neurosci.*, 20, 969-976.

Razin, A. (1998) CpG methylation, chromatin structure and gene silencing-a three-way connection. *EMBO J.*, 17, 4905-4908.

Reeve, S.P., Bassetto, L., Genova, G.K., Kleyner, Y., Leyssen, M., Jackson, F.R. & Hassan, B.A. (2005) The *Drosophila* fragile X mental retardation protein controls actin dynamics by directly regulating profilin in the brain. *Curr. Biol.*, 15, 1156-1163.

Reeve, S.P., Lin, X., Sahin, B.H., Jiang, F., Yao, A., Liu, Z., Zhi, H., Broadie, K., Li, W., Giangrande, A., Hassan, B.A. & Zhang, Y.Q. (2008) Mutational analysis establishes a critical role for the N terminus of fragile X mental retardation protein FMRP. *J. Neurosci.*, 28, 3221-3226.

Robertson, C.E., Ratai, E.M. & Kanwisher, N. (2016) Reduced GABAergic Action in the Autistic Brain. *Curr. Biol.*, 26, 80-85.

Robertson, H.M., Warr, C.G. & Carlson, J.R. (2003) Molecular evolution of the insect chemoreceptor gene superfamily in *Drosophila melanogaster*. *Proc. Natl. Acad. Sci. USA*, 100, 14537-14542.

Rodrigues, S.M., Bauer, E.P., Farb, C.R., Schafe, G.E. & LeDoux, J.E. (2002) The group I metabotropic glutamate receptor mGluR5 is required for fear memory formation and long-term potentiation in the lateral amygdala. *J. Neurosci.*, 22, 5219-5229.

Rogers, S.J., Hepburn, S. & Wehner, E. (2003) Parent reports of sensory symptoms in toddlers with autism and those with other developmental disorders. *J. Autism Dev. Disord.*, 33, 631-642.

Rogers, S.J., Wehner, D.E. & Hagerman, R. (2001) The behavioral phenotype in fragile X: symptoms of autism in very young children with fragile X syndrome, idiopathic autism, and other developmental disorders. *J. Dev. Behav. Pediatr.*, 22, 409-417.

Rolls, E.T. & Tovee, M.J. (1995) Sparseness of the neuronal representation of stimuli in the primate temporal visual cortex. *J. Neurophysiol.*, 73, 713-726.

Root, C.M., Masuyama, K., Green, D.S., Enell, L.E., Nassel, D.R., Lee, C.H. & Wang, J.W. (2008) A presynaptic gain control mechanism fine-tunes olfactory behavior. *Neuron*, 59, 311-321.

Rotschafer, S. & Razak, K. (2013) Altered auditory processing in a mouse model of fragile X syndrome. *Brain Res.*, 1506, 12-24.

Rubenstein, J.L. & Merzenich, M.M. (2003) Model of autism: increased ratio of excitation/inhibition in key neural systems. *Genes Brain Behav.*, 2, 255-267.

Rudelli, R.D., Brown, W.T., Wisniewski, K., Jenkins, E.C., Laure-Kamionowska, M., Connell, F. & Wisniewski, H.M. (1985) Adult fragile X syndrome. Clinico-neuropathologic findings. *Acta Neuropathol.*, 67, 289-295.

Rudy, B. & McBain, C.J. (2001) Kv3 channels: voltage-gated K+ channels designed for high-frequency repetitive firing. *Trends Neurosci.*, 24, 517-526.

Rupert, A., Moushegian, G. & Galambos, R. (1963) Unit responses to sound from auditory nerve of the cat. *J. Neurophysiol.*, 26, 449-465.

Santoro, M.R., Bray, S.M. & Warren, S.T. (2012) Molecular mechanisms of fragile X syndrome: a twenty-year perspective. *Annu. Rev. Pathol.*, 7, 219-245.

Schaefer, G.B. & Mendelsohn, N.J. (2008) Genetics evaluation for the etiologic diagnosis of autism spectrum disorders. *Genet. Med.*, 10, 4-12.

Schilit Nitenson, A., Stackpole, E.E., Truszkowski, T.L., Midroit, M., Fallon, J.R. & Bath, K.G. (2015) Fragile x mental retardation protein regulates olfactory sensitivity but not odorant discrimination. *Chem. Senses*, 40, 345-350.

Schrander-Stumpel, C., Gerver, W.J., Meyer, H., Engelen, J., Mulder, H. & Fryns, J.P. (1994) Prader-Willi-like phenotype in fragile X syndrome. *Clin. Genet.*, 45, 175-180.

Seki, Y., Rybak, J., Wicher, D., Sachse, S. & Hansson, B.S. (2010) Physiological and morphological characterization of local interneurons in the *Drosophila* antennal lobe. *J. Neurophysiol.*, 104, 1007-1019.

Semmelhack, J.L. & Wang, J.W. (2009) Select *Drosophila* glomeruli mediate innate olfactory attraction and aversion. *Nature*, 459, 218-223.

Sengupta, B., Laughlin, S.B. & Niven, J.E. (2013) Balanced excitatory and inhibitory synaptic currents promote efficient coding and metabolic efficiency. *PLoS Comput. Biol.*, 9, e1003263.

Shanbhag, S.R., Müller, B. & Steinbrecht, R.A. (1999) Atlas of olfactory organs of *Drosophila melanogaster*: 1. Types, external organization, innervation and distribution of olfactory sensilla. *Int. J. Insect Morphol. Embryol.*, 28, 377-397.

Shang, Y., Claridge-Chang, A., Sjulson, L., Pypaert, M. & Miesenbock, G. (2007) Excitatory local circuits and their implications for olfactory processing in the fly antennal lobe. *Cell*, 128, 601-612.

Sherman, S.L. (2000) Premature ovarian failure among fragile X premutation carriers: parent-of-origin effect? *Am. J. Hum. Genet.*, 67, 11-13.

Silbering, A.F., Rytz, R., Grosjean, Y., Abuin, L., Ramdya, P., Jefferis, G.S. & Benton, R. (2011) Complementary function and integrated wiring of the evolutionarily distinct *Drosophila* olfactory subsystems. *J. Neurosci.*, 31, 13357-13375.

Singh, B., Ogiwara, I., Kaneda, M., Tokonami, N., Mazaki, E., Baba, K., Matsuda, K., Inoue, Y. & Yamakawa, K. (2006) A Kv4.2 truncation mutation in a patient with temporal lobe epilepsy. *Neurobiol. Dis.*, 24, 245-253.

Snyder, E.M., Philpot, B.D., Huber, K.M., Dong, X., Fallon, J.R. & Bear, M.F. (2001) Internalization of ionotropic glutamate receptors in response to mGluR activation. *Nat. Neurosci.*, 4, 1079-1085.

Sourdet, V., Russier, M., Daoudal, G., Ankri, N. & Debanne, D. (2003) Long-term enhancement of neuronal excitability and temporal fidelity mediated by metabotropic glutamate receptor subtype 5. *J. Neurosci.*, 23, 10238-10248.

Steck, K., Veit, D., Grandy, R., Badia, S.B., Mathews, Z., Verschure, P., Hansson, B.S. & Knaden, M. (2012) A high-throughput behavioral paradigm for *Drosophila* olfaction - The Flywalk. *Sci. Rep.*, 2, 361.

Stocker, R.F. (1994) The organization of the chemosensory system in *Drosophila melanogaster*: a review. *Cell Tissue Res.*, 275, 3-26.

Stocker, R.F. (2001) *Drosophila* as a focus in olfactory research: mapping of olfactory sensilla by fine structure, odor specificity, odorant receptor expression, and central connectivity. *Microsc. Res. Tech.*, 55, 284-296.

Stocker, R.F., Lienhard, M.C., Borst, A. & Fischbach, K.F. (1990) Neuronal architecture of the antennal lobe in *Drosophila melanogaster*. *Cell Tissue Res.*, 262, 9-34.

Stocker, R.F., Singh, R.N., Schorderet, M. & Siddiqi, O. (1983) Projection patterns of different types of antennal sensilla in the antennal glomeruli of *Drosophila melanogaster*. *Cell Tissue Res.*, 232, 237-248.

Stoop, R., Conquet, F., Zuber, B., Voronin, L.L. & Pralong, E. (2003) Activation of metabotropic glutamate 5 and NMDA receptors underlies the induction of persistent bursting and associated long-lasting changes in CA3 recurrent connections. *J. Neurosci.*, 23, 5634-5644.

Strauch, M. & Galizia, C.G. (2012) Fast PCA for processing calcium-imaging data from the brain of *Drosophila melanogaster*. *BMC Med. Inform. Decis. Mak.*, 12 Suppl 1, S2.

Strowbridge, B.W. (2008) A volume control for the sense of smell. *Nat. Neurosci.*, 11, 531-533.

Strumbos, J.G., Brown, M.R., Kronengold, J., Polley, D.B. & Kaczmarek, L.K. (2010) Fragile X mental retardation protein is required for rapid experience-dependent regulation of the potassium channel Kv3.1b. *J. Neurosci.*, 30, 10263-10271.

Suh, G.S., Ben-Tabou de Leon, S., Tanimoto, H., Fiala, A., Benzer, S. & Anderson, D.J. (2007) Light activation of an innate olfactory avoidance response in *Drosophila*. *Curr. Biol.*, 17, 905-908.

Suhl, J.A. & Warren, S.T. (2015) Single-Nucleotide Mutations in FMR1 Reveal Novel Functions and Regulatory Mechanisms of the Fragile X Syndrome Protein FMRP. *J. Exp. Neurosci.*, 9, 35-41.

Sullivan, A.K., Marcus, M., Epstein, M.P., Allen, E.G., Anido, A.E., Paquin, J.J., Yadav-Shah, M. & Sherman, S.L. (2005) Association of FMR1 repeat size with ovarian dysfunction. *Hum. Reprod.*, 20, 402-412.

Sutcliffe, J.S., Nelson, D.L., Zhang, F., Pieretti, M., Caskey, C.T., Saxe, D. & Warren, S.T. (1992) DNA methylation represses FMR-1 transcription in fragile X syndrome. *Hum. Mol. Genet.*, 1, 397-400.

Sutherland, G.R. (1977) Fragile sites on human chromosomes: demonstration of their dependence on the type of tissue culture medium. *Science*, 197, 265-266.

Tanaka, N.K., Dye, L. & Stopfer, M. (2011) Dual-labeling method for electron microscopy to characterize synaptic connectivity using genetically encoded fluorescent reporters in *Drosophila*. *J. Neurosci. Methods*, 194, 312-315.

Tassone, F., Adams, J., Berry-Kravis, E.M., Cohen, S.S., Brusco, A., Leehey, M.A., Li, L., Hagerman, R.J. & Hagerman, P.J. (2007) CGG repeat length correlates with age of onset of motor signs of the fragile X-associated tremor/ataxia syndrome (FXTAS). *Am. J. Med. Genet.*, 144B, 566-569.

Tassone, F., Hagerman, R.J., Taylor, A.K., Gane, L.W., Godfrey, T.E. & Hagerman, P.J. (2000) Elevated levels of FMR1 mRNA in carrier males: a new mechanism of involvement in the fragile-X syndrome. *Am. J. Hum. Genet.*, 66, 6-15.

Tranfaglia, M.R. (2011) The psychiatric presentation of fragile x: evolution of the diagnosis and treatment of the psychiatric comorbidities of fragile X syndrome. *Dev. Neurosci.*, 33, 337-348.

Tucker, B., Richards, R.I. & Lardelli, M. (2006) Contribution of mGluR and Fmr1 functional pathways to neurite morphogenesis, craniofacial development and fragile X syndrome. *Hum. Mol. Genet.*, 15, 3446-3458.

Turner, G., Daniel, A. & Frost, M. (1980) X-linked mental retardation, macro-orchidism, and the Xq27 fragile site. *J. Pediatr.*, 96, 837-841.

v. Békésy, G. (1958) Funneling in the Nervous System and its Role in Loudness and Sensation Intensity on the Skin. *J. Acoust. Soc. Am.*, 30, 399-412.

Vanderklish, P.W. & Edelman, G.M. (2002) Dendritic spines elongate after stimulation of group 1 metabotropic glutamate receptors in cultured hippocampal neurons. *Proc. Natl. Acad. Sci. USA*, 99, 1639-1644.

Verkerk, A.J., Pieretti, M., Sutcliffe, J.S., Fu, Y.H., Kuhl, D.P., Pizzuti, A., Reiner, O., Richards, S., Victoria, M.F., Zhang, F.P. & et al. (1991) Identification of a gene (FMR-1) containing a CGG repeat coincident with a breakpoint cluster region exhibiting length variation in fragile X syndrome. *Cell*, 65, 905-914.

Vianna-Morgante, A.M., Armando, I. & Frota-Pessoa, O. (1982) Escalante syndrome and the marker X chromosome. *Am. J. Med. Genet.*, 12, 237-240.

Vinje, W.E. & Gallant, J.L. (2000) Sparse coding and decorrelation in primary visual cortex during natural vision. *Science*, 287, 1273-1276.

Vosshall, L.B. & Stocker, R.F. (2007) Molecular architecture of smell and taste in *Drosophila*. *Annu. Rev. Neurosci.*, 30, 505-533.

Vosshall, L.B., Wong, A.M. & Axel, R. (2000) An olfactory sensory map in the fly brain. *Cell*, 102, 147-159.

Wahl-Schott, C. & Biel, M. (2009) HCN channels: structure, cellular regulation and physiological function. *Cell. Mol. Life Sci.*, 66, 470-494.

Walker, K., Reeve, A., Bowes, M., Winter, J., Wotherspoon, G., Davis, A., Schmid, P., Gasparini, F., Kuhn, R. & Urban, L. (2001) mGlu5 receptors and nociceptive function II. mGlu5 receptors functionally expressed on peripheral sensory neurones mediate inflammatory hyperalgesia. *Neuropharmacology*, 40, 10-19.

Wan, L., Dockendorff, T.C., Jongens, T.A. & Dreyfuss, G. (2000) Characterization of dFMR1, a *Drosophila melanogaster* homolog of the fragile X mental retardation protein. *Mol. Cell. Biol.*, 20, 8536-8547.

Wang, D.D. & Kriegstein, A.R. (2008) GABA regulates excitatory synapse formation in the neocortex via NMDA receptor activation. *J. Neurosci.*, 28, 5547-5558.

Webb, T., Butler, D., Insley, J., Weaver, J.B., Green, S. & Rodeck, C. (1981) Prenatal diagnosis of Martin-Bell syndrome associated with fragile site at Xq27-28. *Lancet*, 2, 1423.

Weiser, M., Bueno, E., Sekirnjak, C., Martone, M.E., Baker, H., Hillman, D., Chen, S., Thornhill, W., Ellisman, M. & Rudy, B. (1995) The potassium channel subunit KV3.1b is localized to somatic and axonal membranes of specific populations of CNS neurons. *J. Neurosci.*, 15, 4298-4314.

Wilson, R.I. (2013) Early olfactory processing in *Drosophila*: mechanisms and principles. *Annu. Rev. Neurosci.*, 36, 217-241.

Wilson, R.I. & Laurent, G. (2005) Role of GABAergic inhibition in shaping odor-evoked spatiotemporal patterns in the *Drosophila* antennal lobe. *J. Neurosci.*, 25, 9069-9079.

Wilson, R.I., Turner, G.C. & Laurent, G. (2004) Transformation of olfactory representations in the *Drosophila* antennal lobe. *Science*, 303, 366-370.

Wisniewski, K.E., Segan, S.M., Miezejeski, C.M., Sersen, E.A. & Rudelli, R.D. (1991) The Fra(X) syndrome: neurological, electrophysiological, and neuropathological abnormalities. *Am. J. Med. Genet.*, 38, 476-480.

Wong, A.M., Wang, J.W. & Axel, R. (2002) Spatial representation of the glomerular map in the *Drosophila* protocerebrum. *Cell*, 109, 229-241.

Yaksi, E., Judkewitz, B. & Friedrich, R.W. (2007) Topological reorganization of odor representations in the olfactory bulb. *PLoS Biol.*, 5, e178.

Yaksi, E. & Wilson, R.I. (2010) Electrical coupling between olfactory glomeruli. *Neuron*, 67, 1034-1047.

Yan, Q.J., Rammal, M., Tranfaglia, M. & Bauchwitz, R.P. (2005) Suppression of two major Fragile X Syndrome mouse model phenotypes by the mGluR5 antagonist MPEP. *Neuropharmacology*, 49, 1053-1066.

Yasuyama, K. & Salvaterra, P.M. (1999) Localization of choline acetyltransferase-expressing neurons in *Drosophila* nervous system. *Microsc. Res. Tech.*, 45, 65-79.

Zalfa, F., Giorgi, M., Primerano, B., Moro, A., Di Penta, A., Reis, S., Oostra, B. & Bagni, C. (2003) The fragile X syndrome protein FMRP associates with BC1 RNA and regulates the translation of specific mRNAs at synapses. *Cell*, 112, 317-327.

Zhang, Y., Bonnan, A., Bony, G., Ferezou, I., Pietropaolo, S., Ginger, M., Sans, N., Rossier, J., Oostra, B., LeMasson, G. & Frick, A. (2014) Dendritic channelopathies contribute to neocortical and sensory hyperexcitability in Fmr1(-/y) mice. *Nat. Neurosci.*, 17, 1701-1709.

Zhang, Y.Q., Bailey, A.M., Matthies, H.J., Renden, R.B., Smith, M.A., Speese, S.D., Rubin, G.M. & Broadie, K. (2001) *Drosophila* fragile X-related gene regulates the MAP1B homolog Futsch to control synaptic structure and function. *Cell*, 107, 591-603.

Zhang, Y.Q., Matthies, H.J., Mancuso, J., Andrews, H.K., Woodruff, E., 3rd, Friedman, D. & Broadie, K. (2004) The *Drosophila* fragile X-related gene regulates axoneme differentiation during spermatogenesis. *Dev. Biol.*, 270, 290-307.

Zho, W.M., You, J.L., Huang, C.C. & Hsu, K.S. (2002) The group I metabotropic glutamate receptor agonist (S)-3,5-dihydroxyphenylglycine induces a novel form of depotentiation in the CA1 region of the hippocampus. *J. Neurosci.*, 22, 8838-8849.

Publications

In addition to the study of neuronal circuit mechanisms related to fragile X syndrome, I collaborated with other laboratories at KU Leuven in different projects. These collaborations have given rise to three publications, which I describe in the following sections.

The Fungal Aroma Gene *ATF1* Promotes Dispersal of Yeast Cells through Insect Vectors

Yeast cells spend considerable amount of energy to produce esters, which are aromatic compounds that are pleasant for some animals. For instance, the particular smell of wine and beer is in part due to the presence of esters. Yet, little is known about the role of esters in the biology of yeast cells. An interesting hypothesis proposes that these esters are molecular cues that attract insects, such as *Drosophila melanogaster*, which, in turn, can act as vectors to disperse yeast cells throughout the environment. In this regard, it is important to mention that yeast cells lack motile mechanisms such as cilia and flagella. Therefore, the contribution of insect vectors for their dispersal seem to be crucial in the biology of yeast cells.

For this project, I performed olfactory behavioral assays and showed that *Drosophila melanogaster* is preferentially attracted to yeast colonies that produce acetate esters when competed with colonies of the same yeast strain in which the *ATF1* gene, whose protein product is a key acetate ester synthase, has been deleted. Furthermore, I carried out *in vivo* functional imaging in the antennal lobe, which is the first neuronal circuit in the *Drosophila melanogaster* brain that processes olfactory information, and showed that the aroma of yeast colonies that produce acetate esters is encoded differently from the aroma of yeast cells that do not produce acetate esters. This is probably due to the extent of activation of the DM1 glomerulus, which is strongly activated by esters. In fact, activation of DM1 alone has been shown to be enough to drive attraction in *Drosophila melanogaster* (Semmelhack & Wang, 2009). Altogether, these results suggest an interesting mutualism between yeast cells and fruit flies based on chemical communication that help fruit flies to locate food sources but also yeast cells to colonize other substrates.

Cell Reports

Report

The Fungal Aroma Gene *ATF1* Promotes Dispersal of Yeast Cells through Insect Vectors

Graphical Abstract

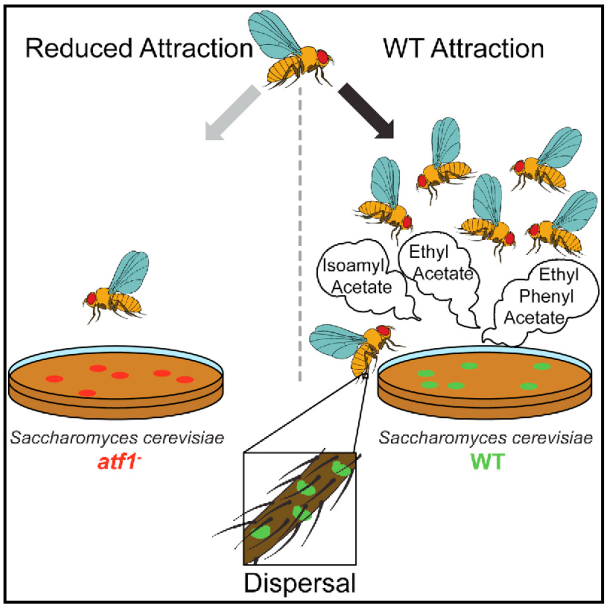

Highlights

The *S. cerevisiae ATF1* gene controls the production of volatile acetate esters

Aroma of *ATF1* mutants elicits different neuronal activity in the fly antennal lobe

Flies are significantly more attracted to wild-type yeast than to atf1-null mutants

Addition of isoamyl acetate and ethyl acetate restores attraction of *Drosophila*

Authors

Joaquin F. Christiaens, Luis M. Franco, ..., Emre Yaksi, Kevin J. Verstrepen

Correspondence

emre.yaksi@nerf.be (E.Y.), kevin.verstrepen@biw.vib-kuleuven.be (K.J.V.)

In Brief

Yeast cells produce several different volatile acetate esters. Whereas these fruity aroma compounds are key contributors to the pleasing aroma of fermented beverages like beer and wine, their physiological role for the yeast cells that produce them remains unknown. Christiaens et al. show that two acetate esters, ethyl acetate and isoamyl acetate, help to attract fruit flies that serve as vectors that promote dispersal of the yeast cells. Deletion of the yeast *ATF1* gene, encoding a key acetate ester synthase, drastically reduces *Drosophila* attraction and therefore limits yeast dispersal.

Christiaens et al., 2014, Cell Reports 9, 425–432
October 23, 2014 ©2014 The Authors
http://dx.doi.org/10.1016/j.celrep.2014.09.009

Cell Reports
Report

The Fungal Aroma Gene *ATF1* Promotes Dispersal of Yeast Cells through Insect Vectors

Joaquin F. Christiaens,[1,2,3,9] Luis M. Franco,[3,4,5,9] Tanne L. Cools,[1,2] Luc De Meester,[6] Jan Michiels,[1] Tom Wenseleers,[6] Bassem A. Hassan,[3,4] Emre Yaksi,[5,7,8,10,*] and Kevin J. Verstrepen[1,2,10,*]
[1]Laboratory for Genetics and Genomics, Centre of Microbial and Plant Genetics (CMPG), Department of Microbial and Molecular Systems, KU Leuven, Gaston Geenslaan 1, 3001 Leuven (Heverlee), Belgium
[2]VIB Laboratory of Systems Biology, Gaston Geenslaan 1, 3001 Leuven (Heverlee), Belgium
[3]Centre for Human Genetics, KU Leuven School of Medicine, Herestraat 49, 3000 Leuven, Belgium
[4]VIB Centre for the Biology of Disease, Herestraat 49, 3000 Leuven, Belgium
[5]Neuroelectronics Research Flanders (NERF), Kapeldreef 75, 3001 Leuven, Belgium
[6]Animal Ecology and Systematics Section, Department of Biology, KU Leuven, Charles Deberiotstraat 32, 3000 Leuven, Belgium
[7]VIB, Kapeldreef 75, 3001 Leuven, Belgium
[8]KU Leuven, Kapeldreef 75, 3001 Leuven, Belgium
[9]Co-first author
[10]Co-senior author
*Correspondence: emre.yaksi@nerf.be (E.Y.), kevin.verstrepen@biw.vib-kuleuven.be (K.J.V.)
http://dx.doi.org/10.1016/j.celrep.2014.09.009

SUMMARY

Yeast cells produce various volatile metabolites that are key contributors to the pleasing fruity and flowery aroma of fermented beverages. Several of these fruity metabolites, including isoamyl acetate and ethyl acetate, are produced by a dedicated enzyme, the alcohol acetyl transferase Atf1. However, despite much research, the physiological role of acetate ester formation in yeast remains unknown. Using a combination of molecular biology, neurobiology, and behavioral tests, we demonstrate that deletion of *ATF1* alters the olfactory response in the antennal lobe of fruit flies that feed on yeast cells. The flies are much less attracted to the mutant yeast cells, and this in turn results in reduced dispersal of the mutant yeast cells by the flies. Together, our results uncover the molecular details of an intriguing aroma-based communication and mutualism between microbes and their insect vectors. Similar mechanisms may exist in other microbes, including microbes on flowering plants and pathogens.

INTRODUCTION

Microbes produce many secondary metabolites, several of which have strong aromas and are central contributors to the flavor of fermented foods and beverages such as cheese, wine, chocolate, and beer (Styger et al., 2011; Swiegers et al., 2005). Flavor formation has been extensively studied in the common brewer's yeast *S. cerevisiae*, which produces several volatile acetate esters such as ethyl acetate (pear aroma), isoamyl acetate (banana aroma), and phenylethyl acetate (flowery aroma; Lambrechts and Pretorius, 2000; Nordström, 1966; Saerens et al., 2008; Verstrepen et al., 2003a). These acetate esters are formed in a condensation reaction, catalyzed by an alcohol acetyl transferase (AAT), between acetyl-coenzyme A and various higher alcohols derived from the central carbon and amino acid metabolism. *S. cerevisiae* has two different genes coding for AATases, *ATF1* and *ATF2*, of which *ATF1* controls the bulk of the acetate ester formation (Lilly et al., 2000; Verstrepen et al., 2003b). Although many studies have focused on the optimization of aroma formation, the physiological role of these compounds remains elusive and highly debated (Mason and Dufour, 2000; Saerens et al., 2010). Some reports argue that some esters might help maintain plasma membrane fluidity in low-oxygen conditions where the synthesis of unsaturated fatty acids is impaired (Mason and Dufour, 2000). Other hypotheses suggest that ester synthesis may help tune the redox balance (Malcorps and Dufour, 1992) or that esterification of small organic acids may facilitate their removal from cells through diffusion through the plasma membrane (Nordström, 1964). However, no evidence has been found for any of these hypotheses, and deletion of *ATF1* does not reduce fitness under laboratory conditions (Saerens et al., 2010). Moreover, the most commonly used *S. cerevisiae* laboratory strains show significantly lower production of aroma compounds compared to their wild and industrial relatives (Verstrepen et al., 2003b), suggesting that the synthesis of these compounds has not been selected for under laboratory culture conditions and might rather be related to survival in complex natural environments.

In this study, we set out to investigate acetate ester production in the context of the well-established relationship between yeasts and their insect vectors (Fogleman et al., 1981; Giglioli, 1897; Phaff et al., 1956; Stefanini et al., 2012; Suh et al., 2005). Numerous studies have shown that, unlike fungi that disperse through air (Roper et al., 2010) or motile bacteria, sessile microbes like yeasts depend on animal and especially insect vectors for their dispersal (Francesca et al., 2012; Ganter et al., 1986; Goddard et al., 2010). In turn, microbes serve as a

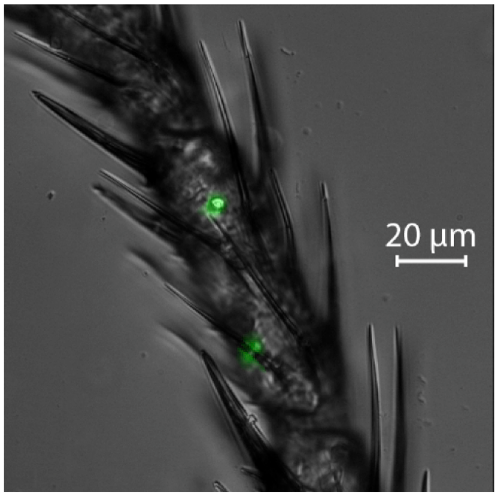

Figure 1. *Drosophila* Transport Yeast Cells in a Laboratory Setup
Yeast cells present on the front leg of a *Drosophila* fly. Sterile individual flies (n = 11) were allowed to roam a plate containing a single fluorescent yeast colony (Movie S1) for 1 hr. Afterward, flies were dissected and yeast cells on the various appendages were visualized using fluorescence microscopy. To quantify the number of cells that were transported, each part of the body was washed in a peptone buffer and the buffer was subsequently plated for cell counting (Table S1).

protein-rich food source for these insects and may even boost their immunocompetence (Anagnostou et al., 2010; Gibson and Hunter, 2010; Sang, 1956; Stamps et al., 2012). Previous studies have demonstrated that fermentation can increase the attractiveness of natural substrates toward *Drosophila* (Becher et al., 2012), even though there appears to be a variability in different yeast strains' ability to do so (Palanca et al., 2013). Additionally, multiple insect species are attracted to fruit and plant aroma mixtures that contain acetate esters (Boch et al., 1962; Galizia et al., 1999; Grosjean et al., 2011; Nojima et al., 2003). Finally, a few seminal studies have demonstrated that *Drosophila* antennae possess specific receptors for certain acetate esters (Elmore et al., 2003; Hallem and Carlson, 2006; Vosshall et al., 2000). Given this complex mutualism between microbes and insects, it seems likely that mechanisms evolved to facilitate these interactions. In this study, we show that a specific yeast gene, *ATF1*, produces acetate esters that change the neural representation of yeast odor in the *Drosophila* antennal lobe and help to attract insect vectors.

RESULTS

Yeast Strain Characterization

Experiments to investigate whether acetate esters help to attract insect vectors were carried out using two biological model systems: the fruit fly *Drosophila melanogaster* and the brewer's yeast *Saccharomyces cerevisiae*. To test the suitability of these organisms for our research, we demonstrated that *Drosophila* do transport yeast cells in a laboratory setup and can indeed act as a vector (Figure 1; Movie S1; Table S1). However, the most commonly used *S. cerevisiae* lab strain, S288c, produces much less aroma compared to wild and industrial *S. cerevisiae* strains (Verstrepen et al., 2003b), making it a poor reference strain for this study. Hence, in order to select a suitable strain, we performed fermentations with 285 genetically diverse *Saccharomyces sensu lato* strains and analyzed their aroma profile (Figure S1). From this collection, we selected a representative diploid strain, coded Y182, for our experimental setup. This *S. cerevisiae* strain was isolated from a vineyard and has an average production of both isoamyl as well as ethyl acetate. Moreover, the strain also shows a relatively high efficiency for genetic transformation, which enabled us to use genetic engineering to create *ATF1* deletion mutants. We deleted both alleles of *ATF1* in this diploid strain and subsequently analyzed the concentration of aroma compounds in the fermentation products of the wild-type and null mutant strains, focusing on higher alcohols, acetate esters, and medium-chain fatty acid esters, as well as ethanol and acetic acid levels, compounds that have been proposed to attract *Drosophila* (Hallem and Carlson, 2006; Hallem et al., 2004). These analyses confirmed that the levels of various acetate esters were severely reduced or even completely abolished in the *atf1* mutant strain, whereas no significant differences in the concentration of other volatile compounds such as acetaldehyde or higher alcohols was observed (Table 1). The effect of the presence of *ATF1* on the yeast's fitness was investigated using an automated multimode plate reader as well as automated time-lapse microscopy. In keeping with previous studies (Saerens et al., 2010), no difference in the growth rate between the wild-type (WT) and *atf1* mutant was observed in liquid or on solid media (see Supplemental Information for more information).

The Presence of *ATF1* Leads to Increased *D. melanogaster* Attraction

To evaluate whether changes in the yeast's aroma profile caused by the deletion of the *ATF1* gene lead *D. melanogaster* to prefer one strain over the other, we used an olfactory behavioral assay in a specially constructed arena (Figure 2). In this computer-controlled system, different airstreams can be released independently from each other out of the four corners of the isolated arena and cleared through a vacuum, applied in the center of the arena (Figure 2A). In this setup, the aromas from two different fermentations are delivered from opposing corners, whereas odorless air is streamed from the two remaining corners. For each olfactory behavioral assay, 50 flies were released in the arena and their positions were recorded with a camera placed above the arena. Subsequently, automated image analysis was used to quantify the number of flies in each of the four quadrants, before, during, and after odor delivery. Based on these numbers, a preference index was calculated for each input (see Figure 2 for details). During the first 2 min of each experiment, odorless air was delivered from all four corners of the arena. During this period, flies did not show preference for any specific quadrant. However, as soon as the airflow was switched so that two out of four corners contained the aroma of WT and *atf1* mutants

Table 1. Aroma Production by WT and *ATF1*$^{-}$ Strain

Compound (ppm)	WT-Y182	SD	*atf1*$^{-}$	SD	p Value
Acetaldehyde	8.98	2.73	9.67	2.89	0.74
Ethyl acetate	**14.54**	**1.53**	**6.45**	**0.43**	**5.20 × 10^{-5}[a]**
Ethyl propionate	0.08	0.01	0.09	0.01	0.19
Ethyl isobutyrate	0.02	0.00	0.02	0.00	0.90
Propyl acetate	**0.03**	**0.01**	**ND**	**ND**	[a]
Isobutyl acetate	**0.09**	**0.03**	**ND**	**ND**	[a]
Ethyl butyrate	20.24	3.26	20.40	2.23	0.94
Isobutanol	13.38	2.57	13.31	1.60	0.96
Isoamyl acetate	**0.82**	**0.20**	**0.13**	**0.06**	**5.68 × 10^{-4}[a]**
Butanol	55.45	2.21	57.67	5.22	0.53
Isoamyl alcohol	37.71	5.69	41.54	3.92	0.31
Ethyl hexanoate	0.13	0.03	0.18	0.01	0.04
Ethyl octanoate	1.08	0.23	1.14	0.13	0.66
Phenyl ethyl acetate	**0.10**	**0.02**	**ND**	**ND**	[a]
Phenyl ethanol	0.13	0.06	0.08	0.03	0.16
Ethanol (% v/v)	6.50	0.05	6.46	0.02	0.14
Acetate (g/l)	24.75	6.25	22.15	3.69	0.32

Concentrations of aroma compounds (in parts per million) produced by the diploid WT Y182 strain and the isogenic *ATF1* double-deletion mutant during fermentation (see Figure S1 for more information on Y182). For each strain, four fermentations were performed and each was analyzed in four technical replicates. Acetate esters are displayed in bold. These results demonstrate that the only compounds significantly affected by the *ATF1*$^{-}$ deletion are acetate esters (ND, not detected). Production of these aroma compounds by non-*Saccharomyces* strains may be found in Table S2.

[a]Significant difference between the WT and deletion strain ($p < 0.05$).

(each in one opposing corner), the flies significantly preferred the quadrant with the WT aroma over the aroma of *atf1* mutants (p value $< 1 \times 10^{-4}$). Afterward, when the airstream at all corners was switched back to odorless control, the flies no longer preferred a specific quadrant and were once again distributed randomly (Figure 2; Movies S2 and S3).

These results indicate that Atf1 activity has a significant effect on the attraction of *Drosophila* by the yeast cells. To verify whether the observed behavioral differences are indeed due to the lower acetate ester levels produced by the *atf1* mutant, we supplemented the *atf1* fermentation medium with phenylethyl acetate, isoamyl acetate, and ethyl acetate (the three important acetate esters most affected by the *ATF1* deletion), so that the final concentration of each ester was equal to that in the WT fermentation medium. We then repeated the olfactory preference tests with this supplemented medium pitted against the fruity WT medium, and no significant difference in preference for either medium was observed, clearly illustrating the central role of phenylethyl, isoamyl, and ethyl acetate in the altered attraction phenotype (Figures 2C and 2D). To further tease apart the specific contribution of each ester, we supplemented the *atf1* medium with each ester separately and tested these against the WT medium. These experiments revealed that ethyl acetate is the most important compound, because addition of this ester is sufficient to make the *atf1* medium as attractive as the WT medium in our olfactory behavioral assay. Addition of isoamyl acetate resulted in increased attraction compared to the unsupplemented *atf1* medium, but the WT attraction was not fully restored. Finally, phenylethyl acetate did not significantly affect *Drosophila* behavior.

To further confirm the role of the yeast *ATF1* gene in *Drosophila* attraction, we set up a second series of preference experiments, this time in larger cages (30 × 30 × 20 cm), allowing flies more freedom of movement in three dimensions, which has been implicated to alter their behavior compared to setups where their movement is more restricted (Becher et al., 2010; Lebreton et al., 2012). Analogous with the olfactory assay in the smaller arena, we placed traps containing either WT or *atf1* mutant fermentation medium in opposing corners of the larger cages and two traps containing only water in the two remaining corners. To account for position effects, the traps were switched across different repeats. Our results further confirmed a clear preference of *D. melanogaster* for the WT strain, attracting 2-fold more flies than the *atf1* strain (see Figure S2 for details).

WT and *atf1* Aromas Are Perceived Differently by *Drosophila*

To further evaluate the effect of isoamyl and ethyl acetate on the *Saccharomyces-Drosophila* interaction, we used in vivo calcium imaging to measure the neuronal responses to *atf1* and WT yeast aroma in the antennal lobe of a ;*Gal4-GH146/UAS-GCaMP6m*; *Drosophila* strain expressing the transgenic calcium indicator GCaMP6m in its projection neurons (Figures 3A and S3A; Chen et al., 2013). These measurements show a clear alteration in the response of projection neurons, which receive direct olfactory input from olfactory sensory neurons, to the mutant yeast strain compared to the WT strain (Figure 3B). To quantify the differences in the olfactory representation of the different yeast strains, we compared the odor-induced neuronal responses using pairwise Pearson's correlations (Figure 3C). Moreover, we further analyzed these activity maps by comparing the autocorrelation of the repetition of the WT yeast odor across different trials to the cross correlation of the odor representations of WT yeast against *atf1* yeast and *atf1* yeast supplemented with the missing esters (Figure S3E). Both analyses revealed that the WT and *atf1* yeast odor are represented by significantly different activity patterns in the fly antennal lobe. Moreover, we observed that the addition of each ester in physiological concentrations to the *atf1* mutant yeast medium shifts the evoked antennal lobe activity more toward the WT activity pattern, as evident by the significant increase in correlations between WT and *atf1* yeast odors when esters are supplemented. Furthermore, the principal component analysis of the antennal lobe odor responses shows that supplementing *atf1* with esters shifts the representation of *atf1* yeast odor toward WT yeast odor (Figure 3F). In summary, all these analyses confirms that *atf1* yeast odor and the WT yeast odor are represented differently in the *D. melanogaster* antennal lobe and the odor representations of *atf1* yeast become more similar to WT yeast when each ester is supplemented to the same levels as found in the WT medium.

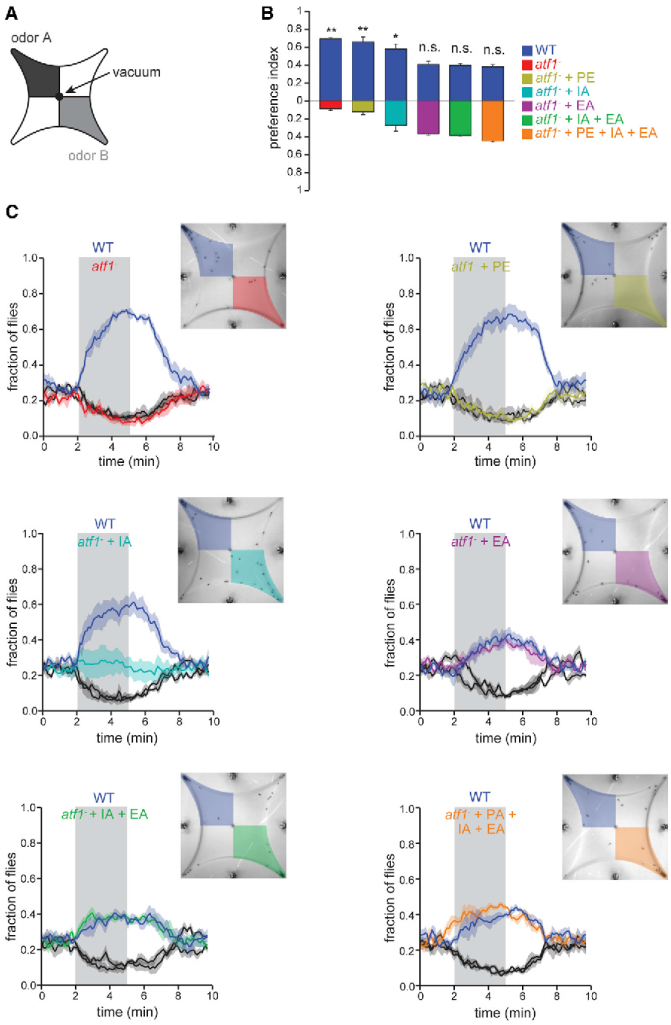

Figure 2. Volatile Acetate Ester Production Affects the Attractiveness of Yeast Cells for *Drosophila melanogaster*

(A) Experimental arena populated with fifty 20 hr-starved *D. melanogaster* CS10 flies. Air is flown from the four corners of the arena, with a common outlet in the center, generating four quadrants that each have their own air profile. Fly movements were recorded during 10 min experiments (odorless air for 2 min from each of the four corners, odors for 3 min from two opposing corners, and odorless air from the other two corners, and finally 5 min of odorless air from all four corners; see also main text for details and Movies S2 and S3).

(B) Preference index defined by the fraction of flies being present in the corresponding odorized quadrant during the last minute of odor exposure. The odors of WT yeast and *atf1*⁻ yeast supplemented with ethyl acetate (EA) and isoamyl acetate (IA) (at concentrations that match the levels present in the WT yeast) exhibit a higher preference index than *atf1*⁻ yeast odor whereas *atf1*⁻ supplemented with phenylethyl acetate (PA) does not (paired t test; $*p < 0.02$; $**p < 0.001$). No significant difference was found when WT yeast odor was competed against *atf1*⁻ yeast odor supplemented with all three esters or with ethyl acetate and isoamyl acetate or with ethyl acetate. The error bars represent SEM. n.s., not significant.

(C) Temporal course of number of flies per quadrant for the different experimental conditions. Colors correspond to the respective media (air shown in black/gray). Shadowed traces represent SEM for the number of flies (n = 200 flies; four experimental sessions; three trials/odor/session). The gray rectangle indicates the time of odor exposure. Inset figures correspond to snapshots taken at the end of the odor delivery period (5th min). For the large cage setup, see Figure S2.

Expression of *ATF1* Results in Increased Yeast Dispersal

The previous experiments revealed that the *ATF1*-mediated production of acetate esters has a significant impact on the attractiveness of yeast cells toward *D. melanogaster*. However, this does not necessarily imply a benefit for the yeast, because increased attraction of flies might merely result in more yeast cells being consumed by the flies. However, we hypothesized that increased fly attraction might also result in increased dispersal of the yeast cells through their insect vectors. To study whether expression of *ATF1* affects yeast dispersal by fruit flies, both the WT and *atf1*⁻ mutant strain were fluorescently labeled by overexpressing either yECitrine or mCherry. These labeled strains were inoculated on one of two designated spots on a specially constructed YPD plate, equidistant from the center of the plate (Figure S4). For each strain, the inoculum contained 1×10^6 cells, corresponding to the amount of *Saccharomyces* cells that may be found on infected grapes (Mortimer and Polsinelli, 1999). Subsequently, a fly was allowed to roam around the test environment overnight in complete darkness, after which it was removed. Then, the spots containing the initial inocula were removed as well so that only dispersed yeast cells remained and the plates were incubated to allow growth of these cells. After 48 hr, the plates were washed and the relative presence of each strain was quantified using a flow cytometer. Because there is no growth difference between the WT and mutant strains (Supplemental Information), the relative presence of each strain indicates the ratio in which the two strains were transported by the fly. Analysis of 100 independent experiments revealed that the fruity WT

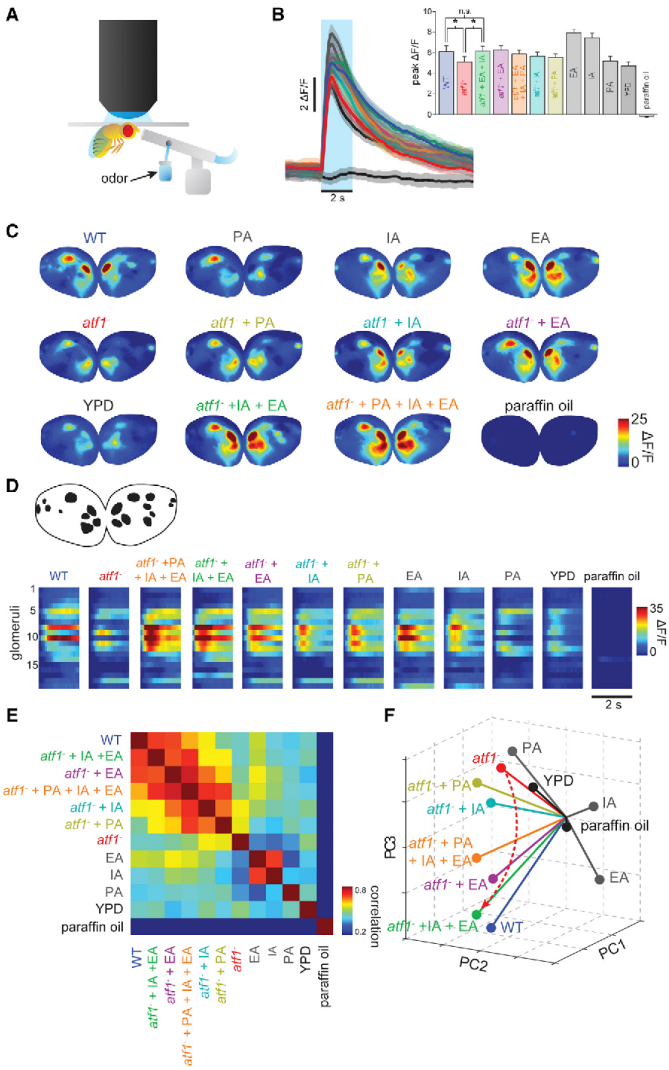

Figure 3. WT and *atf1*⁻ Yeast Odors Are Represented Differently in the Antennal Lobe of *Drosophila melanogaster*

(A) Experimental setup depicting a fly expressing the transgenic calcium indicator GCaMP6 in projection neurons. Briefly, the fly is fixed to an aluminum chamber with wax and the cuticle above the antennal lobes is removed, which allows imaging of the antennal lobes from the dorsal side. A tube is placed in front of its antennae for odors to be delivered (carrier stream flow rate = 2,000 ml/min).

(B) Temporal course of the average fluorescence signal in response to different odors in the entire antennal lobe. Shadowed traces represent SEM for the change in fluorescence. The blue rectangle depicts the 2 s time window after response onset, used for quantitative analyses. Inset bar plot shows that pure *atf1*⁻ yeast odor and *atf1*⁻ odor supplemented with PA elicit significantly weaker responses than WT yeast odor and *atf1*⁻ yeast odor supplemented with EA and IA, respectively ($n = 14$ flies; $^*p < 0.02$; paired t test).

(C) Representative antennal lobe activity maps corresponding to different yeast and ester odors as well as paraffin oil as control, respectively. Calcium responses were averaged during the 2 s window shown in (B).

(D) Regions of interest manually assigned to each responsive glomerulus based on activity maps for the fly shown in (C). On the right, the corresponding glomerulus-based response profiles for the different odors and control are shown. Profiles were constructed for the 2 s window shown in (B).

(E) Correlation matrix representing the pairwise similarities for the different odor response profiles ($n = 14$ flies). Note that *atf1*⁻ yeast odors supplemented with esters are more correlated to WT yeast odor than *atf1*⁻ yeast odor alone.

(F) Principal component analysis of the odor response profiles. The first three components are shown (total variances explained by first three principle components [PCs] = 79.6%; PC1 = 59.4%; PC2 = 12.8%; PC3 = 7.4%). Upon addition of more esters, the *atf1*⁻ yeast odor representations are progressively pushed in the direction of the representations of the WT yeast odor, indicating a more-similar response.

Additional analyses are in Figure S3.

strain was on average transported four times more than the *atf1*⁻ mutant (Figure 4). A separate mirror experiment ($n = 100$) demonstrated that the nature of the fluorescent tag did not influence the dispersal of either strain (Supplemental Information).

DISCUSSION

Together, these results demonstrate that expression of the fungal alcohol acetyl transferase gene *ATF1* promotes attraction of *D. melanogaster*, which in turn promotes dispersal of the yeast cells by the insect vector. Using a combination of molecular, behavioral, and neurobiological tests, we show that acetate esters produced by yeasts change the antennal lobe odor representations of *Drosophila melanogaster* and greatly increase its attraction to yeast. Moreover, we identify two acetate esters, ethyl acetate and isoamyl acetate, as the main signaling molecules associated with this phenotype.

It is interesting to note that compounds like ethyl acetate and isoamyl acetate render ripening fruits their typical aroma (Vermeir et al., 2009). It is therefore tempting to speculate that yeasts

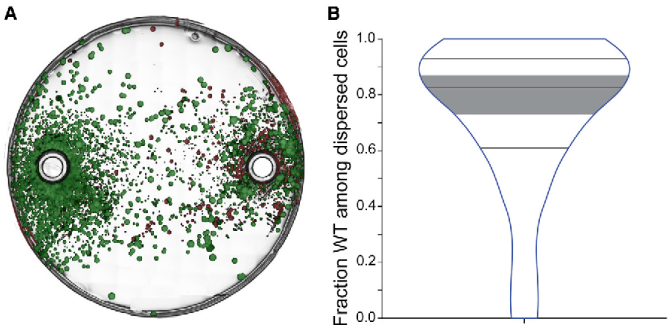

Figure 4. Fruity Yeast Strains Get Dispersed More by *D. melanogaster*

Two fluorescently labeled strains (green or red) were plated equidistantly from the center of a YPD agar plate (black circles; see also Figure S4 for details). A 20 hr-starved CS10 fly was introduced to the plate, which was closed and placed in a container, shielded from external light. After 14 hr, the fly was sedated and removed from the plate, after which the plate was incubated for 48 hr at 30°C to allow growth of dispersed yeast cells. Then, the spots from the initial inoculum were removed and the remaining cells were washed off the plate and analyzed using a flow cytometer.

(A) Image of a representative plate after 48 hr of incubation, before washing. The WT strain is yECitrine-labeled (green-yellow) and the *atf1* strain mCherry-labeled (red). The image clearly shows that the *atf1* (red) strain shows reduced dispersal by the flies.

(B) Violin plot of the fraction of dispersed WT cells (n = 95, excluding five samples where no cells were dispersed); black lines indicate quartiles and median. Fruity WT cells were dispersed significantly more than *atf1* cells, shown by the fact that the estimated fraction (gray band = 95% confidence interval) is significantly higher than the 50% expected if dispersal was equal for both (binomial mixed model; p value < 1×10^{-10}; details in Experimental Procedures).

have evolved the capacity to synthesize these esters to mimic this aroma in order to attract flies. However, it is difficult to show that the yeast *ATF1* gene specifically evolved to stimulate the production of aroma compounds with the aim of attracting insects. Nonetheless, there are compelling arguments for this hypothesis, because several reports demonstrate the intricate mutualism between yeasts and flying insects like fruit flies (Ganter et al., 1986; Giglioli, 1897; Gilliam et al., 1974; Phaff et al., 1956; Reuter et al., 2007; Starmer et al., 1986; Stefanini et al., 2012). For the yeast, dispersal is essential to reach new niches, especially when nutrient levels are running low. Under these conditions, the center of yeast colonies is expected to be a hypoxic environment (Cáp et al., 2012) and hypoxic conditions may increase *ATF1* expression (Fujii et al., 1997), which in turn results in increased acetate ester formation (Lilly et al., 2000; Malcorps and Dufour, 1992; Verstrepen et al., 2003b). Hence, the production of aroma compounds like isoamyl acetate could help alert flies to the presence of yeast cells, a vital component of their diet. Whereas some of the yeast cells are consumed by the insects, a fraction of cells will stick to the fly body and get dispersed to a different environment. Furthermore, yeasts might reap more benefits from this interaction than mere dispersal. Low nutrient levels trigger the formation of spores that can survive passage through the fly gut and promote outbreeding and thus genetic variability (Freese et al., 1982; Reuter et al., 2007). Additionally, it has been demonstrated that certain insects, such as wasps, act as a reservoir for yeasts when environmental conditions are harsh, for example, during a cold winter (Stefanini et al., 2012).

A last important question is whether aroma-based attraction of insects is limited to *S. cerevisiae*. In a first preliminary assay, we observed that many different yeasts can be isolated from the body of *Drosophila* isolated from natural environments and that the vast majority of these yeasts produced aroma-active esters (Table S2). Moreover, we also isolated several strong aroma-producing yeasts from flowers. These preliminary results suggest that aroma production is not restricted to *S. cerevisiae* and may be a much more general theme in microbe-insect interactions. This is further supported by other studies that reported the isolation of many different yeast species from various insects and the discovery that receptors for acetate esters are widespread in insects (Galizia et al., 1999; Phaff et al., 1956). The formation of fungal aroma compounds may even play a role in mimicry and the relation between plants and their pollinators (Dentinger and Roy, 2010; Stökl et al., 2010).

Lastly, our study also highlights the limitations of using standard laboratory conditions with pure single-species cultures. Clearly, studying model organisms in a more complex ecological context will increase our understanding of physiology and may help to reduce the number of genes with unknown functions.

EXPERIMENTAL PROCEDURES

Strains

Both *ATF1* alleles in the Y182 strain were deleted using deletion cassettes based on pUG6, conferring resistance to either Hygromycin B or G-418 disulfate. Both markers were removed through the Cre/LoxP technique using pSH65. Deletions as well as marker removal were confirmed through (lack of) growth on selective media, as well as PCR (primers in Table S3). Fermentations performed with WT and mutant strains were analyzed using a headspace-gas chromatography-flame ionization detector system; ethanol and acetate levels were determined using enzymatic kits. Growth rates in liquid YPD were measured in an automated multimode plate reader, whereas growth rates on solid media were determined using automated time-lapse microscopy (New et al., 2014). Differences between strains were analyzed using Mann-Whitney U tests.

Olfactory Preference Assays

Prior to testing, 50 CS10 flies were starved for 20 hr at ~25°C in scintillation vials containing a wet filter paper and then placed in the four-input arena. A camera placed above the arena filmed each trial, each lasting 10 min (2 min, odorless air; 3 min, odor exposure; 5 min, odorless air); each set of 50 flies was tested three times. The number of flies in each quadrant was detected by an automated MATLAB algorithm, based on binarized images. Paired t tests were used for statistical comparisons. For the assays in large cages, 20 CS10 flies were starved for 20 hr at 25°C in vials containing 2% agarose. Tests lasted 5 hr, after which all flies were sedated and the number of flies in each trap was counted. Statistical analyses were performed using a generalized linear mixed model (GLMM), available in R-package lme4. For the calcium

imaging experiments (Yaksi and Wilson, 2010), principle-component analyses and Pearson's correlations were calculated on the antennal lobe images obtained during 2 s after response onset windows. For statistical analyses, paired t tests were performed on antennal lobe peak responses and Mann-Whitney for correlation coefficients comparisons.

Dispersal Experiments

Flies were starved for 20 hr at 25°C in vials containing 2% agarose. Dispersal experiments were performed with custom-made plates (see Figure S4) filled with YPD-2% agar. Statistical analyses of the dispersal of both strains were performed using a GLMM, available in R-package lme4. Significance of deviation from 50:50 was tested using a Wald z test, also available in lme4.

SUPPLEMENTAL INFORMATION

Supplemental Information includes Supplemental Experimental Procedures, four figures, three tables, and three movies and can be found with this article online at http://dx.doi.org/10.1016/j.celrep.2014.09.009.

AUTHOR CONTRIBUTIONS

J.F.C. and L.M.F. designed, performed, and analyzed experiments and wrote the manuscript. T.L.C. performed experiments. L.D.M., J.M., T.W., and B.A.H. helped with design and interpretation of results and wrote the manuscript. K.J.V. conceived the study, and E.Y. and K.J.V. designed and interpreted experiments and wrote the manuscript.

ACKNOWLEDGMENTS

The authors thank Zeynep Okray; Ine Maes; and all K.J.V., E.Y., and B.A.H. lab members as well as CMPG members for their valuable help and suggestions. Research in B.A.H. lab is supported by VIB; the WiBrain Interuniversity Attraction Pole (BELSPO IUAP) network; and Fonds Wetenschappelijke Onderzoeks (FWO) grants G.0543.08, G.0680.10, G.0681.10, and G.0503.12. Research in the lab of E.Y. is supported by ERC Starting Grant 335561, FWO, VIB, and NERF funding. Research in the lab of K.J.V. is supported by ERC Starting Grant 241426, HFSP program grant RGP0050/2013, VIB, EMBO YIP program, FWO, and IWT.

Received: April 7, 2014
Revised: July 23, 2014
Accepted: September 3, 2014
Published: October 9, 2014

REFERENCES

Anagnostou, C., LeGrand, E., and Rohlfs, M. (2010). Friendly food for fitter flies? Influence of dietary microbial species on food choice and parasitoid resistance in *Drosophila*. Oikos *119*, 533–541.

Becher, P.G., Bengtsson, M., Hansson, B.S., and Witzgall, P. (2010). Flying the fly: long-range flight behavior of Drosophila melanogaster to attractive odors. J. Chem. Ecol. *36*, 599–607.

Becher, P.G., Flick, G., Rozpędowska, E., Schmidt, A., Hagman, A., Lebreton, S., Larsson, M.C., Hansson, B.S., Piškur, J., Witzgall, P., et al. (2012). Yeast, not fruit volatiles mediate *Drosophila melanogaster* attraction, oviposition and development. Funct. Ecol. *26*, 822–828.

Boch, R., Shearer, D.A., and Stone, B.C. (1962). Identification of isoamyl acetate as an active component in the sting pheromone of the honey bee. Nature *195*, 1018–1020.

Cáp, M., Stěpánek, L., Harant, K., Váchová, L., and Palková, Z. (2012). Cell differentiation within a yeast colony: metabolic and regulatory parallels with a tumor-affected organism. Mol. Cell *46*, 436–448.

Chen, T.W., Wardill, T.J., Sun, Y., Pulver, S.R., Renninger, S.L., Baohan, A., Schreiter, E.R., Kerr, R.A., Orger, M.B., Jayaraman, V., et al. (2013). Ultrasensitive fluorescent proteins for imaging neuronal activity. Nature *499*, 295–300.

Dentinger, B.T.M., and Roy, B.A. (2010). A mushroom by any other name would smell as sweet: *Dracula* orchids. Mellvainea *19*, 1–13.

Elmore, T., Ignell, R., Carlson, J.R., and Smith, D.P. (2003). Targeted mutation of a Drosophila odor receptor defines receptor requirement in a novel class of sensillum. J. Neurosci. *23*, 9906–9912.

Fogleman, J.C., Starmer, W.T., and Heed, W.B. (1981). Larval selectivity for yeast species by Drosophila mojavensis in natural substrates. Proc. Natl. Acad. Sci. USA *78*, 4435–4439.

Francesca, N., Canale, D.E., Settanni, L., and Moschetti, G. (2012). Dissemination of wine-related yeasts by migratory birds. Environ. Microbiol. Rep. *4*, 105–112.

Freese, E.B., Chu, M.I., and Freese, E. (1982). Initiation of yeast sporulation of partial carbon, nitrogen, or phosphate deprivation. J. Bacteriol. *149*, 840–851.

Fujii, T., Kobayashi, O., Yoshimoto, H., Furukawa, S., and Tamai, Y. (1997). Effect of aeration and unsaturated fatty acids on expression of the Saccharomyces cerevisiae alcohol acetyltransferase gene. Appl. Environ. Microbiol. *63*, 910–915.

Galizia, C.G., Sachse, S., Rappert, A., and Menzel, R. (1999). The glomerular code for odor representation is species specific in the honeybee Apis mellifera. Nat. Neurosci. *2*, 473–478.

Ganter, P.F., Starmer, W.T., Lachance, M.-A., and Phaff, H.J. (1986). Yeast communities from host plants and associated *Drosophila* in southern Arizona: new isolations and analysis of the relative importance of hosts and vectors on comunity composition. Oecologia *70*, 386–392.

Gibson, C.M., and Hunter, M.S. (2010). Extraordinarily widespread and fantastically complex: comparative biology of endosymbiotic bacterial and fungal mutualists of insects. Ecol. Lett. *13*, 223–234.

Giglioli, I. (1897). Insects and yeasts. Nature *56*, 575–577.

Gilliam, M., Wickerham, L.J., Morton, H.L., and Martin, R.D. (1974). Yeasts isolated from honey bees, Apis mellifera, fed 2,4-D and antibiotics. J. Invertebr. Pathol. *24*, 349–356.

Goddard, M.R., Anfang, N., Tang, R., Gardner, R.C., and Jun, C. (2010). A distinct population of Saccharomyces cerevisiae in New Zealand: evidence for local dispersal by insects and human-aided global dispersal in oak barrels. Environ. Microbiol. *12*, 63–73.

Grosjean, Y., Rytz, R., Farine, J.P., Abuin, L., Cortot, J., Jefferis, G.S., and Benton, R. (2011). An olfactory receptor for food-derived odours promotes male courtship in Drosophila. Nature *478*, 236–240.

Hallem, E.A., and Carlson, J.R. (2006). Coding of odors by a receptor repertoire. Cell *125*, 143–160.

Hallem, E.A., Ho, M.G., and Carlson, J.R. (2004). The molecular basis of odor coding in the Drosophila antenna. Cell *117*, 965–979.

Lambrechts, M.G., and Pretorius, I.S. (2000). Yeast and its importance to wine aroma: A review. S. Afr. J. Enol. Vitic. *21*, 97–129.

Lebreton, S., Becher, P.G., Hansson, B.S., and Witzgall, P. (2012). Attraction of Drosophila melanogaster males to food-related and fly odours. J. Insect Physiol. *58*, 125–129.

Lilly, M., Lambrechts, M.G., and Pretorius, I.S. (2000). Effect of increased yeast alcohol acetyltransferase activity on flavor profiles of wine and distillates. Appl. Environ. Microbiol. *66*, 744–753.

Malcorps, P., and Dufour, J.P. (1992). Short-chain and medium-chain aliphatic-ester synthesis in Saccharomyces cerevisiae. Eur. J. Biochem. *210*, 1015–1022.

Mason, A.B., and Dufour, J.P. (2000). Alcohol acetyltransferases and the significance of ester synthesis in yeast. Yeast *16*, 1287–1298.

Mortimer, R., and Polsinelli, M. (1999). On the origins of wine yeast. Res. Microbiol. *150*, 199–204.

New, A.M., Cerulus, B., Govers, S.K., Perez-Samper, G., Zhu, B., Boogmans, S., Xavier, J.B., and Verstrepen, K.J. (2014). Different levels of catabolite repression optimize growth in stable and variable environments. PLoS Biol. *12*, e1001764.

Nojima, S., Linn, C., Jr., and Roelofs, W. (2003). Identification of host fruit volatiles from flowering dogwood (Cornus florida) attractive to dogwood-origin Rhagoletis pomonella flies. J. Chem. Ecol. *29*, 2347–2357.

Nordström, K. (1964). Formation of esters from acids by brewer's yeast. IV. Effect of higher fatty acids and toxicity of lower fatty acids. Jnl. Institute Brewing *68*, 398–407.

Nordström, K. (1966). Formation of esters from acids by Brewer's yeast: formation from unsaturated acids. Nature *210*, 99–100.

Palanca, L., Gaskett, A.C., Günther, C.S., Newcomb, R.D., and Goddard, M.R. (2013). Quantifying variation in the ability of yeasts to attract Drosophila melanogaster. PLoS ONE *8*, e75332.

Phaff, H.J., Miller, M.W., and Shifrine, M. (1956). The taxonomy of yeasts isolated from Drosophila in the Yosemite region of California. Antonie van Leeuwenhoek *22*, 145–161.

Reuter, M., Bell, G., and Greig, D. (2007). Increased outbreeding in yeast in response to dispersal by an insect vector. Curr. Biol. *17*, R81–R83.

Roper, M., Seminara, A., Bandi, M.M., Cobb, A., Dillard, H.R., and Pringle, A. (2010). Dispersal of fungal spores on a cooperatively generated wind. Proc. Natl. Acad. Sci. USA *107*, 17474–17479.

Saerens, S.M., Delvaux, F., Verstrepen, K.J., Van Dijck, P., Thevelein, J.M., and Delvaux, F.R. (2008). Parameters affecting ethyl ester production by Saccharomyces cerevisiae during fermentation. Appl. Environ. Microbiol. *74*, 454–461.

Saerens, S.M., Delvaux, F.R., Verstrepen, K.J., and Thevelein, J.M. (2010). Production and biological function of volatile esters in Saccharomyces cerevisiae. Microb. Biotechnol. *3*, 165–177.

Sang, J.H. (1956). The quantitative nutritional requirements of *Drosophila melanogaster*. J. Exp. Biol. *33*, 45–72.

Stamps, J.A., Yang, L.H., Morales, V.M., and Boundy-Mills, K.L. (2012). Drosophila regulate yeast density and increase yeast community similarity in a natural substrate. PLoS ONE *7*, e42238.

Starmer, W.T., Barker, J.S., Phaff, H.J., and Fogleman, J.C. (1986). Adaptations of Drosophila and yeasts: their interactions with the volatile 2-propanol in the cactus-microorganism-Drosophila model system. Aust. J. Biol. Sci. *39*, 69–77.

Stefanini, I., Dapporto, L., Legras, J.L., Calabretta, A., Di Paola, M., De Filippo, C., Viola, R., Capretti, P., Polsinelli, M., Turillazzi, S., and Cavalieri, D. (2012). Role of social wasps in Saccharomyces cerevisiae ecology and evolution. Proc. Natl. Acad. Sci. USA *109*, 13398–13403.

Stökl, J., Strutz, A., Dafni, A., Svatos, A., Doubsky, J., Knaden, M., Sachse, S., Hansson, B.S., and Stensmyr, M.C. (2010). A deceptive pollination system targeting drosophilids through olfactory mimicry of yeast. Curr. Biol. *20*, 1846–1852.

Styger, G., Prior, B., and Bauer, F.F. (2011). Wine flavor and aroma. J. Ind. Microbiol. Biotechnol. *38*, 1145–1159.

Suh, S.O., McHugh, J.V., Pollock, D.D., and Blackwell, M. (2005). The beetle gut: a hyperdiverse source of novel yeasts. Mycol. Res. *109*, 261–265.

Swiegers, J.H., Bartowsky, E.J., Henschke, P.A., and Pretorius, I.S. (2005). Yeast and bacterial modulation of wine aroma and flavour. Aust. J. Grape Wine Res. *11*, 139–173.

Vermeir, S., Hertog, M.L.A.T.M., Vankerschaver, K., Swennen, R., Nicolai, B.M., and Lammertyn, J. (2009). Instrumental based flavour characterisation of banana fruit. LWT - Food Sci. Technol. *42*, 1647–1653.

Verstrepen, K.J., Derdelinckx, G., Dufour, J.P., Winderickx, J., Thevelein, J.M., Pretorius, I.S., and Delvaux, F.R. (2003a). Flavor-active esters: adding fruitiness to beer. J. Biosci. Bioeng. *96*, 110–118.

Verstrepen, K.J., Van Laere, S.D., Vanderhaegen, B.M., Derdelinckx, G., Dufour, J.P., Pretorius, I.S., Winderickx, J., Thevelein, J.M., and Delvaux, F.R. (2003b). Expression levels of the yeast alcohol acetyltransferase genes ATF1, Lg-ATF1, and ATF2 control the formation of a broad range of volatile esters. Appl. Environ. Microbiol. *69*, 5228–5237.

Vosshall, L.B., Wong, A.M., and Axel, R. (2000). An olfactory sensory map in the fly brain. Cell *102*, 147–159.

Yaksi, E., and Wilson, R.I. (2010). Electrical coupling between olfactory glomeruli. Neuron *67*, 1034–1047.

Gustatory-mediated avoidance of bacterial lipopolysaccharides via TRPA1 activation in *Drosophila*

Detection of pathogens is crucial for animal health. However, immune responses require a high metabolic demand, not to mention that it can be potentially dangerous if the immune system becomes too active. In this regard, a mechanism that allows an early detection of pathogens can be advantageous. Such mechanism could, in principle, involve the neural system to alert the animal of potential danger.

The bacterial endotoxins lipopolysaccharides (LPS) are cues that are recognized by the immune system. Interestingly, previous studies have shown that when fruit flies get in contact with LPS they begin cleaning themselves, which might help prevent infection. Nevertheless, it was not clear whether fruit flies can actually detect LPS. In this project, I performed *in vivo* functional imaging and showed that gustatory neurons that are normally activated by bitter compounds are also activated by LPS in *Drosophila melanogaster* (Figure P1). Furthermore, unlike bitter compounds such as caffeine, which activate these neurons via the Gr66a gustatory receptor, LPS seems to drive excitation of these gustatory neurons through the membrane protein TRPA1. These findings suggest that fruit flies detect bacterial endotoxins via a gustatory pathway, which might help them to avoid contaminated food. Moreover, as TRPA1 has also been associated with mediating detection of pungent chemicals contained in ordinary food items such as mustard, garlic and wasabi in humans, it is likely that a conserved mechanism involving TRPA1 has been preserved throughout evolution to help animals identify potential dangerous toxins in their food.

The results of the experiments I carried out for this project were initially included in the manuscript (Figure P1). Nevertheless, due to editorial decision, these results were excluded in the final version of the manuscript.

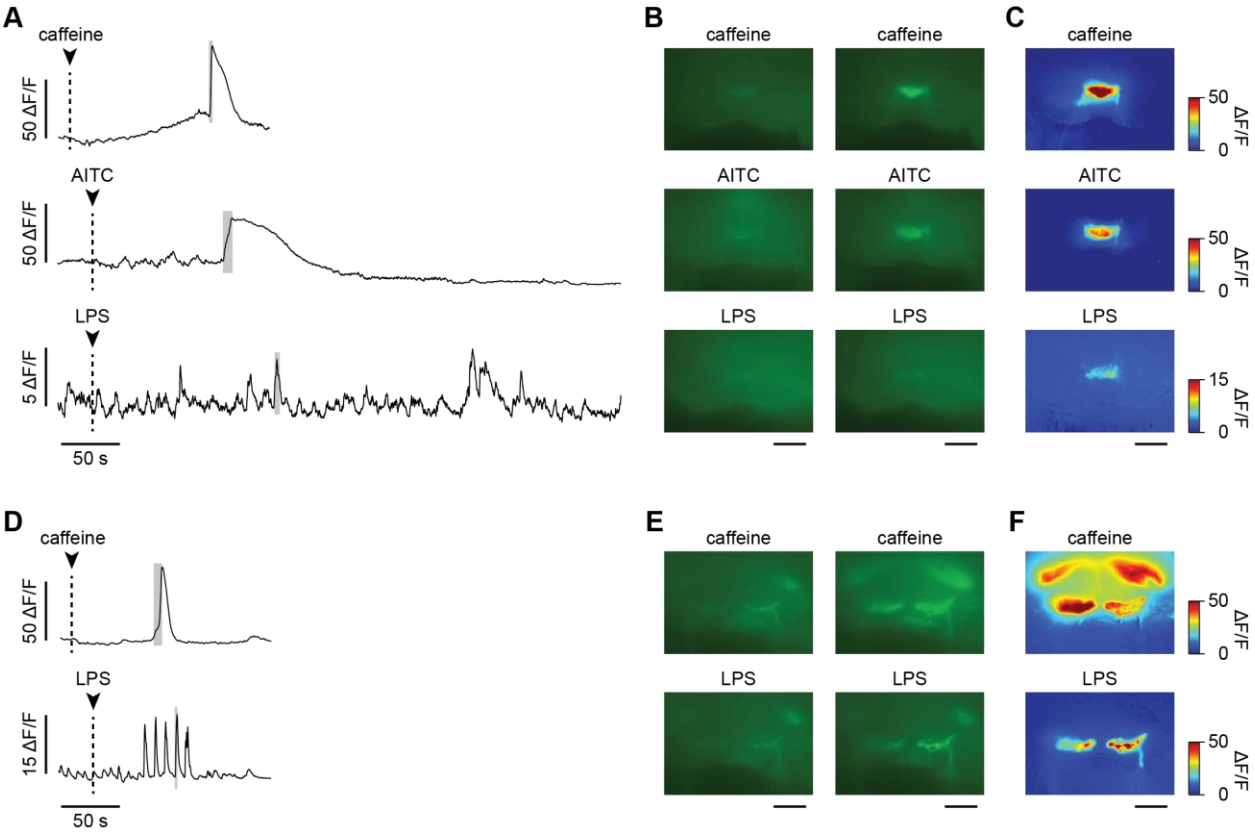

Figure P1. LPS activates neuronal populations in SOG. A,D. Time course of the percentage of fluorescence intensity (ΔF/F) in the projections of Gr66a positive (A) and TRPA1 positive (D) gustatory neurons, respectively, imaged in the subesophageal ganglion. Dashed lines indicate the start of drug application. The neurons were stimulated with 100 mM caffeine, 300 µM allyl isothiocyanate (AITC) or 500 µg/mL lipopolysaccharide (LPS). **B-C,E-F.** Activity maps obtained by calculating the percentage of fluorescence intensity (ΔF/F) during the time window denoted by contour gray boxes in A and D. Scale bar = 20 µm.

eLIFE elifesciences.org

SHORT REPORT

Gustatory-mediated avoidance of bacterial lipopolysaccharides via TRPA1 activation in *Drosophila*

Alessia Soldano[1,2,3], Yeranddy A Alpizar[1], Brett Boonen[1], Luis Franco[2,3,4], Alejandro López-Requena[1], Guangda Liu[2,3], Natalia Mora[2,3], Emre Yaksi[4,5], Thomas Voets[1], Rudi Vennekens[1], Bassem A Hassan[2,3,6,7]*, Karel Talavera[1]*

[1]Laboratory of Ion Channel Research and TRP Research Platform Leuven, Department of Cellular and Molecular Medicine, KU Leuven, Leuven, Belgium; [2]VIB Center for the Biology of Disease, VIB, Leuven, Belgium; [3]Center for Human Genetics, University of Leuven School of Medicine, Leuven, Belgium; [4]Neuroelectronics Research Flanders, Leuven, Belgium; [5]Kavli Institute for Systems Neuroscience and Centre for Neural Computation, NTNU, Trondheim, Norway; [6]Institut du Cerveau et de la Moelle Epinière, Hôpital Pitié-Salpétrière, Paris, France; [7]Ecole Doctorale Cerveau Cognition Comportement, Université Pierre et Marie Curie, Sorbonne Universités, Paris, France

Abstract Detecting pathogens and mounting immune responses upon infection is crucial for animal health. However, these responses come at a high metabolic price (***McKean and Lazzaro, 2011***, ***Kominsky et al., 2010***), and avoiding pathogens before infection may be advantageous. The bacterial endotoxins lipopolysaccharides (LPS) are important immune system infection cues (***Abbas et al., 2014***), but it remains unknown whether animals possess sensory mechanisms to detect them prior to infection. Here we show that *Drosophila melanogaster* display strong aversive responses to LPS and that gustatory neurons expressing Gr66a bitter receptors mediate avoidance of LPS in feeding and egg laying assays. We found the expression of the chemosensory cation channel dTRPA1 in these cells to be necessary and sufficient for LPS avoidance. Furthermore, LPS stimulates *Drosophila* neurons in a TRPA1-dependent manner and activates exogenous dTRPA1 channels in human cells. Our findings demonstrate that flies detect bacterial endotoxins via a gustatory pathway through TRPA1 activation as conserved molecular mechanism.
DOI: 10.7554/eLife.13133.001

***For correspondence:** bassem.hassan@icm-institute.org (BAH); karel.talavera@med.kuleuven.be (KT)

Competing interests: The authors declare that no competing interests exist.

Funding: See page 12

Received: 18 November 2015
Accepted: 12 May 2016
Published: 14 June 2016

Reviewing editor: Kristin Scott, University of California, Berkeley, United States

Results and discussion

In the past decade, increasing attention has been paid to the interactions between the immune and nervous systems (***McMahon et al., 2015***). In particular, there is evidence that sensory neurons can directly detect bacterial components as potentially damaging stimuli, and initiate acute inflammatory and nocifensive responses (***Chiu et al., 2013***; ***Meseguer et al., 2014***). It has been shown that the Gram-negative bacterial wall component LPS induces hygienic grooming in *Drosophila*, an important behavioral defense against pathogens, via contact chemosensation (***Yanagawa et al., 2014***). Thus, LPS may represent important sensory cues of food contamination with Gram-negative bacteria. To test whether LPS can be perceived by flies during food ingestion we used a binary food choice assay (***Isono and Morita, 2010***) (***Figure 1—figure supplement 1A***). We found that control flies displayed significant avoidance towards food supplemented with LPS (***Figure 1A*** and ***Figure 1—figure***

eLife digest An immune system can fight bacterial infections, ensuring an animal's health and survival. However, mounting an immune response to a bacterial infection requires a lot of energy. It also can be potentially dangerous if the immune system becomes too active. Therefore, avoiding bacteria and not getting infected to begin with may be a better strategy to stay healthy. Fruit flies, like humans, can detect dangerous substances in the environment via their sense of smell, but it is not known whether they also detect disease-causing organisms through their sense of taste.

Bacterial molecules called lipopolysaccharides (LPS) can alert the immune system to the presence of dangerous bacteria. Previous studies have found that when flies get in contact with LPS they begin cleaning themselves, which might help prevent infection. However it was not clear how the flies actually detected the LPS. Now, Soldano et al. show that fruit flies can taste LPS and avoid eating or laying eggs on food contaminated with LPS and bacteria. A series of experiments showed that when a fly tastes LPS it stimulates bitter-sensing neurons in the fly's mouth and throat. The experiments also revealed that the protein that activates these neurons in response to LPS is the same protein that acts in humans as detector of pungent chemicals contained in ordinary food items like mustard, garlic and wasabi. This suggests this protein, called TRPA1, is part of a key survival mechanism that has been preserved in many species throughout evolution.

Soldano et al. showed that a fly's senses and nervous system are actively involved in protecting it from bacterial infection. This is particularly important to flies, because unlike humans they don't develop resistance to future infections with the same bacteria. Future studies are needed to determine if flies use their sense of taste to detect other chemicals that are signs of infections. Additionally, studies are needed to determine if the activated bitter-sensing nerves alert the fly's immune system to a potential infection.

DOI: 10.7554/eLife.13133.002

supplement 1B). Because LPS is non-volatile we determined if this avoidance is mediated by gustatory neurons known to detect aversive compounds (Gr66a) (***Marella et al., 2006***). Blocking neurotransmission in these neurons by expressing the light chain of tetanus toxin (TNT) abolished avoidance of LPS (***Figure 1B***), indicating that flies can detect LPS through a gustatory mechanism.

A subset of Gr66a neurons innervating the labral sense organ and the labellum express TRPA1 (***Kim et al., 2010***; ***Kang et al., 2011***), a chemosensory cation channel (***Story et al., 2003***; ***Nilius et al., 2012***; ***Zygmunt and Högestätt, 2014***) that mediates acute nocifensive responses to LPS in mice (***Meseguer et al., 2014***) and avoidance of bitter and noxious compounds in *Drosophila* (***Kim et al., 2010***; ***Kang et al., 2010***; ***Du et al., 2015***). We tested whether TRPA1 mediates gustatory avoidance of LPS in flies. We found that loss of *dTrpA1* (w^{1118};$dTrpA1^{1}$, ***Figure 1C*** and $dTrpA1^{1}/dTrpA1^{ins}$, ***Figure 1—figure supplement 1C***) and pan-neuronal *dTrpA1* knockdown by two independent RNAi lines (***Figure 1—figure supplement 1D***) lead to impaired avoidance of LPS. Therefore, neuronal expression of *dTrpA1* is required for LPS avoidance. Furthermore, *Gr66a*-specific knockdown of *dTrpA1* abolished the LPS-induced behavior (***Figure 1D***), and restoration of *dTrpA1* expression using either of two different *dTrpA1* isoforms (A and B) in the entire *dTrpA1* pattern or only in Gr66a gustatory neurons of $dTrpA1^{1}/dTrpA1^{ins}$ flies rescued the avoidance of LPS (***Figure 1E***).

Female flies use gustatory detection of non-volatile compounds via Gr66a neurons to select oviposition sites (***Joseph and Heberlein, 2012***). In a binary oviposition choice assay control females showed preference for control food over food supplemented with LPS (***Figure 2A***). This behavior was lost in $dTrpA1^{-/-}$ flies (***Figure 2A***), upon silencing *Gr66a*-expressing neurons (***Figure 2B***), and in *Gr66a*-specific *dTrpA1* knockdown flies (***Figure 2C***). Altogether, these data show that LPS is avoided during feeding and oviposition and that *dTrpA1* expression in bitter-sensing gustatory neurons is necessary and sufficient for LPS avoidance. These data indicate that a TRPA1-dependent mechanism of avoidance of LPS may serve flies to prevent infection with Gram-negative bacteria. Indeed, we found that control animals, but not $dTrpA1^{-/-}$ mutants, preferred laying eggs on control food, rather than on food contaminated with *E. coli* (***Figure 2D***).

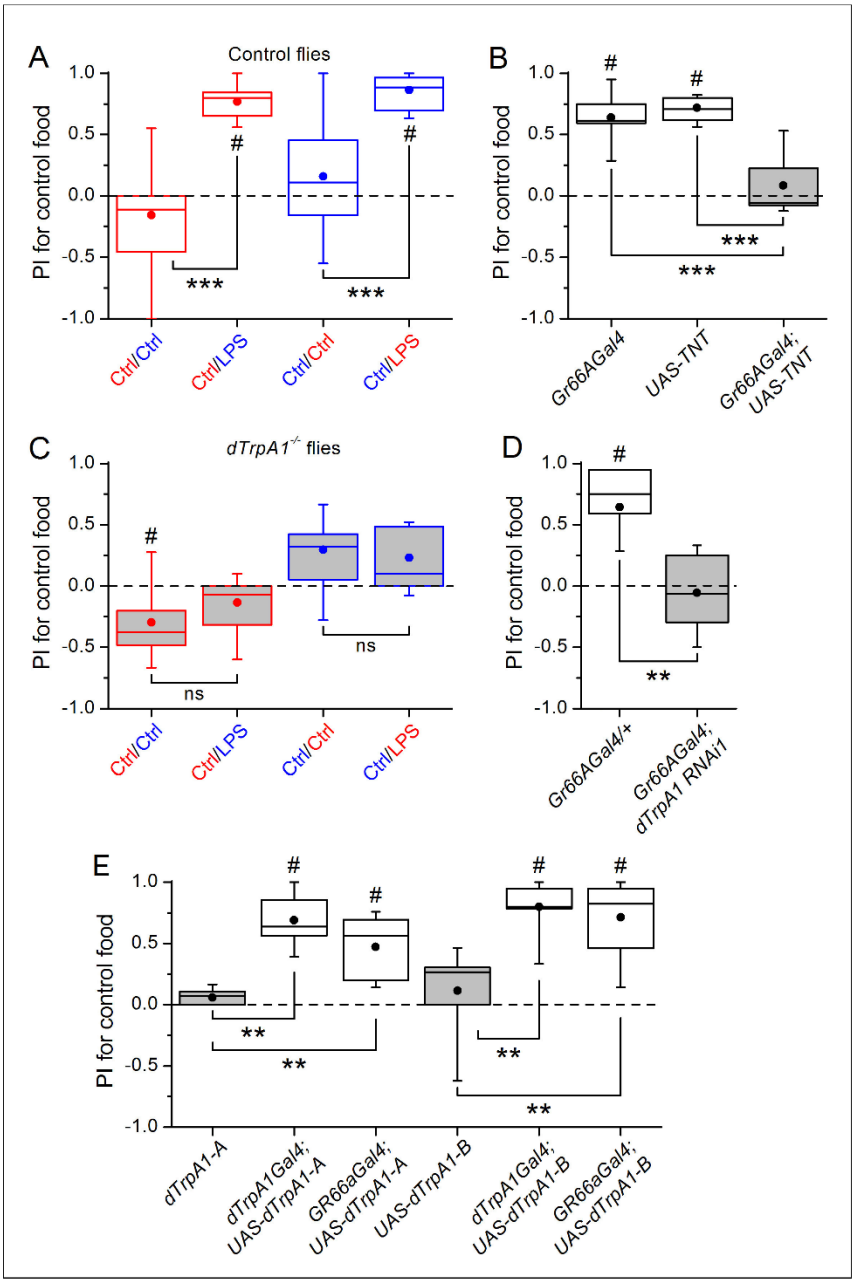

Figure 1. Gustatory *dTrpA1*-dependent avoidance of LPS in *Drosophila melanogaster*. (**A**,**C**) Preference index (PI) of control *CS10w*^{1118} (**A**) and *dTrpA1*-deficient (**C**) male flies for control food over LPS-supplemented food. PI was calculated for the consumption of the control solution mixed with the color

Figure 1 continued on next page

Figure 1 continued

of the corresponding data symbol (n ≥ 6). (**B**) PI for control food of *Gr66a>TNT* flies and in the corresponding driver-only and responder-only control flies (n ≥ 6). (**D**) PI for control food of *Gr66a>dTrpA1 RNAi* flies (n ≥ 4–8). (**E**) Rescue of LPS avoidance in $dTrpA1^{1}/dTrpA1^{ins}$; *dTrpA1>dTrpA1* and $dTrpA1^{1}/dTrpA1^{ins}$; *Gr66a>dTrpA1-A/B* flies (n ≥ 5). *P < 0.05; **P < 0.01; ***P < 0.001; 'ns', P > 0.05 (two-tailed Mann-Whitney *U* test). #, statistically significant differences from the no-preference zero level (two-tailed *t* test).

DOI: 10.7554/eLife.13133.003

The following figure supplement is available for figure 1:

Figure supplement 1. *dTrpA1*-dependent aversion to LPS in *Drosophila*.

DOI: 10.7554/eLife.13133.004

dTRPA1 is expressed in the mouthpart in a subset of gustatory neurons in the esophagus (***Figure 3A,B*** and ***Kang et al., 2010***) and in a few neurons in the labellum that also express Gr66a (data not shown and ***Kang et al., 2011***). However, no co-localization between *dTrpA1* and *Gr66a* was observed in the leg (***Figure 3—figure supplement 1***). To test whether avoidance of LPS is mediated by labellar or esophageal chemosensors we performed a proboscis extension reflex (PER) assay in wild type animals. LPS did not inhibit PER (***Figure 3—figure supplement 2***), suggesting that avoidance of LPS is not mediated by the labellar neurons, but by the gustatory neurons of the esophagus. We attempted to record neuronal responses in these neurons using flies expressing the genetically encoded Ca^{2+} indicator GCaMP6m in *Gr66a* neurons but Ca^{2+} imaging access to these neurons proved impossible in our assays. Next, we attempted direct brain stimulation. All preparations (5/5) responded robustly to the application of the dTRPA1 agonist allyl isothiocyanate (AITC) or the classical bitter compound caffeine, indicating that they were healthy. However, application of LPS gave varying results (small responses in 40% (2/5) of the flies; data not shown) precluding definitive conclusions. Therefore, in order to further test whether dTRPA1 mediates responses to LPS in vivo we monitored intracellular Ca^{2+} dynamics in the ventral nerve cord of larvae, a preparation that allows better accessibility of chemical stimuli. Application of LPS or the dTRPA1 agonist allyl isothiocyanate (AITC) induced robust Ca^{2+} responses, effects that were strongly reduced by incubation with the TRPA1 inhibitor HC030031 (***Figure 4—figure supplement 1***). In contrast, HC030031 did not affect the responses to a depolarizing solution containing high K^{+} concentration.

To test the role of TRPA1 in neuronal responses to LPS at the cellular level we examined primary cultures of larva brain neurons (***Figure 4—figure supplement 2***, ***Harzer et al., 2013***) expressing the Ca^{2+} indicator GCaMP5 under the control of *dTrpA1Gal4*. LPS (30 µg/ml) reversibly stimulated more than 40% of neurons isolated from control larvae (122/289), and 80% of these were also activated by the dTRPA1 agonist N-ethyl maleimide (NEM, 300 µM) (***Kim and Cavanaugh, 2007***) (***Figure 4A,B***). Notably, the proportion of neurons responding to both agents was strongly reduced in cultures derived from $dTrpA1^{1}$ null animals (20/153, $P < 10^{-4}$, Fisher exact test), as well as by pharmacological inhibition of dTRPA1 with HC030031 in neurons isolated from control animals (4/32, $P < 10^{-3}$, Fisher exact test). Intriguingly, the responses to LPS or NEM were not fully abolished by genetic or pharmacological ablation of dTRPA1. This suggests that dTRPA1 mediates some, though not all, Ca^{2+} responses of larva brain neurons to these compounds. To verify this indication in other experimental settings we evaluated the responses of cells isolated from brains of wild type larvae using the ratiometric Ca^{2+} indicator Fura2, and AITC as reference TRPA1 agonist. Application of LPS (60 µg/ml) reversibly stimulated more than 70% (39/54) of neurons isolated from control larvae (***Figure 4—figure supplement 3A,E,F***). A large proportion of LPS-sensitive neurons (23/39, 59%) were also activated by 100 µM AITC (***Figure 4—figure supplement 3A,E***), which indicates that LPS stimulates cells functionally expressing dTRPA1 channels. No Ca^{2+} response was observed when LPS was applied in the absence of extracellular Ca^{2+} (0/14, $P < 10^{-4}$, Fisher exact test; ***Figure 4—figure supplement 3B,E,F***). This indicates that LPS-induced responses result from Ca^{2+} influx through channels in the plasma membrane, rather than from release from intracellular stores. To directly assess whether LPS induces neuronal responses through the activation of dTRPA1, we tested its effects on wild type neurons in the presence of HC030031 (***Figure 4—figure supplement 3C***). In these experiments, LPS-induced responses were significantly less frequent (9/32, 28%, $P < 10^{-3}$, Fisher exact test, ***Figure 4—figure supplement 3E***) and smaller in amplitude ($P < 10^{-3}$, Mann-Whitney U test, ***Figure 4—figure supplement 3F***) than in control experiments. To confirm these data genetically, we tested the effects of LPS on neurons isolated from *dTrpA1*-null larvae. These cells responded to

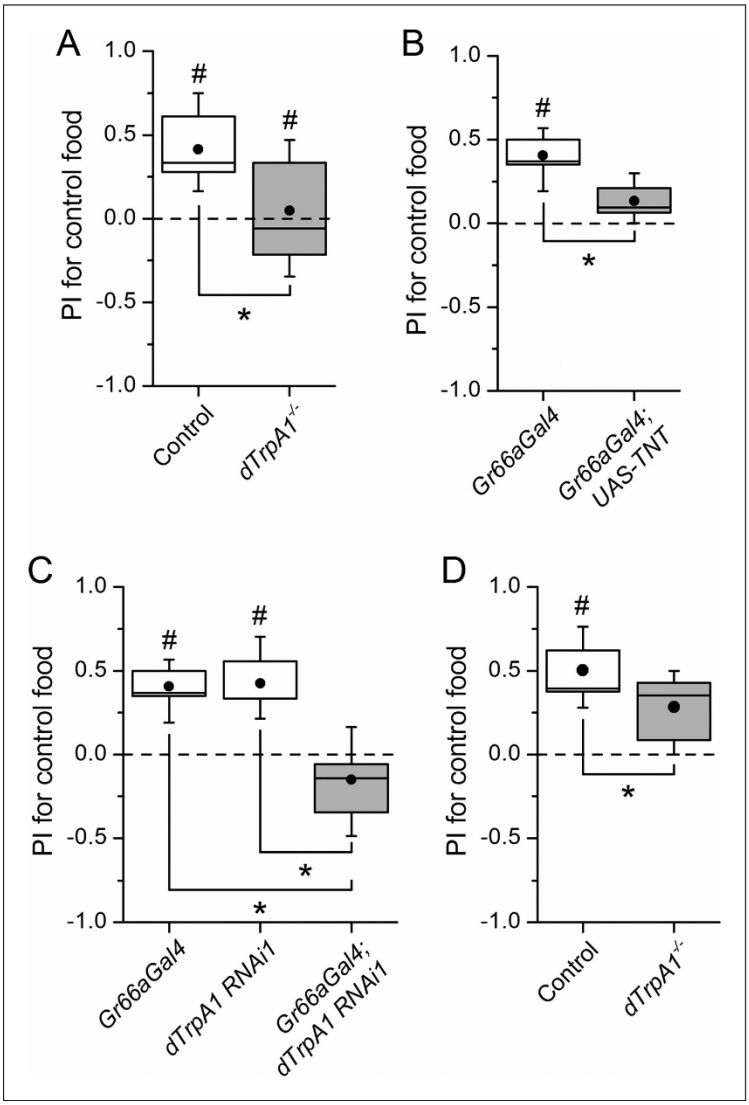

Figure 2. *dTrpA1* expression in gustatory neurons is required for avoidance of LPS during oviposition. (**A**) Preference index for oviposition in control food of wild type versus *dTrpA1*$^{-/-}$ flies ($n \geq 5$). (**B**) Oviposition preference of *Gr66a>TNT* flies ($n \geq 6$). (**C**) Oviposition preference of *Gr66a>dTrpA1 RNAi* flies ($n \geq 6$). (**D**) Oviposition preference of wild type versus *dTrpA1*$^{-/-}$ flies in presence of *E. coli*. ($n \geq 8$) *P < 0.05; **P < 0.01; ***P < 0.001 (two-tailed Mann-Whitney *U* test). #, statistically significant differences from the no-preference zero level (two-tailed *t* test).

DOI: 10.7554/eLife.13133.005

LPS with significantly lower frequency (5/23, 22%, $P < 10^{-4}$, Fisher exact test, ***Figure 4—figure supplement 3D,E***) and amplitude ($P < 10^{-4}$, Mann-Whitney U test, ***Figure 4—figure supplement 3F***) than control neurons. Importantly, the subpopulation of neurons responsive to both LPS and AITC in cultures from control larvae was absent in cultures from *dTrpA1*-null animals (***Figure 4—figure***

supplement 3E). Taken together, these data indicate that dTRPA1 channels expressed in the plasma membrane mediate at least part of the Ca^{2+} influx triggered by stimulation with in *Drosophila* neurons. Interestingly, as for the experiments with NEM, neither the LPS- nor the AITC-induced responses were fully absent in *TrpA1*-null neurons. This demonstrates that receptors other than TRPA1 may be also sensitive to these compounds in cultured brain neurons. This is in line with previous reports showing that sensory neurons isolated from *Trpa1* knockout mice showed reduced, but not completely abrogated responses to LPS (*Meseguer et al., 2014*), and that TRPA1 is not the only target of electrophilic compounds in sensory neurons (*Alpizar et al., 2014*; *Everaerts et al., 2011*; *Gees et al., 2013*; *Ohta et al., 2007*; *Salazar et al., 2008*). Here it is important to note that we used the larval fillet preparation and the neuron cultures as experimental models for native functional expression of dTRPA1.

Finally, we determined whether dTRPA1 can be activated by LPS in the HEK293T heterologous expression system. We found that 60 µg/ml LPS induced only very few responses in non-transfected cells (7/110), but stimulated a significantly larger fraction of cells transiently transfected with dTRPA1-A (42/74, $P < 10^{-4}$, Fisher exact test) or dTRPA1-B (14/67, P = 0.007, Fisher exact test) (*Figure 4—figure supplement 4*). These responses were more variable in amplitude and less frequent than those triggered by AITC, indicating that LPS is a relatively weak agonist of dTRPA1 channels (*Alpizar et al., 2013*). Further evidence for dTRPA1 activation by LPS was obtained in whole-cell patch-clamp experiments, in which application of LPS significantly enhanced both outward and inward currents in dTRPA1-A transfected HEK293T cells, but not control cells (*Figure 4C,D*). Application of HC030031 reduced the amplitude of currents recorded in the presence of LPS (35 ± 4% at -75 mV, n = 6, *Figure 4C*), further confirming the TRPA1-dependence of these responses. Previous results suggest that LPS activates mouse TRPA1 channels by inducing mechanical perturbations in the plasma membrane upon insertion of the lipophilic moiety of the molecule (*Meseguer et al., 2014*). It is conceivable that LPS activates dTRPA1 channels via the same mechanism, but additional experiments are required to verify this.

Taken together, our data demonstrate that fruit flies possess a gustatory mechanism underlying the detection and avoidance of LPS. The avoidance of LPS-contaminated food during feeding and oviposition may serve to prevent Gram-negative bacterial infections, potentially compensating for the lack of adaptive immunity in these animals. The fact that this sensory mechanism exploits dTRPA1 suggests a broadly conserved principle whereby these channels play a crucial role in LPS detection by sensory neurons in flies and mammals, regardless of the particular sensory modality involved. Our findings, together with previous evidence of an olfactory-based detection of secondary metabolites of Gram-positive bacteria (*Stensmyr et al., 2012*), underscore the need to consider the function of the sensory nervous system as a crucial part of a broad mechanistic understanding of pathogen-host interactions.

Materials and methods

Drosophila stocks

Drosophila melanogaster strains were raised on standard cornmeal/agar medium supplemented with dry yeast at 25 °C with a 12 hr light/dark cycle. The wild type stock was a w^{1118}strain. The following stocks were obtained from Bloomington Stock Center: w^{1118};*dTrpA1*^{1} (BL26504), *dTrpA1 RNAi1* (BL31384), *w*;dTrpA1*^{1}, *dTrpA1-Gal4* (BL36922), *w*; dTrpA1-Gal4* (BL 27593), UAS-RFP (BL 27391), *UAS-GCaMP5* (BL 42037), *UAS-GCaMP6m* (BL 42748). The Gr66a-IRES-GFP vector was kindly provided by Kristin Scott, the *NSyB-Gal4;UAS-GCaMP3* was obtained by Patrick Verstreken. The lines *Gr66aGal4, UAS-dTrpA1(A);dTrpA1*^{ins}*,dTrpA1GAL4, UAS-dTrpA1(B);dTrpA1*^{ins}*,dTrpA1-Gal4* and the *dTrpA1 RNAi 2* were kindly provided by the laboratory of Paul Garrity.

Binary choice food preference

Groups of 20–30 adult males (2–7 days old) were starved for 20 hr in plastic tubes provided with humidified filter paper. After starvation, the animals were allowed to feed on a microtiter dish containing wells alternating 100 mM sucrose alone or with 1 mg/ml LPS, mixed with either a red or blue dye (Supplementary *Figure 1*, left). This concentration of LPS was chosen in accordance with a previous study reporting concentrations between 250 and 800 µg/ml in water used to rinse fruits and

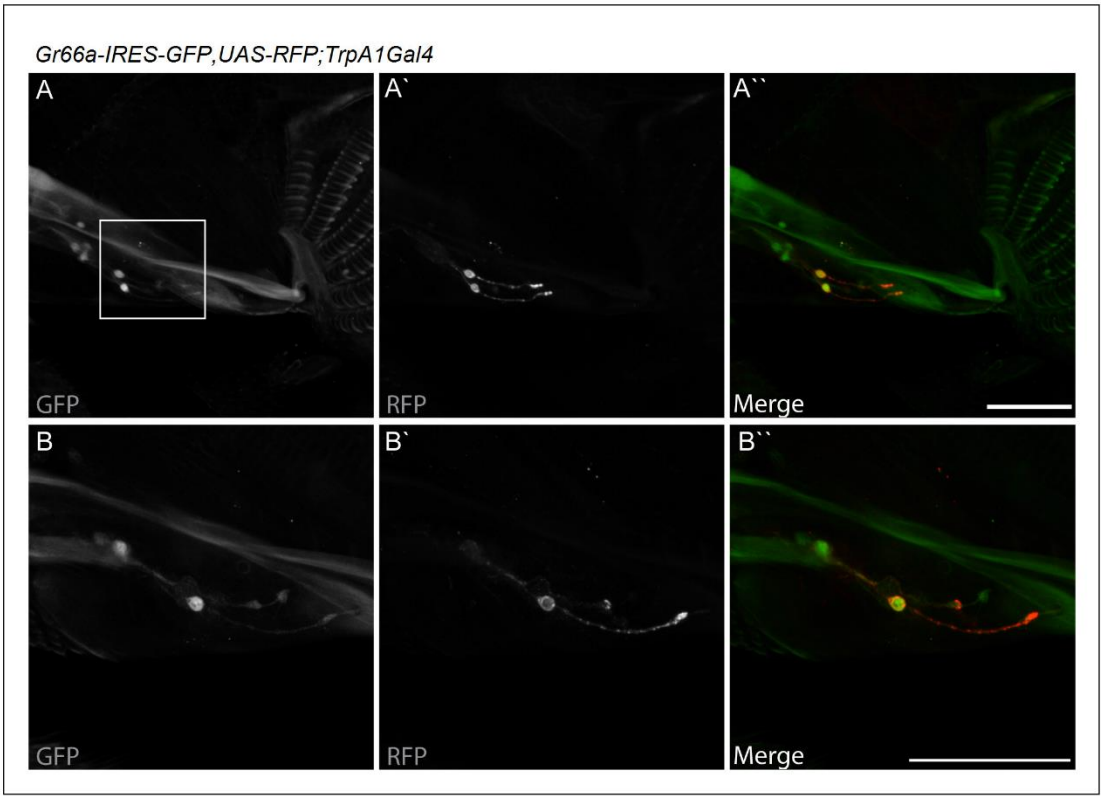

Figure 3. *dTrpA1* is expressed in a subset of *Gr66a*-expressing neurons that can be directly stimulated by LPS. (**A**) Immunofluorescence analysis of *Gr66a-IRES-GFP,UAS-RFP;dTrpA1Gal4* adult proboscis. Anti-GFP immunohistochemistry (in green in the Merge panel) labels taste neurons while anti-RFP (in red in the Merge panel) labels *dTrpA1*-expressing cells. Scale bar = 50 μm. (**B**) High magnification image of esophageal neurons expressing *Gr66a* and *TrpA1*.

DOI: 10.7554/eLife.13133.006

The following figure supplements are available for figure 3:

Figure supplement 1. dTRPA1 is not expressed in tarsal Gr66a-expressing neurons.

DOI: 10.7554/eLife.13133.007

Figure supplement 2. LPS does not alter the proboscis extension reflex.

DOI: 10.7554/eLife.13133.008

vegetables contaminated with *E. coli* (***Wang et al., 2011***). The concentrations in the surface of the food would be therefore much higher than these values, and hence the concentration of 1 mg/ml is likely to be relevant for real scenarios. The feeding preference was assessed by examining the colors of the abdomen and by classifying the flies as red, blue or purple (Supplementary ***Figure 1***, right). The preference index (PI) for the control-containing solutions was calculated as: $(n_{Control} - n_{Test})/(n_{Control} + n_{Test})$, where $n_{Control}$ and n_{Test} are the number of flies that ate the control solution (in red or blue color) and the test solution (containing control or LPS, both in red or blue color), respectively. The test solutions were colored with food dyes that showed comparable results: red (food dye or Sulforhodamine B sodium salt, 1 mg/ml) and blue (food dye or Erioglaucine disodium salt, 0.16 mg/ml). Preference data was always represented in box charts in which lines and the dots inside the boxes represent the median and the mean of the data, respectively.

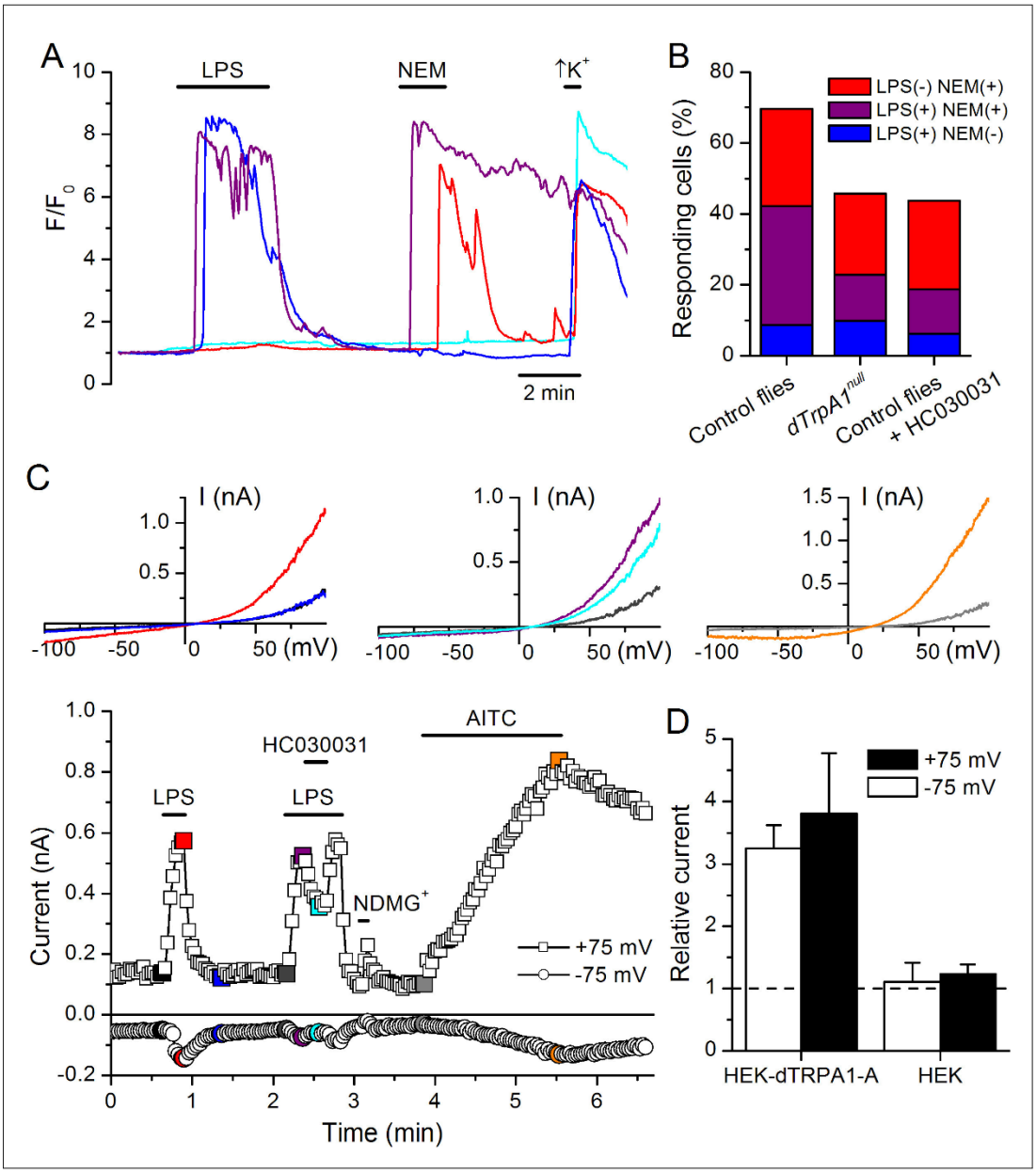

Figure 4. LPS stimulates dTRPA1. (**A**) Intracellular Ca^{2+} imaging in cultured brain L3 neurons expressing RFP and GCaMP5 under the control of *dTrpA1Gal4* in baseline conditions and during extracellular perfusion with LPS (30 µg/ml), NEM (300 µM) or high K^+ (50 mM KCl). (**B**) Proportions of neurons responding to LPS (red), NEM (blue) or both (purple). (**C**) Time course of the currents amplitude measured at +75 and -75 mV during whole-cell patch-clamp recording in dTRPA1-A transfected HEK293T cell. The colored data points correspond to current traces shown at the top of the panel. (**D**)

Figure 4 continued on next page

Figure 4 continued

Average effects of LPS on the current amplitudes recorded at +75 and -75 mV in dTRPA1-A-transfected (n = 7) and non-transfected (n = 3) HEK293T cells. For each cell, the current amplitudes measured in the presence of LPS were normalized to those measured in control condition.

DOI: 10.7554/eLife.13133.009

The following figure supplements are available for figure 4:

Figure supplement 1. LPS stimulates dTRPA1 in vivo.

DOI: 10.7554/eLife.13133.010

Figure supplement 2. Images of a culture of cells from third instar larvae brains.

DOI: 10.7554/eLife.13133.011

Figure supplement 3. LPS stimulates Drosophila neurons in vitro in a dTRPA1-dependent manner.

DOI: 10.7554/eLife.13133.012

Figure supplement 4. LPS-induced responses in HEK293T cells transfected with dTRPA1 channels.

DOI: 10.7554/eLife.13133.013

Egg-laying assay

Adult flies were allowed to mate for 48 hr prior to test. Males were subsequently discarded and females were transferred to a test tube on top of a 35 mm dish containing food. The food was covered on one side with control solution (water) and on the other side with test solution. The test solution consisted of either *E. coli* or 1 mg/ml LPS in water. The flies were allowed to lay eggs for 20 hr at 25 °C in a light-proof chamber, after which the amount of eggs on each side of the plate was counted. A preference index (PI) for laying eggs in the control side was calculated as: $(n_{ControlSide} - n_{OtherSide})/(n_{ControlSide} + n_{OtherSide})$, where $n_{Control}$ and $n_{OtherSide}$ are the number of eggs laid in the control and in the other side (containing control, *E. coli* or LPS), respectively.

Proboscis extension reflex assay

Two to seven day old flies were starved overnight on wet wipes, anaesthetized on ice, and gently pushed into a pipette tip. The flies were positioned with the head and the proboscis protruding outside the tip edge and the body immobilized within the tip. Flies recovered for 5–10 min before the test and then satiated with water. The solutions were presented as a liquid drop on a syringe tip and the proboscis was touched with the drop for 5 consequent times. During the assay flies were first stimulated with water, to exclude that any response would be due to thirst, and subsequently with 100 mM sucrose alone, as positive control, 100 mM sucrose + 1 mg/ml LPS and finally with 100 mM sucrose again. The extension frequency was calculated as mean frequency of all the samples (n = 19 animals).

In vivo intracellular Ca^{2+} imaging on the *Drosophila* sub-esophageal ganglion

For each experiment, a fly was secured to an aluminum chamber with wax. The antennae and the surrounding cuticle were removed. The brain was immerged into a bath containing adult hemolymph-like (AHL) solution. The proboscis was partially severed to allow easier penetration of the chemicals. The sub-esophageal ganglion was imaged in vivo from the dorsal side while constantly perfusing the brain with oxygenated AHL saline. The saline containing (in mM): 108 NaCl, 5 KCl, 2 $CaCl_2$, 8.2 $MgCl_2$, 4 $NaHCO_3$, 1 NaH_2PO_4, 5 trehalose, 15 ribose, 5 HEPES (pH 7.3). GCaMP fluorescence was imaged at 4 Hz using an EMCCD camera (Hamamatsu Photonics) installed on an Olympus BX51 fluorescence microscope (Olympus Corporation).

Drosophila larval fillet preparation and *in vivo* intracellular Ca^{2+} imaging

In vivo intracellular Ca^{2+} imaging was performed in larvae fillets, consisting on surgically exposed brains and ventral nerve cords of wandering third instar larvae. Briefly, larvae were immobilized using pins and stretched out lengthwise in a dish coated with silica and filled with a HL3 solution containing (in mM): 70 NaCl, 5 KCl, 20 $MgCl_2$, 10 $NaHCO_3$, 5 trehalose, 115 sucrose and 5 HEPES (pH 7.3). The larval skin was cut vertically along the dorsal midline towards the rostral end of the larva using spring scissors. At the rostrum of the animal horizontal incisions were made to the left and right. This created a left and a right flap in the body wall. These flaps were then pulled and pinned on the

side of the larva to better expose the brain. The organs were removed with forceps and the preparation was immediately used for imaging.

Intracellular Ca^{2+} imaging was performed using a monochromator-based system consisting of a Polychrome V monochromator (TILL Photonics GmbH, Germany), an upright microscope (Olympus, U-TV1X-2, Japan) and a 10X water immersion objective. Images were obtained with an iXon3 888 (Andor, Germany) camera controlled by LiveAcquisition software (TILL Photonics GmbH, Germany). The bath temperature was controlled by a SC-20 dual in-line heater/cooler (Warner Instruments, USA) and an Objective Heater® System (Bioptech, USA). The data were classified semi-automatically using a function programmed in MATLAB (MathWorks, MA) and analyzed with Origin 7.0 (OriginLab Corporation, Northamptom, MA, USA).

Primary cultureof *Drosophila* larval neurons

Primary neuronal cultures were obtained by dissection of the brain complex of third instar larvae, as described elsewhere (***Harzer et al., 2013***). Dissociated neurons were plated as a 50 µl drop in the center of a coverslip previously coated with a poly-D-lysine/laminin solution. Approximately 40 larvae were dissociated to seed 10 coverslips. Primary neurons were allowed to attach on a coverslip for 2 hr at 25 ˚C after dissociation. Imaging experiments were performed 3 hr after seeding the cells.

Immunostaining and intracellular Ca^{2+} imaging in cultured primary neurons

Primary neurons in coverslips were washed three times with PBS and subsequently fixed with 4% paraformaldehyde (PFA) for 20 min. After 10 min incubation with 0.1 M glycine, the cells were permeabilize with 0.1% Triton X-100, followed by 20 min incubation with 3% BSA to reduce unspecific protein bindings. Neuronal subset was stained using a rat anti-Elav (Molecular Probes, 1 hr, dilution 1:100), followed by 30 min incubation with a donkey anti-rat Alexa 488 antibody. Three washes with PBS were used to rinsed cells during all experimental steps described during fixation, permeabilization and staining. After immunostaining coverslips were covered with Vectashield mounting medium (Vector Labs) and imaged on an A1-R confocal (Nikon) mounted on a Ti-2000 inverted microscope (Nikon). The images were processed using ImageJ.

Experiments were performed at 25 ˚C using a standard Krebs solution containing (in mM): 150 NaCl, 6 KCl, 1 $MgCl_2$, 1.5 $CaCl_2$, 10 glucose, 10 HEPES and titrated to pH 7.4. In experiments on cells expressing GCaMP5 the fluorescence was measured during excitation at 488 nm using a Nikon Eclipse Ti microscope (Nikon) and the NIS Elements 4.30 software. In experiments on cells isolated from wild type flies we used Fura2 as Ca^{2+} indicator. Neurons were functionally identified at the end of each experiment by their responsiveness to the application of an extracellular solution containing high K^+ concentration. The data were classified semi-automatically using a function programmed in MATLAB (MathWorks, MA) and analyzed with Origin 7.0 (OriginLab Corporation, Northamptom, MA, USA).

Immunostainings of fly tissue

For the proboscis staining adult heads were dissected in phosphate buffered saline (PBS) and fixed in 3.7% formaldehyde in PBT (PBS + TritonX100 0.1%) for 15 min. The samples were subsequently rinsed three times in PBT and the proboscis were detached from the heads before being blocked in PAX-DG for 1 hr. Following these steps, the samples were incubated with mouse anti-GFP (Roche) and rabbit anti-dsRED (Clonetech) diluted in PAX-DG overnight at 4 ˚C. This incubation was followed by three washes with PBT and a subsequent incubation with the appropriate fluorescent secondary antibodies for 2 hr at 25 ˚C. After three rinses in PBT, the proboscis were transferred in 50% Glycerol diluted in PBS and then mounted in Vectashield (Vector Labs) mounting medium.

For the legs staining the procedure was modified as follows. Flies were fixed in 3.7% formaldehyde in PBT (PBS + TritonX100 3%) for 4 hr, then subsequently rinsed three times in PBT. The legs were then separated from the body and left O/N in the fixing solution.

Culture and transfection of HEK293T cells

Human embryonic kidney cells, HEK293T, were seeded on 18 mm glass coverslips coated with poly-L-lysine (0.1 mg/ml) and grown in Dulbecco's modified Eagles medium containing 10% (v/v) fetal calf

serum, 2 mM L-glutamine, 2 U/ml penicillin and 2 mg/ml streptomycin at 37 ˚C in a humidity controlled incubator with 10% CO_2. Cells were transiently transfected using Trans-IT-293 reagents (Mirus, Madison, MI, USA) with dTRPA1-A or dTRPA1-B (kindly provided by Paul Garrity) cloned into the pCAGGSM2-IRES-GFP vector.

Intracellular Ca^{2+} imaging in HEK293T cells

For intracellular Ca^{2+} imaging experiments cells were incubated at 37 ˚C with 2 µM Fura2-AM ester for 30 min before the recordings. Intracellular Ca^{2+} concentration was measured on an Olympus CellM system at 23 ˚C. Fluorescence was measured during excitation at 340 and 380 nm, and after correction for the individual background fluorescence signals, the ratio of the fluorescence at both excitation wavelengths (F340/F380) was monitored. In all experiments transfected cells were identified by GFP expression and sensitivity to the TRPA1 agonist AITC.

Patch-clamp experiments

Whole-cell membrane currents were measured at 23 ˚C with an EPC-10 patch-clamp amplifier and the softwares Pulse (HEKA, Lambrecht/Pfalz, Germany) and Clampex (Axon Instruments, Sunnyvale CA, US). Currents were digitally filtered at 2.9 kHz, acquired 20 kHz and stored for off-line analysis on a personal computer. Cells were recorded in an extracellular solution containing (in mM): 140 NaCl, 5 KCl, 10 HEPES, 2 $CaCl_2$, 2 $MgCl_2$, 10 glucose, pH titrated to 7.4 with NaOH. The pipette solution contained (in mM): 120 Cs-Aspartate, 5 EGTA, 10 HEPES, 1 $MgCl_2$, pH titrated to 7.4 with CsOH. Non-transfected HEK cells were used as control. Whole-cell currents were elicited using a 200 ms voltage ramp from -110 mV to +110 mV every 2 s from a holding potential of -40 mV. $NMDG^+$ (N-methyl-D-glucamine) was used to monitor the size of the leak currents during the patch-clamp recordings (***Meseguer et al., 2011***). Electrophysiological data were analyzed using WinASCD software (Guy Droogmans, KU Leuven) and Origin (OriginLab Corporation, Northamptom, MA, USA). Origin was also used for statistical analysis and data display.

Reagents

We used LPS extracted from *E. coli*, strains 055:B5 and 0127:B8. AITC was kept at 4 ˚C as a 100 mM stock solution in ethanol and fresh dilutions were prepared daily. All chemicals were purchased from Sigma-Aldrich (Bornem, Belgium).

Acknowledgements

We are very grateful to Paul Garrity for reagents and discussion of the data during the initial part of the project and to Patrik Verstreken for the *NSyB-Gal4;UAS-GCaMP3* flies. We thank Zeynep Okray for her help with larval dissections, Koenraad Philippaert for his help with in vivo Ca^{2+} imaging experiments, and members of the laboratories of Ion Channel Research (KU Leuven) and Neurogenetics (VIB) for helpful discussions. This work was funded by grants from the Belgian Federal Government (Belspo; IUAP P7/13), the Research Council of the KU Leuven (GOA/14/011, OT/12/091 and PF-TRPLe), VIB and the Research Foundation-Flanders (FWO) (G.0702.12, G.0C77.15, G.0680.10, G.0681.10, G.0503.12, G.0654.15, G.0761.10N, G.0596.12 and G.0565.07). AS and YAA hold Postdoctoral Mandates from KU Leuven. BB is funded by a Ph.D. grant of the Agency for Innovation by Science and Technology (IWT, Flanders, Belgium), GL by the FliAct Marie-Curie Initial Training Network, and LF is by a fellowship from the VIB International Ph.D. Program. BAH is an Allen Distinguished Investigator and an Einstein Visiting Fellow of the Berlin Institute of Health.

Additional information

Funding

Funder	Grant reference number	Author
Vlaams Instituut voor Biotechnologie		Alessia Soldano Luis Franco Guangda Liu Natalia Mora Emre Yaksi Bassem A Hassan
Fonds Wetenschappelijk Onderzoek	G.0702.12	Alessia Soldano Yeranddy A Alpizar Brett Boonen Alejandro López-Requena Natalia Mora Thomas Voets Rudi Vennekens Bassem A Hassan Karel Talavera
Fonds Wetenschappelijk Onderzoek	G.0C77.15	Alessia Soldano Yeranddy A Alpizar Brett Boonen Alejandro López-Requena Natalia Mora Thomas Voets Rudi Vennekens Bassem A Hassan Karel Talavera
Fonds Wetenschappelijk Onderzoek	G.0680.10	Alessia Soldano Yeranddy A Alpizar Brett Boonen Alejandro López-Requena Natalia Mora Thomas Voets Rudi Vennekens Bassem A Hassan Karel Talavera
Fonds Wetenschappelijk Onderzoek	G.0680.10	Alessia Soldano Yeranddy A Alpizar Brett Boonen Alejandro López-Requena Natalia Mora Thomas Voets Rudi Vennekens Bassem A Hassan Karel Talavera
Fonds Wetenschappelijk Onderzoek	G.0680.10	Alessia Soldano Yeranddy A Alpizar Brett Boonen Alejandro López-Requena Natalia Mora Thomas Voets Rudi Vennekens Bassem A Hassan Karel Talavera
Fonds Wetenschappelijk Onderzoek	G.0681.10	Alessia Soldano Yeranddy A Alpizar Brett Boonen Alejandro López-Requena Natalia Mora Thomas Voets Rudi Vennekens Bassem A Hassan Karel Talavera

Fonds Wetenschappelijk Onderzoek	G.0503.12	Alessia Soldano Yeranddy A Alpizar Brett Boonen Alejandro López-Requena Natalia Mora Thomas Voets Rudi Vennekens Bassem A Hassan Karel Talavera
Fonds Wetenschappelijk Onderzoek	G.0654.15	Alessia Soldano Yeranddy A Alpizar Brett Boonen Alejandro López-Requena Natalia Mora Thomas Voets Rudi Vennekens Bassem A Hassan Karel Talavera
Fonds Wetenschappelijk Onderzoek	G.0761.10N	Alessia Soldano Yeranddy A Alpizar Brett Boonen Alejandro López-Requena Natalia Mora Thomas Voets Rudi Vennekens Bassem A Hassan Karel Talavera
Fonds Wetenschappelijk Onderzoek	G.0596.12	Alessia Soldano Yeranddy A Alpizar Brett Boonen Alejandro López-Requena Natalia Mora Thomas Voets Rudi Vennekens Bassem A Hassan Karel Talavera
Fonds Wetenschappelijk Onderzoek	G.0565.07	Alessia Soldano Yeranddy A Alpizar Brett Boonen Alejandro López-Requena Natalia Mora Thomas Voets Rudi Vennekens Bassem A Hassan Karel Talavera
KU Leuven	GOA/14/011	Alessia Soldano Yeranddy A Alpizar Brett Boonen Luis Franco Alejandro López-Requena Guangda Liu Natalia Mora Emre Yaksi Thomas Voets Rudi Vennekens Bassem A Hassan Karel Talavera
European Commission	IUAP P7/13	Alessia Soldano Yeranddy A Alpizar Brett Boonen Luis Franco Alejandro López-Requena Guangda Liu Natalia Mora Emre Yaksi Thomas Voets Rudi Vennekens

KU Leuven	OT/12/091	Alessia Soldano Yeranddy A Alpizar Brett Boonen Luis Franco Alejandro López-Requena Guangda Liu Natalia Mora Emre Yaksi Thomas Voets Rudi Vennekens Bassem A Hassan Karel Talavera
KU Leuven	PF-TRPLe	Alessia Soldano Yeranddy A Alpizar Brett Boonen Luis Franco Alejandro López-Requena Guangda Liu Natalia Mora Emre Yaksi Thomas Voets Rudi Vennekens Bassem A Hassan Karel Talavera

The funders had no role in study design, data collection and interpretation, or the decision to submit the work for publication.

Author contributions

AS, YAA, Conception and design, Acquisition of data, Analysis and interpretation of data, Drafting or revising the article; BB, LF, GL, NM, Acquisition of data, Analysis and interpretation of data; AL-R, Drafting or revising the article, Contributed unpublished essential data or reagents; EY, Conception and design, Analysis and interpretation of data; TV, RV, Analysis and interpretation of data, Drafting or revising the article; BAH, KT, Conception and design, Analysis and interpretation of data, Drafting or revising the article

Author ORCIDs

Alejandro López-Requena, http://orcid.org/0000-0002-6951-8321
Thomas Voets, http://orcid.org/0000-0001-5526-5821
Bassem A Hassan, http://orcid.org/0000-0001-9533-4908

References

Abbas AK, Lichtman AH, Pillai S. 2014. Innate immunity. In: *Cellular and Molecular Immunology*. Elsevier Saunders.

Alpizar YA, Boonen B, Gees M, Sanchez A, Nilius B, Voets T, Talavera K. 2014. Allyl isothiocyanate sensitizes TRPV1 to heat stimulation. *PflüGers Archiv : European Journal of Physiology* **466**:507–515. doi: 10.1007/s00424-013-1334-9

Alpizar YA, Sanchez A, Radwan A, Radwan I, Voets T, Talavera K. 2013. Lack of correlation between the amplitudes of TRP channel-mediated responses to weak and strong stimuli in intracellular ca2+ imaging experiments. *Cell Calcium* **54**:362–374. doi: 10.1016/j.ceca.2013.08.005

Chiu IM, Heesters BA, Ghasemlou N, Von Hehn CA, Zhao F, Tran J, Wainger B, Strominger A, Muralidharan S, Horswill AR, Wardenburg JB, Hwang SW, Carroll MC, Woolf CJ. 2013. Bacteria activate sensory neurons that modulate pain and inflammation. *Nature* **501**:52–57. doi: 10.1038/nature12479

Du EJ, Ahn TJ, Choi MS, Kwon I, Kim HW, Kwon JY, Kang K. 2015. The mosquito repellent citronellal directly potentiates drosophila TRPA1, facilitating feeding suppression. *Molecules and Cells* **38**:911–917. doi: 10.14348/molcells.2015.0215

Everaerts W, Gees M, Alpizar YA, Farre R, Leten C, Apetrei A, Dewachter I, van Leuven F, Vennekens R, De Ridder D, Nilius B, Voets T, Talavera K. 2011. The capsaicin receptor TRPV1 is a crucial mediator of the noxious effects of mustard oil. *Current Biology : CB* **21**:316–321. doi: 10.1016/j.cub.2011.01.031

Gees M, Alpizar YA, Boonen B, Sanchez A, Everaerts W, Segal A, Xue F, Janssens A, Owsianik G, Nilius B, Voets T, Talavera K. 2013. Mechanisms of transient receptor potential vanilloid 1 activation and sensitization by allyl isothiocyanate. *Molecular Pharmacology* **84**:325–334. doi: 10.1124/mol.113.085548

Harzer H, Berger C, Conder R, Schmauss G, Knoblich JA. 2013. FACS purification of drosophila larval neuroblasts for next-generation sequencing. *Nature Protocols* **8**:1088–1099. doi: 10.1038/nprot.2013.062

Isono K, Morita H. 2010. Molecular and cellular designs of insect taste receptor system. *Frontiers in Cellular Neuroscience* **4**. doi: 10.3389/fncel.2010.00020

Joseph RM, Heberlein U. 2012. Tissue-specific activation of a single gustatory receptor produces opposing behavioral responses in drosophila. *Genetics* **192**:521–532. doi: 10.1534/genetics.112.142455

Kang K, Panzano VC, Chang EC, Ni L, Dainis AM, Jenkins AM, Regna K, Muskavitch MAT, Garrity PA. Modulation of TRPA1 thermal sensitivity enables sensory discrimination in drosophila. *Nature* **481**:76–80. doi: 10.1038/nature10715

Kang K, Pulver SR, Panzano VC, Chang EC, Griffith LC, Theobald DL, Garrity PA. 2010. Analysis of drosophila TRPA1 reveals an ancient origin for human chemical nociception. *Nature* **464**:597–600. doi: 10.1038/nature08848

Kim D, Cavanaugh EJ. 2007. Requirement of a soluble intracellular factor for activation of transient receptor potential A1 by pungent chemicals: Role of inorganic polyphosphates. *The Journal of Neuroscience : The Official Journal of the Society for Neuroscience* **27**:6500–6509. doi: 10.1523/JNEUROSCI.0623-07.2007

Kim SH, Lee Y, Akitake B, Woodward OM, Guggino WB, Montell C. 2010. Drosophila TRPA1 channel mediates chemical avoidance in gustatory receptor neurons. *Proceedings of the National Academy of Sciences of the United States of America* **107**:8440–8445. doi: 10.1073/pnas.1001425107

Kominsky DJ, Campbell EL, Colgan SP. 2010. Metabolic shifts in immunity and inflammation. *Journal of Immunology* **184**:4062–4068. doi: 10.4049/jimmunol.0903002

Marella S, Fischler W, Kong P, Asgarian S, Rueckert E, Scott K. 2006. Imaging taste responses in the fly brain reveals a functional map of taste category and behavior. *Neuron* **49**:285–295. doi: 10.1016/j.neuron.2005.11.037

McKean KA, Lazzaro B. 2011. The costs of immunity and the evolution of immunological defense mechanisms. In: eds *Mechanisms of Life History Evolution: The Genetics and Physiology of Life History Traits and Trade-Offs, T. Flatt and A. Heyland*. Oxford University Press . doi: 10.1093/acprof:oso/9780199568765.003.0023

McMahon SB, La Russa F, Bennett DL. 2015. Crosstalk between the nociceptive and immune systems in host defence and disease. *Nature Reviews. Neuroscience* **16**:389–402. doi: 10.1038/nrn3946

Meseguer V, Alpizar YA, Luis E, Tajada S, Denlinger B, Fajardo O, Manenschijn JA, Fernández-Peña C, Talavera A, Kichko T, Navia B, Sánchez A, Señarís R, Reeh P, Pérez-García MT, López-López JR, Voets T, Belmonte C, Talavera K, Viana F. 2014. TRPA1 channels mediate acute neurogenic inflammation and pain produced by bacterial endotoxins. *Nature Communications* **5** . doi: 10.1038/ncomms4125

Meseguer VM, Denlinger BL, Talavera K. 2011. Methodological considerations to understand the sensory function of TRP channels. *Current Pharmaceutical Biotechnology* **12**:3–11. doi: 10.2174/138920111793937871

Nilius B, Appendino G, Owsianik G. 2012. The transient receptor potential channel TRPA1: from gene to pathophysiology. *PflüGers Archiv : European Journal of Physiology* **464**:425–458. doi: 10.1007/s00424-012-1158-z

Ohta T, Imagawa T, Ito S. 2007. Novel agonistic action of mustard oil on recombinant and endogenous porcine transient receptor potential V1 (ptrpv1) channels. *Biochemical Pharmacology* **73**:1646–1656. doi: 10.1016/j.bcp.2007.01.029

Salazar H, Llorente I, Jara-Oseguera A, García-Villegas R, Munari M, Gordon SE, Islas LD, Rosenbaum T. 2008. A single n-terminal cysteine in TRPV1 determines activation by pungent compounds from onion and garlic. *Nature Neuroscience* **11**:255–261. doi: 10.1038/nn2056

Stensmyr MC, Dweck HK, Farhan A, Ibba I, Strutz A, Mukunda L, Linz J, Grabe V, Steck K, Lavista-Llanos S, Wicher D, Sachse S, Knaden M, Becher PG, Seki Y, Hansson BS. 2012. A conserved dedicated olfactory circuit for detecting harmful microbes in drosophila. *Cell* **151**:1345–1357. doi: 10.1016/j.cell.2012.09.046

Story GM, Peier AM, Reeve AJ, Eid SR, Mosbacher J, Hricik TR, Earley TJ, Hergarden AC, Andersson DA, Hwang SW, McIntyre P, Jegla T, Bevan S, Patapoutian A. 2003. ANKTM1, a trp-like channel expressed in nociceptive neurons, is activated by cold temperatures. *Cell* **112**:819–829. doi: 10.1016/S0092-8674(03)00158-2

Wang A, Molina G, Prima V, Wang K. 2011. Anti-LPS test strip for the detection of food contaminated with salmonella and E. coli. *Journal of Microbial & Biochemical Technology* **03**:26–29. doi: 10.4172/1948-5948.1000046

Yanagawa A, Guigue AM, Marion-Poll F. 2014. Hygienic grooming is induced by contact chemicals in drosophila melanogaster. *Frontiers in Behavioral Neuroscience* **8**. doi: 10.3389/fnbeh.2014.00254

Zygmunt PM, Högestätt ED. 2014. TRPA1. *Handbook of Experimental Pharmacology* **222**:583–630. doi: 10.1007/978-3-642-54215-2_23

Neural circuits mediating olfactory-driven behavior in fish

Danio rerio has become increasingly important as animal model for brain research during the last decade. This is mostly due to the increasing number of genetic lines that permit the manipulation of its neuronal circuits. *Danio rerio* is a vertebrate with a brain that features several structural and functional similarities with other vertebrates, such as mammals, but with the advantage of being more genetically tractable. Importantly, *Danio rerio* allows the recording of neuronal activity in the intact animal while its behavior is simultaneously monitored. These characteristics have helped to consolidate *Danio rerio* as a useful animal model in Neuroscience. For this manuscript, I contributed to review the anatomy, physiology and behavioral output of neuronal circuits involved in olfactory information processing in *Danio rerio* and other vertebrates, and to discuss how recent technological advancements could help to elucidate the function of brain target areas of the olfactory system.

frontiers in NEURAL CIRCUITS

REVIEW ARTICLE
published: 11 April 2013
doi: 10.3389/fncir.2013.00062

Neural circuits mediating olfactory-driven behavior in fish

Florence Kermen[1,2†], *Luis M. Franco*[1,2,3†], *Cameron Wyatt*[1,2] *and Emre Yaksi*[1,2,3*]

[1] Neuroelectronics Research Flanders, Leuven, Belgium
[2] Vlaams Instituut voor Biotechnologie, Leuven, Belgium
[3] KU Leuven, Leuven, Belgium

Edited by:
German Sumbre, Ecole Normal Supérieure, France

Reviewed by:
Peter Brunjes, University of Virginia, USA
Suresh Jesuthasan, Duke/NUS Graduate Medical School, Singapore

***Correspondence:**
Emre Yaksi, Neuroelectronics Research Flanders, Imec Campus, Kapeldreef 75, Leuven, Belgium.
e-mail: emre.Yaksi@nerf.be

† Florence Kermen and Luis M. Franco have contributed equally to this work.

The fish olfactory system processes odor signals and mediates behaviors that are crucial for survival such as foraging, courtship, and alarm response. Although the upstream olfactory brain areas (olfactory epithelium and olfactory bulb) are well-studied, less is known about their target brain areas and the role they play in generating odor-driven behaviors. Here we review a broad range of literature on the anatomy, physiology, and behavioral output of the olfactory system and its target areas in a wide range of teleost fish. Additionally, we discuss how applying recent technological advancements to the zebrafish (*Danio rerio*) could help in understanding the function of these target areas. We hope to provide a framework for elucidating the neural circuit computations underlying the odor-driven behaviors in this small, transparent, and genetically amenable vertebrate.

Keywords: teleost, zebrafish, anatomy and physiology, behavior, olfactory bulb, olfactory epithelium, habenula, hypothalamus

INTRODUCTION

Teleosts, the infraclass to which zebrafish belong, account for nearly half of all extant vertebrate species. The diversity of forms in these closely related species provide opportunities to study similar but distinct brain organizations and behavioral programs. Due to this, there already exists a wealth of literature on the teleost olfactory system, pre-dating many genetic and optical techniques, in such members as goldfish and catfish. Despite these variations, the architecture of the zebrafish olfactory system is fundamentally similar to that of other vertebrates. On the molecular level, families of receptor proteins expressed by the olfactory sensory neurons are comparable within most vertebrates, with zebrafish possessing a modest repertoire several times smaller than that of mammals (Alioto and Ngai, 2005).

The olfactory system is of particular relevance to systems neuroscience due to the large variety of stimuli that need to be encoded as well as the simple but interesting computations it performs, such as gain control, pattern decorrelation, categorization, and detecting weak stimuli despite highly dynamic background "noise." Furthermore, olfactory stimuli can trigger a wide range of behaviors related to reproduction, appetite, fear, and anxiety, which allow the study of the brain circuits that are involved in generating these essential behaviors. Finally, the activity patterns evoked by these odors can be readily recorded in highly conserved structures of the olfactory system, i.e., the olfactory epithelium, the olfactory bulb, and olfactory telencephalic and diencephalic centers, owing to the accessibility of these brain regions in zebrafish.

Over the past decade, the zebrafish (*Danio rerio*) has become increasingly popular in systems neuroscience. The success of this model organism is mainly due to its small brain that is amenable to functional imaging and genetic manipulations. The extensive genetic toolbox of the zebrafish can readily be combined with optical and electrophysiological techniques and quantitative behavioral assays to perform experiments that were impossible only a few years ago. Here we review a wide range of literature on the anatomy and the function of the olfactory system in zebrafish and other teleosts and discuss how the novel experimental tools of the zebrafish can and will transform this field. We hope to provide a framework for elucidating the neural circuit computations underlying the odor-driven behaviors in this small, transparent, and genetically amenable vertebrate.

ODORANTS SENSED BY FISH

The fish olfactory system can detect a wide range of water soluble compounds which elicit, or contribute to, behaviors crucial for survival such as feeding, reproduction, social interaction, and avoiding predation. Amino acids and nucleotides indicate the presence of food. Nucleotides, such as adenosine-5′-triphosphate (ATP), indicate food freshness in carp (Hara and Zielinski, 2007). Amino acids induce appetitive swimming behavior characterized by increased number of turns and swimming speed in zebrafish (Lindsay and Vogt, 2004). Steroids and prostaglandin F2α, which are hormones produced in the gonads and released in urine, were shown to trigger species and sex specific reproductive behaviors in a variety of teleosts (Hurk and Lambert, 1983; Stacey and Kyle, 1983). Bile acids are steroids secreted by the liver and released in urine, which have been implicated in migration to spawning sites in lampreys (Sorensen et al., 2005). While bile acids are agreed upon as one of the main classes of odorant in fish, their putative role as social pheromones, indicating the presence of other fish, is not yet conclusively proven in teleosts (Doving et al., 1980). Compounds released from the skin of injured fish have long been known to elicit a vigorous, stereotyped alarm response from many species of fish (von Frisch, 1941). This alarm response is characterized by darting followed by slow swimming or freezing (Speedie and Gerlai, 2008; Doving and Lastein, 2009).

OLFACTORY EPITHELIUM

Odorants are detected upon interaction with olfactory receptors (ORs) in the nose. Teleosts have two nasal cavities, one on each side of the head at the extremity of the snout (Hansen and Zielinski, 2005). Unlike in mammals, there is no sniffing in teleost fish. Each nasal cavity is composed of an anterior nostril, through which water enters the nose, and a posterior nostril, through which water exits the nose. The olfactory epithelium lies between these two nostrils (Hara and Zielinski, 2007). In zebrafish, it is multilamellar and rosette-shaped. Zebrafish olfactory sensory neurons are comprised of three morphologically distinct types of cells: (1) ciliated cells, with long dendrites and few cilia, (2) microvillous sensory neurons, with shorter dendrites and microvilli, (3) crypt cells, pear-shaped cells specific to fish, with microvilli and few cilia (Hansen and Zielinski, 2005). While ciliated and microvillous cells are present in higher vertebrates, crypt cells have only been found in fish (Hansen et al., 1999; Schmachtenberg, 2006; Vielma et al., 2008). The soma of olfactory sensory neurons are located at different depths in the olfactory epithelium: ciliated cells are situated in the deep layer, microvillous cells are located in the intermediate layer and mature crypt cells are located in the most superficial layer, forming the pseudo-stratified structure of the olfactory epithelium. Scattered amongst the olfactory sensory neurons are ciliated non-sensory cells, which help to move the mucus covering the olfactory epithelium (Zeiske et al., 1992). Crypt, microvillous, and ciliated cells are dispersed throughout the epithelium. They represent respectively 2, 8, and 90% of the total olfactory sensory neuron population, in trout and mackerel (Sato and Suzuki, 2001; Schmachtenberg, 2006). Olfactory sensory neurons are constantly renewed throughout adult life or following chemical lesion of the epithelium (Cancalon, 1982; Julliard et al., 1996; Bettini et al., 2006). This regeneration is mediated by the division of basal cells located in the deepest layer of the olfactory epithelium (Cancalon, 1982).

In fish, as in mammals, the detection of odorants by olfactory sensory neurons is mediated by different families of G-protein-coupled receptors. The zebrafish genome contains 143 OR genes, 56 vomeronasal receptor (VR) genes, and 109 trace amine-associated receptor (TAAR) genes (Alioto and Ngai, 2005; Hashiguchi and Nishida, 2006, 2007; Saraiva and Korsching, 2007). Ciliated cells express ORs whereas microvillous cells express VRs (Yoshihara, 2009). The precise identity of the receptor mediating the odor response in crypt cells is not known. However, a recent study found that crypt cells express a member of the VR family in zebrafish (Oka et al., 2012). Subsets of zebrafish olfactory sensory neurons express members of the TAAR gene family (Hussain et al., 2009).

As in other vertebrates, most olfactory sensory neurons express only one receptor (Sato et al., 2007). As a consequence, the response profile of a given neuron is constrained by the receptive field of the receptor it expresses. Patch clamp recordings of neurons isolated from fish olfactory epithelium provided insights into the repertoire of ligands that bind to ORs and VRs. In channel catfish, both ciliated and microvillous cells respond to amino acids (Sato and Suzuki, 2001; Hansen et al., 2003; Schmachtenberg and Bacigalupo, 2004). Ciliated cells also respond to urine extracts containing bile acids and might be involved in alarm substance detection (Sato and Suzuki, 2001; Doving and Lastein, 2009). Nucleotides activate microvillous cells (Hansen et al., 2003). However, the ligands of crypt cells have proven more elusive. Since their discovery, crypt cells have been hypothesized to participate in reproductive pheromone detection. Their density and depth in the olfactory epithelium was shown to vary depending on the seasons in sexually mature carp (Hamdani el et al., 2008). Moreover crypt cell density is sex-dependent in certain fish species (Bettini et al., 2012). A large majority of crypt cells respond to only one category of odorants. Intracellular recordings and calcium imaging studies carried out on mackerel and juvenile trout showed that different subsets of crypt cells respond either to amino acids, bile acids, or reproductive pheromones (Schmachtenberg, 2006; Vielma et al., 2008; Bazaes and Schmachtenberg, 2012). However, in mature trout, the majority of crypt cells respond to reproductive pheromones of the opposite sex and not to the other categories, indicating a change in the response profile of crypt cells during life, depending on sexual maturity and sex of the fish (Bazaes and Schmachtenberg, 2012).

As in other vertebrates, zebrafish olfactory sensory neurons expressing the same receptor are dispersed throughout the epithelium (Baier et al., 1994; Weth et al., 1996). They project their axons via the olfactory nerve to the same glomerulus in the ipsilateral olfactory bulb (Hansen and Zielinski, 2005; Sato et al., 2007). Moreover, the bulbar projection pattern of the three types of olfactory sensory neurons shows a coarse spatial organization. Using a double transgenic zebrafish line labeling ciliated and microvillous cells with different fluorophores, studies have shown that ciliated cells mainly project to the dorsal and medial olfactory bulb, whereas microvillous cells project to the lateral olfactory bulb (Sato et al., 2005, 2007). Retrograde labeling of the olfactory epithelium following lipophilic tracer application to different bulbar domains showed that crypt cells project to the ventral olfactory bulb in carp and to the dorsomedial olfactory bulb in zebrafish (Hamdani el and Doving, 2006; Gayoso et al., 2012). This projection pattern, shown in **Figure 1**, is well-conserved between the two bulbs of the same zebrafish, as well as among individual zebrafish (Baier and Korsching, 1994; Braubach et al., 2012).

Additionally, a subset of fibers originating from the nose reach the telencephalon without contacting the olfactory bulb in several teleosts (Honkanen and Ekstrom, 1990; Riddle and Oakley, 1992; Gayoso et al., 2011). Extrabulbar primary olfactory projections to telencephalic centers have also been described in amphibians but not in mammals (Pinelli et al., 2004). In white sturgeon, these fibers terminate in the posterior tubercle, a diencephalic region (Northcutt, 2011). In trout, these fibers innervate the ventral nucleus of the ventral telencephalon (Vv) and the dorsal telencephalon, as well as the preoptic area and the hypothalamus (Becerra et al., 1994; Anadon et al., 1995). In zebrafish, lipophilic tracer application in the Vv retrogradely labels a few bipolar olfactory sensory neurons in the olfactory epithelium, indicating that ciliated and/or microvillous cells send direct projections to Vv (Gayoso et al., 2011). Nevertheless, the functional role of these extrabulbar primary connections remains unknown.

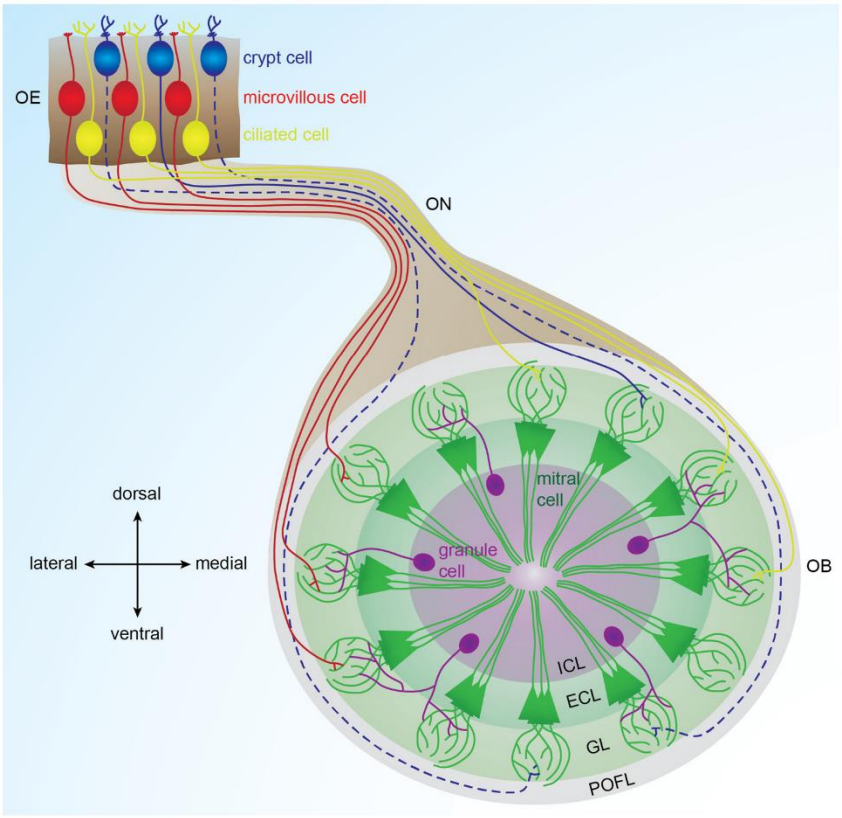

FIGURE 1 | Organization of the olfactory bulb network. Odorants are detected in the olfactory epithelium by three types of sensory neurons (microvillous, ciliated, and crypt cells) that project to different glomeruli located in different areas of the olfactory bulb. Ciliated cells mainly project to the dorsal and medial olfactory bulb; microvillous cells project to the lateral olfactory bulb (Sato et al., 2005, 2007). Crypt cells project to a dorsomedial domain in zebrafish and to a ventral domain in carp (Hamdani el and Doving, 2006; Gayoso et al., 2012). In each glomerulus, olfactory sensory neuron axons contact dendrites of mitral cells, the output cells of the olfactory bulb. Inhibitory interneurons called granules cells are located in the deepest layer of the bulb and modulate the activity of mitral cells. Solid lines represent connections described in zebrafish. Dotted lines represent connections described in other fish species. OE: olfactory epithelium, OB: olfactory bulb, ON: olfactory nerve, POFL: primary olfactory fiber layer, GL: glomerular layer, ECL: external cell layer, ICL: internal cell layer.

THE OLFACTORY BULB: PRIMARY PROCESSING OF ODOR INFORMATION

The olfactory bulb is the vertebrate brain structure that receives the large majority of olfactory sensory neuron inputs through the olfactory nerve. Understanding the neurophysiological mechanisms governing odor processing in the olfactory bulb requires a profound comprehension of its neuronal connectivity and physiological properties. In zebrafish, the olfactory bulb is comprised of approximately 20,000 neurons (Friedrich et al., 2009) organized in four concentric layers (**Figure 1**). From superficial to deep, these are: (1) primary olfactory fiber layer, formed by olfactory sensory neuron axons (Sato et al., 2007); (2) glomerular layer, containing approximately ≈140 spherical modules of neuropil named glomeruli (Braubach et al., 2012); (3) external cell layer, consisting of mitral and ruffed cell somas (Fuller and Byrd, 2005; Fuller et al., 2006); and (4) internal cell layer, containing cell bodies of different interneurons, namely juxtaglomerular, periglomerular, and granular cells (Edwards and Michel, 2002; Bundschuh et al., 2012).

Glutamatergic mitral and ruffed cells are the principal cells of the olfactory bulb in fish (Edwards and Michel, 2002). In zebrafish, apical dendrites of mitral cells receive direct synaptic inputs from olfactory sensory neurons in glomeruli and project to the telencephalon and diencephalon (Fuller et al., 2006; Miyasaka et al., 2009). Teleost ruffed cells are not innervated by olfactory sensory neurons. Nevertheless, ruffed cells receive synaptic contacts from

mitral cells and bulbar interneurons (Kosaka and Hama, 1979, 1981, 1982; Kosaka, 1980).

Interneurons are localized deeper in the olfactory bulb. They mediate lateral interactions within bulbar neurons. The ratio of interneurons to mitral cells is 10:1 in zebrafish (Wiechert et al., 2010), whereas in mammals it is 100:1 (Rosselli-Austin and Altman, 1979). In zebrafish, GABAergic granule cells, which lack axons, are located in the inner layer of the olfactory bulb and extend their processes to make dendrodendritic synaptic connections with principal cells. Juxtaglomerular and periglomerular cells are apposed to glomeruli and express glutamate and dopamine, respectively, in addition to GABA (Byrd and Brunjes, 1995; Edwards and Michel, 2002).

ODOR CODING IN THE OLFACTORY BULB

Each glomerulus receives convergent input from olfactory sensory neurons expressing the same odorant receptor (Sato et al., 2005, 2007). Individual odorant receptors respond to different odors and a given odor generally activates several odorant receptors. As a consequence, odor stimulation in zebrafish and goldfish activates spatially distributed ensembles of glomeruli (Friedrich and Korsching, 1997, 1998; Speca et al., 1999; Fuss and Korsching, 2001). Glomeruli responding to similar molecular features are organized into defined zones within the olfactory bulb, forming chemotopic maps. Yet, odorants frequently activate glomeruli beyond their chemotopical domain. As a consequence, odorants are represented as fractured maps in the olfactory bulb (Friedrich and Korsching, 1997, 1998). In zebrafish, first-order chemical features, such as molecular categories, are encoded by large glomerular domains. Second-order features, such as carbon chain length or branching, are encoded by local differences of glomerular activity patterns within chemotopical domains (Friedrich and Korsching, 1997, 1998; Fuss and Korsching, 2001; Korsching, 2001). Chemotopic maps are therefore hierarchically organized such that fine maps of secondary features are nested within coarse maps of primary features (Friedrich and Korsching, 1997, 1998).

In zebrafish, the lateral subregion of the olfactory bulb responds preferentially to amino acids and to nucleotides, whereas the medial subregion responds to bile acids (Friedrich and Korsching, 1997, 1998; Koide et al., 2009). Genetic ablation of subsets of synaptic inputs to the olfactory bulb from the olfactory epithelium has revealed that the lateral glomerular cluster is responsible for feeding behavior evoked by amino acids (Koide et al., 2009). Fish skin extract is a mixture of several compounds that trigger alarm responses in zebrafish and one of its components is shown to activate mediodorsal posterior and anterolateral olfactory glomeruli (Mathuru et al., 2012). In addition, a group of ventral glomeruli responds to prostaglandin (Friedrich and Korsching, 1998). Amino acids, bile acids, and nucleotides evoke combinatorial glomerular activity patterns that overlap but are sufficiently complex so that even very similar odorants can be discriminated. In contrast, pheromones are represented in a non-combinatorial fashion, suggesting a direct relay to brain structures controlling sex behavior and endocrine states (Friedrich and Korsching, 1997, 1998).

In goldfish, ruffed cells are spontaneously active, and are inhibited by granule cells which are activated by mitral cells (Zippel et al., 1999). Upon odor stimulation, mitral cells respond with high frequency burst-like firing rates triggered by olfactory sensory neuron activity, whereas ruffed cell firing rates are low. Moreover, mitral and ruffed cells frequently respond with contrasting activity patterns. Excitation of mitral cells drives ruffed cell inactivation via granule cells, and inhibition of mitral cells releases ruffed cells from inactivation (Zippel et al., 1999).

In zebrafish, mitral cell activity patterns are dynamically reorganized during the initial phase (~400 ms) of an odor response before they reach a steady state (Friedrich and Laurent, 2001, 2004). Mitral cell activity patterns evoked by similar odorants overlap during the early phase of the odor response but subsequently diverge. Hence initially overlapping odor responses decorrelate over time (Friedrich and Laurent, 2001, 2004). It has been suggested that mitral cell firing patterns convey multiplexed information about odors simultaneously (Friedrich et al., 2004). This study proposed that the mitral cell action potentials, which are phase-locked to the local field potential oscillations, carry information about the odor category and the remaining mitral cell activity informs about precise odorant identity. Thus, multiplexed mitral cell activity patterns simultaneously convey information about complementary odorant features (Friedrich et al., 2004). Although glomerular responses to different odors are highly variable, total mitral cell firing remains within a relatively narrow range, suggesting a gain control, probably through inhibitory circuits (Friedrich and Laurent, 2004; Friedrich et al., 2009).

SYNAPTIC INPUTS TO THE OLFACTORY BULB FROM HIGHER BRAIN AREAS

In zebrafish, the olfactory bulb receives serotonergic inputs from raphe nuclei (Lillesaar et al., 2009) and cholinergic inputs through the terminal nerve ganglion (Edwards et al., 2007). In rodents, serotonin and acetylcholine increase the activity of interneurons while reducing the excitability of principal cells (Castillo et al., 1999; Ghatpande et al., 2006; Pressler et al., 2007; Petzold et al., 2009; Liu et al., 2012). In carp, noradrenaline enhances postsynaptic long term potentiation evoked by tetanic stimulation of mitral cell–granule cell synapses (Satou et al., 2006). In addition, centrifugal fibers originating from the telencephalon terminate in the olfactory bulb internal cell layer of teleosts, probably making synaptic contact with granule cells, raising the possibility that cortical feedback modulates the bulbar network (Munz et al., 1982; Stell et al., 1984; Zucker and Dowling, 1987). Nevertheless, further studies are needed in order to elucidate the physiological role of these neuromodulators onto bulbar neural circuits in fish.

ORGANIZATION OF OLFACTORY BULB PROJECTIONS

Mitral cells extend their axons through the medial and lateral olfactory tracts to different higher brain centers (**Figure 2**). In carp and zebrafish, the lateral olfactory tract contains mainly fibers originating in the lateral olfactory bulb, whereas the medial olfactory tract contains mainly fibers originating from the medial olfactory bulb (Sheldon, 1912). Anatomical tracing studies have shown that the teleost medial olfactory tract is subdivided into medial and lateral regions (Sheldon, 1912; Finger, 1975; Bass, 1981; von Bartheld et al., 1984). The lateral part of the medial olfactory tract is comprised largely of centrifugal fibers projecting to the olfactory

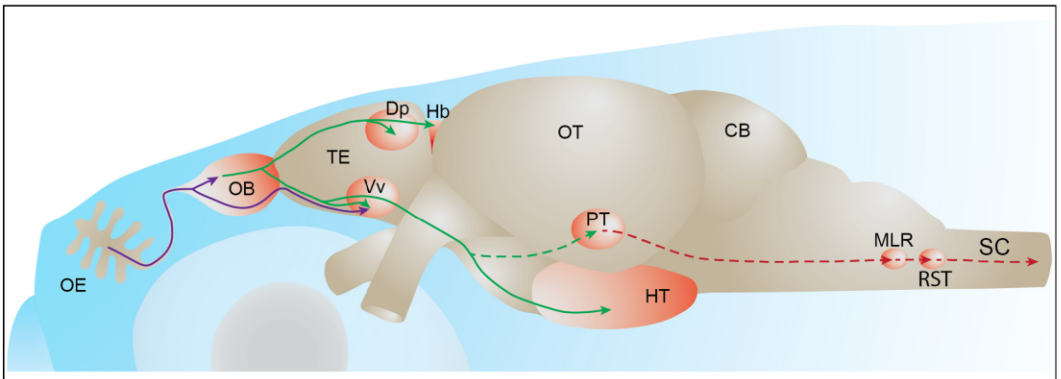

FIGURE 2 | Fish olfactory system. Primary projections from olfactory sensory neurons to the olfactory bulb or telencephalon are depicted in purple. Secondary olfactory projections from the olfactory bulb to the telencephalon and diencephalon are depicted in green. A putative olfacto-motor pathway connecting the posterior tubercle to executive motor centers in the mesencephalon, described in lampreys, is depicted in red. Solid lines represent connections described in zebrafish. Dotted lines represent connections described in other fish species. OE: olfactory epithelium, OB: olfactory bulb, TE: telencephalon, Dp: dorsal-posterior part of the telencephalon, Hb: habenula, Vv: ventral nucleus of the ventral telencephalon, OT: optic tectum, PT: posterior tubercle, HT: hypothalamus, CB: cerebellum, MLR: mesencephalic locomotor region; RST: reticulo-spinal tract, SC: spinal cord.

bulb whereas the medial part of the medial olfactory tract as well as the lateral olfactory tract contain mitral cell axons projecting to telencephalic and diencephalic areas (von Bartheld et al., 1984). In addition, the medial part of the medial olfactory tract carries mitral cell axons that project to the contralateral olfactory bulb (von Bartheld et al., 1984).

The medial and lateral olfactory tracts are separate, anatomically well-defined axon bundles, which enables the study of their physiological function by several experimental manipulations across different fish species (Stacey and Kyle, 1983; Hamdani et al., 2000, 2001). It was shown that the electrical stimulation of the medial olfactory tract induces alarm reaction or reproductive behavior, while lateral olfactory tract stimulation induces feeding behaviors in cod (Doving and Selset, 1980). These different functions could arise from different projection profiles of these two tracts to higher brain centers. In the goldfish, fibers carried by the medial and lateral olfactory tracts reach target areas in the telencephalon and the posterior tubercle of the diencephalon (von Bartheld et al., 1984). This study also showed that the lateral olfactory tract specifically innervates the habenula while the medial olfactory tract also sends projections to the Vv. These projection patterns have been confirmed by anatomical tracing studies in other fish species (Huesa et al., 2000; Folgueira et al., 2004; Northcutt, 2011). In zebrafish, the mitral cells are shown to project to Vv and the dorsal-posterior part of the telencephalon (Dp) and to the right habenula and the hypothalamus in the diencephalon (Rink and Wullimann, 2004; Miyasaka et al., 2009; Gayoso et al., 2011).

OLFACTORY BULB TARGETS

TELENCEPHALON

Dp in teleosts corresponds to the mammalian primary olfactory (piriform) cortex, whereas teleost Vv is the homolog of the septal area, a part of the limbic system, in mammals. Whether the chemotopic odor maps in the olfactory bulb are maintained in Dp and Vv in fishes remains a subject of debate. Recording of single neurons in the channel catfish pallium showed a spatial segregation of neurons preferentially responding to odorants belonging to the same biological categories (Nikonov et al., 2005). This study showed that bile acids preferentially activate the medial pallium whereas amino acids and nucleotides preferentially activate the lateral pallium (comprising Dp), indicating a gross chemotopical organization in the telencephalic targets of the olfactory bulb. However, a recent functional imaging study suggested that the spatial segregation of odor responses was not prominent in Vv and Dp neurons of zebrafish (Yaksi et al., 2009). This study showed that Vv and Dp display overlapping and distributed activity in response to various odor categories (bile acids, amino acids, nucleotides). Hence odor representations in the telencephalon do not display strong chemotopy (although slight differences between the distribution of amino acid and bile acid-evoked activity can be observed in the Dp). This is in accordance with work in rodents, where optical imaging in the mouse primary olfactory cortex shows that odor-evoked activity is not spatially segregated in the main bulbar target (Stettler and Axel, 2009).

Vv and Dp neurons were shown to have different response properties. Vv neurons are broadly tuned resulting in overlapping representation of odor categories, whereas Dp neurons respond to odors more specifically (Yaksi et al., 2009). The activity of mitral cell ensembles was shown to carry multiplexed information about stimulus features such as category and identity (Friedrich et al., 2004). How is the multiplexed output provided by the olfactory bulb decrypted in the telencephalic targets? Dp cells were shown to be relatively insensitive to oscillatory mitral cell activity, which informs about odor categories (Blumhagen et al., 2011). This study suggests that Dp establishes

specific and decorrelated odor representations. However a previous study suggests that the pattern correlation in Dp neurons is not significantly different from the pattern correlation in mitral cells (Yaksi et al., 2009). Further studies are needed to examine whether the multiplexed olfactory bulb output is read and used by its targets.

Importantly, Vv and Dp receive substantial neuromodulatory inputs which could participate in odor response refinement in these areas. In zebrafish, the pallium (comprising Dp) and the subpallium (comprising Vv) share inputs from locus coeruleus (noradrenergic), raphe nuclei (serotoninergic), and posterior tubercle (dopaminergic; Rink and Wullimann, 2004; Scharer et al., 2012). The subpallium additionally receives inputs from the cholinergic superior reticular nucleus and the histaminergic caudal hypothalamus (Rink and Wullimann, 2004). It was shown that dopamine selectively decreases inhibitory but not excitatory odor responses in the Dp (Scharer et al., 2012). Calcium imaging further showed that the amplitude of odor responses was increased in the presence of dopamine, without affecting the spatial response pattern. Therefore, dopamine mediated increase of odor response gain might mediate changes in odor saliency during learning.

DIENCEPHALON

Habenula

The habenula is a highly conserved brain region that connects the forebrain to brainstem nuclei such as the interpeduncular nucleus, the serotonergic raphe nuclei and the ventral tegmental area containing dopaminergic neurons (Tomizawa et al., 2001; Hikosaka, 2010). The habenula is divided into two parts based on connectivity and functional heterogeneity: the medial and lateral mammalian habenulae, which are homologous to the dorsal and ventral fish habenulae, respectively (Amo et al., 2010). It was shown in several teleost species that mitral cells project to the habenula (Wedgwood, 1974; von Bartheld et al., 1984; Miyasaka et al., 2009; Northcutt, 2011). In zebrafish, bulbar projections to the habenula are asymmetric. Indeed, it has been shown that mitral cells located in both olfactory bulbs send axons that terminate in the medial compartment of the right habenula (Miyasaka et al., 2009).

The mammalian homolog of the fish ventral habenula has been proposed to participate in the control of motor behaviors depending on stimulus values by influencing the activity of dopaminergic neurons (Hikosaka, 2010). Moreover, two recent studies showed that when the dorsal habenula is genetically inactivated, zebrafish display altered responses to conditioned fear stimuli (Agetsuma et al., 2010; Lee et al., 2010). These studies indicate a role for the habenula in experience-dependent modulation of fear responses. The role of habenula in odor processing and the functional architecture of its circuitry remain to be uncovered.

Posterior tubercle

The posterior tubercle is a ventral region of the posterior diencephalon. Because the posterior tubercle contains dopaminergic cells, it has been proposed to be functionally similar to the mammalian mesolimbic dopaminergic system (Rink and Wullimann, 2001). Bulbar efferents have been shown to terminate in the posterior tubercle of several teleost fish (Matz, 1995; Von Bartheld, 2004; Derjean et al., 2010; Northcutt, 2011; Northcutt and Rink, 2012). However, it is currently not known whether this projection also exists in zebrafish.

A recent work suggested that the projections from the olfactory bulb to the posterior tubercle play a role in the generation of olfactory-driven locomotor activity in the sea lamprey (Derjean et al., 2010). This study showed that stimulation of the medial olfactory bulb by glutamate injection generated rhythmical electrical activity in reticulospinal cells and in the ventral root of the spinal cord, which resembles fictive locomotion. The proposed olfacto-motor pathway is comprised of a medial glomerulus projecting to the posterior tubercle, which would then transmit the olfactory input to the mesencephalic locomotor region that in turn excites reticulospinal cells which are command neurons responsible for the activation of spinal locomotor networks. This study is the first demonstration of a functional connection between the olfactory system and the spinal locomotor network in vertebrates.

Hypothalamus

In mammals, the hypothalamic nuclei, located in the ventral diencephalon, play a pivotal role in the regulation of a number of vital physiological functions via direct synaptic stimulation of a wide range of targets or the secretion of various neuropeptides (Machluf et al., 2011). Homologs of diverse hypothalamic cell types secreting oxytocin, gonadotropin-releasing hormone, neuropeptide Y, and hypocretin have been identified in teleosts (Machluf et al., 2011). Hence it is likely that the zebrafish and terrestrial vertebrates have similar hypothalamic functions such as regulation of sleep, blood pressure, temperature, thirst and satiety, stress, reproduction, and social behavior. Mitral cells send direct projections to the hypothalamic area in fish but the exact localization of mitral cell terminals in hypothalamic nuclei and the functional significance of these projections remain unknown. In rodents, a ventral glomerulus projects to vasopressin or oxytocin secreting hypothalamic neurons (Hatton and Yang, 1989; Smithson et al., 1992; Bader et al., 2012). Vasopressin and oxytocin are known to modulate social behaviors in rodents as well as in fish (Godwin and Thompson, 2012). Olfactory cues are very important in signaling the presence of food or sexual partners in fish. The monosynaptic bulbo-hypothalamic projection in fish is therefore probably involved in the modulation of feeding and reproductive behaviors.

CONCLUSION

Olfactory computations performed by the upstream olfactory brain areas in relation to behavior are well-documented in teleosts. Despite minor anatomical differences, the general principles and computations performed by the fish olfactory system are highly similar to what is described in terrestrial vertebrates. Odors are detected in a combinatorial manner by receptors expressed in olfactory sensory neurons. Olfactory sensory neurons expressing the same receptor are dispersed in the olfactory epithelium and project to one spatially confined glomerulus. Hence, the shuffled peripheral epithelial activation is reorganized into odor specific glomerular maps in the olfactory bulb. Odor-evoked activity patterns among mitral cell ensembles become less correlated with

time, potentially helping discrimination of similar odorants. Ethologically relevant classes of odors tend to activate specific bulbar domains, resulting in a coarse topographic organization of different odor categories. Odor responses in the telencephalon do not seem to be topologically organized and the precise circuit mechanisms underlying the transformations of olfactory information in telencephalic targets still remain to be discovered. Odor responses in diencephalic areas such as the hypothalamus and habenula are currently not documented. Zebrafish lines that express calcium indicators in these areas are already available, which should allow the function of these areas to be revealed in the near future.

Currently, the neural pathways connecting the olfactory system to brain regions involved in the execution of different behaviors are not known in zebrafish. However, new techniques are rapidly being adopted which allow the tracing of functional connectivity in the olfacto-motor pathway. For example, the green fluorescent protein reconstitution across synaptic partners (GRASP) method, where non-fluorescent green fluorescent protein fragments expressed in two different neurons assemble to form the fluorophore at the synapse, is mainly used in invertebrates but is being adapted for vertebrates (Yamagata and Sanes, 2012). Additionally, links must be established between neural activity in olfactory bulb targets and relevant behavioral outputs. In this regard, the possibility of activating and deactivating genetically targeted neural populations offers new perspectives to understand how circuits elicit or modulate behavior. For example, the precise and non-invasive optogenetic stimulation of olfactory sensory neuron subsets already enables specific swimming patterns to be elicited in freely behaving zebrafish larvae (Zhu et al., 2009). In summary, thanks to its innate properties and a timely convergence of new techniques, the zebrafish olfactory system is an increasingly attractive model to understand the function of neural circuits involved in olfactory processing.

ACKNOWLEDGMENT

This work was supported by Fyssens post-doctoral fellowship to Florence Kermen, VIB-PhD program funding to Luis M.Franco, AXA research post-doctoral fellowship to Cameron Wyatt and NERF funding to Emre Yaksi.

REFERENCES

Agetsuma, M., Aizawa, H., Aoki, T., Nakayama, R., Takahoko, M., Goto, M., et al. (2010). The habenula is crucial for experience-dependent modification of fear responses in zebrafish. *Nat. Neurosci.* 13, 1354–1356.

Alioto, T. S., and Ngai, J. (2005). The odorant receptor repertoire of teleost fish. *BMC Genomics* 6:173. doi: 10.1186/1471-2164-6-173

Amo, R., Aizawa, H., Takahoko, M., Kobayashi, M., Takahashi, R., Aoki, T., et al. (2010). Identification of the zebrafish ventral habenula as a homolog of the mammalian lateral habenula. *J. Neurosci.* 30, 1566–1574.

Anadon, R., Manso, M. J., Rodriguez-Moldes, I., and Becerra, M. (1995). Neurons of the olfactory organ projecting to the caudal telencephalon and hypothalamus: a carbocyanine-dye labelling study in the brown trout (Teleostei). *Neurosci. Lett.* 191, 157–160.

Bader, A., Klein, B., Breer, H., and Strotmann, J. (2012). Connectivity from OR37 expressing olfactory sensory neurons to distinct cell types in the hypothalamus. *Front. Neural Circuits* 6:84. doi: 10.3389/fncir.2012.00084

Baier, H., and Korsching, S. (1994). Olfactory glomeruli in the zebrafish form an invariant pattern and are identifiable across animals. *J. Neurosci.* 14, 219–230.

Baier, H., Rotter, S., and Korsching, S. (1994). Connectional topography in the zebrafish olfactory system: random positions but regular spacing of sensory neurons projecting to an individual glomerulus. *Proc. Natl. Acad. Sci. U.S.A.* 91, 11646–11650.

Bass, A. H. (1981). Telencephalic efferents in channel catfish, *Ictalurus punctatus*: projections to the olfactory bulb and optic tectum. *Brain Behav. Evol.* 19, 1–16.

Bazaes, A., and Schmachtenberg, O. (2012). Odorant tuning of olfactory crypt cells from juvenile and adult rainbow trout. *J. Exp. Biol.* 215, 1740–1748.

Becerra, M., Manso, M. J., Rodriguez-Moldes, I., and Anadon, R. (1994). Primary olfactory fibres project to the ventral telencephalon and preoptic region in trout (*Salmo trutta*): a developmental immunocytochemical study. *J. Comp. Neurol.* 342, 131–143.

Bettini, S., Ciani, F., and Franceschini, V. (2006). Recovery of the olfactory receptor neurons in the African *Tilapia mariae* following exposure to low copper level. *Aquat. Toxicol.* 76, 321–328.

Bettini, S., Lazzari, M., and Franceschini, V. (2012). Quantitative analysis of crypt cell population during postnatal development of the olfactory organ of the guppy, *Poecilia reticulata* (Teleostei, Poecilidae), from birth to sexual maturity. *J. Exp. Biol.* 215, 2711–2715.

Blumhagen, F., Zhu, P., Shum, J., Scharer, Y. P., Yaksi, E., Deisseroth, K., et al. (2011). Neuronal filtering of multiplexed odour representations. *Nature* 479, 493–498.

Braubach, O. R., Fine, A., and Croll, R. P. (2012). Distribution and functional organization of glomeruli in the olfactory bulbs of zebrafish (*Danio rerio*). *J. Comp. Neurol.* 520, 2317–2339.

Bundschuh, S. T., Zhu, P., Scharer, Y. P., and Friedrich, R. W. (2012). Dopaminergic modulation of mitral cells and odor responses in the zebrafish olfactory bulb. *J. Neurosci.* 32, 6830–6840.

Byrd, C. A., and Brunjes, P. C. (1995). Organization of the olfactory system in the adult zebrafish: histological, immunohistochemical, and quantitative analysis. *J. Comp. Neurol.* 358, 247–259.

Cancalon, P. (1982). Degeneration and regeneration of olfactory cells induced by ZnSO4 and other chemicals. *Tissue Cell* 14, 717–733.

Castillo, P. E., Carleton, A., Vincent, J. D., and Lledo, P. M. (1999). Multiple and opposing roles of cholinergic transmission in the main olfactory bulb. *J. Neurosci.* 19, 9180–9191.

Derjean, D., Moussaddy, A., Atallah, E., St-Pierre, M., Auclair, F., Chang, S., et al. (2010). A novel neural substrate for the transformation of olfactory inputs into motor output. *PLoS Biol.* 8:e1000567. doi: 10.1371/journal.pbio.1000567

Doving, K. B., and Lastein, S. (2009). The alarm reaction in fishes–odorants, modulations of responses, neural pathways. *Ann. N. Y. Acad. Sci.* 1170, 413–423.

Doving, K. B., and Selset, R. (1980). Behavior patterns in cod released by electrical stimulation of olfactory tract bundlets. *Science* 207, 559–560.

Doving, K. B., Selset, R., and Thommesen, G. (1980). Olfactory sensitivity to bile acids in salmonid fishes. *Acta Physiol. Scand.* 108, 123–131.

Edwards, J. G., Greig, A., Sakata, Y., Elkin, D., and Michel, W. C. (2007). Cholinergic innervation of the zebrafish olfactory bulb. *J. Comp. Neurol.* 504, 631–645.

Edwards, J. G., and Michel, W. C. (2002). Odor-stimulated glutamatergic neurotransmission in the zebrafish olfactory bulb. *J. Comp. Neurol.* 454, 294–309.

Finger, T. E. (1975). The distribution of the olfactory tracts in the bullhead catfish, *Ictalurus nebulosus*. *J. Comp. Neurol.* 161, 125–141.

Folgueira, M., Anadon, R., and Yanez, J. (2004). An experimental study of the connections of the telencephalon in the rainbow trout (*Oncorhynchus mykiss*). I: olfactory bulb and ventral area. *J. Comp. Neurol.* 480, 180–203.

Friedrich, R. W., Habermann, C. J., and Laurent, G. (2004). Multiplexing using synchrony in the zebrafish olfactory bulb. *Nat. Neurosci.* 7, 862–871.

Friedrich, R. W., and Korsching, S. I. (1997). Combinatorial and chemotopic odorant coding in the zebrafish olfactory bulb visualized by optical imaging. *Neuron* 18, 737–752.

Friedrich, R. W., and Korsching, S. I. (1998). Chemotopic, combinatorial, and noncombinatorial odorant representations in the olfactory bulb revealed using a voltage-sensitive axon tracer. *J. Neurosci.* 18, 9977–9988.

Friedrich, R. W., and Laurent, G. (2001). Dynamic optimization of odor representations by slow temporal patterning of mitral cell activity. *Science* 291, 889–894.

Friedrich, R. W., and Laurent, G. (2004). Dynamics of olfactory bulb input and output activity during odor stimulation in zebrafish. *J. Neurophysiol.* 91, 2658–2669.

Friedrich, R. W., Yaksi, E., Judkewitz, B., and Wiechert, M. T. (2009). Processing of odor representations by neuronal circuits in the olfactory bulb. *Ann. N. Y. Acad. Sci.* 1170, 293–297.

Fuller, C. L., and Byrd, C. A. (2005). Ruffed cells identified in the adult zebrafish olfactory bulb. *Neurosci. Lett.* 379, 190–194.

Fuller, C. L., Yettaw, H. K., and Byrd, C. A. (2006). Mitral cells in the olfactory bulb of adult zebrafish (*Danio rerio*): morphology and distribution. *J. Comp. Neurol.* 499, 218–230.

Fuss, S. H., and Korsching, S. I. (2001). Odorant feature detection: activity mapping of structure response relationships in the zebrafish olfactory bulb. *J. Neurosci.* 21, 8396–8407.

Gayoso, J., Castro, A., Anadon, R., and Manso, M. J. (2012). Crypt cells of the zebrafish *Danio rerio* mainly project to the dorsomedial glomerular field of the olfactory bulb. *Chem. Senses* 37, 357–369.

Gayoso, J. A., Castro, A., Anadon, R., and Manso, M. J. (2011). Differential bulbar and extrabulbar projections of diverse olfactory receptor neuron populations in the adult zebrafish (*Danio rerio*). *J. Comp. Neurol.* 519, 247–276.

Ghatpande, A. S., Sivaraaman, K., and Vijayaraghavan, S. (2006). Store calcium mediates cholinergic effects on mIPSCs in the rat main olfactory bulb. *J. Neurophysiol.* 95, 1345–1355.

Godwin, J., and Thompson, R. (2012). Nonapeptides and social behavior in fishes. *Horm. Behav.* 61, 230–238.

Hamdani, E. H., Kasumyan, A., and Doving, K. B. (2001). Is feeding behaviour in crucian carp mediated by the lateral olfactory tract? *Chem. Senses* 26, 1133–1138.

Hamdani, E. H., Stabell, O. B., Alexander, G., and Doving, K. B. (2000). Alarm reaction in the crucian carp is mediated by the medial bundle of the medial olfactory tract. *Chem. Senses* 25, 103–109.

Hamdani el, H., and Doving, K. B. (2006). Specific projection of the sensory crypt cells in the olfactory system in crucian carp, *Carassius carassius*. *Chem. Senses* 31, 63–67.

Hamdani el, H., Lastein, S., Gregersen, F., and Doving, K. B. (2008). Seasonal variations in olfactory sensory neurons–fish sensitivity to sex pheromones explained? *Chem. Senses* 33, 119–123.

Hansen, A., Rolen, S. H., Anderson, K., Morita, Y., Caprio, J., and Finger, T. E. (2003). Correlation between olfactory receptor cell type and function in the channel catfish. *J. Neurosci.* 23, 9328–9339.

Hansen, A., and Zielinski, B. S. (2005). Diversity in the olfactory epithelium of bony fishes: development, lamellar arrangement, sensory neuron cell types and transduction components. *J. Neurocytol.* 34, 183–208.

Hansen, A., Zippel, H. P., Sorensen, P. W., and Caprio, J. (1999). Ultrastructure of the olfactory epithelium in intact, axotomized, and bulbectomized goldfish, *Carassius auratus*. *Microsc. Res. Tech.* 45, 325–338.

Hara, T. J., and Zielinski, B. (2007). "Olfaction," in *Sensory Systems Neuroscience* (Oxford: Elsevier Academic Press), 1–43.

Hashiguchi, Y., and Nishida, M. (2006). Evolution and origin of vomeronasal-type odorant receptor gene repertoire in fishes. *BMC Evol. Biol.* 6:76. doi: 10.1186/1471-2148-6-76

Hashiguchi, Y., and Nishida, M. (2007). Evolution of trace amine associated receptor (TAAR) gene family in vertebrates: lineage-specific expansions and degradations of a second class of vertebrate chemosensory receptors expressed in the olfactory epithelium. *Mol. Biol. Evol.* 24, 2099–2107.

Hatton, G. I., and Yang, Q. Z. (1989). Supraoptic nucleus afferents from the main olfactory bulb–II. Intracellularly recorded responses to lateral olfactory tract stimulation in rat brain slices. *Neuroscience* 31, 289–297.

Hikosaka, O. (2010). The habenula: from stress evasion to value-based decision-making. *Nat. Rev. Neurosci.* 11, 503–513.

Honkanen, T., and Ekstrom, P. (1990). An immunocytochemical study of the olfactory projections in the three-spined stickleback, *Gasterosteus aculeatus*, L. *J. Comp. Neurol.* 292, 65–72.

Huesa, G., Anadon, R., and Yanez, J. (2000). Olfactory projections in a chondrostean fish, *Acipenser baeri*: an experimental study. *J. Comp. Neurol.* 428, 145–158.

Hurk, R. V. D., and Lambert, J. G. D. (1983). Ovarian steroid glucuronides function as sex pheromones for male zebrafish, *Brachydanio rerio*. *Can. J. Zool.* 61, 2381–2387.

Hussain, A., Saraiva, L. R., and Korsching, S. I. (2009). Positive Darwinian selection and the birth of an olfactory receptor clade in teleosts. *Proc. Natl. Acad. Sci. U.S.A.* 106, 4313–4318.

Julliard, A. K., Saucier, D., and Astic, L. (1996). Time-course of apoptosis in the olfactory epithelium of rainbow trout exposed to a low copper level. *Tissue Cell* 28, 367–377.

Koide, T., Miyasaka, N., Morimoto, K., Asakawa, K., Urasaki, A., Kawakami, K., et al. (2009). Olfactory neural circuitry for attraction to amino acids revealed by transposon-mediated gene trap approach in zebrafish. *Proc. Natl. Acad. Sci. U.S.A.* 106, 9884–9889.

Korsching, S. I. (2001). Odor maps in the brain: spatial aspects of odor representation in sensory surface and olfactory bulb. *Cell. Mol. Life. Sci.* 58, 520–530.

Kosaka, T. (1980). Ruffed cell: a new type of neuron with a distinctive initial unmyelinated portion of the axon in the olfactory bulb of the goldfish (*Carassius auratus*): II. Fine structure of the ruffed cell. *J. Comp. Neurol.* 193, 119–145.

Kosaka, T., and Hama, K. (1979). Ruffed cell: a new type of neuron with a distinctive initial unmyelinated portion of the axon in the olfactory bulb of the goldfish (*Carassius auratus*) I. Golgi impregnation and serial thin sectioning studies. *J. Comp. Neurol.* 186, 301–319.

Kosaka, T., and Hama, K. (1981). Ruffed cell: a new type of neuron with a distinctive initial unmyelinated portion of the axon in the olfactory bulb of the goldfish (*Carassius auratus*). III. Three-dimensional structure of the ruffed cell dendrite. *J. Comp. Neurol.* 201, 571–587.

Kosaka, T., and Hama, K. (1982). Synaptic organization in the teleost olfactory bulb. *J. Physiol. (Paris)* 78, 707–719.

Lee, A., Mathuru, A. S., Teh, C., Kibat, C., Korzh, V., Penney, T. B., et al. (2010). The habenula prevents helpless behavior in larval zebrafish. *Curr. Biol.* 20, 2211–2216.

Lillesaar, C., Stigloher, C., Tannhauser, B., Wullimann, M. F., and Bally-Cuif, L. (2009). Axonal projections originating from raphe serotonergic neurons in the developing and adult zebrafish, *Danio rerio*, using transgenics to visualize raphe-specific pet1 expression. *J. Comp. Neurol.* 512, 158–182.

Lindsay, S. M., and Vogt, R. G. (2004). Behavioral responses of newly hatched zebrafish (*Danio rerio*) to amino acid chemostimulants. *Chem. Senses* 29, 93–100.

Liu, S., Aungst, J. L., Puche, A. C., and Shipley, M. T. (2012). Serotonin modulates the population activity profile of olfactory bulb external tufted cells. *J. Neurophysiol.* 107, 473–483.

Machluf, Y., Gutnick, A., and Levkowitz, G. (2011). Development of the zebrafish hypothalamus. *Ann. N. Y. Acad. Sci.* 1220, 93–105.

Mathuru, A. S., Kibat, C., Cheong, W. F., Shui, G., Wenk, M. R., Friedrich, R. W., et al. (2012). Chondroitin fragments are odorants that trigger fear behavior in fish. *Curr. Biol.* 22, 538–544.

Matz, S. P. (1995). Connections of the olfactory bulb in the chinook salmon (*Oncorhynchus tshawytscha*). *Brain Behav. Evol.* 46, 108–120.

Miyasaka, N., Morimoto, K., Tsubokawa, T., Higashijima, S., Okamoto, H., and Yoshihara, Y. (2009). From the olfactory bulb to higher brain centers: genetic visualization of secondary olfactory pathways in zebrafish. *J. Neurosci.* 29, 4756–4767.

Munz, H., Claas, B., Stumpf, W. E., and Jennes, L. (1982). Centrifugal innervation of the retina by luteinizing hormone releasing hormone (LHRH)-immunoreactive telencephalic neurons in teleostean fishes. *Cell Tissue Res.* 222, 313–323.

Nikonov, A. A., Finger, T. E., and Caprio, J. (2005). Beyond the olfactory bulb: an odotopic map in the forebrain. *Proc. Natl. Acad. Sci. U.S.A.* 102, 18688–18693.

Northcutt, R. G. (2011). Olfactory projections in the white sturgeon, *Acipenser transmontanus*: an experimental study. *J. Comp. Neurol.* 519, 1999–2022.

Northcutt, R. G., and Rink, E. (2012). Olfactory projections in the lepidosirenid lungfishes. *Brain Behav. Evol.* 79, 4–25.

Oka, Y., Saraiva, L. R., and Korsching, S. I. (2012). Crypt neurons express a single V1R-related ora gene. *Chem. Senses* 37, 219–227.

Petzold, G. C., Hagiwara, A., and Murthy, V. N. (2009). Serotonergic modulation of odor input to the mammalian olfactory bulb. *Nat. Neurosci.* 12, 784–791.

Pinelli, C., D'aniello, B., Polese, G., and Rastogi, R. K. (2004). Extrabulbar olfactory system and nervus terminalis FMRFamide immunoreactive components in *Xenopus laevis* ontogenesis. *J. Chem. Neuroanat.* 28, 37–46.

Pressler, R. T., Inoue, T., and Strowbridge, B. W. (2007). Muscarinic receptor activation modulates granule cell excitability and potentiates inhibition onto mitral cells in the rat olfactory bulb. *J. Neurosci.* 27, 10969–10981.

Riddle, D. R., and Oakley, B. (1992). Immunocytochemical identification of primary olfactory afferents in rainbow trout. *J. Comp. Neurol.* 324, 575–589.

Rink, E., and Wullimann, M. F. (2001). The teleostean (zebrafish) dopaminergic system ascending to the subpallium (striatum) is located in the basal diencephalon (posterior tuberculum). *Brain Res.* 889, 316–330.

Rink, E., and Wullimann, M. F. (2004). Connections of the ventral telencephalon (subpallium) in the zebrafish (*Danio rerio*). *Brain Res.* 1011, 206–220.

Rosselli-Austin, L., and Altman, J. (1979). The postnatal development of the main olfactory bulb of the rat. *J. Dev. Physiol.* 1, 295–313.

Saraiva, L. R., and Korsching, S. I. (2007). A novel olfactory receptor gene family in teleost fish. *Genome Res.* 17, 1448–1457.

Sato, K., and Suzuki, N. (2001). Whole-cell response characteristics of ciliated and microvillous olfactory receptor neurons to amino acids, pheromone candidates and urine in rainbow trout. *Chem. Senses* 26, 1145–1156.

Sato, Y., Miyasaka, N., and Yoshihara, Y. (2005). Mutually exclusive glomerular innervation by two distinct types of olfactory sensory neurons revealed in transgenic zebrafish. *J. Neurosci.* 25, 4889–4897.

Sato, Y., Miyasaka, N., and Yoshihara, Y. (2007). Hierarchical regulation of odorant receptor gene choice and subsequent axonal projection of olfactory sensory neurons in zebrafish. *J. Neurosci.* 27, 1606–1615.

Satou, M., Hoshikawa, R., Sato, Y., and Okawa, K. (2006). An in vitro study of long-term potentiation in the carp (*Cyprinus carpio* L.) olfactory bulb. *J. Comp. Physiol. A Neuroethol. Sens. Neural Behav. Physiol.* 192, 135–150.

Scharer, Y. P., Shum, J., Moressis, A., and Friedrich, R. W. (2012). Dopaminergic modulation of synaptic transmission and neuronal activity patterns in the zebrafish homolog of olfactory cortex. *Front. Neural Circuits* 6:76. doi: 10.3389/fncir.2012.00076

Schmachtenberg, O. (2006). Histological and electrophysiological properties of crypt cells from the olfactory epithelium of the marine teleost *Trachurus symmetricus*. *J. Comp. Neurol.* 495, 113–121.

Schmachtenberg, O., and Bacigalupo, J. (2004). Olfactory transduction in ciliated receptor neurons of the Cabinza grunt, *Isacia conceptionis* (Teleostei: Haemulidae). *Eur. J. Neurosci.* 20, 3378–3386.

Sheldon, R. E. (1912). The olfactory tracts and centers in teleosts. *J. Comp. Neurol.* 22, 177–339.

Smithson, K. G., Weiss, M. L., and Hatton, G. I. (1992). Supraoptic nucleus afferents from the accessory olfactory bulb: evidence from anterograde and retrograde tract tracing in the rat. *Brain Res. Bull.* 29, 209–220.

Sorensen, P. W., Fine, J. M., Dvornikovs, V., Jeffrey, C. S., Shao, F., Wang, J., et al. (2005). Mixture of new sulfated steroids functions as a migratory pheromone in the sea lamprey. *Nat. Chem. Biol.* 1, 324–328.

Speca, D. J., Lin, D. M., Sorensen, P. W., Isacoff, E. Y., Ngai, J., and Dittman, A. H. (1999). Functional identification of a goldfish odorant receptor. *Neuron* 23, 487–498.

Speedie, N., and Gerlai, R. (2008). Alarm substance induced behavioral responses in zebrafish (*Danio rerio*). *Behav. Brain Res.* 188, 168–177.

Stacey, N. E., and Kyle, A. L. (1983). Effects of olfactory tract lesions on sexual and feeding behavior in the goldfish. *Physiol. Behav.* 30, 621–628.

Stell, W. K., Walker, S. E., Chohan, K. S., and Ball, A. K. (1984). The goldfish nervus terminalis: a luteinizing hormone-releasing hormone and molluscan cardioexcitatory peptide immunoreactive olfactoretinal pathway. *Proc. Natl. Acad. Sci. U.S.A.* 81, 940–944.

Stettler, D. D., and Axel, R. (2009). Representations of odor in the piriform cortex. *Neuron* 63, 854–864.

Tomizawa, K., Katayama, H., and Nakayasu, H. (2001). A novel monoclonal antibody recognizes a previously unknown subdivision of the habenulo-interpeduncular system in zebrafish. *Brain Res.* 901, 117–127.

Vielma, A., Ardiles, A., Delgado, L., and Schmachtenberg, O. (2008). The elusive crypt olfactory receptor neuron: evidence for its stimulation by amino acids and cAMP pathway agonists. *J. Exp. Biol.* 211, 2417–2422.

Von Bartheld, C. S. (2004). The terminal nerve and its relation with extrabulbar "olfactory" projections: lessons from lampreys and lungfishes. *Microsc. Res. Tech.* 65, 13–24.

von Bartheld, C. S., Meyer, D. L., Fiebig, E., and Ebbesson, S. O. (1984). Central connections of the olfactory bulb in the goldfish, *Carassius auratus*. *Cell Tissue Res.* 238, 475–487.

von Frisch, K. (1941). Über einen Schreckstoff der Fischhaut und seine biologische Bedeutung. *Z. Vgl. Physiol.* 29, 46–145.

Wedgwood, M. (1974). Proceedings: Connections between the olfactory bulb and the habenula and dorsomedial thalamic nuclei. *J. Physiol.* 239, 88P–89P.

Weth, F., Nadler, W., and Korsching, S. (1996). Nested expression domains for odorant receptors in zebrafish olfactory epithelium. *Proc. Natl. Acad. Sci. U.S.A.* 93, 13321–13326.

Wiechert, M. T., Judkewitz, B., Riecke, H., and Friedrich, R. W. (2010). Mechanisms of pattern decorrelation by recurrent neuronal circuits. *Nat. Neurosci.* 13, 1003–1010.

Yaksi, E., Von Saint Paul, F., Niessing, J., Bundschuh, S. T., and Friedrich, R. W. (2009). Transformation of odor representations in target areas of the olfactory bulb. *Nat. Neurosci.* 12, 474–482.

Yamagata, M., and Sanes, J. R. (2012). Transgenic strategy for identifying synaptic connections in mice by fluorescence complementation (GRASP). *Front. Mol. Neurosci.* 5:18. doi: 10.3389/fnmol.2012.00018

Yoshihara, Y. (2009). Molecular genetic dissection of the zebrafish olfactory system. *Results Probl. Cell Differ.* 47, 97–120.

Zeiske, E., Theisen, B., and Breucker, H. (1992). "Structure, development and evolutionary aspects of the peripheral olfactory system," in *Fish Chemoreception* (London: Chapman and Hall), 13–39.

Zhu, P., Narita, Y., Bundschuh, S. T., Fajardo, O., Scharer, Y. P., Chattopadhyaya, B., et al. (2009). Optogenetic dissection of neuronal circuits in Zebrafish using viral gene transfer and the tet system. *Front. Neural Circuits* 3:21. doi: 10.3389/neuro.04.021

Zippel, H. P., Reschke, C., and Korff, V. (1999). Simultaneous recordings from two physiologically different types of relay neurons, mitral cells and ruffed cells, in the olfactory bulb of goldfish. *Cell. Mol. Biol. (Noisy-le-grand)* 45, 327–337.

Zucker, C. L., and Dowling, J. E. (1987). Centrifugal fibres synapse on dopaminergic interplexiform cells in the teleost retina. *Nature* 330, 166–168.

Conflict of Interest Statement: The authors declare that the research was conducted in the absence of any commercial or financial relationships that could be construed as a potential conflict of interest.

Received: 31 January 2013; paper pending published: 19 February 2013; accepted: 18 March 2013; published online: 11 April 2013.

Citation: Kermen F, Franco LM, Wyatt C and Yaksi E (2013) Neural circuits mediating olfactory-driven behavior in fish. Front. Neural Circuits 7:62. doi: 10.3389/fncir.2013.00062

Curriculum Vitae

Personal Information

Name, Surname	Luis Manuel, Franco Méndez
Place of birth	Mexicali, Baja California, Mexico
Date of birth	July 11th, 1985
Work address	VIB Center for the Biology of Disease Herestraat 49, 3000 Leuven, Belgium
E-mail address	lmfrancomendez@gmail.com

Education

Doctor of Philosophy	Cognitive and Molecular Neurosciences (2016) Doctoral School of Biomedical Sciences University of Leuven (KU Leuven)
Master of Science	Molecular Cell Neurobiology (2011) Department of Physiology, Biophysics and Neuroscience Center for Research and Advanced Studies (CINVESTAV)
Bachelor of Science	Biochemical Engineering in Biotechnology (2008) Department of Biochemical Engineering Celaya Institute of Technology (ITC)

Publications

Franco L. M., Okray Z., Linneweber, G., Hassan B. A., Yaksi E. Impaired lateral inhibition alters neuronal representations in a *Drosophila* model of Fragile X Syndrome. *Curr Biol. In revision.*

Soldano, A., Alpizar, Y.A., Boonen, B., **Franco, L.M.**, Lopez-Requena, A., Liu, G., Mora, N., Yaksi, E., Voets, T., Vennekens, R., Hassan, B.A. & Talavera, K. (2016) Gustatory-mediated avoidance of bacterial lipopolysaccharides via TRPA1 activation in *Drosophila*. *eLife*, 5.

Franco L. M., Beltrán J. Q., Tapia J. A., Franco O., Manjarrez E., Gutiérrez R. (2016) Differential frequency-dependent antidromic resonance of the Schaffer collaterals and mossy fibers. *Brain Struct Funct* 221, 1793-1807.

Christiaens J. F.*, **Franco L. M.***, Cools T., de Meester L., Michiels J., Wenseleers T., Hassan B. A., Yaksi E., Verstrepen K. J. (2014) The fungal aroma gene *ATF1* promotes dispersal of yeast cells through insect vectors. *Cell Rep* 9, 425-432.
***equal contribution**

Kermen F.*, **Franco L. M.***, Wyatt C., Yaksi E. (2013) Neural circuits mediating olfactory-driven behavior in fish. *Front Neural Circuits* 7.
***equal contribution**

Awards

International Brain Research Organization/Society for Neuroscience (IBRO/SfN)	Travel fellowship awarded to present my work entitled *Reduced lateral inhibition impairs olfactory computations and behaviors in a Drosophila model of fragile X syndrome* at the Society for Neuroscience annual meeting: Neuroscience 2016. (November 12th – 16th, 2016)
Fonds Wetenschappelijke Onderzoeks (FWO)	Grant for participation in an international conference awarded to present my work entitled *Reduced lateral inhibition impairs olfactory computations and behaviors in a Drosophila model of fragile X syndrome* at the biennial Cold Spring Harbor meeting on Neuronal Circuits. (April 6th – 9th, 2016)
Vlaams Instituut voor Biotechnologie (VIB)	Fellowship for doctoral studies in Cognitive and Molecular Neurosciences to be carried out in Neuroelectronics Research Flanders (NERF) and VIB Center for the Biology of Disease awarded by the VIB PhD International Program in Life Sciences. (September 2012 – November 2016)
National Council for Science and Technology (CONACyT)	Fellowship for the research project entitled *Electrophysiological characterization of mixed chemical-electrical synapses established by mossy fibers onto CA3 pyramidal neurons* (reference: 79408) carried out in the Department of Physiology, Biophysics and Neuroscience of the Center for Research and Advanced Studies (CINVESTAV). (August 2010 – July 2012)
National Council for Science and Technology (CONACyT)	Fellowship for master studies (CVU/Fellow: 267382/219216) in Molecular Cell Neurobiology carried out in the Department of Physiology, Biophysics and Neuroscience of the Center for Research and Advanced Studies (CINVESTAV). (August 2008 – July 2010)
Secretariat of Public Education (SEP)	Fellowship for bachelor studies in Biochemical Engineering carried out in Celaya Institute of Technology awarded by the National Program of Fellowships to Academic Achievement and Excellence. (September 2006 – June 2007)

Research experience

Neuroelectronics Research Flanders (NERF), IMEC
Leuven, Belgium
Advisor: Dr. Emre Yaksi

- *In vivo* whole-cell patch-clamp recordings and calcium imaging.
- Optogenetic and odor stimulation of neurons.
- *D. melanogaster* preparation for *in vivo* neurophysiological experiments.
- Behavioral assays on populations of *D. melanogaster*.
- MATLAB programming for data acquisition and analysis.
- Building of computer-controlled devices for odor stimulation and behavioral assays.

(September 2012 – November 2016)

VIB Center for the Biology of Disease, KU Leuven
Leuven, Belgium
Advisor: Dr. Bassem Hassan

- Immunostainings on *D. melanogaster* brains.
- Selection of *D. melanogaster* phenotypic markers.
- Breeding and handling of *D. melanogaster*.

(September 2012 – November 2016)

Department of Physiology, Biophysics and Neuroscience, CINVESTAV
Mexico City, Mexico
Advisor: Dr. Rafael Gutierrez

- *In vitro* field potential and intracellular recordings.
- Preparation of acute rat hippocampal slices.
- Building of microscale bipolar stimulation electrodes.
- Data analysis on pClamp 10, OriginPro and SigmaPlot.

(August 2009 – July 2012)

Center for Multidisciplinary Studies in Biotechnology (CMEB), UMSNH
Morelia, Mexico
Advisor: Dr. Victor Baizabal

- Electrophoresis.
- RT-PCR.
- RNA extraction.
- Cell culture.

(July 2007 – May 2008)

Workshops

FLiACT Workshop
Janelia Farm, HHMI
Ashburn, VA, USA

Emerging techniques to map and functionally characterize neural circuits in *Drosophila melanogaster*.
European Commission, Marie Curie Actions
(October 4th – 7th, 2013)

FLiACT Workshop
MPI of Neurobiology
Munich, Germany

Behavioral assay design and screening techniques in *Drosophila melanogaster*.
European Commission, Marie Curie Actions
(April 16th – 19th, 2013)

FLiACT Workshop
MPI for Chemical Ecology
Jena, Germany

Electrophysiology in *Drosophila melanogaster*.
European Commission, Marie Curie Actions
(December 10th – 13th, 2012)

Poster presentations

Neuroscience 2016 **San Diego, CA, USA**	**Franco L. M.**, Okray, Z., Hassan B. A., Yaksi E. Reduced lateral inhibition impairs olfactory computations and behaviors in a *Drosophila* model of Fragile X Syndrome. (November 14th, 2016)
FENS Forum 2016 **Copenhagen, Denmark**	**Franco L. M.**, Okray, Z., Hassan B. A., Yaksi E. Reduced lateral inhibition impairs olfactory computations and behaviors in a *Drosophila* model of Fragile X Syndrome. (July 4th, 2016)
ISDN 2016 **Juan-les-Pins, France**	**Franco L. M.**, Okray, Z., Yaksi E., Hassan B. A. Reduced lateral inhibition impairs olfactory computations and behaviors in a *Drosophila* model of Fragile X Syndrome. (May 12th, 2016)
Neuronal Circuits **Cold Spring Harbor, NY, USA**	**Franco L. M.**, Okray, Z., Hassan B. A., Yaksi E. Reduced lateral inhibition impairs olfactory computations and behaviors in a *Drosophila* model of Fragile X Syndrome. (April 7th, 2016)
2nd Belgian Neuroinformatics Congress **Leuven, Belgium**	**Franco L. M.**, Hassan B. A., Yaksi E. Extraction of dendrite activity in dense neural circuits by independent component analysis. (December 4th, 2015)
VIB-NERF PhD Symposium **Leuven, Belgium**	**Franco L. M.**, Okray Z., Hassan, B. A., Yaksi, E. Functional Characterization of Fragile X Syndrome. (September 20th, 2015)
Flies, Worms and Robots **ESF-EMBO Symposium** **Sant Feliu de Guíxols, Spain**	**Franco L. M.**, Christiaens J. F., Hassan B. A., Verstrepen K. J., Yaksi E. Beer aroma: a yeast product that attracts fruitflies (…and humans). (November 10th, 2014)
FENS Forum 2014 **Milan, Italy**	**Franco L. M.**, Christiaens J. F., Hassan B. A., Verstrepen K. J., Yaksi E. Ester production in yeast alters neural responses in the fruitfly antennal lobe, increases their attractiveness and promotes their dispersal. (July 8th, 2014)
FLiACT Workshop **Janelia Farm, HHMI** **Ashburn, VA, USA**	**Franco L. M.**, Okray Z., Hassan, B. A., Yaksi, E. Functional Characterization of Fragile X Syndrome. (October 6th, 2013)
VIB-NERF PhD Symposium **Leuven, Belgium**	**Franco L. M.**, Okray Z., Hassan, B. A., Yaksi, E. Functional Characterization of Fragile X Syndrome. (September 20th, 2013)
Neuroscience 2011 **Washington, DC, USA**	**Franco L. M.**, Beltrán J. Q., Manjarrez E., Gutiérrez R. Hippocampal mossy fibers, but not Schaffer collaterals, present resonance. (November 12th, 2011)

Oral presentations

Neuroelectronics Research Flanders (NERF), IMEC Leuven, Belgium	"Studying neural circuit mechanisms underlying fragile X syndrome in *Drosophila melanogaster*" NERF Seminar (June 2nd, 2016)
Kavli Institute for Systems Neuroscience, NTNU Trondheim, Norway	"Studying neural circuit mechanisms underlying fragile X syndrome in *Drosophila melanogaster*" Invited Speaker (July 20th, 2015)
Neuroelectronics Research Flanders (NERF), IMEC Leuven, Belgium	"Studying neural circuit mechanisms underlying fragile X syndrome in *Drosophila melanogaster*" NERF Seminar (January 29th, 2015)
VIB Center for the Biology of Disease, KU Leuven Leuven, Belgium	"Studying neural circuit mechanisms underlying fragile X syndrome in *Drosophila melanogaster*" NERF-VIB11 PhD Symposium (September 26th, 2014)
Neuroelectronics Research Flanders (NERF), IMEC Leuven, Belgium	"Functional Characterization of Fragile X Syndrome" NERF Seminar (May 16th, 2013)
VIB Headquarters Ghent, Belgium	"Resonance increases fidelity of transmission in the hippocampal DG-CA3 circuit" VIB PhD International Program in Life Sciences (May 21st, 2012)